Spring 2002

The development of h Homogeneous nucleation rate model for thermoplastic foams based on a molecular partition function and Fickian diffusion

Ronald G. Gabbard
New Jersey Institute of Technology

ABSTRACT

THE DEVELOPMENT OF A HOMOGENEOUS NUCLEATION RATE MODEL FOR THERMOPLASTIC FOAMS BASED ON A MOLECULAR PARTITION FUNCTION AND FICKIAN DIFFUSION

by
Ronald G. Gabbard

An improved homogeneous nucleation rate model for thermoplastic foams has been developed. This model does not rely on experimentally determined parameters and only uses pure component physical property data and a binary diffusion coefficient. This model, like those derived from classical nucleation theory, is made up of two parts, one that determines the size of the energy barrier in the nucleation process and one that estimates the forward rate of the process. A statistical-mechanical approach was used to create an energy term that is based on a molecular partition function. In this approach, the bulk phase (polymer and blowing agent mixture) of the system is treated as a regular solution and the potential energy of this phase is estimated from regular solution theory. The rate component of the model is obtained by utilizing a diffusion-based model derived from Fick's law. Additional approaches including a diffusion only based approach, a fluctuation theory based approach, and a lattice model based approach were all unsuccessfully investigated.

The predictions obtained from the model have been compared to a polymethylmethacrylate/carbon dioxide system with limited success. Although the model results do not match the experimental data, there is a significant improvement over the results obtained from current models available in the literature. The data is limited to

the one system described above as there was significant evidence of heterogeneous nucleation in most other systems identified in the literature.

Finally, the work also provides a comprehensive review of the literature on foam nucleation in thermoplastics. The review covers both homogeneous and heterogeneous models and looks at results obtained experimentally and theoretically. This review clearly identifies the need for an improved nucleation model that is not dependent on experimental parameters like the one developed in this work.

THE DEVELOPMENT OF A HOMOGENEOUS NUCLEATION RATE MODEL FOR THERMOPLASTIC FOAMS BASED ON A MOLECULAR PARTITION FUNCTION AND FICKIAN DIFFUSION

by
Ronald G. Gabbard

A Dissertation
Submitted to the Faculty of
New Jersey Institute of Technology
in Partial Fulfillment of the Requirements for the Degree of
Doctor of Philosophy in Chemical Engineering

Department of Chemical Engineering

May 2002

APPROVAL PAGE

THE DEVELOPMENT OF A HOMOGENEOUS NUCLEATION RATE MODEL FOR THERMOPLASTIC FOAMS BASED ON A MOLECULAR PARTITION FUNCTION AND FICKIAN DIFFUSION

Ronald G. Gabbard

Dr. Dana E. Knox, Dissertation Advisor — Date
Associate Professor of Chemical Engineering, New Jersey Institute of Technology

---

Dr. Robert B. Barat, Committee Member — Date
Associate Professor of Chemical Engineering, New Jersey Institute of Technology

---

Dr. Norman Loney, Committee Member — Date
Associate Professor of Chemical Engineering, New Jersey Institute of Technology

---

Dr. Marino Xanthos, Committee Member — Date
Professor of Chemical Engineering, New Jersey Institute of Technology

---

Dr. William E. Volz, Committee Member — Date
Global Quality Manager, BASF Corporation, Portsmith, Va.

BIOGRAPHICAL SKETCH

Author: Ronald G. Gabbard

Degree: Doctor of Philosophy

Date: May, 2002

Undergraduate and Graduate Education

- Doctor of Philosophy in Chemical Engineering
  New Jersey Institute of Technology, Newark, NJ, 2002

- Master of Science in Chemical Engineering
  New Jersey Institute of Technology, Newark, NJ, 1993

- Bachelors of Science in Chemical Engineering
  New Jersey Institute of Technology, Newark, NJ, 1985

Major: Chemical Engineering

Presentations and Publications:

Gabbard, R. G. and Knox, D. E., A Supercritical Extraction Experiment for the Unit Operations Laboratory. Chemical Engineering Education, **35**, 96-101, 2001.

Ober, R.D. and Gabbard, R. G., A Plant Scale Expandable Polystyrene "Stopper System": α-Tocopherol as an Alternative to tert-Butyl Catechol, 222nd American Chemical Society National Meeting, Chicago, Ill., August, 2001.

Gabbard, R.G. and Knox, D.E., The Solubility of Blowing Agents in Polymers and Its Impact on Nucleation Rate and Cell Number in Foamed Polymers. 9th Int. Symp. on Solubility Phenomena (IUPAC), Hammamet, Tunisia, 2000.

Gabbard, R. G. and Knox, D. E., Nucleation of Thermoplastic Foams. American Institute of Chemical Engineers Annual Meeting, Los Angeles, California, 2000.

Arora, V.J., G.V. Jones, J. M. Kovtun, and R. G. Gabbard, "Evaporation Process for Producing Coffee Glass", Assignee: Kraft General Foods, United States Patent #5035908, 1991.

This thesis is dedicated to my wonderful family;
my beautiful wife, Anna and my three delightful children;
Nicole, Jacqueline, and Louis, for all of their sacrifices and
persistent encouragement, and yes Louis, Daddy can come out and play now!

ACKNOWLEDGMENT

The author wishes to express his deepest gratitude to his advisor, Dr. Dana Knox for guidance and friendship throughout this work. Special thanks go to Dr. Robert Barat, Dr. Norman Loney, and Dr. Marino Xanthos for serving as members of my thesis committee and for all their helpful suggestions and support. Additional special thanks go to Dr. William E. Volz of BASF, Corp. who has taken the time from his busy schedule to also participate as a committee member.

The author is especially grateful to BASF, Corp. for supporting this work and providing the equipment, materials, analytical support, and time so that this work could be completed. The author is also especially grateful to Lizle Laqui and Eric Weisenbach, for all their help in the lab. Finally, a very special thanks is owed to Petra Knox, who was kind enough to tolerate the author's invasion of her home on many late nights and weekends so that this work could be completed.

TABLE OF CONTENTS

TABLE OF CONTENTS
(Continued)

Chapter **Page**

TABLE OF CONTENTS
(Continued)

Chapter **Page**

LIST OF TABLES

LIST OF FIGURES

LIST OF FIGURES
(Continued)

Figure **Page**

LIST OF FIGURES
(Continued)

LIST OF SYMBOLS

Symbol	Description and units if applicable
a	Activity
A	Surface Area [cm^2]
A_{iji}	Hamaker constant for material j between material i [ergs]
A_n	Helmholtz energy of a cluster [ergs]
A^*_{nv}	Internal Helmholtz energy of a cluster for clusters with number of molecules and volume varying independently [ergs]
A_T	Total surface area of the critical clusters in the system [cm^2]
b	van der Waals volume parameter [cm^3]
B(T)	Bulk modulus of the polymer [dyne/cm^2]
$\mathscr{B}$	Generic pure component property
$\mathscr{B}_m$	Generic mixture property
$\bar{c}$	Average speed of a molecule [cm/sec]
C	Concentration [moles/cm^3]
c_P	Heat capacity (constant pressure) [ergs/mole-K]
c_v	Heat capacity (constant volume) [ergs/mole-K]
C_V	Concentration in the vapor [moles/cm^3]
C_l	Concentration in the liquid [moles/cm^3]
C_0	Initial gas concentration in the system [moles/cm^3]
C_B	Concentration of blowing agent in the bulk phase [mole/cm^3]
$C_e(t)$	Equilibrium concentration corresponding to the partial pressure of the volatile component in the vapor phase at time t [moles/cm^3]
C_{Het}	Initial concentration of heterogeneous nucleation sites in the system [number/liter]
$\mathscr{C}$	Combinatorial factor
d	Dipole moment [Debyes]
d_{ij}	Hard sphere diameter [cm]
D	Dummy variable
D_{AB}	Liquid diffusion coefficient [cm^2/sec]
D_p	Diameter of a particle [cm]
D(T)	Temperature dependent diffusivity [cm^2/sec]
E	Energy [ergs]
$\bar{E}$	Average energy [ergs]
ΔE^v	Complete energy of vaporization [ergs/mole]
E_t	Total energy of an ensemble system [ergs]
ε	Probabilistic event
f^v	Fugacity of the vapor [dyne/cm^2]
f^l	Fugacity of the liquid [dyne/cm^2]
f_i^{sat}	Fugacity of the i^{th} component at the saturation pressure [dyne/cm^2]
$f_{n,s}$	Steady state cluster distribution function
$f_{n,0}$	Equilibrium cluster distribution function
f(n,t)	Cluster size distribution that is a function of time
f_n	Steady state cluster size distribution

LIST OF SYMBOLS
(Continued)

Symbol	Description and units if applicable
f_{nv}	Cluster size distribution for clusters that have number of molecules and volume varied independently
F	Function derived from wetting angle, also know as contact angle, see Equation 2.3.4
g	Modulus [dyne/cm^2]
g_c	Composite modulus [dyne/cm^2]
G	Gibbs free energy [ergs]
ΔG	Change in Gibbs free energy [ergs]
ΔG^*	Corrected Gibbs free energy [ergs]
ΔG_{Het}	Gibbs free energy for heterogeneous systems [ergs]
ΔG_m	Maximum value of ΔG [ergs]
ΔG_p	Corrected Gibbs energy [ergs]
ΔG_s	Gibbs energy corrected for non equilibrium [ergs]
ΔG_t	Gibbs energy corrected for presence of solvent molecules [ergs]
G_k*	Modulus [dyne/cm^2]
G(Z)	Non-retarded Liftshitz-van der Waals free energy [dyne/cm]
h	Planks constant [6.6262 x^{-27} ergs-sec]
h_v	Heat of vaporization [ergs/mol]
h_c	Convective heat transfer coefficient [W/m^{2}K]
H	Hamiltonian [ergs]
$\mathcal{H}$	Conditional probability event that was required to occur before the probabilistic event could be fulfilled
I	Elasticity number for nucleation [dyne/cm^2]
J(n,t)	Flux of clusters in cluster size space as a function of n and t
J	Steady state nucleation rate [bubbles/cm^3-sec]
J_{AB}	Molar flux [moles of A/cm^2-sec]
J_i	Transport corrected steady-state nucleation rate [bubbles/cm^3-sec]
k	Boltzmann's constant [1.380662 X 10^{-16} ergs/K]
K:	Thermal conductivity [ergs/cm-K-sec]
K_h	Henry's constant [cm^3(STP)/cm^3-atm]
L	Avogadro's number [6.022045 X 10^{23} molecules/mole]
ℓ	Radius of gyration for a molecule [cm]
m	Mass of a molecule [g]
m_V	Ratio of molar volumes of polymer to solvent in Flory-Huggins theory
M	Mass of the system [g]
MW	Molecular weight [g/mole]
n	Number of molecules in a cluster
$n_1, n_2, \ldots, n_j$	Number of systems in the canonical ensemble, applies only to Appendix A
n_c	Number of molecules in a critically sized cluster
N	Total number of molecules
N_B	Number of molecules in bulk phase
N_{exc}	Number of vapor molecules outside the clusters

LIST OF SYMBOLS
(Continued)

Symbol	Description and units if applicable
N_G	Number of blowing agent molecules initially in the system per cm^3
N_P	Number of polymer repeat units
N_0	Concentration of molecules that will form new phase once nucleation begins [moles or molecules/cm^3]
$\mathcal{N}_p$	Number of particles in the system
$\mathcal{N}$	Lattice sites occupied by polymer repeat units
$\mathcal{N}_0$	Total occupied lattice sites
$\mathcal{N}_T$	Total lattice sites
$\mathcal{N}_V$	Vacant lattice sites
O1	Calculated intermediate values [cm-molecules]
O2	Calculated intermediate value [ergs]
$\mathbf{p}_i$	Momentum of the i^{th} molecule [g-cm/sec]
P	Pressure [dyne/cm^2]
ΔP	Change in pressure [dyne/cm^2]
P_G	Pressure inside a gas bubble [dyne/cm^2]
P_B	Pressure of the bulk polymer phase [dyne/cm^2]
P^{sat}	Saturation pressure [dyne/cm^2]
P_0	Reference pressure [dyne/cm^2]
$\mathcal{P}$	Symbol for a probability term
$\mathcal{P}_D$	Diffusion probability defined by Equation 2.4.7
$\mathcal{P}_n$	Probability that a single cluster with volume v centered on the c.m.
$\mathcal{P}_{nv}$	Probability that a single nv cluster will be found in V
$\mathcal{P}_0$	Probability that the c.m. of a cluster will be found at the origin
$\mathcal{P}_r$	Probability a given microvoid is size r
q_n	Individual cluster partition function (similar to partition function for individual molecule)
q_{nv}	Individual cluster partition function that has the number of molecules and the volume varied independently
Q	System partition function
Q_{nv}	Partition function for the molecules in the nv cluster
Q_n	Partition function for all of the molecules in the system
Q'	Intermediate Step in the development of the Partition Function
r	Bubble or cluster radius [cm]
$\bar{r}$	Average bubble or cluster radius [cm]
r_p	Radius of a particle (i.e. rubber particle in HIPS) [cm]
r_c	Critical bubble or cluster radius [cm]
r_0	Initial radius of a microvoid [cm]
$\mathbf{r}_i$	Position vector for the i^{th} molecule in the c.m. coordinate system
$\mathbf{r}_i'$	Position vector for the i^{th} molecule in any arbitrary coordinate system
$\mathbf{R}$	Position vector of the c.m. of a cluster
R_1^*	Dimensionless radius defined in Equation 3.2.39

LIST OF SYMBOLS
(Continued)

Symbol	Description and units if applicable
R_p	Radius of the mouth in the porous cavity in the cavity model [cm]
R	Ideal gas constant, Applies only to Appendix D
$\mathcal{R}$	Lagrange multiplier
s	Super-saturation ratio
S	Entropy [ergs/K])
$\mathcal{S}$	Lagrange multiplier
t	Time
t_c	Bubble growth time [sec]
T	Temperature [K]
T_c	Critical Temperature [K]
T_0	Reference Temperature [K]
T_e	Equilibrium temperature of the bulk phase [K]
T_g	Glass transition temperature of a thermoplastic polymer [K]
T_i	Initial temperature [K]
T^{sat}	Saturation temperature [K]
u	Potential energy of an individual cluster [ergs]
u'	Potential energy of an individual cluster in the transformed coordinate system [ergs]
u_{shell}	Potential energy of the shell molecule [ergs]
$u_n(r^n)$	Pairwise additive potential [ergs]
U	Potential energy [ergs]
v	Volume of a cluster [cm^3]
v'	Arbitrary upper limit to cluster volume [cm^3]
v_m	Volume of a molecule [cm^3]
$\bar{v}$	Average linear velocity in the system [cm/sec]
V	Volume [cm^3]
V_l	Lattice site volume [cm^3]
V_L	Liquid molar volume [mole/cm^3]
V_{exc}	Volume of the system not occupied by molecules or clusters [cm^3]
V_f	Free volume excluding clusters [cm^3]
$\bar{V}_f$	Free volume including clusters [cm^3]
V_{Free}	Free volume of a polymer [cm^3]
V_G	Volume of blowing agent [cm^3]
V_p	Volume of polymer surrounding a bubble [cm^3]
V_0	Volume of pure polymer @ reference temperature T_0 [cm^3]
V_{vdw}	van der Waals volume [cm^3]
$\bar{V}$	Molar volume of a component [moles/cm^3]
w_i	Weight fraction of the i^{th} component
$\mathcal{W}$	Substituted variable for integration defined by Equation 4.1.30
x_i	Number of moles of the i^{th} species [moles]
x_i	Liquid mole fraction of the i^{th} component, applies only to Appendix D

LIST OF SYMBOLS
(Continued)

Symbol	Description and units if applicable
χ	Substituted variable for integration defined by Equation 4.1.29
y	Convected coordinate transformation variable, applies only to Equation 3.3.4
y_i	Mole fraction of the i^{th} component
z	Linear Distance or distance between polymer chains or molecules [cm]
z_i	Interaction distance between point charges [cm]
z_1	Intermolecular separation distance [cm]
z_2	Repeat unit interaction distance [cm]
Z	Zeldovich Factor
Z'	Compressibility of a gas
Z_{nv}	Classic configuration integral for the nv cluster
Z_n	Classic configuration integral for the bulk phase of the system
Z_R	Classic configuration integral for a cluster
Z_0	Classic configuration integral for a system that is constrained to the origin of the original system
Z_0	Equilibrium inter-chain distance [cm]
ζ	Substituted variable for integration defined by Equation 4.1.32

Greek Symbols	Description and units if applicable
α	Coefficient of thermal expansion [1/K]
α_i, α_j	Point charges of the ith and jth particles [coulombs]
β	Collision Factor defined in Equation 2.2.13 [1/cm^2-sec]
β_0	Condensation coefficient (accounts for rate that molecules add to clusters)
γ	Surface tension [dyne/cm]
γ_a	Activity coefficient, applies only to appendix D
γ_{local}	Local or microscopic surface tension [dyne/cm]
$\dot{\gamma}$	Shear rate (if with over-bar, the average shear rate) [1/sec]
Γ_n	Curvature Correction for Surface Tension
Γ_θ	Function of angles between dipoles
δ	Solubility parameter [(J/cm^3)$^{0.5}$]
δ_i	General correction factor for transport limited nucleation
ε	Surface energy parameter
ε_0	Evaporation rate (accounts for rate that molecules leave clusters)
ζ	Gradient energy coefficient, [ergs cm^2]
η	Solution viscosity [cp]
η_1, η_2	Parameter selected to fit saturated vapor pressure and second viral coefficient data
θ	Wetting angle, also known as the contact angle

LIST OF SYMBOLS
(Continued)

Greek Symbol	Description and units if applicable
$\theta_1, \theta_2, \theta_3$	Orientation angles for a dipole
Θ	Defined in Equation 2.6.3
ι_m	Permittivity of the medium containing point charges [usually taken to be 9 x 10^9 N-m^2/$coulomb^2$]
κ	Surface mass coefficient
λ	Lagrange undetermined multiplier
λ_t	Relaxation time [sec]
Λ	Modified Thermal deBroglie wave-length cubed [1/cm^3]
μ	Chemical potential [ergs/mole of i]
μ_l	Chemical potential of solvent in polymer solution [ergs/mole of i]
μ_l^0	Chemical potential of pure solvent [ergs/mole of i]
$\mu_G^{(L)}$	Chemical potential of the blowing agent in the liquid phase [ergs/mole of i]
ν	Poisson's ratio (Change in width per unit width/Change in length per unit length)
ξ	Dummy variable
ρ	Mass density [g/cm^3]
ρ_l	Mass density of the liquid phase [g/cm^3]
ρ_g	Mass density of the vapor phase [g/cm^3]
$\bar{\rho}$:	Molar density [moles/cm^3]
ρ^*	Number density [molecules/cm^3]
$\rho^{(G)}$	Density of the blowing agent in the vapor phase [moles/cm^3]
σ	Standard deviation
σ_{LJ}	Characteristic length parameter for Lennard-Jones potential energy function [cm]
$\Sigma_{rr}, \Sigma_{\phi\phi}, \Sigma_{\theta\theta}$	Triaxial tensile stresses [dynes]
τ	Differential volume [cm^3]
τ_{f_G}	Differential free volume of blowing agent [cm^3]
τ_{f_P}	Differential free volume of polymer agent [cm^3]
τ_L	Larson parameter
υ_1, υ_2	Parameter selected to fit the critical density and pressure of a substance
$\varphi_G^{(L)}$	Activity coefficient of the blowing agent in the liquid phase
φ	Activity coefficient
ϕ	Long range attractive part of the potential energy function [ergs]
ϕ_{LJ}	Lennard-Jones potential energy [ergs]
ϕ_S	Stockmayer potential energy function [ergs]
$\hat{\phi}$	Fugacity coefficient of ith component in a mixture, applies only to Appendix D

LIST OF SYMBOLS
(Continued)

Greek Symbols	Description and units if applicable
ϕ_i^{sat}	Fugacity coefficient of i^{th} component at saturation pressure, applies only to Appendix D
Φ_i	Volume fraction as defined by Flory-Huggins theory
χ	Flory-Huggins interaction parameter
χ_0	Entropic contribution to the Flory-Huggins parameter, usually taken to be 0.34
ψ	Frequency factor in Fokker-Planck equation [1/sec]
ψ_a, ψ_b	Constants for ψ determined experimentally based on nucleation rate data
ψ_0	Homogeneous frequency factor [1/sec]
ψ_1	Heterogeneous frequency factor [1/sec]
ω	Total number of systems in an ensemble
Ω	Grand Potential in Density Functional Theory [ergs]
Ω_c	Critical Grand Potential in Density Functional Theory [ergs]

Special Symbols	Description and units if applicable
ϑ	Ratio of characteristic bubble radius to actual bubble radius
ϵ	Characteristic energy parameter for the Lennard-Jones potential energy function [ergs]
$\wp$	Area correction term in Equation 3.2.43
$\Re$	Cohesive-energy density [ergs/cm^3]

LIST OF SYMBOLS
(Continued)

Dimensionless Numbers	Description
N_{Bi}	Biot Number $\left[\frac{h_c\left(r_p/3\right)}{K}\right]$
N_{Ca}	Capillary Number $\left[\frac{R_p\eta\dot{\gamma}_{avg}}{4\gamma}\right]$
N_{De}	Deborah Number $\left[\frac{\lambda}{t_c}\right]$
N_{Pe}	Peclet Number $\left[\frac{\gamma^2}{D_{AB}\Delta P\eta}\right]$
N_{So}	Solubility Number $[K_h RT]$

Useful Abbreviations

AIBN	Azo bis(iso-butyronitrile)
CFC	Chlorofluorocarbon
c.m.	Center of mass of a cluster
CNT	Classical Nucleation Equation
EPS	Expandable Polystyrene
HCFC	Hydrochloroflourocarbon
MPF	Molecular Partition Function
PET	Polyethylene terephthalate
PMMA	Polymethyl methacrylate
SEM	Scanning Electron Microscopy
TEM	Transmission Electron Microscopy
VOC	Volatile Organic Compound

CHAPTER 1

INTRODUCTION

1.1 Fundamentals of Polymeric Foam

Polymeric foams are made by dispersing a large number of tiny gas bubbles throughout the polymer matrix. These foams have existed since at least the mid 1930's when polystyrene foam was invented in Sweden and can be made from many different types of polymers (Benning, 1969). In the 1950's and 1960's, commercial activity surrounding foams significantly increased. Some of the manufacturers leading the way included BASF Aktiengesellschaft AG (BASF), Bayer AG, and the Dow Chemical Company (Benning, 1969). Benning also notes that since then many different polymers such as polyolefin, polyvinyl-chloride, phenolic, urea-formaldehyde, epoxy, and synthetic rubber, to name a few, have been used to produce foams commercially. To date, polystyrene and polyurethane foams continue to dominate as the two most widely produced foams in the polymer industry (Best, 2001).

These polymeric foams have evolved into an important class of engineered materials with widespread applications. Historically, foams had been used predominately as thermal insulation, however, today they are used in a wide variety of different engineering and packaging applications. The diversity of these applications includes the traditional use as insulation to newer uses in cushioning, packaging, special building and construction applications, buoyancy, and weight reduction (Zhang, Xanthos, Dey, 2001). The cushioning applications include everything from seat cushions to energy absorbing foams like bumper cores and side impact panels in automobiles, while the packaging applications include everything from electronics to food. The essential role of

a packaging application is to protect the article in transit. The article can be anything from expensive electronics to priceless people (when the protective package is a bicycle helmet). Some of the more interesting construction applications include insulating concrete forms and structural panels combining both strength and structural support with thermal and/or sound insulation in an integrated design. Buoyancy applications include things such as dock floatation, personal floatation devices, and weight reduction in watercraft. One of the most unique buoyancy applications is one that involves expandable polystyrene (EPS). The fourteenth green (see Figure 1.1) at Coeur d'Alene Country Club and Golf Resort in Idaho is a man-made movable island that floats on an EPS base (Hagadone Hospitality, 2001). This application not only highlights the buoyant properties of the foam, but also its strength and structural support properties. This floating green also demonstrates the flexibility that plastic foams can provide for engineering design.

One important reason why polymer foams are so successful in such a wide variety of different applications is the fact that their physical properties are not based on the polymer alone. These foams are complicated structures and their physical and functional properties are based on a number of important factors. These include the morphology or structure of the foam, the density of the foam, the cell gas, and the base polymer. The cell gas can be either air or residual blowing agent that is left after the foaming process has been completed.

The foam morphology can be broken down into two sub-categories. The first category relates to the size of the bubbles in the foam and the second relates to the foam structure. Polymeric foams that have bubbles or cells with diameters greater than ten

Figure 1.1 Fourteenth Green at Coeur d'Alene Country Club and Golf Resort in Idaho. The 15,000 ft^2 green is a man-made island that floats on an expandable polystyrene base, which is used to provide structural support and integrity while also providing the necessary buoyancy. Photo from Hagadone Hospitality, 2001.

microns are typically referred to as "cellular" while those foams with cell diameters of less than ten microns are typically referred to as "micro-cellular". The foam structure is made up of either closed cells or open cells. Closed-cell foam is predominantly made up of cells where the cell walls are intact and the cells look like tiny individual bubbles. Each cell or bubble is made up of a group of struts, which act as the supports for the bubble, and a group of membranes. These membranes connect to the struts creating the closed foam structure. Figure 1.2 shows a cross sectional microscopic image of closed-cell foam. Open-cell foams have a majority of the cell walls broken leaving only struts (without the membranes). Figure 1.3 shows a cross sectional microscopic image of an open-celled foam. In general, open cell foams tend to be more resilient and flexible

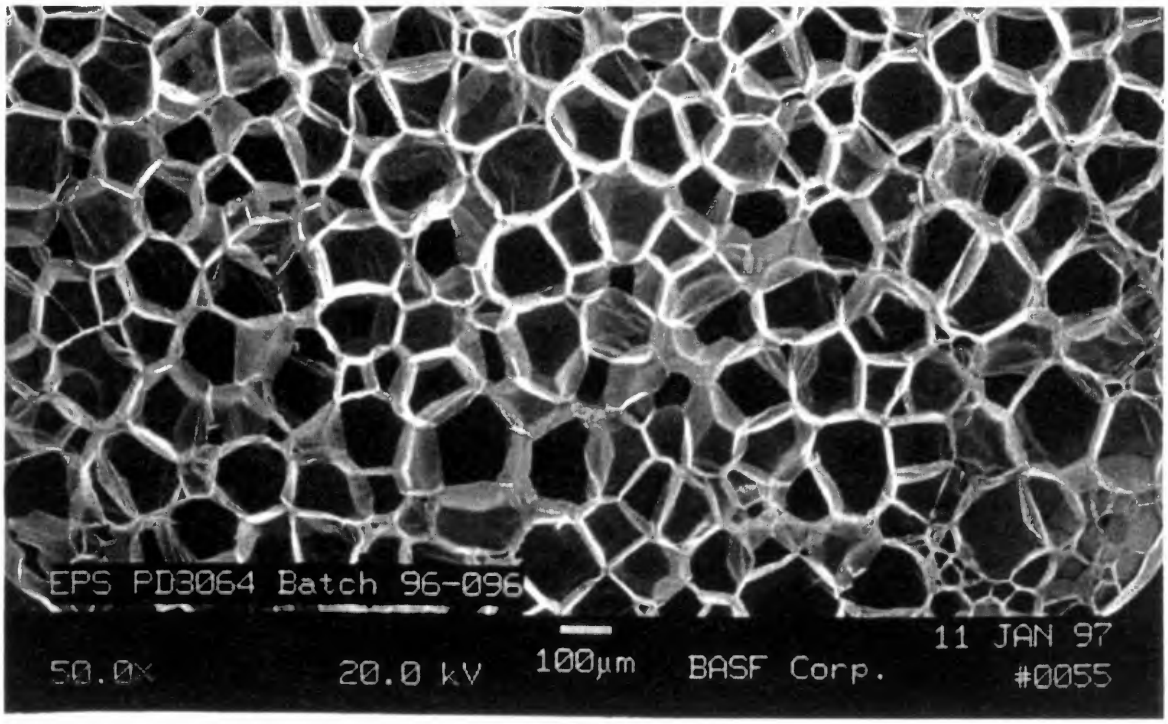

Figure 1.2 Closed-cell Foam (An Electron Scanning Microscopy Photo of Expandable Polystyrene Foam at 50X).

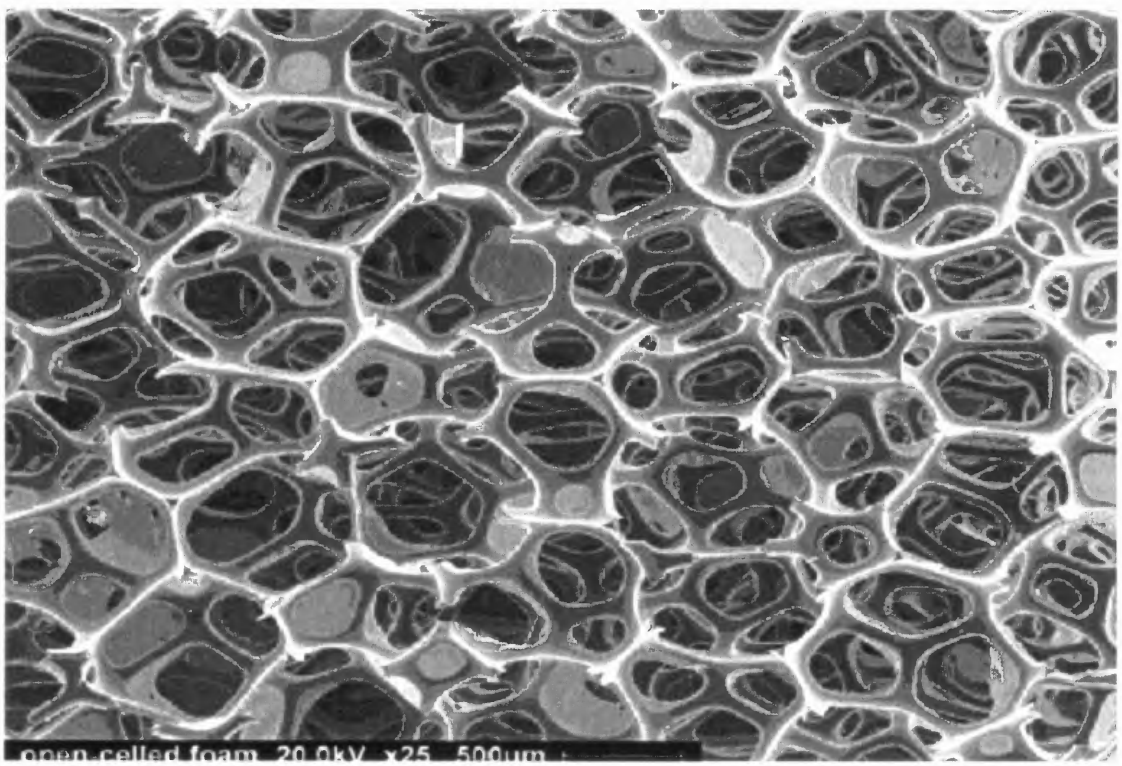

Figure 1.3 Open-cell Foam (An Electron Scanning Microscopy Photo of a Flexible Polyurethane Foam at 25X).

while closed cell foams tend to be rigid with better thermal insulating properties. The rate of gas flow through closed cell foams tends to be relatively slow because the permeating gas must actually diffuse through the polymer membranes stretched across the struts. Gas flow through open celled foams on the other hand is relatively fast as the gas simply moves through the various pores of the structure established by the broken cell walls. The difference in the path of the gas flow caused by the structural differences is the predominant reason why closed-cell foams have better thermal insulating performance. (Benning, 1969)

Three other important characteristics of the foam morphology are the homogeneity of the cell size, the distribution of polymer within the foam, and the actual shape of the cells (Meineche and Clark, 1973). Foams with uniformly sized cells are considered homogeneous while those with cells that are not uniform are considered inhomogeneous. This can play an important role in some of the physical properties of the foam such as flexural or compressive strength and insulating performance. The distribution of the polymer within the foam between the cell membranes and struts can also have a dramatic influence on the compressive and flexural properties of the foam. This polymer distribution determines the actual thickness of each of the struts and membranes, which in turn, determines how the foam reacts to a given load. This distribution can be controlled in part by adding nucleating agents that control the number of cells and improve the homogeneity of the cell size distribution. Finally, while most nucleation models assume spherical symmetry of the cells or bubbles, the actual shape of the cells will influence the physical properties of the foam. Meineche and Clark contend that the extent to which each of these morphological influences actually affects the

performance of the foam is related, in part, to what type of strain (or load) is placed on the foam.

The density of the foam plays a significant role in its physical properties. Benning (1969) points out that foams are made up largely of air (or residual blowing agent) and the only physically tangible material is the polymer structure. The amount of polymer in a foam doubles for example, when the foam density is increased from 1 lb/ft^3 to 2 lb/ft^3. This has a very dramatic effect on physical properties such as flexural and compressive strength. The downside in this example above is that the material costs for the foam also doubles. Foams do have an excellent cost to weight performance ratio, however, and when these low-density foams (5 lb/ft^3) are compared to their high density (60 lb/ft^3) ridged polymer counterparts they usually are an excellent economic choice.

The cell gas can also play an important role in determining the performance of these foams. Certain cell gases (i.e. chloroflourocarbons or CFC) have better insulating properties as compared with others (e.g. air) while some have more pronounced effects on mechanical properties of the foam, especially if they act as plasticizers for the base polymer (e.g. pentane in polystyrene). In general, however, the cell gas only influences the properties of the foam during its formation and then for a "relatively" short time period thereafter. It has been shown that the cell gas eventually diffuses out of the foam and is replaced with air (Alsoy, 1999). This process may take up to a few years but in typical construction applications, the life of the foam is usually measured in decades.

An important factor influencing the physical properties of the foam is the type of polymer used to create it. Polymers are typically broken down into two classes, thermoplastics and thermosets. Thermoplastic materials (e.g. polystyrene) are

characterized as materials that exhibit a second order thermal phase transitions (i.e. a glass transition temperature, T_g) when heated (Rosen, 1993). This causes them to become soft and pliable, which then allows them to be easily molded or formed into different shapes. Thermoset materials (i.e. polyurethanes) are characterized as those materials that do not exhibit a second order thermal phase transition. These materials remain stable during heating and cannot be made to flow or melt; however, they will decompose (Billmeyer, 1984).

A further distinction that can be made with regard to the resin is the degree of crystallinity in thermoplastic polymer. Some polymers can exhibit a high degree of crystallinity like polyethylene or they can be completely amorphous like polystyrene. Highly crystalline polymers will exhibit a melting point transition in addition to the T_g transition (Brandrup and Immergut, 1989).

The actual formation of a polymeric foam occurs in three fundamental steps. The first step is to add the blowing agent (or a chemical precursor that will form a gas at an appropriate decomposition temperature) into the polymer matrix. This step also includes distributing the blowing agent throughout the polymer matrix homogeneously. The second step, which in part controls the morphology of the foam, is the nucleation step. The third and final step, which also contributes to the foam morphology, is the growth of the bubbles. After the foam is formed, it then needs to harden and stabilize.

The blowing agent is usually added into the polymer matrix by one of three methods. The first is to introduce a chemical blowing agent such as sodium bicarbonate (Han and Yoo, 1981), N,N'-dinitroso, N,N'-dimethyl terephthalamide (Fehn, 1967) or p,p'-oxybisbenzenesulfonyl hydrazide (Fehn, 1967) into the polymer matrix. Such

chemical blowing agents typically decompose at high temperatures (typical extrusion processing temperatures) to form gases that produce the bubbles. Alternatively, for thermosetting materials such as polyurethanes, the chemical blowing agent can be the reaction byproducts of the polymerization. In these types of foam systems, the resulting blowing agent is carbon dioxide, which is formed from the reaction of water with isocyanate. Auxiliary blowing agents such as CFCs and HCFCs for example can also be added to aid in the foaming process. The second method used to make foams is to melt a thermoplastic in an extrusion type operation (either an extrusion process or some other melt blending process) and inject a gas (a physical blowing agent) into the molten polymer matrix. Typically, the physical blowing agent is an inert material such as carbon dioxide or nitrogen. It can also be a volatile organic compound (VOC) such as a pentane or butane. This method is not suitable for thermoset materials. The third way polymeric foams can be produced is by supersaturating or impregnating a physical blowing agent into a polymer (not in the melt as stated above), usually at elevated pressures. The foam is created in a subsequent step by heating the polymer to releasing the blowing agent. The impregnation can be done to finished polymers or it can be done during the polymerization. This method is typically not used with thermoset materials, however, additional blowing agent could theoretically be injected directly into the mold cavity during the thermoset polymerization reaction.

The nucleation step can be envisioned as the agglomeration of the blowing agent molecules into critically sized clusters that ultimately grow into bubbles. The agglomeration of blowing agent molecules is driven by the local density fluctuations that

are present in the system. These fluctuations, which are present in any system, can be considered similar to the fluctuations that govern typical diffusion based processes.

The final step in the process is the growth of the bubbles. This phase of the foam formation process is governed by the sophisticated rheology of polymeric systems. Numerous complex mathematical models (to be touched on briefly in Chapter 3) have been developed to predict this bubble growth phenomena.

1.2 Objective

There still exists a significant lack of understanding regarding how polymeric foams are produced even though these foams have been made commercially for over half a century. As discussed earlier, one of the important properties of a thermoplastic foam is its foam morphology, and an important step in controlling the foam morphology is the nucleation step. The current nucleation models are based on empirical parameters that significantly restrict the range of applicability of the current theory, especially for polymeric systems. If any part of the foam system (polymer or blowing agent) is altered or if the processing conditions are varied sufficiently, then the empirical model becomes essentially useless. This results in an inability to understand and predict the nucleation process and subsequently other polymeric foam properties.

It is the aim of this work to develop an improved theoretical model to better predict the steady state nucleation rate in thermoplastic foams. This will be accomplished in two steps. The first will be to develop a model for the cluster distribution function in a polymeric system. The second is to incorporate this cluster distribution function into a diffusion –based nucleation model. The intent is to focus on homogeneous systems and

develop a theory that stands on its own merits from first principles without the use of empirical parameters.

The focus on homogeneous systems is to allow for a better evaluation of how the model fits experimental data. Unfortunately, in polymeric systems, it is very difficult to find such homogeneous systems. Another goal of this work then is to identify a suitable homogeneous system, preferably already in the existing body of knowledge to evaluate the effectiveness of the model. Although both, heterogeneous and mixed mode nucleation remain as topics outside the scope of this work, it is the author's intention that the homogeneous model developed here from first principles will also extend readily to these other types of nucleation.

1.3 Summary of Contents: A Reader's Guide

The purpose of this work is to investigate homogeneous nucleation models in thermoplastic foams. Before this topic can be adequately discussed, however, an understanding of the basic theories behind nucleation is required. As such, Chapter 2 is a comprehensive review of general nucleation theory as it applies to any system. The first section of this chapter, 2.1 discusses the thermodynamic definition of "Stability" and what is required for a system to phase split. The phase split, which is the formation of the new phase, starts with nucleation. The next two sections (2.2 and 2.3) cover classical homogeneous and heterogeneous nucleation theories respectively. Section 2.4 describes a model that is, in part, based on diffusion. This section will be used as the foundation for part of the work in Chapter 4. Section 2.5 takes a detailed look at nucleation from a statistical mechanical viewpoint and describes how the molecular partition function for a

single pure component system can be developed. This section will be used as one of the key building blocks for the work that is discussed in Chapter 5. The last section in the chapter covers application of alternative theories such as "Density Functional Theory". Readers not interested in a detailed review of nucleation or those already familiar with the topic can skip to Chapter 3 where the application of nucleation theory to thermoplastic foams is discussed.

Chapter 3 is divided up into four sections. The first section is a brief review of bubble growth models. These models were first used in early attempts to describe nucleation in viscous fluids. Section 3.2 describes, in detail, the work that has been done to modify the classical nucleation equations developed in Chapter 2 so they can be used for homogeneous and heterogeneous polymeric systems. Section 3.3 describes alternative models that have been developed. In general, these models are only applicable to heterogeneous systems. This review is also quite detailed. Finally, the last section (3.4) of Chapter 3 briefly summarizes the works reviewed in Sections 3.2 and 3.3 and then discusses the motivation behind the need for a new nucleation model for thermoplastic foams. Readers interested in a brief literature review of the pertinent topics are encouraged to start with section 3.4. They can then refer back to the other sections in Chapter 3 if they are interested in a more detailed examination of the topics.

Chapter 4 is broken down into two basic sections. The first section, 4.1, develops a diffusion-based nucleation model for thermoplastics. The second section, 4.2 will discuss the two key alternative approaches, "Fluctuation Theory" and "A Lattice Model" that were examined. These two sections are then further broken down into the theoretical development followed by a discussion of the results that were obtained.

Chapter 5 develops a multi-component molecular partition function (MPF) for a thermoplastic system that contains a blowing agent in Section 5.1 and then uses that MPF to develop a nucleation rate equation in Section 5.2. The development of the MPF in Section 5.1 is broken into three topics, each covered in its own sub-section. The first section, 5.1.1 defines the molecular cluster. This definition is important to the success of the MPF approach. The second section (5.1.2) actually develops the MPF and the third section (5.1.3) identifies the most probable or equilibrium distribution for the MPF. In the first sub-section of Section 5.2, the MPF is combined with the diffusions model developed in Chapter 4. This forms the final homogeneous nucleation rate equation. The last sub-section of this chapter, 5.2.2 discusses the results that were obtained with this new model. In closing, Chapter 6 summarizes the contributions of this work and Chapter 7 suggests areas for future investigation.

CHAPTER 2

CLASSICAL NUCLEATION THEORY

A variety of different nucleation phenomena exist. The formation of liquid droplets or aerosols from supersaturated vapors (Feder et al., 1966), crystals from supersaturated solutions (Lydersen, 1983), and bubbles from supersaturated liquids (Blander and Katz, 1975) are just a few common types that can be found in the literature. In all cases, the phenomenon describes the formation of a new more stable second phase from an original phase which is metastable. The formation of this second phase occurs spontaneously after the metastable phase has been sufficiently perturbed to cause a phase split.

Classical nucleation theory (CNT) historically has been used to describe the rate of formation of this new more stable second phase (Becker, R. and Döring, 1935; Farkas, 1927; Feder, et al. 1966; Volmer, 1929 and 1939; Zeldovich, 1942). CNT can be broken down into three types: homogeneous, heterogeneous, and a combination of the two which has been referred to as mixed mode. These designations generally refer to the state of the original metastable phase. Homogeneous nucleation occurs when the metastable phase is a single phase, usually either liquid or vapor. The single phase can be a pure component or it can be comprised of multiple components that are completely miscible. Heterogeneous nucleation occurs when the metastable phase exists in the presence of another phase. The presence of a second phase is usually the result of an immiscible impurity. This impurity is thought to reduce the energy barrier for nucleation and the formation of the new stable phase is believed to develop at the interface between the two phases (Colton and Suh, 1987). Mixed mode nucleation is a combination of both types of nucleation occurring simultaneously.

For polymer systems, homogeneous nucleation generally refers to a system that contains a pure homopolymer and a dissolved blowing agent. The system will not contain immiscible impurities and the blowing agent is present in concentrations where it is also completely miscible. Heterogeneous systems are those that are made up of polymers with immiscible impurities or copolymers. The impurities are often added deliberately as nucleating agents or are present in the polymer for other purposes (i.e. mold releases, coloring agents, flame retardant agents, etc.). The polymers in these heterogeneous systems may be homopolymers or they may be copolymers. Generally, any commercially available polymer, even a homopolymer will contain sufficient levels of impurities to make it a heterogeneous system.

2.1 Stability

A phase exists in either a stable or metastable state. Stable phases are those which exist at or above the equilibrium curve in a typical P-V diagram otherwise known as the binodal curve (Tester, 1996). Metastable phases exist between the binodal and spinodal curves. The spinodal curve is the lower boundary of a metastable phase and phases below the spinodal curve are unstable (Tester, 1996). A typical P-V diagram illustrating these curves is shown in Figure 2.1. A spinodal or binodal point is simply a particular point on either curve, respectively at a given pressure and temperature. Nucleation is the phenomenon of a metastable phase being subjected to a suitable perturbation resulting in a phase split (La Mer, 1952; Blander and Katz, 1975). The size of the perturbation required to move the meta-phase to an unstable condition depends on how close the phase is to the spinodal curve.

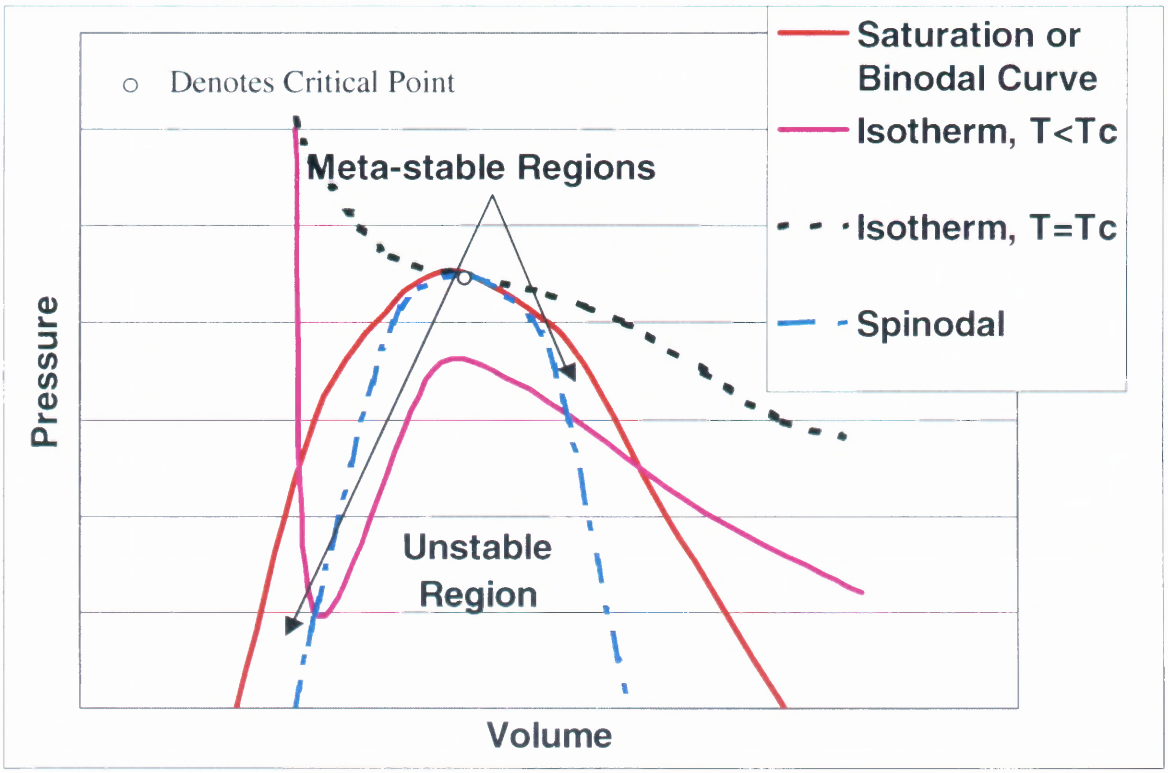

Figure 2.1 P-V Diagram Showing Two Different Isotherms, the Binodal or Saturation Curve and the Spinodal Curve. The term T_c in the figure refers to the critical temperature.

Phases far removed from the spinodal curve (close to the binodal curve) require fairly large perturbations to move to the unstable region and phase split. This phenomenon is what gives rise to the notion of superheat in boiling liquids (Blander and Katz, 1975). A metastable phase closer to the spinodal curve requires a smaller perturbation to move to the unstable region while a metastable phase on the spinodal curve only requires an infinitesimally small perturbation to move into the unstable region.

Illustrations of each of the different phases can be given using the example of a solute dissolved in a solvent. A stable phase is obtained when a solute is dissolved in the solvent at a given pressure and temperature at or below its solubility limit, otherwise known as the binodal point. The phase becomes metastable when the solute

concentration is increased above the solubility limit but below the spinodal point creating a supersaturated solution. The unstable phase occurs when the system is at the spinodal point and the addition of an infinitesimally small amount of the solute or other perturbation causes spontaneous precipitation.

A simple way to visualize the difference between these phases is through an analogy of a brick with one of its corners cut off (La Mer, 1952). This brick is depicted in Figure 2.2. The first illustration represents the brick as a stable system and requires a significant perturbation to change position. The second position depicts the brick, balanced precariously on its corner as a system at the spinodal limit. This is essentially an unstable system. It will fall to a more stable position with only an infinitesimally small perturbation. The brick in the third position is also stable, and is actually in a more stable position than the first brick. This third brick when compared to the first brick is symbolic of a system further from the binodal curve. Finally, the brick resting on the cut

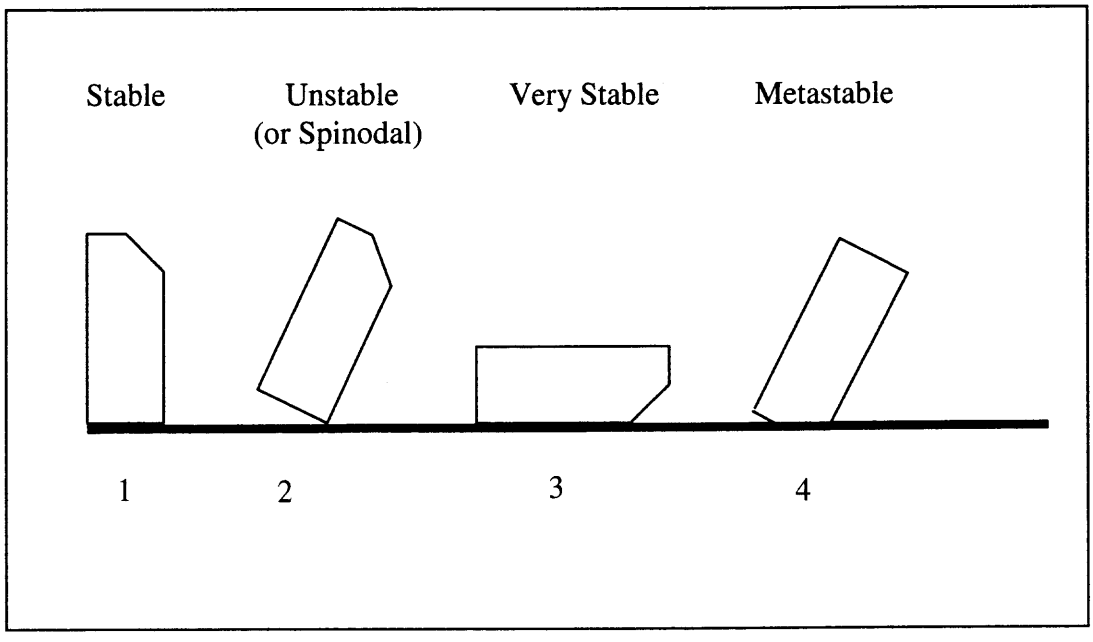

Figure 2.2 La Mer's (1952) Brick Analogy for Stability.

corner, represents a metastable system. Unlike the unstable brick, this brick can withstand certain small perturbations without changing position. It is not stable enough, however, to sustain most of the perturbations the bricks (1 and 3) in the other two more stable positions can withstand and relatively small perturbations will cause this brick to fall to a more stable position.

2.2 Development of the Classical Homogeneous Nucleation Equation

This section will focus on the development of Classical Nucleation Theory for the formation of liquid droplets from a condensing vapor as this is where most of the literature surrounding this topic is concentrated. In order for a first order phase transition like nucleation to occur, a certain activation or free energy barrier needs to be overcome. The driving force behind this event is the Gibbs free energy for the formation of a cluster. The term cluster is introduced here and defined as a collection of molecules in a specified volume that will form the new more stable second phase. The clusters can be described as the precursors to liquid droplets that result from the nucleation process of a condensing supersaturated vapor. In classical nucleation theory, this free energy is calculated by assuming that the microscopic cluster has the same properties (i.e. surface tension, density, etc.) as a bulk phase of the molecules in the same physical state. For example, the cluster molecules of a condensing vapor have the same properties as the bulk liquid. Traditionally, this is known as the capillary approximation (Laaksonen, Talanquer, and Oxtoby, 1995).

A system of two (or more) partially miscible materials will phase split, if by doing so, the system can obtain a lower Gibbs energy (Prausnitz, et al., 1986). The most

general form of the Gibbs free energy for the creation of a new phase is given by (Bromberg, 1980; Prausnitz, et al. 1986):

$$dG = -SdT + VdP + \sum \mu_i dx_i + Ad\gamma \tag{2.2.1}$$

where G is the Gibbs free energy of formation of the new phase, S is the entropy, T is the temperature, V is the volume of the new phase, P is the pressure, μ_i is the chemical potential of the i^{th} species, x_i is the moles of species i, A is the surface area of the new phase, and γ is surface tension. Generally speaking, $d\gamma$, which is γ_{final}-$\gamma_{initial}$, is taken to be the value of the surface tension between the original metastable phase and the newly created phase (final condition) which will be denoted simply as γ. For closed isothermal systems in chemical equilibrium, Equation 2.2.1 reduces to:

$$\Delta G = V\Delta P + \gamma A \tag{2.2.2}$$

If spherical symmetry is assumed for the clusters, then Equation 2.2.2 becomes

$$\Delta G = \frac{4\pi r^3}{3}\Delta P + 4\pi r^2 \gamma \tag{2.2.3}$$

where r is the radius of the individual cluster being evaluated.

Equation 2.2.3, which is a fundamental result in CNT, can be used to calculate ΔG as a function of cluster size. Clusters are present in varying sizes throughout the metastable phase prior to and during the nucleation process. When the change in Gibbs energy calculated from Equation 2.2.3 is plotted vs. the cluster size, one obtains a curve similar to the one in Figure 2.3 which is for a PMMA/CO_2 (PMMA is poly methyl methacrylate) system (data used to develop Figure 2.3 from Goel and Beckman, 1994). This curve shows that a maximum value of ΔG is obtained at a critical radius, $r = r_c$, of

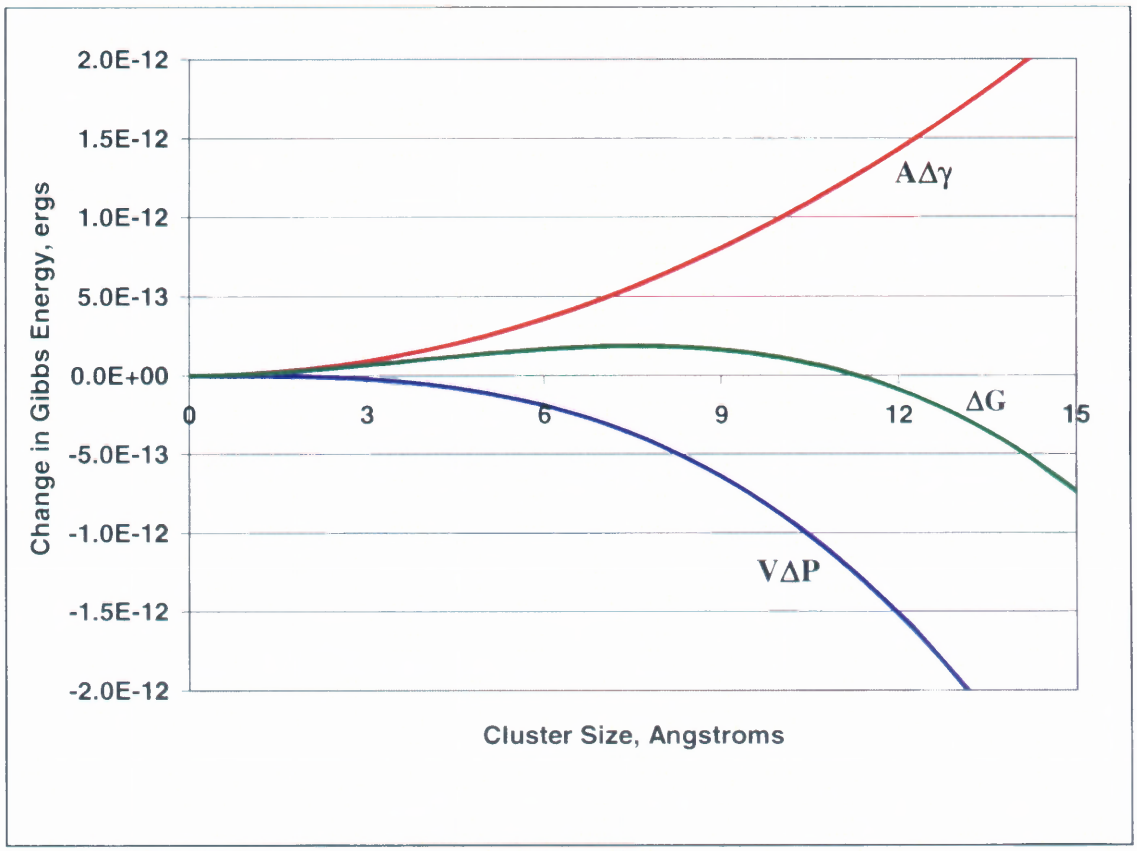

Figure 2.3 ΔG vs. Cluster Size (radius) for PMMA/CO_2 System @ 313 K and 21 MPa.

the cluster. This value of r (which provides the maximum) is easily obtained by differentiating Equation 2.2.3 with respect to r, the radius of the cluster, then setting the result equal to zero, and solving for r. The result is:

$$\frac{d\Delta G}{dr} = 0 \rightarrow r_c = \frac{2\gamma}{(P_G - P_B)} \tag{2.2.4}$$

This is the well-known Laplace-Kelvin equation (Blander and Katz, 1975) where P_B is the pressure in the bulk phase and P_G is the pressure inside the cluster of gas molecules. As it is the tendency of any system to minimize ΔG for a given temperature and pressure, one can see from Figure 2.3 that clusters that are formed with a radius smaller than r_c

(about 8 Angstroms in Figure 2.3) will minimize this energy by following a path that is equivalent to moving to the left on this curve. Physically, these clusters are re-absorbed into the bulk metastable phase and the blowing agent molecules become free to join other clusters. Clusters that have a radius greater than r_c are considered to have already nucleated into bubbles and are undergoing bubble growth. These bubbles minimize the excess energy as they grow by following a path to the right in Figure 2.3. This is a result of the negative $V\Delta P$ term being larger than the positive γA term past r_c. The $V\Delta P$ term is negative because the final pressure is lower than the initial pressure for the PMMA/CO_2 system resulting in a negative quantity. Once bubble growth has begun, the bubbles will not be re-absorbed and will only shrink if they undergo bubble collapse. In CNT, clusters with a radius equal to r_c are considered metastable and will either nucleate into bubbles or become re-absorbed based on the local fluctuations of the blowing agent molecules.

The expression for ΔG in Equation 2.2.3 may also be expressed in terms of the number of molecules that each cluster contains by using the ideal gas law. A short derivation yields:

$$\Delta G = -nkT + (4\pi)^{1/3}\left(\frac{3kT}{P_B}\right)^{2/3}\gamma n^{2/3} \tag{2.2.5}$$

In Equation 2.2.5, ΔP is often substituted for P_B for convenience. This result is substituted into r in the second term of Equation 2.2.3. In this case, the excess energy is maximized with respect to n, the number of molecules in the cluster and the following equation for n_c results:

$$\frac{d\Delta G}{dn} = 0 \rightarrow n_c = \frac{32\pi\gamma^3}{3kTP_B^{\,2}} \tag{2.2.6}$$

The values of ΔG can be plotted against the number of molecules in the cluster (Figure 2.4). The critical value of n, n_c, occurs at the maximum value of ΔG as did the critical value of r, r_c in Figure 2.3. Note that the curves in Figure 2.3 and 2.4 have different scales for the change in Gibbs free energy. The scale used in Figure 2.3 was chosen to clearly show the contributions of the individual VΔP and γA terms as well as their sum. The scale used in Figure 2.3 was chosen to easily identify the maximum. The maximum value of ΔG is the same in both figures, however.

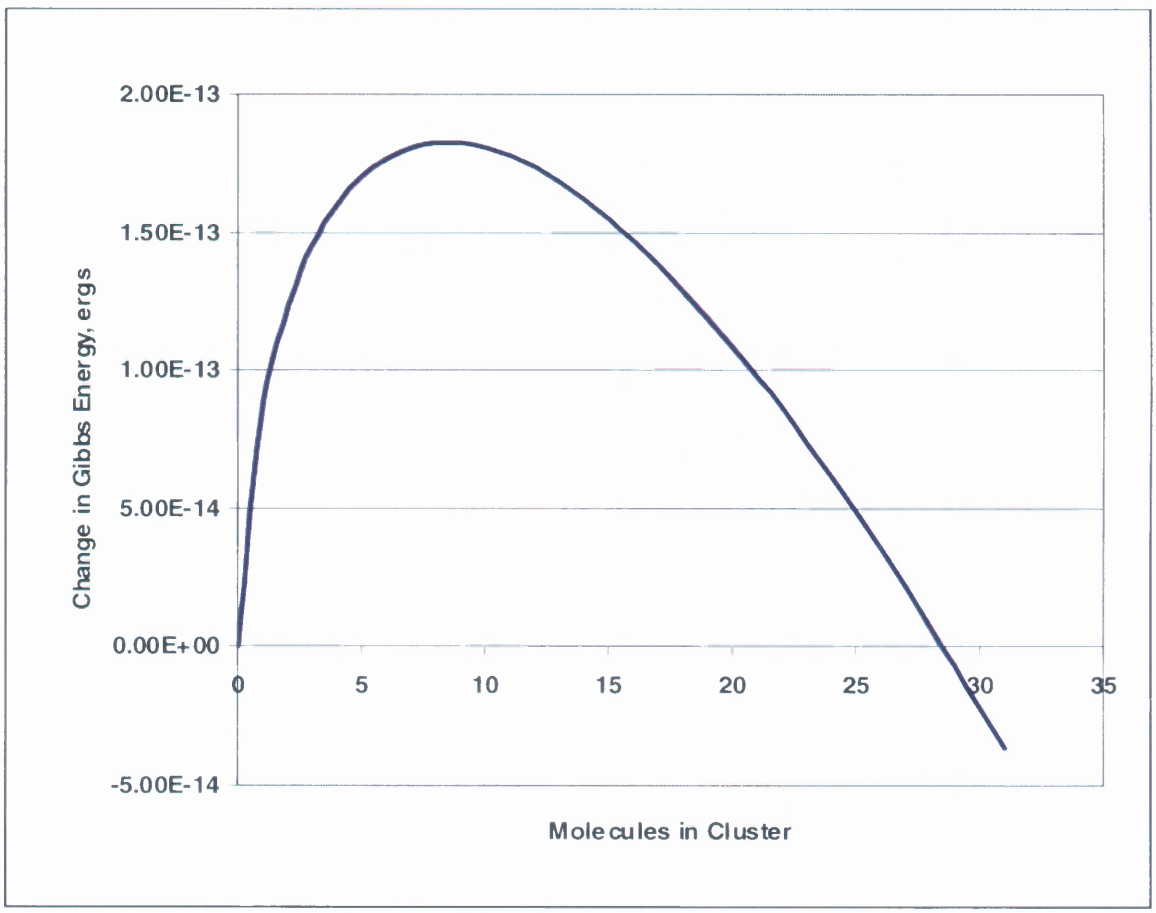

Figure 2.4 ΔG vs. Number of Molecules in the Cluster for PMMA/CO_2 System @ 313 K.

The maximum value of ΔG is obtained by substituting the value of r_c into Equation 2.2.3 or n_c into Equation 2.2.5. Both equations obtain the same result:

$$\Delta G_m = \frac{16\pi\gamma^3}{3(\Delta P)^2} \tag{2.2.7}$$

This value, ΔG_m, (subscript m indicates a maximum value) can be looked at as the energy barrier for the nucleation process for CNT (Blander and Katz, 1975; Frenkel, 1955; Feder, et al., 1966; McDonald, 1962; Reiss and Katz, 1967). Clusters need to obtain this level of energy to be able to move to the right of the maximum in Figure 2.3 (or Figure 2.4), otherwise, they will be reabsorbed. Clusters obtain or lose energy through the addition or loss of individual molecules. Hence, a cluster of critical size r_c or n_c will move forward in the process if a molecule of sufficient energy adds to the cluster before a molecule with equal or greater energy already contained in the cluster leaves it. It is this net rate of addition of the molecules to the critical clusters that determines the nucleation rate. This process for accounting for the addition and subtraction of molecules to a cluster is often referred to as a "detailed balance" in the literature (Becker and Döring, 1935; Zeldovich, 1942; Feder, et al. 1966, Monette, 1994; Slezov, et al. 1996). Each author has a slightly different approach to the derivation of the CNT, but in general, all ultimately arrive at a form of the Fokker-Planck equation:

$$\frac{\partial f(n,t)}{\partial n} = \frac{\partial}{\partial n}\left\{\psi\left[\frac{\partial f(n,t)}{\partial n} + \frac{f(n,t)}{kT}\frac{\partial \Delta G(n)}{\partial n}\right]\right\} \tag{2.2.8}$$

In Equation 2.2.8, f(n,t) is the distribution of n sized clusters (n is the number of molecules in a cluster) as a function of time, ψ is a coefficient that, in part, accounts for the net impingement rate of molecules on the clusters commonly referred to as a frequency factor in the literature, and k is the Boltzmann constant. The Fokker-Planck

Equation is the result of estimating a finite difference equation with a differential equation that is obtained after the difference equation is expanded in a Taylor series (McQuarrie, 1976). In CNT, the difference equation is obtained from the concept of the detailed balance.

The detailed balance starts with the premise that the rate of change of the cluster distribution function, f(n,t) is only related to the rate at which molecules either leave or add to clusters (Becker and Döring, 1935; Zeldovich, 1942; Feder, et al. 1966, Monette, 1994). This process is due to the "evaporation" and "condensation" of molecules and can be viewed mathematically as (Feder, et al., 1966):

$$\frac{\partial f(n,t)}{\partial t} = -f(n,t)[\beta_0 A(n) + \varepsilon_0(n)A(n)] + f(n-1,t)\beta_0 A(n-1) + f(n+1,t)\varepsilon_0(n+1)A(n+1) \tag{2.2.9}$$

where β_0 is a condensation rate and ε_0 is an evaporation rate for the molecules joining and leaving the clusters from the bulk vapor phase. N is the total number of molecules in the system and A is the surface area of a cluster, which is a function of n, the number of molecules in the cluster. In Equation 2.2.9, the first term accounts for the number of clusters of size n that lose or gain a molecule, the second term accounts for clusters of size n-1 that become clusters of size n by the addition of a molecule and the last term accounts for clusters of size n+1 that become size n through the loss of a molecule. At steady state f(n,t) is replaced with f(n,0) and the evaporation frequency is given by:

$$f(n,0)\beta_0 A(n) = f(n,0)(n+1)\varepsilon_0(n+1)A(n+1) \tag{2.2.10}$$

where the (n) refers to clusters of size n and (n+1) refers to clusters of size n + 1. This can be substituted into Equation 2.2.9 yielding the following difference equation:

$$\frac{\partial f(n,t)}{\partial t} = \beta_0 A(n) f(n,0)\left\{\frac{f(n,t)(n+1)}{f(n,0)(n+1)} - \frac{f(n,t)(n)}{f(n,0)(n)}\right\} - \beta_0 A(n-1) f(n,0)(n-1)\left\{\frac{f(n,t)(n)}{f(n,0)(n)} - \frac{f(n,t)(n-1)}{f(n,0)(n-1)}\right\} \tag{2.2.11}$$

This difference equation is expanded in a Taylor series to obtain the Fokker-Planck Equation (2.2.8). One can now see that ψ, the coefficient used for the net impingement rate in Equation 2.2.8 is a combination of the evaporation rate, ε_0 and the condensation rate, β_0 found in Equations 2.2.9-2.2.11.

At this point, Frenkel, (1955); Feder, et al., (1966); Zeldovich, (1942); Blander and Katz, (1975) along with most other authors assume that the equilibrium cluster distribution follows a Boltzmann-like distribution:

$$f_n = N_G \exp\left(-\frac{\Delta G(n)}{kT}\right) \tag{2.2.12}$$

where N_G is defined as the number density or concentration (in molecules/cm^3) of molecules initially present. It should be pointed out that the cluster distribution, f_n in Equation 2.2.12 is not a function of time because at equilibrium, the net number of clusters of a given size, n, is not changing.

The coefficient, ψ, in Equation 2.2.8 was defined by Feder, et al., 1966 and Wilt, 1986 as:

$$\psi = \beta A \tag{2.2.13}$$

As before, A is the surface area of the cluster and β is derived from the kinetic theory of gases. It is defined as (McDonald, 1962; Bromberg, 1980):

$$\beta = \frac{P}{(2\pi mkT)^{1/2}} \tag{2.2.14}$$

where m is the mass of a molecule.

Using Equations 12 and 14, the following integral equation for the steady state nucleation rate, J, is obtained from Equation 2.2.8 (Zeldovich, 1942; Frenkel, 1955; Feder, et al., 1966; Blander and Katz, 1975; Wilt, 1986):

$$J = \frac{\beta}{\int \frac{dn}{AN_G \exp-\left(\frac{\Delta G(n)}{kT}\right)}} \tag{2.2.15}$$

To complete the integration, the change in Gibbs energy is expanded in a Taylor series about n_c and then truncated after two terms resulting in a quadratic approximation for ΔG:

$$\Delta G \approx \frac{16\pi\gamma^3}{3\Delta P^2} - \frac{(kT\Delta P)^2}{64\pi\gamma^3}(n-n_c)^2 \tag{2.2.16}$$

Before continuing with the derivation, a comment regarding the use of a truncated Taylor series expansion about $(r - r_c)$ to approximate ΔG is appropriate. The use of this quadratic estimation is adequate because the largest contributions from the integral used to estimate ΔG occur at radii very near the critical radius. The contributions to ΔG from higher order terms in this expansion contribute negligibly as the radii depart further and farther from r_c (Cohen, 1970; Blander and Katz, 1975). After substituting Equation 2.2.16 into 2.2.15 and extending the limits of integration from 0 to ∞, the following result is obtained for the steady state nucleation rate:

$$J = \frac{(kT)^{1/2}\Delta PA\beta N_G}{8\pi\gamma^{3/2}}\exp(-\Delta G/kT) \tag{2.2.17}$$

In Equation 2.2.15, the limits of integration were extended essentially by the same argument that allowed a quadratic approximation for ΔG to be used. The majority of the contributions to the integral occur at or near $n = n_c$. Hence, extending the limits of integration for mathematical formality does not introduce a significant error.

When comparing Equation 2.2.17 to the nucleation equations found in the literature (Frenkel, 1955; Feder, et al., 1966; Blander and Katz, 1975), it is obvious that all of the equations have the same form:

$$J = ZA\beta N_G \exp(-\Delta G/kT) \tag{2.2.18}$$

The term Z, known as the Zeldovich factor, in Equation 2.2.18 is defined as (White, 1969, Wegener, 1987; Shafi and Flumerfelt, 1996, 1997):

$$Z = \left[\frac{1}{2\pi kT}\frac{d^2\Delta G(n)}{dn^2}\right]^{1/2} = \frac{(kT)^{1/2}\Delta P}{8\pi\gamma^{3/2}} \tag{2.2.19}$$

The Zeldovich factor accounts for the differences between the number of n sized clusters that exist in the metastable phase at equilibrium and the number of these clusters that exist during steady state nucleation (Shafi and Flumerfelt, 1996). It is clear that Equations 2.2.17 and 2.2.18 are the same once Equation 2.2.19 is substituted for Z in Equation 2.2.18.

Finally, after some algebraic manipulation, it can be shown that when Equations 2.2.4, 2.2.14, and 2.2.19 are substituted into Equation 2.2.18, the result is the classical homogeneous nucleation equation in its most familiar Arrhenius form:

$$J = N_G\left(\frac{2\gamma}{\pi m}\right)^{1/2}\exp\left(-\frac{\Delta G}{kT}\right) \tag{2.2.20}$$

The term $N_G(2\gamma/\pi m)^{1/2}$ in Equation 2.2.20 is often represented as a single pre-exponential term in many published works.

2.3 Development of the Classical Heterogeneous Nucleation Equation

In heterogeneous nucleation, like in homogeneous nucleation, the formation of gas bubbles in a liquid (or liquid drops in a condensing vapor) as a more stable second phase is associated with a change in the Gibbs free energy. The difference is that the Gibbs energy is defined differently because of the presence of the additional interface between the miscible phase and the immiscible impurity. The derivation of the heterogeneous nucleation equation, however, is exactly the same as that for the homogeneous equation, therefore, only the relevant equations that differ between the two derivations are summarized here.

Using the concept of bubbles forming in a liquid, Blander and Katz (1975) define the Gibbs energy for heterogeneous nucleation as:

$$\Delta G = \gamma_{g,l} A_{g,l} + (\gamma_{g,s} - \gamma_{s,l}) A_{g,s} + V\Delta P \tag{2.3.1}$$

In Equation 2.3.1, $\gamma_{g,l}$ is the surface tension between the bubble and the bulk liquid phase, $A_{g,l}$ is the surface area of the corresponding surface, $\gamma_{g,s}$ is the surface tension between the bubble and the solid impurity, $\gamma_{s,l}$ is the surface tension between the solid impurity and the bulk liquid phase, and $A_{g,s}$ is the area of the interfacial surface formed between the bubble and the solid impurity. Blander and Katz (1975) and Colton and Suh (1987) evaluate the volume and surface area associated with this new interface through geometric arguments. In order to do this, a force balance on the bubble is performed by using the different surface tensions in the system:

$$\gamma_{s,l} = \gamma_{g,s} + \gamma_{g,l}\cos(\pi - \theta) \tag{2.3.2}$$

where θ is the wetting angle between the insoluble impurity and the bulk metastable phase. The wetting angle is the angle formed between the two immiscible phases, see Figure 2.5.

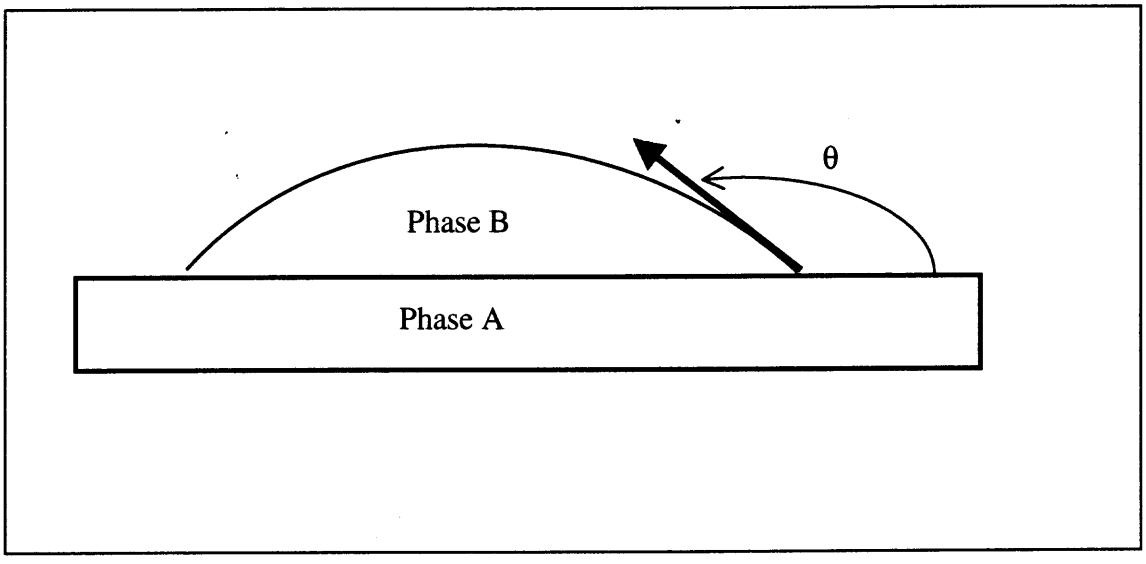

Figure 2.5 Representation of the Wetting Angle Between a Solid (Phase A) and a Liquid (Phase B). The solid that denotes Phase A can be any insoluble impurity in the system.

Once the necessary area and volume are known, the same procedure used in the homogeneous case is followed; the derivative of ΔG with respect to r (or n) is taken, it is set equal to zero, solved for r_c (or n_c), and then the maximum value of ΔG is found. This led Blander and Katz (1975) to:

$$\Delta G_m = \frac{16\pi\gamma^3 F}{3(P_G - P_B)^2} \tag{2.3.3}$$

where F is a function based on the wetting angle (Blander and Katz, 1975; Colton and Suh, 1987):

$$F = \frac{1}{4}\left(2 + 3\cos\theta - \cos^3\theta\right) \tag{2.3.4}$$

Blander and Katz also point out that the pre-exponential factor takes on a slightly different form in the heterogeneous case. This is because the nucleation rate should be proportional to a surface rather than a volume. This results in the number density, N_G, changing to $N_G^{2/3}$. The function based on the wetting angle also appears in the pre-exponential for the heterogeneous case as does the wetting angle itself. The new pre-exponential term is

$$= N_G^{\frac{2}{3}} \frac{1+\cos\theta}{2}\left(\frac{2\gamma}{\pi m F}\right)^{1/2} \tag{2.3.5}$$

This leads to the final form of the heterogeneous classical nucleation equation below.

$$J = N_G^{\frac{2}{3}} \frac{1+\cos\theta}{2}\left(\frac{2\gamma}{\pi m F}\right)^{1/2} \exp\frac{-16\pi\gamma^3 F}{3kT\left(P_G - P_B\right)^2} \tag{2.3.6}$$

2.4 A Nucleation Model Based on Diffusion

The governing equation for nucleation in the classical sense is comprised of two parts, an exponential term and a pre-exponential term. The exponential term accounts for the free energy required to form the new phase. The pre-exponential term describes the rate at which the new phase forms. This pre-exponential is usually comprised of a term that accounts for the concentration of molecules in the system, N, a surface area term for the critically sized clusters, A and a rate term, β; see Equation 2.2.18. Often, Z, the Zeldovich factor is also included (see Equation 2.2.19). In CNT, β, is always based on the molecular movement of gaseous molecules, most likely because almost all of the work done on nucleation during the early development of CNT was with condensing

supersaturated vapors. The formation of bubbles from supersaturated liquids has received far less attention in the literature.

From Bromberg (1980), β can derived from the number of molecules impinging on a surface A, in a given period of time, t, as follows:

$$\frac{dn}{dt} = \frac{1}{4}\frac{N}{V}\bar{c}A \tag{2.4.1}$$

where N is the number of molecules, V is the volume and $\bar{c}$ is the average speed of a molecule given as:

$$\bar{c} = \left(\frac{8kT}{\pi m}\right)^{1/2} \tag{2.4.2}$$

Inserting Equation 2.4.2 into 2.4.1 and utilizing the ideal gas law to replace N/V with P/kT leads to:

$$\frac{dn}{dt} = \frac{1}{4}\left(\frac{8kT}{\pi m}\right)^{1/2}\frac{P}{kT}A = \beta A \tag{2.4.3}$$

where

$$\beta = \frac{P}{(2\pi mkT)^{1/2}} \tag{2.4.4}$$

This simple derivation is based on the concept of an ideal gas. With this concept, there are two fundamental assumptions. The first is that the intermolecular potential energy between the gas molecules is assumed to be zero. The second is that the low density of the ideal gas provides sufficient separation between the molecules so that drag forces do not affect them. Drag forces result when the moving molecules have to squeeze through small openings created in between the other molecules in the system. These drag forces that occur in high-density systems like liquids are often combined with the intermolecular

potential but have been separated here to highlight the effect of density on the system. Based on these assumptions, the motion of the molecules is related only to their kinetic energy. Such a system of gas molecules can be visualized in Figure 2.6.

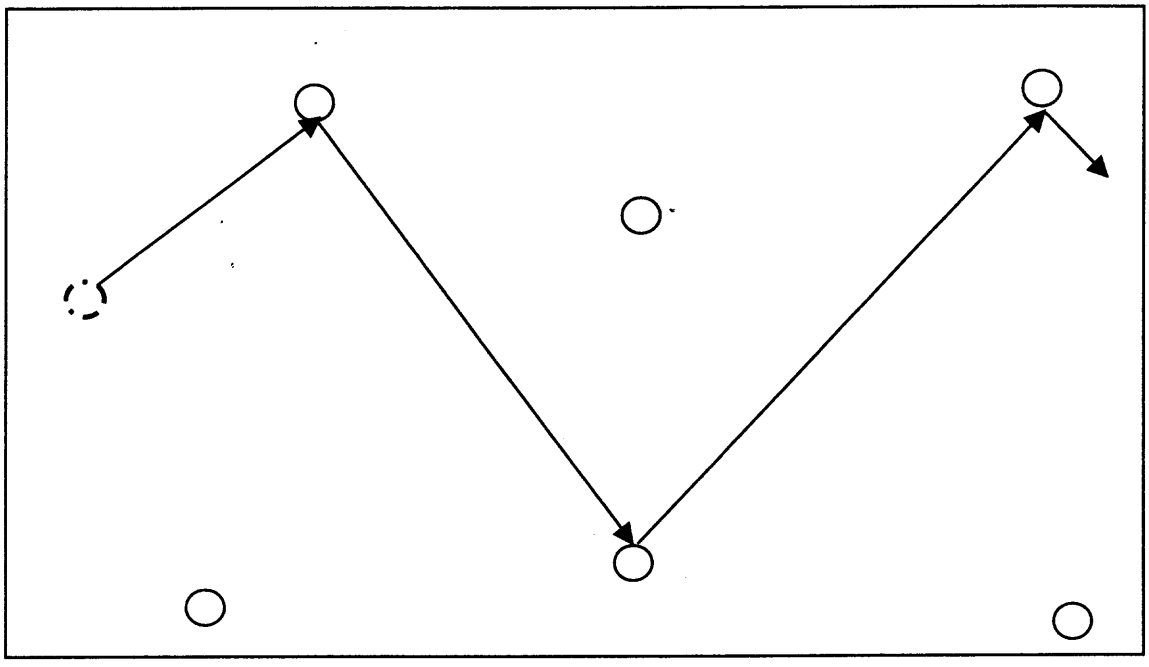

Figure 2.6 The Movement of a Molecule Through an Ideal Gas.

For gas bubbles forming in a liquid system (simple liquid or polymer melt), the assumptions related to an ideal gas are no longer valid. The movement of the molecules is affected by the intermolecular potential energy and by the drag forces due to the higher densities of the liquid. This higher density results in the molecules being more tightly packed, see Figure 2.7. In Figure 2.7, the drag forces are highlighted in the circled areas of the figure. Thus, the notion of accurately modeling these molecular movements with β is unrealistic. It is well know that vapor phase diffusion coefficients can be up to 5 orders of magnitude larger than their liquid counterparts (Lydersen, 1983; Reid, et al., 1987).

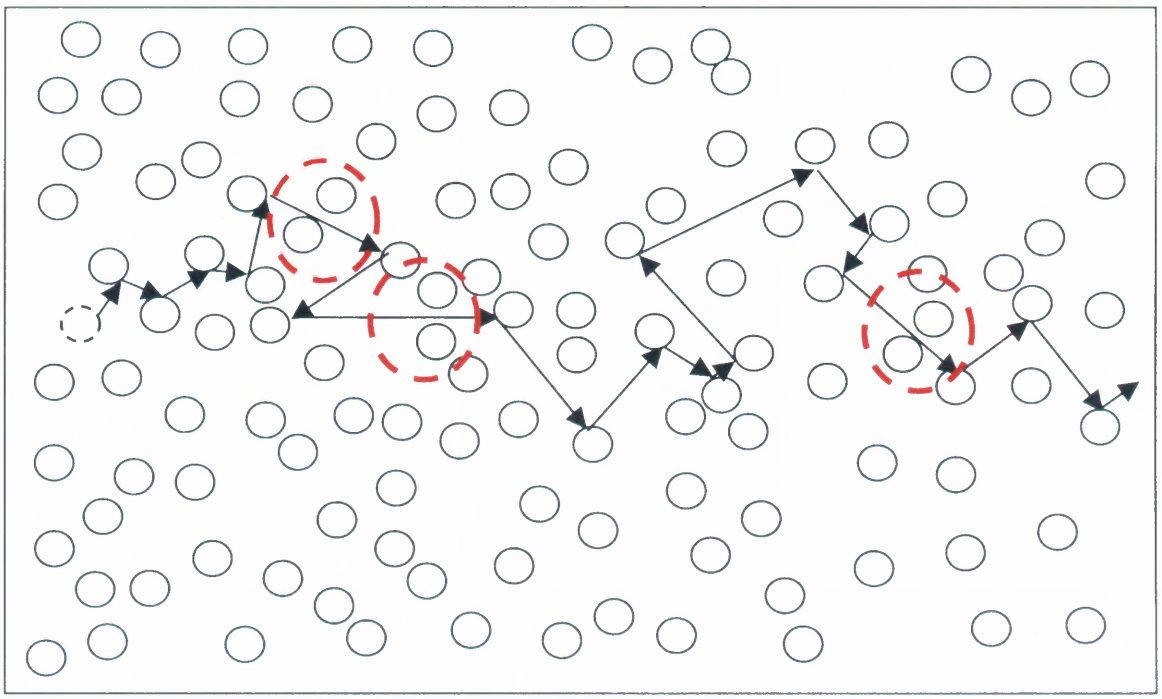

Figure 2.7 The Movement of a Molecule Through a Liquid Often Referred to as a "Random Walk". The red circled areas highlight the influence of "drag" on the molecules.

Finally, given the large difference between vapor and liquid diffusion rates, one would expect a significant over prediction for the nucleation rate of bubbles in a liquid system by the CNT model. This expected over prediction is exactly what is observed when the unmodified CNT is used to predict the nucleation rate of bubbles in a PMMA/CO_2 system, see Figure 2.8. Given the discrepancy between theoretical predictions and experimental results, a better model is needed to describe the motion of the molecules in a liquid system.

One such improved model is based on diffusion. In general, diffusion occurs through two basic mechanisms, the first is molecular and the second is convective. Convective diffusion, which results in systems undergoing a momentum change, is

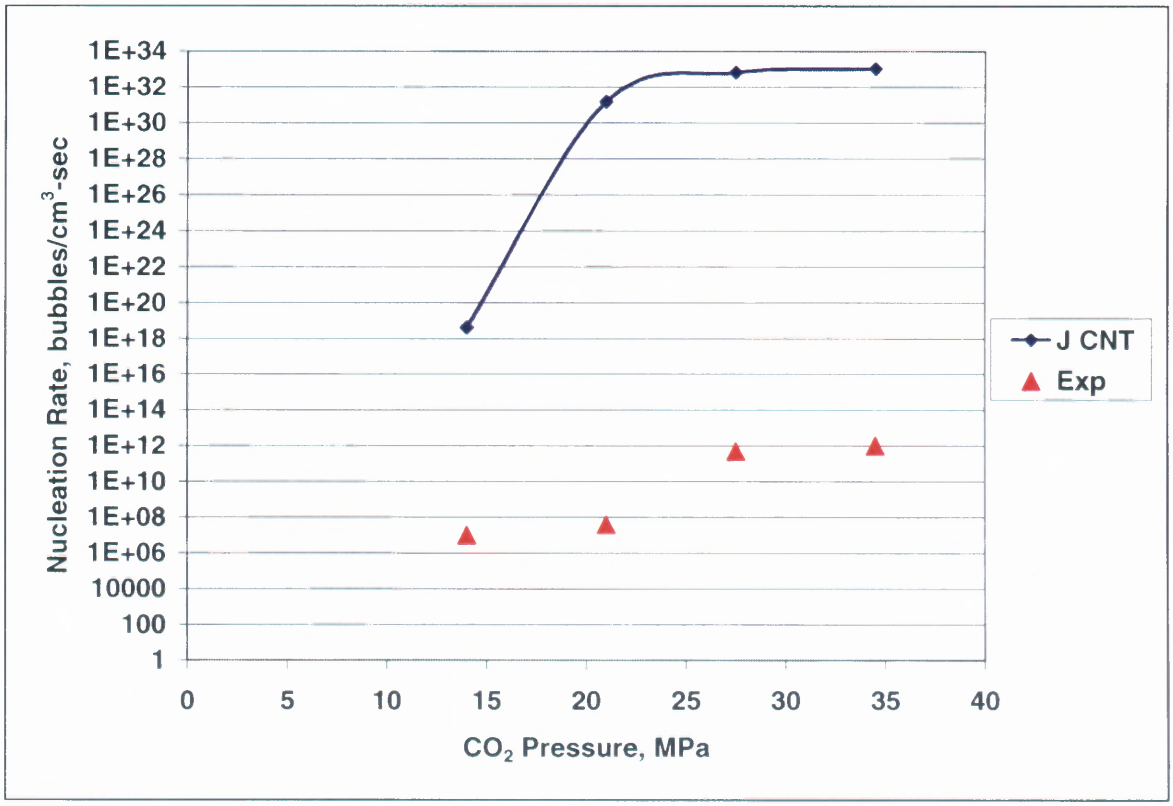

Figure 2.8 Nucleation Rate as a Function of Pressure in the PMMA/CO_2 System @ 313 as Predicted by CNT. Data from Goel and Beckman (1994).

generally of no concern in the study of nucleation. This is because most experiments are done on stagnant or non-flowing and non-agitated systems. Examples of such experiments are discussed in Laaksonen et al. (1995). This being the case, the focus here will be on molecular diffusion.

The molecular diffusion rate of a substance (call it A) through another substance (call it B) in either a vapor or a liquid is driven by a concentration gradient and can be described by Fick's Law (Bird, Stewart, and Lightfoot, 1960, Geankoplis, 1983; Lydersen, 1983) as:

$$J_{AB} = -\frac{N}{V} D_{AB} \frac{dy_A}{dz} \tag{2.4.5}$$

In Equation 2.4.5, N is the total moles in the system, V is the volume, y_A is the mole fraction of A in the system, z is a linear distance A has to travel, and D_{AB} is the diffuison coefficient. For systems of constant density, y_A can be replaced with the concentration, C, in the equation above giving:

$$J_{AB} = -D_{AB} \frac{dC}{dz} \tag{2.4.6}$$

In the case of nucleation experiments, however, there is generally no such concentration gradient to provide the driving force for diffusion. This is because these experiments are often carried out under constant conditions (i.e. volume and composition) and in many cases are comprised of only a single component undergoing a phase change, either condensation or evaporation (Laaksonen et al. 1995). When this is the case, where is the driving force for diffusion? The answer is found in looking at the system on a microscopic level.

Diffusion is often referred to as a random walk process because if one looks at the path of an individual molecule, it randomly moves through the system in short steps frequently changing direction based on collisions with other molecules, see Figure 2.6 (Geankoplis, 1983). This constant random motion is often referred to as Brownian motion and was first used to describe the random motion of microscopic pollen grains suspended in water by R. Brown (Bromberg, 1980).

From a statistical thermodynamic point of view, this behavior is described in fluctuation theory (Hill, 1986; McQuarrie, 1976). Fluctuation theory, which is based on statistics, states that there will be local or microscopic deviations from the macroscopic

average of a particular variable in a system. Fluctuations can be identified in almost any "mechanical" variable associated with a system. They cannot be identified for "non-mechanical" variables, however (Hill, 1986). The term mechanical is used here to describe a variable of the system that has a well-defined value in a given quantum state. Examples of such variables are energy, number of molecules, and volume. Examples of variables that are not "mechanical" are entropy and temperature as they are the average or cumulative property of many molecules. A detailed development of the statistically based equations for fluctuation theory can be reviewed in Appendix A.

These deviations or fluctuations are constantly changing because of the movement of the molecules. It is these fluctuations in the number of molecules in a given volume that provides the "energy" or gradient for the diffusion process to occur and this leads to nucleation (La Mer, 1952; Blander and Katz, 1975). To envision this diffusion process, one needs to think of a series of microscopic volume elements. Each of these elements can contain a number of molecules less than, equal to, or greater than the bulk average number of molecules in the system. If two adjacent volumes contain a number of molecules greater than and less than the average number of molecules respectively, then the necessary concentration gradient is established at the microscopic level and molecules will tend to move from the point of higher concentration to lower concentration. This allows the use of a diffusion coefficient to model the behavior. It seems obvious that one should use a liquid based diffusion coefficient when working with liquid systems.

While not part of their principle concern, Slezov, et al. (1996) did incorporate this type of a diffusional approach into their work. The intent of their work was to show that the number of clusters was independent of the kinetic limitations of the system and only

dependent on the thermodynamic parameters. The authors recognized that the growth of the newly forming phase is limited kinetically by the rate at which molecules can join the segregating phase and in a liquid, this limit is better described by diffusion. As such, the authors incorporate a diffusion coefficient into the nucleation model by defining a diffusion probability term:

$$\mathcal{P}_D = \frac{4\pi r^2 D_{AB} N_0}{\ell} \tag{2.4.7}$$

where N_0 is the concentration of molecules that will form the segregating or second stable phase once nucleation has occurred, and ℓ is an estimate of the linear size of those molecules or a characteristic length.

The authors further defined the volume of a molecule based on the characteristic length, ℓ, as:

$$v_m = \frac{4}{3}\pi \ell^3 \tag{2.4.8}$$

The number of molecules in a critical cluster, n_c, is obtained by taking the ratio of a critically sized cluster volume ($4\pi r_c^3/3$) relative to a molecule volume, v_m, which results in:

$$n_c = \left(\frac{r_c}{\ell}\right)^3 \tag{2.4.9}$$

Using the Fokker-Plank equation, Slezov et al. replaced the kinetic term, β, traditionally used in CNT with the probability term defined in Equation 2.4.7. While the mathematical development in all the classic references cited earlier is very similar, Slezov et al. (1996) provided additional detail not generally found in these other works on how to transform the Fokker-Plank equation into a nucleation rate equation. The

present author found these details helpful in understanding the development and as such, these insights are captured here.

Starting with the Fokker-Plank equation,

$$\frac{\partial f(n,t)}{\partial n} = \frac{\partial}{\partial n}\left\{\psi\left[\frac{\partial f(n,t)}{\partial n} + \frac{f(n,t)}{kT}\frac{\partial \Delta G(n)}{\partial n}\right]\right\} \tag{2.4.10}$$

changes in the cluster size distribution with time are related to the flux in the cluster space by:

$$\frac{\partial f(n,t)}{\partial t} = -\frac{\partial J(n,t)}{\partial n} \tag{2.4.11}$$

where J(n,t), the flux in the cluster size space, is given by:

$$J(n,t) = -\mathcal{P}_D\left[\frac{\partial f(n,t)}{\partial n} + \frac{f(n,t)}{kT}\frac{\partial \Delta G(n)}{\partial n}\right], n \le g \tag{2.4.12}$$

The term, g, in Equation 2.4.12 is somewhat of an arbitrary limit to cluster size and will be described later. At steady state, J(n,t) is not a function of time and further, if a Boltzmann-like distribution of clusters is presumed, then the distribution function takes on the same form as the cluster distribution function in the classical theory (see Equation 2.2.12):

$$f_n = \xi \exp\left(-\frac{\Delta G}{kT}\right) \tag{2.4.13}$$

The only difference is that the term ξ is yet to be defined in Equation 2.4.13. Differentiating Equation 2.4.13 and substituting it into Equation 2.4.12 results in the following equation for the steady state flux of clusters in the cluster size space:

$$J = -\mathcal{P}_D \frac{\partial \xi}{\partial n}\exp\left(-\frac{\Delta G(n)}{kT}\right) \tag{2.4.14}$$

At this point, Slezov et al. note that the value of ΔG(n) must be equal to zero if there are no clusters. Hence, in Equation 2.4.13, as the limit of no clusters is approached, the value of f_n is equal to ξ. This must then be equal to the initial concentration of blowing agent molecules in the system, C_0, if there are no clusters. Integrating Equation 2.4.14 with respect to n from zero to n clusters results in:

$$\xi = C_0 - J\int_0^n \frac{\exp\left(\frac{\Delta G}{kT}\right)}{\mathcal{P}_D} dn \tag{2.4.15}$$

Then, for the smallest value of n for which ξ is approximately equal to zero, this gives:

$$J = \frac{C_0 \mathcal{P}_D}{\int_0^g \exp\left(\frac{\Delta G}{kT}\right) dn} \tag{2.4.16}$$

This smallest value of n that allows ξ to approximate 0 is the upper size limit of a cluster, g, identified earlier in Equation 2.4.12. Equation 2.4.16 is of the same form as Equation 2.2.12 from the classical theory, however, β, which was based on the kinetic theory of gases, has now been replaced with $\mathcal{P}_D$, a diffusion based term. Integrating, as in Equation 2.2.15, after ΔG has been expanded in a Taylor series provides the final nucleation rate equation:

$$J = C_0 \mathcal{P}_D(n_c) Z \exp\left(-\frac{\Delta G}{kT}\right) \tag{2.4.17}$$

In comparing Equations 2.4.17 and 2.2.18, it is easy to see the similarities.

$$J = ZA\beta N_G \exp(-\Delta G/kT) \tag{2.2.18}$$

In fact, the only difference is the desired change to an equation based on diffusion. In Equation, 2.4.17, the area term, A, does not appear because it is incorporated into the diffusion probability, $\mathcal{P}_D$, refer to Equation 2.4.7.

2.5 Statistical Approach to Nucleation Focused on Droplet Formation from an Ideal Super-saturated Vapor

Contributors to the early development of CNT recognized the role of statistical mechanics in the development of the CNT, but the theory seems to be driven more by kinetic considerations (Becker and Döring, 1935; Farkas, 1927; Feder, et al. 1966; Volmer, 1929 and 1939; Zeldovich, 1942). Incorporation of a statistical approach can be seen in the literature, however, as early as in the 1960's (Lothe and Pound, 1962; Reiss and Katz, 1967; and Reiss, Katz, and Cohen, 1968). Work by Reiss and co-workers continued in a series of manuscripts in the early 1990's (Reiss, Tabazadeh, and Talbot, 1990; Ellerby, Weakliem, and Reiss, 1991; Ellerby and Reiss, 1992). All of these works focus on the condensation of a liquid from a supersaturated vapor and do not address the issue of a vapor bubble forming in a supersaturated liquid. They are important, however, in building a fundamental understanding of the nucleation process and how a metastable phase is transformed into more stable phases.

Reiss, Katz, and Cohen (1968), building on the work of Lothe and Pound (1962) attempted to rigorously develop a nucleation theory based on statistical principles. Their work started by defining a system of N monatomic molecules contained in a volume, V. The molecules are assumed to be in their lowest electronic and nuclear energy states. The intermolecular potential energy of these molecules is denoted as $U(\mathbf{r}_1 \ldots \mathbf{r}_n)$ which

depends on positions $\mathbf{r}_1 \ldots \mathbf{r}_n$. If the momentum of each molecule is denoted as $\mathbf{p}_i$, then the classical partition function, Q, for the ideal vapor can be written as:

$$Q = \frac{1}{N! h^{3N}} \int_{-\infty}^{\infty} \cdots \int \exp\left[\frac{1}{kT} \left(\sum_N \frac{\mathbf{p}_n^2}{2m} + U(\mathbf{r}_1 \cdots \mathbf{r}_N) \right) \right] d\mathbf{r}_1 \cdots d\mathbf{r}_N d\mathbf{p}_1 \cdots d\mathbf{p}_N \qquad (2.5.1)$$

where h is Planck's constant. The outside integrations over the momenta go from -∞ to +∞ while the inner integrations over the positions cover the entire system volume, V. The Hamiltonian in the exponent is separable in the momenta but not in the position coordinates, and is given by:

$$H = \sum_n \frac{\mathbf{p}_n^2}{2m} + U(\mathbf{r}_1 \cdots \mathbf{r}_n) \qquad (2.5.2)$$

Reiss, Katz, and Cohen view the system through a series of "snap shots" to look at how the N molecules will be partitioned in the volume. In other words, they use the snap shots to freeze the molecules in time and then locate and count them. The molecules will partition naturally into a number of clusters of different sizes in different snap shots. The different configurations that result in these different snap shots are the result of the density fluctuations that are present in the system.

The cluster distribution function is denoted by f_n and describes the size and number of each of the different clusters present in the system. It is assumed that the clusters are sufficiently separated in space such that they do not interact with each other. With this in mind, the potential energy, U, in the Hamiltonian can be separated into individual terms, one for each cluster. Additionally, the N! in the denominator of Equation 2.5.1 corrects for the fact that the indistinguishable molecules are being treated as distinguishable molecules in the counting process facilitated by the snap shots. The distinguishable

molecules can be placed in a number of different configurations (one for each different snap shot) resulting in f_n clusters given by:

$$Q' = \frac{N!}{\prod_n (n!)^{f_n}} \tag{2.5.3}$$

where Q' is an intermediate step in defining the molecular partition function for the system. Some of these configurations are simply the result of all of the molecules of a given cluster of size n exchanging position with another cluster of the same size. These configurations do not accomplish anything other than a switch of position and are incorrectly counted more than once. In order to correct this, the factor:

$$\frac{1}{\prod_n f_n!} \tag{2.5.4}$$

is introduced. Using Equations 2.5.3 and 2.5.4 and the fact that each cluster can be treated as an independent entity with no interactions allowed Reiss, Katz, and Cohen to re-write Equation 2.5.1 as:

$$Q = \prod_n \frac{q_n^{f_n}}{f_n!} \tag{2.5.5}$$

where q is the partition function for an individual cluster given as:

$$q_n = \frac{1}{n!h^{3n}} \int_{\infty}^{\infty} \cdots \int \exp\left[\frac{1}{kT}\left(\sum_n \frac{\mathbf{p}_1^2 + \mathbf{p}_2^2 + \cdots \mathbf{p}_n^2}{2m} + u_n(\mathbf{r}_1 \cdots \mathbf{r}_n)\right)\right] d\mathbf{r}_1 \cdots d\mathbf{r}_n d\mathbf{p}_1 \cdots d\mathbf{p}_n \tag{2.5.6}$$

The individual cluster partition function, q, in Equation 2.5.5 is raised to the f_n power to account for each of the f_n clusters' contributions to the partition function. The cumulative product in Equation 2.5.5 is to account for the contributions from every possible configuration.

Each cluster, as defined, will have a center of mass. It is desirable to have this center of mass reside at the center of the volume of the n molecules (in other words, be spherically symmetric). This helps define the cluster in the counting process. Using this idea, Reiss, Katz, and Cohen (1968) transform their coordinate system from an arbitrary one to one based on the center of mass (c.m.) of the clusters. They do this by introducing vector quantities

$$\mathbf{r}_j' = \mathbf{r}_j - \mathbf{R}, \quad j = 1, 2, 3, \cdots, n\text{-}1 \tag{2.5.7}$$

and

$$\mathbf{R} = \frac{\sum_{j=1}^{j=n} \mathbf{r}_j}{n} \tag{2.5.8}$$

where $\mathbf{R}$ is a vector that identifies the c.m. of the cluster, $\mathbf{r}_j$' is the position vector of the j^{th} molecule in the arbitrary coordinate system and $\mathbf{r}_j$ is the position vector of the same j^{th} molecule in the c.m. or relative coordinate system. An example of a cluster coordinate system is shown in Figure 2.9.

Blander and Katz (1968) re-evaluate Equation 2.5.6 in the c.m. coordinate system and after integration of the momenta, the individual cluster partition function, q, becomes:

$$q_n = \frac{\Lambda^n}{n!} \int_V dR \left[n^3 \int \cdots \int_{v_n} \exp\left[\frac{1}{kT} u'(\mathbf{r}'_1 \cdots \mathbf{r}'_{n-1}) \right] d\mathbf{r}'_1 \cdots d\mathbf{r}'_{n-1} \right] \tag{2.5.9}$$

In Equation 2.5.9, the n^3 comes from the coordinate transformation from the arbitrary coordinate system to the relative one and u' is the transformed potential energy. The integrations over the primed coordinates, $\mathbf{r}'_1$, $\mathbf{r}'_2$, etc. are only carried out over the volume of the cluster. The quantity:

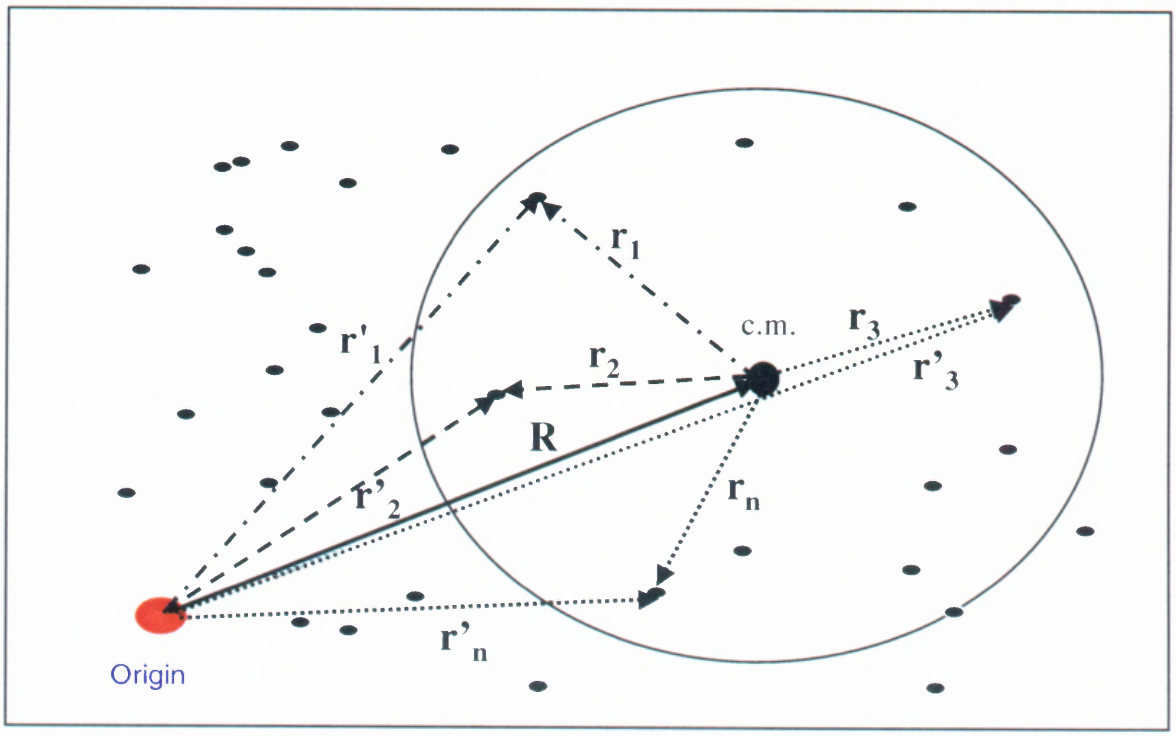

Figure 2.9 Cluster Coordinate System Indicating the Position Vectors $\mathbf{r}_n$ and $\mathbf{r}_n'$. The center of mass is designated by the position vector **R**.

$$\Lambda = \left(\frac{2\pi nkT}{h^2} \right)^{1/2} \tag{2.5.10}$$

results from the integration over the momenta and is related to the thermal deBroglie wavelength which is often referred to in standard statistical thermodynamics texts such as Hill (1986).

Finally, Equation 2.5.9 can be integrated over dR resulting in

$$q_n = \left[\Lambda V n^{1/2} \right] \left[\frac{\Lambda^{n-1} n^{1/2}}{n!} \int \cdots \int_{V_n} \exp\left[\frac{1}{kT} u'(\mathbf{r}'_1 \cdots \mathbf{r}'_{n-1}) \right] d\mathbf{r}'_1 \cdots d\mathbf{r}'_{n-1} \right] \tag{2.5.11}$$

In the first term of Equation 2.5.11, the authors have grouped a factor of $n^{3/2}$, V, and Λ together to indicate that this term is clearly the translational partition function of the cluster. They then conclude that the second term in the equation represents the internal partition function including rotation.

The next step undertaken by the authors is to define the cluster distribution function. They start with a well-known expression for the chemical potential:

$$\mu_n = -kT\left(\frac{\partial \ln Q}{\partial f_n}\right)_{T,V} = -kT(\ln q_n - \ln f_n) \tag{2.5.12}$$

Further, they conclude that since n single molecules must combine to form a cluster of size n, then at equilibrium, it follows that:

$$\mu_n = n\mu_1 \tag{2.5.13}$$

where u_1 is the chemical potential of one molecule in the bulk phase. Using Equation 2.5.13 in Equation 2.5.12 and solving for f_n, the cluster distribution function can be obtained:

$$f_n = q_n \exp\left(\frac{n\mu_1}{kT}\right) \tag{2.5.14}$$

Reiss, Katz, and Cohen then apply Equation 2.5.9 to a cluster. The only differences in this application of Equation 2.5.9 are that the integration over **R** is restricted to the volume of the drop or cluster and that the volume is not centered on the c.m. Equation 2.5.9 becomes:

$$q'_n = \frac{\Lambda^n}{n!}\int_{v_n} Z_R d\mathbf{R} \tag{2.5.15}$$

where $Z_{\mathbf{R}}$ is the classical configuration integral and the q'_n is for the liquid drop. The authors use Equation 2.5.9 for a cluster again, this time restricting the c.m. of the cluster to the origin of the arbitrary coordinate system. The result is:

$$q_n = \frac{\Lambda^n}{n!}\int_V Z_0 d\mathbf{R} = \frac{\Lambda^n}{n!} V Z_0 \tag{2.5.16}$$

In Equation 2.5.16, Z_0 is the configuration integral with the c.m. of the cluster constrained to remain at the origin and the integration is now over the entire system V. This leads to the following result:

$$q_n = q'_n V\left[\frac{Z_0}{Z_R d\mathbf{R}}\right] = q'_n V\mathcal{P}_o \tag{2.5.17}$$

In this equation, $\mathcal{P}_0$ is the probability that the c.m. will be found at the origin. Equation 2.5.17 and 2.5.14 are combined resulting in:

$$f_n = V\mathcal{P}_o q'_n \exp\left(\frac{n\mu_1}{kT}\right) \tag{2.5.18}$$

The authors then write the Helmholtz free energy of the cluster in the following form:

$$A_n = kT \ln q'_n = n\mu_1 + \varepsilon_n^{2/3} - P_B v \tag{2.5.19}$$

where v is the cluster volume and ε is ill-defined in the original manuscript but is believed to be related to the surface tension and area of the cluster or drop. This equation is solved for q'_n and the result is used in Equation 2.5.18 to obtain the final form of the cluster distribution function:

$$f_n = V\mathcal{P}_o \exp\left[\frac{-\left(n(\mu_1 - \mu_n) + \varepsilon_n^{2/3}\right)}{kT}\right] \tag{2.5.20}$$

The last issue remaining is the evaluation of $\mathcal{P}_0$. Reiss, Katz, and Cohen resorted to a statistical argument to accomplish this task. They assumed that the probability function $\mathcal{P}_D$, where D indicates a distribution function, is adequately described by a Gaussian distribution:

$$\mathcal{P}_D = \frac{1}{(2\pi)^{-3/2}\sigma^3} \exp\left(\frac{-D^2}{2\sigma^2}\right) \tag{2.5.21}$$

where σ is the standard deviation of a fluctuation in any one of the three Cartesian coordinates of the c.m. The probability at the center of mass (which is limited to the origin) is then given by:

$$\mathcal{P}_o = \frac{1}{(2\pi)^{-3/2}\sigma^3} \tag{2.5.22}$$

The value of the standard deviation, σ, is easily obtained by taking the square root of the variance, σ^2, which is given by:

$$\sigma^2 = \left[\frac{(1-f)}{12n}\right] v_n^{2/3} \tag{2.5.23}$$

The authors have now completely defined a distribution function for the clusters. This can be multiplied by a kinetic-based pre-exponential factor as typically found in classical nucleation theory to predict nucleation rates. Unfortunately, as the work focused on condensing vapors, it is not readily applicable to the formation of vapor bubbles in either liquids or polymers.

More recently, Reiss and co-workers published a series of manuscripts that expanded and improved on the partition function approach described above. The first (Reiss, Tabazadeh, and Talbot, 1990) focused on creating a more rigorous definition of a cluster. The intent of the manuscript was to create a cluster model that was physically consistent and could be used to predict the equilibrium cluster distribution function. The second manuscript (Ellerby, Weakliem, and Reiss, 1991) tried to identify average thermodynamic properties of the clusters and defined a cluster distribution function. A third manuscript (Ellerby and Reiss, 1992) outlined a probabilistic method for developing the cluster distribution function. Each of these works will be touched on in more detail below.

Reiss, Tabazadeh, and Talbot (1990) modified the original work of Reiss et al. (1968) by accounting for the effects of the surrounding ideal vapor. This was done by defining the cluster in such a way that the contributions of all of the molecules could be accurately combined into the partition function. The cluster definition they employed follows. A spherical shell of volume v is centered on the center of mass of a group of n molecules. The density of the cluster is defined as n/v and is greater than the density of the bulk phase because of normal density fluctuations. It is important to note that clusters can have the same density n/v, but different total v's (i.e. clusters of different size) or they can have the same n and different v's (i.e. different n/v's or densities) in this cluster definition. Clusters of only a critical size will still be the ones to nucleate but this definition suggests that the size of the critical cluster does not have to be unique.

Based on this cluster definition, the following changes to the molecular partition function result. First, Equation 2.5.5 is modified to account for the contributions of the vapor outside the clusters:

$$Q = \sum_{f_n} \frac{1}{N_{exc}!} (\Lambda V_{exc})^{N_{exc}} \prod_n \frac{q_n^{f_n}}{f_n!} \tag{2.5.24}$$

where N_{exc} is the number of individual vapor molecules outside the clusters identified in the system. The individual cluster partition function, q, given by Equation 2.5.6 is also modified; the limits of integration for the inner integrals now are over v, the cluster volume, not V, the system volume. The change results in:

$$q_{nv} = \frac{1}{n!h^{3n}} \int \cdots \int \exp\left[\frac{1}{kT}\left(\sum_n \frac{\mathbf{p}_1^2 + \mathbf{p}_2^2 + \cdots \mathbf{p}_n^2}{2m} + u_n(\mathbf{r}_1 \cdots \mathbf{r}_n)\right)\right] d\mathbf{r}_1 \cdots d\mathbf{r}_n d\mathbf{p}_1 \cdots d\mathbf{p}_n \tag{2.5.24}$$

Finally, V_{exc} is the part of the system volume not occupied by molecules in a cluster and is given by:

$$V_{exc} = V - \sum_{n}\sum_{v} v f_n \tag{2.5.26}$$

Equation 2.5.26 simply states that the cluster volume of each individual cluster, v, is multiplied by the corresponding number of clusters of that size; this is repeated for every cluster size in the system. The results are then summed over all cluster sizes and then, this quantity is subtracted from the total system volume yielding the excluded volume, V_{exc}. The cluster distribution function will now be identified as f_{nv}.

The authors transform to center of mass coordinates in exactly the same way as the previous work and the partition function takes on its final form:

$$Q = \sum_{f_{nv}} \frac{(\Lambda V_{exc})^{N_{exc}}}{N_{exc}!} \prod_{n}\prod_{v} \frac{\left(\Lambda n^{3/2} \exp - \left(\frac{A^*_{nv}}{kT}\right)\right)^{f_{nv}}}{f_{nv}!} \tag{2.5.27}$$

In Equation 2.5.27, the original product over n has been replaced by a double product, one over n and the other over v since Reiss et al (1990) have chosen to let both of these quantities vary in defining the cluster and A^*_{nv} is defined as internal Helmholz energy of the cluster. The cluster distribution function is found from maximizing Equation 2.5.27 by the method of Lagrange multipliers subject to the following constraining equation:

$$N_{exc} + \sum_{n}\sum_{v} n f_{nv} - N = 0 \tag{2.5.28}$$

The result after simplification is given as:

$$N_{exc} = \Lambda V_{exc} \exp \frac{\mu_1}{kT} \tag{2.5.29}$$

and

$$f_{nv} = \exp\left[-\frac{1}{kT}\left(A^*_{nv} - kT \ln \Lambda n^{3/2} V + Pv - n\mu_1\right)\right] \tag{2.5.30}$$

The first three terms in the parentheses of Equation 2.4.30 represent the final Gibbs energy of the cluster; A^*_{nv} representing the internal Helmholz energy, $kTln\Lambda Vn^{3/2}$ representing the translational free energy and the pv term which when added converts the entire expression to a Gibbs energy. The last term in the parentheses, $n\mu_1$, represents the initial Gibbs energy of the system. Reiss et al. (1990) suggest that the evaluation of A^*_{nv} can be obtained from computer simulations.

The theory was further developed by Ellerby, Weakliem, and Reiss (1991) when they refined the definition of the cluster. Ellerby et al. recognized that the original cluster definition given by Reiss, Tabazadeh, and Talbot makes the cluster not only a function of n, but also of v, with v being able to vary continuously. The problem is that for the cluster distribution function to have any meaning, the volume needs to be made discrete (analogous to creating discrete quantum energy states) and the function needs to be multiplied by this discrete volume. In multiplying by a discrete volume, i.e. Δv, the cluster distribution would carry units of volume, however, the cluster distribution function in Equation 2.4.30 originally derived by Reiss et al (1990) is a pure number having no units.

To correct this problem, Ellerby et al. redefined the cluster model proposed by Reiss, Tabazadeh, and Talbot to include a shell molecule. This shell molecule, which intersects the original shell, is contained in a differential volume element, $d\tau$ (See Figure 2.10).

The contribution of this molecule and its corresponding volume then need to be accounted for in the development of the partition function. The resulting partition function that Ellerby et al.(1991) obtain is given by:

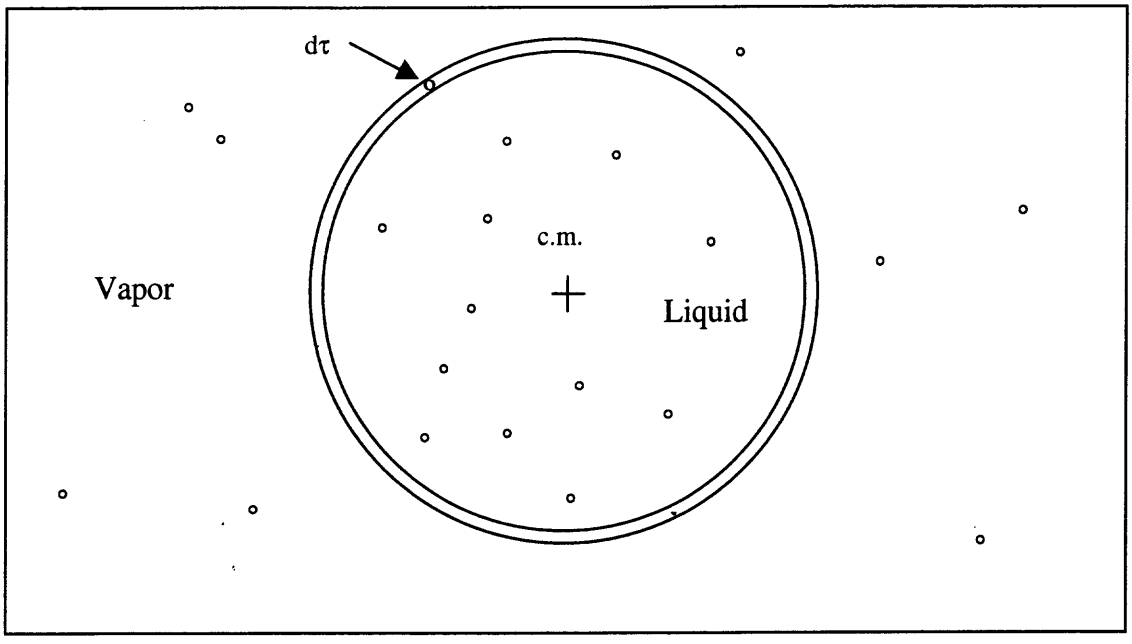

Figure 2.10 Cluster Model as Defined by Ellerby, Weakliem, and Reiss (1991) for a Liquid Cluster in an Ideal Vapor.

$$Q = \sum_{f_{nv}} \frac{(\Lambda V_{exc})^{N_{exc}}}{N_{exc}!} \prod_{nv} \frac{(q_{nv} V)^{f_{nv}}}{f_{nv}!} (\Lambda dv)^{f_{nv}} \tag{2.5.31}$$

where the term Λdv accounts for the contributions of the shell molecule. The cluster distribution function is found by maximizing the partition function, again by the method of Lagrange multipliers subject to the following constraining equation:

$$N_{exc} + \sum_{nv} (n+1) f_{nv} - N = 0 \tag{2.5.32}$$

Equation 2.5.32 differs slightly from 2.5.28 in that the sum over all possible cluster sizes and molecular content (shown here to be consistent with the original manuscript as a single sum) is multiplied by n+1 to account for the shell molecule, not simply n, the number of molecules in the cluster. The resulting equilibrium cluster distribution that is obtained is nearly identical to that obtained by Reiss, Tabazadeh, and Talbot (1990) with the only difference being the existence of a pre-exponential term, (Ndv/V):

$$f_{nv} = \left(\frac{Ndv}{V}\right)\exp\left[-\frac{1}{kT}\left(A^*_{nv} - kT\ln\Lambda n^{3/2}V + Pv - n\mu_1\right)\right] \tag{2.5.33}$$

In a follow-up manuscript, Ellerby and Reiss (1992) take a different approach to determining what the cluster distribution function is, they look at the phenomena of a cluster forming from local density fluctuations in a probabilistic approach. They hypothesize that the formation of exactly one cluster of size nv in V is related to three probabilistic events that all must happen together. The first probability is the absolute probability that all of the molecules other than the n molecules contained in the cluster are found outside the cluster. This probability is given by

$$\mathcal{P}\{\mathcal{E}_{N-n}\} = \prod_{n=1}^{N-n}\left(1-\frac{v}{V}\right) = \left(1-\frac{v}{V}\right)^{N-n} \tag{2.5.34}$$

In Equation 2.5.34, the probability of finding the molecules in space is related to the size or volume of the space in question, hence the probability of finding a molecule inside the cluster is simply the cluster volume, v divided by total volume, V. One minus this quantity is the probability that the molecule will be found outside v. The term is taken over the product from n = 1 to n = N-n to account for all the molecules not in the cluster. The authors' note that taking the log of Equation 2.5.34 and then expanding it in a Taylor series and taking the limit as N and V both go to ∞ gives the following exponential form for this probability:

$$\mathcal{P}\{\mathcal{E}_{N-n}\} = \exp\left(-\rho^* v\right) \tag{2.5.35}$$

where ρ* is N/V.

The second probability, a conditional probability that states that any one molecule will be found in the differential shell volume, dτ centered about **r** given that the first event (that the N-n molecules are outside the cluster volume, v) has occurred, is:

$$\mathcal{P}\{\mathcal{E}_{n+1}|\mathcal{H}_{N-n}\}=\sum^{N-n}\frac{dv}{V}=\left(N-n\frac{dv}{v}\right)\approx\frac{N}{V}dv=\rho^{*}dv \tag{2.5.36}$$

The conditional probability is again simply related to the size or volume of the space that the molecule can be found in.

The third and final probability is the conditional probability that the center of a cluster of n molecules in volume v corresponds to the center of mass of the cluster volume v, again assuming the first event (that the N-n molecules are outside the cluster volume, v) has occurred. This probability is related to the ratio of the n molecules in the cluster volume to the N molecules in the system volume V. In order to determine what this probability is, the arbitrary coordinate system needs to be transformed to the center of mass coordinate system and this is done as before, utilizing Equations 2.5.7 and 2.5.8.

The resulting probability is given as:

$$\mathcal{P}\{\mathcal{E}_{nv}|\mathcal{H}_{N-n}\}=\frac{n^{3}\int_{V}dR\int_{0}^{v'}\cdots\int_{0}^{v'}d\mathbf{r}_{1}\cdots d\mathbf{r}_{n-1}}{V^{n}} \tag{2.5.37}$$

In Equation 2.5.37, the n^3 term results from the coordinate transformation. The authors use the notation of v' as the upper limit on the inner integrations as an imposed arbitrary size limit for the clusters rather than v, the actual cluster volume. This is done to ensure that the clusters do not grow too large and interfere with each other. Ellerby, et al (1991) argue that the limit is of no real consequence because the actual kinetic limit imposed on the clusters will be far more severe than this arbitrary limit.

This probability needs to be corrected to account for the fact that the N distinct molecules can be taken without regard to selection order which is simply the combination of N items taken n at a time or,

$$= \frac{N!}{(N-n)!n!} \tag{2.5.38}$$

Equation 2.5.38 is the binomial coefficient and in the limit of N>>n, simplifies to:

$$= \frac{N(N-1)\cdots(N-1+n)}{n!} = \frac{N^n}{n!} \tag{2.5.39}$$

Multiplying Equation 2.5.37 by Equation 2.5.39 and integrating over dR results in the desired probability:

$$\mathcal{P}\{\mathcal{E}_{nv}|\mathcal{H}_{N-n}\} = \frac{N^n n^3 V \int_0^{v'}\cdots\int_0^{v'} d\mathbf{r}_1 \cdots d\mathbf{r}_{n-1}}{n!V^n} \tag{2.5.40}$$

Ellerby and Reiss correct this term for the non-ideality of the "condensed" cluster by adding a Boltzmann factor, $\exp(-u_n(\mathbf{r}^n)/kT)$ assuming a pairwise-additive potential, $u_n(\mathbf{r}^n)$ giving:

$$\mathcal{P}\{\mathcal{E}_{nv}|\mathcal{H}_{N-n}\} = \frac{N^n n^3 V \int_0^{v'}\cdots\int_0^{v'} \exp\left(-\frac{u_n(\mathbf{r}^n)}{kT}\right) d\mathbf{r}_1 \cdots d\mathbf{r}_{n-1}}{n!V^n} \tag{2.5.41}$$

The three probabilities (Equations 2.5.32, 2.5.35, and 2.5.41) are then combined to give the probability of forming a single cluster of volume v centered on the c.m.:

$$\mathcal{P}_n = \frac{N}{V} dv \exp-\left(\frac{N}{V}v\right)\left[\frac{\left(\frac{N^n}{n!}\right) n^3 V \int_0^{v'}\cdots\int_0^{v'} \exp\left(-\frac{u_n(\mathbf{r}^n)}{kT}\right) d\mathbf{r}_1 \cdots d\mathbf{r}_{n-1}}{V^n}\right] \tag{2.5.42}$$

or

$$\mathcal{P}_n = \frac{N}{V} dv \exp-\left(\frac{N}{V}v\right)\frac{Z_{nv}}{Z_n} \tag{2.5.43}$$

recognizing that:

$$\frac{Z_{nv}}{Z_n} = \frac{\left(\frac{N^n}{n!}\right) n^3 V \int_0^{v'} \cdots \int_0^{v'} \exp\left(-\frac{u_n(\mathbf{r}^n)}{kT}\right) d\mathbf{r}_1 \cdots d\mathbf{r}_{n-1}}{V^n} \tag{2.5.44}$$

where Z_{nv} and Z_n are the classic configuration integrals. The authors recognize that Equation 2.5.42 or 2.5.43 must be corrected for the molecules being indistinguishable and a momentum term needs to be added for completeness. Incorporating these terms (n! for indistinguishablility and Λ for momentum or translational contributions) to both configuration integrals yields:

$$\mathcal{P}_n = \frac{N}{V} dv \exp - \left(\frac{N}{V} v\right) \left[\frac{\frac{\Lambda^n \left(\frac{N^n}{n!}\right) n^3 V \int_0^{v'} \cdots \int_0^{v'} \exp\left(-\frac{u_n(\mathbf{r}^n)}{kT}\right) d\mathbf{r}_1 \cdots d\mathbf{r}_{n-1}}{n!}}{\frac{\Lambda^n}{n!} V^n} \right] \tag{2.5.45}$$

This modification allows the numerator to be written as the partition function for the n molecules in the cluster, Q_{nv}, and the denominator to be written as the partition function, Q_n, for the n molecules in the ideal bulk phase or:

$$Q_{nv} = \frac{\Lambda^n \left(\frac{N^n}{n!}\right) n^3 V \int_0^{v'} \cdots \int_0^{v'} \exp\left(-\frac{u_n(\mathbf{r}^n)}{kT}\right) d\mathbf{r}_1 \cdots d\mathbf{r}_{n-1}}{n!} \tag{2.5.46}$$

and

$$Q_n = \frac{\Lambda^n}{n!} V^n \tag{2.5.47}$$

Finally, using the ratio of these partition functions, the probability of forming a single cluster of volume v centered on the center of mass is written as:

$$\mathcal{P}_n = \frac{N}{V} dv \exp - \left(\frac{N}{V} v\right) \frac{Q_{nv}}{Q_n} \tag{2.5.48}$$

Ellerby and Reiss suggest that this form of the equation represents the physical process very nicely. The first part of the equation, Ndv/V is the probability that a shell molecule exists in dv and exp(-Nv/V) is the probability of forming a hole of exactly the correct size for the cluster by doing pv work until a volume v is centered on r. This, Ellerby and Reiss claim is the first part of the nucleation process. The second part of the process, filling the volume, v, with n molecules through density fluctuations is then given by the ratio of the partition functions, Q_{nv}/Q_n.

The authors use this probability to obtain a cluster distribution function in the following manner. They note that the probability of one or more clusters (i.e. at least one) will be found somewhere in the volume V is the sum from j = 1 to j = ∞ of the mutually exclusive probabilities of exactly one j cluster being found or

$$\mathcal{P}_{nv} = \mathcal{P}_{nv}^{1} + \mathcal{P}_{nv}^{2} + \mathcal{P}_{nv}^{3} + \cdots = \sum_{j=1}^{\infty} \mathcal{P}_{nv}^{j} \tag{2.5.49}$$

The probability of exactly one cluster being found in V is Equation 2.5.48. Noting that the clusters do not interact with each other, the probability for more than one cluster can be expressed as the product of the j identical uncorrelated probabilities of exactly one cluster being found for the j total clusters in the system, or:

$$\mathcal{P}_{nv} = \left(\mathcal{P}_{nv}^{1}\right)^{j} = \left[\frac{N}{V}\exp-\left(\frac{N}{V}v\right)\frac{Q_{nv}}{Q_n}\right]^{j} dv^{j} \tag{2.5.50}$$

Ellerby and Reiss state that the higher order terms (j ≥ 2) can be neglected in comparison to $\mathcal{P}^{1}_{nv}$ because these higher order terms are multiplied by the infinitesimally small volume, dv, raised to the corresponding power.

The ensemble average number of clusters (i.e. the cluster distribution function) can be expressed as:

$$f_{nv} = 1\mathcal{P}_{nv}^{1} + 2\mathcal{P}_{nv}^{2} + 3\mathcal{P}_{nv}^{3} + \cdots = \sum_{j=1}^{\infty} j\mathcal{P}_{nv}^{j} \tag{2.5.51}$$

Neglecting higher order terms as before leads to:

$$f_{nv} = 1\mathcal{P}_{nv}^{1} + 0 + 0 + \cdots = \frac{N}{V} dv \exp - \left(\frac{N}{V} v\right) \frac{Q_{nv}}{Q_n} \tag{2.5.52}$$

Ellerby and Reiss re-write Equation 2.5.52 in exponential form to obtain a free energy for the cluster formation. Utilizing the ideal gas law (N/V = p/kT), this exponential form is:

$$f_{nv} = \frac{N}{V} dv \exp\left[-\frac{1}{kT}\left(-kT \ln \frac{Q_{nv}}{Q_n} + Pv \right)\right] \tag{2.5.53}$$

With this in mind, they note that the first term ($-kT\ln Q_{nv}/Q_n$) in the exponential is the Helmholtz free energy change for the formation of the cluster. The second term, pv is the pv work required to create the empty volume v. It is a straightforward result of elementary thermodynamics that adding pv to the Helmholz free energy gives the Gibbs free energy. Knowing this, the authors claim, that Equation 2.5.53 can be put into the same form as Equation 2.4.33 after some manipulation:

$$f_{nv} = \left(\frac{Ndv}{V}\right) \exp\left[-\frac{1}{kT}\left(A_{nv}^{*} - kT \ln \Lambda n^{3/2} V + Pv - n\mu_1 \right)\right]$$

As before A^{*}_{nv} needs to be estimated by some method, most likely via computer simulation. Once this is complete, the distribution function can be multiplied by a standard pre-exponential term from classical nucleation theory to yield a nucleation rate.

In summary, the above works provide a method for determining a molecular partition function for the formation of clusters (which have liquid like densities) from a supersaturated ideal vapor. Finally, with a look forward to the polymeric systems that will be discussed in the remaining chapters, the use of a molecular partition function

approach can be seen as early as 1975 (Helfand, 1975). Helfand, extending the Flory and Huggins lattice concept, created molecular partition functions to model the interfacial free energy between dissimilar polymers. The issue of dealing with liquid and vapor phases, however, was not addressed in Helfand's work as it was focused on interfacial energies between polymers rather than nucleation.

2.6 Other Theories

So far, all of the nucleation theories touched on have been based on one significant simplifying assumption; that is the capillary approximation. This approximation states that a cluster of molecules will have the same physical and chemical properties as a bulk phase of the molecules in the same physical state (i.e. liquid or vapor). Dillmann and Meier (1991) propose a correction factor to account for deviations in the actual surface free energy for the clusters from that which is estimated from macroscopic fluid properties. In their work, they were specifically concerned with the condensation of supersaturated vapors. They define the following curvature correction factor:

$$\Gamma_n = 1 + \eta_1 n^{-1/3} + \eta_2 n^{-2/3} \tag{2.6.1}$$

where η_1 and η_2 are selected to fit the saturated vapor pressure and second viral coefficient for the material under investigation. They then use this correction factor in the expression for ΔG:

$$\frac{\Delta G}{kT} = \Gamma_n \Theta n^{2/3} + \upsilon_1 \ln n - \ln(\upsilon_2 V) - n \ln s \tag{2.6.2}$$

In Equation 2.6.2, s is the super-saturation ratio of the system and the terms υ_1 and υ_2 are

parameters chosen to fit the critical density and pressure of the material. The term, Θ, is given by Equation 2.6.3 below:

$$\Theta = \frac{(36\pi)^{1/3}\gamma\rho_l^{-2/3}}{kT} \tag{2.6.3}$$

Here, γ is the surface tension and ρ_l the liquid density of the system. A variety of authors (Delale and Meier, 1993; Ford, 1993; Laaksonen, Ford, and Kulmala, 1994) attempted to improve the theory by reducing or eliminating the need for the many parameters needed in the Dillmann and Meier correction with mixed success.

Another approach that has been examined in some detail is the application of "Density Functional Theory" for predicting nucleation rates. Laaksonen et al. (1995) points out that the premise behind Density Functional Theory is to treat the newly forming second phase as an inhomogeneous fluid. In doing this, the theory obtains properties of the critical nucleus from the free energy of the non-uniform system which is a unique functional of the average density. The minimum of this density functional determines the thermodynamically stable states at a given temperature. Further, the theory does not rely on the classical premise (the capillary approximation) that there is a sharp interface or boundary between the nucleating phase and the metastable phase, which is what makes the capillary approximation valid.

The first attempt at using density functional theory dates back to the late 1950's (Cahn and Hilliard, 1959). They proposed the following form for the grand potential of the system:

$$\Omega[\rho(\mathbf{r})] = \int d\mathbf{r}\left\{A[\rho(\mathbf{r})] - \mu\rho(\mathbf{r}) + \zeta[\nabla\rho(\mathbf{r})]^2\right\} \tag{2.6.4}$$

where the grand potential is derived from the grand canonical partition function and is for systems that do not have constant N. It is defined as the total internal energy minus the chemical potential for the system. In Equation 2.6.4, A is the Helmholtz free energy per unit volume of the homogeneous system with density ρ and μ is the chemical potential. The last term, which is a gradient term squared, accounts for non-local contributions to the free energy. In an earlier manuscript, Cahn and Hilliard (1958) define ζ as a gradient energy coefficient that depends on the concentration and temperature of the system. They define it as a constant for regular solutions, however, so that it can be evaluated. Cahn and Hilliard (1959) indicate that at a given supersaturation, the functional has a saddle point in the functional space. This solution gives the density profile of the critical nucleus and the free energy required to form a liquid droplet of critical size from the unstable vapor.

Oxtoby and Evans (1988) take a slightly different approach to density functional theory. They express the free energy of the non-uniform fluid in terms of the free energy of a suitable reference system. The authors use a hard-sphere perturbation theory to write the free energy as the sum of the hard-sphere repulsive contribution and a long-range attractive contribution. They view the repulsive term as a local contribution and the long-range term as a non-local contribution. Their grand potential has the form of:

$$\Omega[\rho(\mathbf{r})] = \int d\mathbf{r}[A[\rho(\mathbf{r})] - \mu\rho(\mathbf{r})] + \iint d\mathbf{r}d\mathbf{r}'\phi(|\mathbf{r}-\mathbf{r}'|)\rho(\mathbf{r})\rho(\mathbf{r}') \qquad (2.6.5)$$

Here the squared gradient term has been replaced with the double integral term. This is done to increase the range of applicability of Equation 2.6.5. In Equation 2.6.4, the gradient term is only useful when the average density of the system varies slowly over the atomic distance scale (Laaksonen et al., 1995) but Equation 2.6.5 does not have this

limitation. In Equation 2.6.5, Oxtoby and Evans (1988) use the Yukawa potential energy function to model the long-term attractive part of the potential, ϕ. This is given by (Lee, 1988):

$$\phi = \frac{\alpha_i \alpha_j}{4\pi r^2 \iota_m} \exp\left(-z_i\left(z - d_{ij}\right)\right) \tag{2.6.6}$$

In Equation 2.6.6, α_i and α_j are the point charges of particles i and j, ι_m is the permittivity of the medium containing the two charges, usually taken to be 9 x 10^9 N-m^2/coulomb^2 for vacuum or air, z_i is an interaction distance of the point charges, z is the distance between the point charges, and d_{ij} represents the hard sphere diameter for the system. For $z < d_{ij}$, u is ∞, and for $z > d_{ij}$, u is given by Equation 2.6.6. For $z_i = 0$ in Equation 2.6.6, Coulomb's law is recovered.

The Yukawa potential energy function is not necessarily the most realistic for many fluids. Oxtoby and Evans state that their choice of the Yukawa potential was for its mathematical simplicity and because the interfacial properties of hard-sphere Yukawa fluids had been extensively studied. To improve on this, Zeng and Oxtoby (1991) replaced the long-range attractive contribution given by the Yukawa potential in the Oxtoby and Evans (1988) work with a more realistic Lennard-Jones potential energy function:

$$\phi_{LJ}(r) = 4\epsilon\left[\left(\frac{\sigma_{LJ}}{r}\right)^{12} - \left(\frac{\sigma_{LJ}}{r}\right)^{6}\right] \tag{2.6.7}$$

In Equation 2.6.7, ϵ is the depth of the energy well or the minimum potential energy, r is the distance between the molecules, and σ_{LJ} is the collision diameter. In either case, Oxtoby and Evans, or Zeng and Oxtoby, the density functional theory allowed the

authors to calculate a critical grand potential function for nucleation, $\Delta\Omega_c$, which is used in place of the traditional change in free energy, ΔG_m in a typical Arrhenius nucleation equation:

$$J = \psi \exp - \frac{\Delta\Omega_c}{kT} \tag{2.6.8}$$

The term ψ is used in Equation 2.6.8 as the traditional pre-exponential frequency factor found in CNT.

Talanquer and Oxtoby have extended density functional theory to include fluids modeled with a Stockmayer potential energy function (1993) and mixtures of binary fluids (1995). A Stockmayer potential is a combination of a Lennard-Jones 6-12 potential coupled with a dipole-dipole interaction (Prausnitz et al., 1986):

$$\phi_S(r) = 4\epsilon\left[\left(\frac{\sigma_{LJ}}{r}\right)^{12} - \left(\frac{\sigma_{LJ}}{r}\right)^{6}\right] + \frac{d^2}{r^3}\Gamma_\theta(\theta_1\theta_2\theta_3) \tag{2.6.9}$$

where d is the dipole moment and Γ_θ is a function of the three angles, θ_1, θ_2, and θ_3 which determine the relative orientation of the two dipoles. In their work with binary fluids, Talanquer and Oxtoby use the standard form of the Lennard-Jones potential energy function. They address the issues surrounding a mixture by introducing mixing rules into the grand potential given by Equation 2.6.5. This leads to the following grand potential for the binary mixture:

$$\Omega[\rho(\mathbf{r})] = \int d\mathbf{r} A[\rho_1(\mathbf{r}), \rho_2(\mathbf{r})] + \frac{1}{2}\sum_{i,j=1} \iint d\mathbf{r} d\mathbf{r}' \phi_{i,j}(|\mathbf{r} - \mathbf{r}'|)\rho_i(\mathbf{r})\rho_j(\mathbf{r}') - \sum_{i=1}^{2} \mu_i \int d\mathbf{r}\rho_i(\mathbf{r}) \tag{2.6.10}$$

In order to evaluate this grand potential, Talanquer and Oxtoby use a mixture Lennard-Jones potential given by:

$$\phi_{i,j}(r) = 4\epsilon_{i,j}\left[\left(\frac{\sigma_{i,j}}{r}\right)^{12} - \left(\frac{\sigma_{i,j}}{r}\right)^{6}\right] \tag{2.6.11}$$

In their work, however, the authors assume that both fluids are of equal size and Equation 2.6.11 reduces to the standard Lennard-Jones potential given by Equation 2.6.7. An interesting outcome of their work is that they hypothesize that the nucleation process may actually occur in two steps for binary systems, first a liquid-liquid phase split and then a vapor-liquid phase split.

Additional work by Talanquer and Oxtoby (1994) looked at improving the density functional theory to be a "dynamic" theory that could estimate both forward and backward addition rates of molecules to the critical clusters. This approach in some ways mirrors the very early works (Becker and Döring, 1935; Zeldovich, 1942; Feder, et al. 1966) that utilized the concept of a detailed balance to develop cluster distribution functions in CNT (refer to section 2.2). Recent work done by Shen and Debenedetti (2001) focused on defining the limit at which point the classical capillary approximation failed and at which point the application of density functional theory improved results obtained from a theoretical model. This in essence defines the limit of applicability of the CNT.

In their work, they use a Lennard-Jones potential energy function and follow the same approach used by Zeng and Oxtoby (1991). The authors show that the ratio of the density functional free energy barrier to the classical nucleation theory free energy barrier scales to the ratio of two different differences in the chemical potential, $\Delta\mu/\Delta\mu_{spin}$. The first difference in chemical potential, $\Delta\mu$, is between the bulk superheated vapor and the saturated liquid. The second difference in chemical potential, $\Delta\mu_{spin}$, is the chemical

potential difference between the liquid at the spinodal and saturated liquid. They show that at low values of this ratio (i.e. $\Delta\mu/\Delta\mu_{spin} < 0.5$) the classical capillary approximation is reasonable because a sharp interface exists between the two phases. As the value of $\Delta\mu/\Delta\mu_{spin}$ decreases, this approximation improves. At values around 0.5 for $\Delta\mu/\Delta\mu_{spin}$, the capillary approximation is no longer valid because the sharp interface between the two phases becomes fuzzy and more diffuse. As the ratio is increased to $\Delta\mu/\Delta\mu_{spin} > 0.5$, non-classical behavior becomes progressively more evident and the vapor density inside the bubble becomes more liquid-like, making the distinction between the phases more difficult to discern.

Finally, a variety of manuscripts focused on computer simulation techniques and semi-empirical approaches can be found. In most cases, these approaches utilize Monte-Carlo simulation techniques to determine the stable cluster distribution function. This approach is employed to calculate many of the necessary quantities used in the density functional theory approach described above (Talanquer and Oxtoby, 1994). The earliest notable work in computer simulation/Monte Carlo methods on cluster dynamics was done by Lee, Barker and Abraham (1973). In their work, the authors modeled cluster formation in argon vapor using a Lennard-Jones 6-12 potential function. This work, however, did not address nucleation.

The first attempt to adopt the approach of Lee et al. to nucleation was by Garcia and Soler Torroja (1981). The authors tried to model nucleation of argon gas condensing but were forced to make several assumptions that included using an arbitrary cluster volume. Weakliem and Reiss (1993) attempted to correct the problems associated with this arbitrary selection of a cluster volume. They adopted the cluster definition developed

by Ellerby, Weakliem, and Reiss (1991) and also modeled nucleation phenomena (condensation) in argon vapor. They were able to estimate the free energy of formation of the argon clusters and then suggested that this could be coupled with the concept of a detailed balance similar to the classical theory to estimate nucleation rates.

The above fairly detailed review of liquid-vapor nucleation theory ranges from the classical approach, which rests heavily on the capillary approximation to more modern theories such as density functional theory, which eliminate the need for this assumption. Some of these theories will next be applied to the prediction of nucleation phenomena in polymeric foams.

CHAPTER 3

PREDICTION OF FOAM FORMATION RATES IN THERMOPLASTICS

A brief overview of the literature pertinent to nucleation in thermoplastic foams is given in last section of this chapter, 3.4. It provides the relevant findings in the field and summarizes the need for additional work. Some readers may prefer to start with this section and then return to the more detailed reviews in the earlier sections for more comprehensive information. The first three sections of the chapter focus on developing the state of the existing theory and are broken down as follows. Section 3.1, "Early Approaches" focuses on the last step of the foam formation process, bubble growth. This is because these bubble growth mechanisms dominated the early literature. It was not until the 1980's that investigators began to look at CNT to predict the rate of bubble formation in viscous polymer systems. Section 3.2, "Application of CNT" examines, in detail, some of the modifications that were incorporated into CNT to improve the model results. Finally, Section 3.3, "Other Mechanisms", provides a detailed look at foam formation through a variety of models that differ in approach from those found in the first two sections.

3.1 Early Approaches: Bubble Growth

The early approaches to modeling the formation of thermoplastic foams were largely based on bubble growth models in viscous fluids. Barlow and Langlois (1962) were the first to extend the earlier works of Scriven (1959) on bubble growth in low viscosity fluids to a viscous polymer solution. The model is based on transport mechanisms (mass,

momentum, and heat transfer) and assumes that the bubble is growing in an infinite pool under isothermal conditions. This model also assumes spherical symmetry and takes into account mass transfer between the viscous liquid and the "gas" bubble. Rosner and Epstein (1972) and Patel (1980) apply similar transport phenomena driven approaches to the problem and obtain similar models for the bubble growth. There are two areas that differentiate these three models. The first area is in how each of the investigators used the boundary and initial conditions to develop the governing transport equations. The second area is in what type of numerical method is used to solve the resulting equations.

Street, Fricke, and Reiss (1971) and Ramesh, Rasmussen, and Campbell (1991) extended the theory to include Ostwald-de Waele power law fluids. The work of Street et al. is more of a theoretical exercise and also includes the introduction of a non-isothermal system where the bubble interface temperature is different from the actual bubble temperature. Using a polystyrene-nitrogen system, Ramesh et al. conducted a number of experiments to investigate the influences of temperature, saturation pressure, molecular weight, and the nature of the blowing agent on bubble growth. The authors use the Newtonian fluid model developed by Patel (1980) and then extend it to a power law fluid. They also compare their experimental results to the cell model proposed by Amon and Denson (1984).

Amon and Denson introduced the concept of a cell model in which multiple bubbles are in cells bounded by thin layers of polymer. Prior works had assumed that a single bubble was growing in an infinite pool. Amon and Denson's (1984) model recognizes the fact that each bubble is not an independent entity and that it must compete with neighboring bubbles for mass and energy. Arefmanesh (1991) also uses the concept of a

group of bubbles growing in a liquid pool. In his work, the bubbles are also only separated by a thin boundary layer. The primary difference between the last two approaches discussed is in the way the initial and boundary conditions are set up to establish the governing transport equations.

Han and Yoo (1981) incorporate the effects of injection rate (polymer flow rate) into a mold cavity on bubble formation. They worked with commercially supplied polystyrene and used sodium bicarbonate as a chemical blowing agent. In some experiments, they added citric acid as a nucleating agent in addition to the chemical blowing agent. This work investigated the effects of the varied injection rates (into the mold cavity) on the final foam morphology and bubble growth phenomena, however, it did not specifically examine nucleation rates. The work, in large part, focuses very heavily on the rheology of the system and includes the effects of the dissolved gas on the rheological properties of the polymer.

These manuscripts above have been chosen to provide an overview of the state of bubble growth theory. They do not fully represent the large body of work that has been compiled on this complicated subject, but they do address the significant technical considerations involved in bubble growth. These areas include Newtonian and non-Newtonian fluids, isothermal and non-isothermal conditions, systems with and without mass transfer limiting steps, and finally, single bubble and multi-bubble models. Additionally, they look at some of the effects that the processing equipment will have on bubble growth. Understanding bubble growth by itself, however, does not provide insight into the physics of the nucleation process. It does, however, remain as an

important topic, which when combined with an adequate nucleation model, can be used to predict the formation of polymeric foams.

3.2 Application of CNT

One of the first attempts to apply CNT to a viscous system was not in a polymeric system, but rather in coal pyrolysis (Attar, 1978). Attar attempted to model the formation of gas bubbles in coal melts. The gas, presumed to be methane, is a reaction byproduct of the pyrolysis process and the bubbles are believed to occur when a certain critical concentration of methane is exceeded. The author uses the same standard form of the CNT equation given in Section 2.2 (Equation 2.2.20) as a starting point for his work with one small difference. The usual form of the CNT equation has a factor of 2 in the pre-exponential term, but Attar uses a factor of 3. This changes Equation 2.2.20 to:

$$J = N_G\left(\frac{3\gamma}{\pi m}\right)^{1/2}\exp\left(-\frac{\Delta G}{kT}\right) \tag{3.2.1}$$

The equation (with either a factor of 2 or 3) will provide the "maximum" possible nucleation rate based on thermodynamics and the actual nucleation rate may be significantly lower (Attar, 1978). The decrease in the nucleation rate can be attributed to mass, heat or momentum transport limitations in the viscous material. Additionally, a kinetic limitation on the pyrolysis reaction rate is theoretically possible but unlikely given the other transport limitations. The author defines a corrected nucleation rate for each limiting transport phenomena case. Each equation has the same general form:

$$J_i = \frac{J}{1+\delta_i} \tag{3.2.2}$$

The i's in Equation 3.2.2 carry a subscript of t, η or m when the nucleation is limited by thermal, momentum or mass transfer respectively. The δ_i's represent the correction factor based on whichever particular transport mechanism is limiting. Blander and Katz (1975) use a similar approach to correct for mass transfer limitations for non-viscous liquids. Specifically for thermally-limited nucleation, Attar (1978) defines δ_t as:

$$\delta_t = \left(\frac{h_v}{kT}\right)^2 \frac{\gamma}{K}\left(\frac{2k}{\pi m T}\right)^{1/2} \frac{P_G}{(P_G - P_B)} \tag{3.2.3}$$

In Equation 3.2.3, h_v is the heat of vaporization and K is the thermal conductivity, both of the bulk phase. Substituting Equation 3.2.3 into 3.2.2 leads to a thermally controlled (or limited) nucleation rate of :

$$J_t \approx N \frac{K}{\gamma}\left(\frac{3\gamma T}{2k}\right)^{1/2}\left(\frac{kT}{h_v}\right)^2\left(1-\frac{P_B}{P_G}\right)\exp\left(-\frac{\Delta G_m}{kT}\right) \tag{3.2.4}$$

For momentum limited cases, Attar defines δ_η as:

$$\delta_\eta = \frac{\eta}{\gamma}\left(\frac{3kT}{\pi m}\right)^{1/2} \frac{P_G}{(P_G - P_B)} \tag{3.2.5}$$

where η is the viscosity of the viscosity of the bulk phase. This gives a momentum limited nucleation rate of:

$$J_\eta \approx N \frac{\gamma}{\eta}\left(\frac{\gamma}{kT}\right)^{1/2}\left(1-\frac{P_B}{P_G}\right)\exp\left(-\frac{\Delta G_m}{kT}\right) \tag{3.2.6}$$

Finally, the corresponding δ_m for mass transfer limited nucleation is:

$$\delta_m = \frac{2\gamma}{D_{AB}(2\pi m k T)^{1/2}(C_v - C_l)} \tag{3.2.7}$$

which leads to:

$$J_m \approx ND_{AB}(C_v - C_l)\left(\frac{kT}{\gamma}\right)^{1/2}\left(1-\frac{P_B}{P_G}\right)\exp\left(-\frac{\Delta G_m}{kT}\right) \qquad (3.2.8)$$

where C_v is the concentration of the vapor and C_l is the concentration of the liquid or bulk phase.

Attar also discusses heterogeneous nucleation in the manuscript and develops criteria by which to determine if the mode of nucleation is homogeneous or heterogeneous. Unfortunately, these criteria are based on the diffusion coefficient of the system, a diffusion characteristic length, and in part, on the reaction rate constant for the pyrolysis decomposition reaction. The dependence of this approach on the reaction rate constant limits the range of applicability of his criteria only to similar systems with decomposition reactions.

In general, Attar claims that the bubble formation in coal is momentum transport limited. His approach of developing different limiting nucleation rate equations, however, has not been widely adopted in literature pertaining to bubble formation or nucleation in viscous polymer systems.

Colton and Suh (1987) were some of the first investigators to use classical nucleation theory to model the formation of a thermoplastic foam. They looked at both homogeneous and heterogeneous nucleation of a micro-cellular polystyrene foam. Nitrogen gas was used as the blowing agent.

The authors start with the standard expression for the Gibbs free energy (Equation 2.2.3):

$$\Delta G = \frac{4\pi r^3}{3}\Delta P + 4\pi r^2 \gamma$$

They assume that ΔP can be reasonably approximated as the saturation pressure used to impregnate the nitrogen into the polymer. They also assume that the surface tension needed for Equation 2.2.3 can be estimated by a simple weighted average of the different components in the system:

$$\gamma = \gamma_p w_p + \gamma_n w_n \tag{3.2.9}$$

where γ_p and γ_n are the surface tension of the polymer and the nitrogen respectively, w_p is the weight percent of the polymer in the mixture, and w_n is the weight percent of the nitrogen that has been absorbed in the polymer.

Colton and Suh saw the need to modify Equation 2.2.3, however, because it does not adequately represent ΔG for polymeric systems. In these polymeric systems, ΔG should incorporate changes in the free volume of the polymer associated with the nucleation process. In order to account for these changes, the authors propose a number of volumetric corrections. These include the volume changes due to: thermal expansion, the addition of the dissolved gas, and the presence of other insoluble additives contained in the polymer matrix.

The volume change due to thermal expansion is estimated by using the coefficient for thermal expansion, α:

$$\Delta V_{Temp} = \alpha(T - T_0) \tag{3.2.10}$$

where T is the system temperature and T_0 is a reference temperature. The volume change due to insoluble or immiscible materials contained in the polymer matrix is generally assumed to be equal to the volume on a mass basis (as opposed to a molar basis) of the additives. Finally, the volume change due to the dissolved gas (nitrogen) can be estimated from:

$$\Delta V_{Gas} = \frac{V\Delta P}{3B(T)} \tag{3.2.11}$$

In Equation 3.2.11, V is the volume of the polymer after the changes due to temperature and other additives have already been considered and B(T) is the bulk modulus of the polymer which is a function of temperature.

Each of these terms are combined into a single correction for the polymer volume:

$$V(T,P,C) = [V_0 + \alpha(T - T_0)]\left[1 + \frac{\Delta P}{3B(T)}\right] + V_{Additives} \tag{3.2.12}$$

Here, V_0 is the volume of the pure polymer at the reference temperature, T_0. The change in free volume is then calculated assuming that the free volume is a known percentage of the total polymer volume. In the case of polystyrene near its glass transition temperature, Russel (1980) indicates that the free volume is about 13 percent. Based on this, Colton and Suh (1987) write the free volume of the polymer as:

$$V_{Free} = 0.13V(T,P,C) \tag{3.2.13}$$

The authors attempt to incorporate these changes in free volume into the free energy and the nucleation rate. They note that changes in free volume affect the distances between the polymer chains thus affecting the potential energy of the system. They try to model the interactions between chains by assuming that the chains act as points with spherically symmetric potential fields around them. To do this, the authors estimate the distance between the chains, z, is:

$$z(T,P,C) = 2\left[\left(\frac{3}{4\pi L}\right)V(T,P,C)\right]^{1/3} \tag{3.2.14}$$

where L is Avogadro's number. The potential energy is estimated by using a Lennard-Jones 6-12 potential:

$$U(z(T,P,c)) = \epsilon \left[\left(\frac{z_0}{z(T,P,c)} \right)^{12} - 2 \left(\frac{z_0}{z(T,P,c)} \right)^{6} \right] \tag{3.2.15}$$

In Equation 3.2.15, ϵ is the depth of the energy minimum and z_0 is the equilibrium inter-chain distance. Colton and Suh use a zero-point enthalpy method cited in van Krevelen (1990) to estimate ϵ and cite a value of 6.7 Angstroms for z_0 (Yannas and Luise, 1983). Based on this, Colton and Suh calculate a change in potential energy for the system from:

$$\Delta U = U(z(T,P,c)) - U(z(T_0,P_0)) \tag{3.2.16}$$

They modify the free energy calculated from Equation 2.2.3 by subtracting this change in potential energy, ΔU, leading to a modified free energy:

$$\Delta G^{*} = \Delta G - \Delta U \tag{3.2.17}$$

Substituting Equation 3.2.17 for ΔG into the classical nucleation equation gives it the following form:

$$J = \psi_0 C_0 \exp\left(\frac{\Delta G^{*}}{kT} \right) \tag{3.2.18}$$

where ψ_0 is the frequency at which critically sized clusters are transformed into stable bubbles by the addition of gas molecules and C_0 is the initial gas concentration.

With regard to heterogeneous nucleation, Colton and Suh take a more traditional approach and do not apply any correction or modification for changes in free volume to the Gibbs free energy. The resulting equation for the heterogeneous nucleation rate is:

$$J_{Het} = \psi_1 C_{Het} \exp\left(\frac{\Delta G_{Het}}{kT} \right) \tag{3.2.19}$$

In this equation, C_{Het} is the concentration of heterogeneous nucleation sites and ψ_1 is identified as a frequency factor similar to ψ_0, which represents the frequency that gas

molecules impinge on clusters. They describe ψ_1 as a complex function based on the vibrational frequencies of the gas atoms and the activation energy of diffusion in the polymer matrix. They do not define this term, however, in any mathematical sense. In Equation 3.2.19, ΔG_{Het} is defined as:

$$\Delta G_{Het}\Big|_{n_c} = \frac{16\pi\gamma^3 F}{3\Delta P^2} \tag{3.2.20}$$

The term, F, which is a function based on a wetting angle, is defined in Equation 2.3.4 (Section 2.3) and is consistent with other heterogeneous nucleation literature.

In a follow-up manuscript, which presents the experimental work to support the theoretical developments, Colton and Suh (1987) revert back to the traditional expression for the homogeneous excess free energy given in Chapter 2, Equation 2.2.7:

$$\Delta G_m = \frac{16\pi\gamma^3}{3(\Delta P)^2}$$

They do not use the modified form of ΔG (Equation 3.2.17) that they developed when comparing experimental results and model predictions for the polystyrene/nitrogen system because the change to ΔG is insignificant. The authors investigated a variety of different polystyrenes manufactured commercially by Dow and Monsanto covering a fairly wide range of molecular weights and polydispersities (number average molecular weights from about 43,000 to 120,000 and polydispersities from 2.38 to 4.12 were reported in the work). Additionally, the authors investigated a wide range of N_2 saturation pressures from 1.5 MPa to 13.8 MPa. During the gas saturation step, all of the samples were held at a constant temperature of 294 K. The results they obtain for the homogeneous case, however, are not adequate.

In the heterogeneous experiments, zinc stearate was the most popular nucleating agent. It was either already present in the polystyrene Colton and Suh used in their investigation or it was compounded into the polymer matrix in an extruder. Other nucleating agents described in the work included stearic acid and carbon black. No data or reference is given for the wetting angles used to calculate the heterogeneous nucleation rates in the second manuscript, however, Colton and Suh discuss the values of typical wetting angles as being about 20° in their first manuscript. The results obtained using Colton and Suh's (1987) heterogeneous model are similar in quality to those obtained from their homogeneous model. As with the homogeneous case, the model and experimental data cannot be correlated and additional work on their theory is necessary.

Kumar and Weller (1992) use the Colton and Suh model, also with very poor results for the prediction of nucleation rates (measured as cell density in cells/cm^3) in a polycarbonate system impregnated with carbon dioxide that they thought was homogeneous. In all cases, the model predicted saturation pressures above 50 MPa, while experimentally only pressures between 2-7MPa were needed to obtain the same cell densities. It appears that the classical homogeneous model provides an unrealistically high energy barrier for the nucleation phenomena and that the system is in fact a heterogeneous one. As such, their results may have been better described by a heterogeneous model. The heterogeneous model would predict a lower energy barrier because of the influence of the wetting angle in the calculation. This would result in higher nucleation rates at lower pressures. If the heterogeneous model had been used, however, it would have been difficult to determine the concentration and type (wetting angles, etc.) of heterogeneous impurities.

Han and Han (1990) also attempt to improve CNT by modifying the Gibbs free energy for the system. While the method they use is different from Colton and Suh (1987), the basic concept of modifying ΔG is similar. Han and Han propose two distinct changes to the free energy of formation. The first is based on the non-ideality of polymer solutions and the second is the fact that CNT assumes that the critical clusters are in equilibrium with the metastable bulk phase. In a polymer system, nucleation always occurs under supersaturated conditions. The equilibrium vapor pressure and the pressure inside the gas bubble are not necessarily expected to be equal. It is also important to point out that Han and Han were not working with polymer melts, but rather concentrated polymer solutions.

In order to address the issue of the polymer system being far from ideal, Han and Han note that according to Flory-Huggins theory (Flory, 1953) the change in chemical potential for the solvent will be:

$$\mu_l - \mu_l^0 = kT\left[\ln\Phi_1 + \left[1 - \frac{1}{m_V}\right]\Phi_2 + \chi\Phi_2^2\right] \tag{3.2.21}$$

The terms in Equation 3.2.21 are defined as follows: μ_l is the chemical potential of the solvent in the mixture, μ_l^0 is the chemical potential of pure solvent, Φ_1 and Φ_2 are the volume fractions of the solvent and polymer respectively, and m is the ratio of the molar volume of the polymer to the molar volume of the solvent. Assuming that m is a very large number, Han and Han reduce Equation 3.2.21 to:

$$\mu_l - \mu_l^0 = kT\left(\ln\Phi_1 + \Phi_2 + \chi\Phi_2^2\right) \tag{3.2.22}$$

They derive the free energy change of the solvent molecules in the presence of the polymer molecules, ΔG_t, by multiplying Equation 3.2.22 by n, where n is the number of solvent molecules in a critical cluster to get:

$$\Delta G_t = nkT\left(\ln \Phi_1 + \Phi_2 + \chi \Phi_2^2\right) \tag{3.2.23}$$

The second step Han and Han (1990) take is to correct for the fact that the critical cluster is not in equilibrium with the bulk metastable phase. They define the degree of super-saturation as s:

$$s(t) = \frac{(C_0 - \Delta C(t))}{C_e(t)} \tag{3.2.24}$$

The term C_0 is the initial concentration of the volatile component (or blowing agent) at time t = 0, ΔC is the change in concentration of the volatile component at time t, and $C_e(t)$ is the equilibrium concentration corresponding to the partial pressure of the volatile component in the vapor phase at time t. Han and Han use this to write the free energy change due to supersaturation, ΔG_s:

$$\Delta G_s = nkT \ln\left[\frac{(C_0 - \Delta C(t))}{C_e(t)}\right] \tag{3.2.25}$$

Finally, ΔG_t and ΔG_s are combined with the classical ΔG_m to obtain a modified free energy for polymer systems, ΔG^*:

$$\Delta G^* = \Delta G_m - \Delta G_t - \Delta G_s \tag{3.2.26}$$

Equation 3.2.26 is then used in the typical Arrhenius style nucleation rate equation:

$$J = N\psi \exp\left(-\frac{\Delta G^*}{kT}\right) \tag{3.2.27}$$

The pre-exponential contains the usual terms, N for the number of blowing agent molecules in the system and ψ is the frequency factor as in CNT described in Chapter 2, however, it does not explicitly contain a Zeldovich correction. At this point, Han and Han, deviate further from the CNT treatment of this factor. While they cite that ψ represents the frequency that gas molecules impinge on the critical clusters in their work, they do not adopt the usual values based on the kinetic theory of gases. Instead, they propose an empirical equation that has two fitted parameters.

$$\psi = \psi_a \left(\frac{D(T)}{4\pi r_c^2} \right) \exp\left(-\frac{\psi_b}{T} \right) \tag{3.2.28}$$

In Equation 3.2.28, ψ_a and ψ_b are constants based on experimentally determined nucleation rate data and D(T) is the diffusivity of the volatile (or blowing agent) molecule which is a function of temperature. Han and Han reference a free volume theory method for estimating D(T) developed by Vrentas, Duda, and Hsieh (1983).

The specific system studied by the authors was polystyrene with helium as the blowing agent. Toluene was used as the solvent and polymer concentrations of 40, 50 and 60 wt% were used. Experiments were run in two groups. The first group included three temperatures, 423, 433, and 443 K at a pressure of about 2.9 MPa. All three weight fractions were included in this group. The second group included two temperatures, 433 and 443 K at a pressure of about 4.2 MPa. Only the 50 and 60 wt% solutions were included in this group. The authors had the polystyrene made specifically for this test with no additives to minimize or eliminate heterogeneous nucleation sources. Additionally, the authors took care to minimize the possibility of contamination in their sample preparation steps to avoid unwanted sites for heterogeneous nucleation. Laser

light scattering was used to measure the nucleation phenomena. The development of this experimental technique was a significant aspect of the first Han and Han manuscripts. The authors point out several advantages over the rising drop method previously used to measure nucleation temperatures in a polystyrene benzene system (Prud'homme, Gregory, and Andres, 1985). The advantages include the ability to examine the size distribution of the bubbles as well as the critical bubble or cluster size.

Given the use of fitted parameters, it is not surprising that Han and Han have reasonably good correlation between their model and the experimental data obtained from the polystyrene-(toluene)/helium system examined. Ultimately, they provide a nucleation rate equation for the system with the values of the necessary fitted parameters as a final conclusion for their work. Unfortunately, this equation is specific to that system and cannot be generalized. Further, utilizing Han and Han's method for other systems requires experimental nucleation rate data that is, in general, not readily available.

Goel and Beckman (1994) also attempted to use CNT to model the formation of a polymeric foam. They studied polymethylmethacrylate (PMMA) saturated with supercritical carbon dioxide. The CNT model they use maintains the same exponential term (Equation 2.2.7 for ΔG) as Colton and Suh's (1987) model with a slightly different pre-exponential:

$$J_{Homo} = C_0 Z \psi_1 \exp\left(\frac{-\Delta G}{kT}\right) \tag{3.2.29}$$

The pre-exponential factor is similar to the one used by Colton and Suh in that it is a combination of the concentration of gas molecules initially present in the system and a frequency factor for the net impingement rate of these molecules joining the clusters.

The difference is that Goel and Beckman included the Zeldovich factor in this frequency factor in their manuscript whereas Colton and Suh did not. This factor, which was included implicitly in the original work has been separated out here in Equation 3.2.29 to be consistent with the derivation in Chapter 2 (Equation 2.2.20).

Goel and Beckman use the traditional Gibbs free energy similar to Colton and Suh's final work, however, they do make one significant change to the way that they calculate the surface tension. Rather than using the simple weight fraction approach of Colton and Suh, they use a correlation provided by Reid, et al (1987):

$$\gamma_{mix}^{1/4} = \overline{\rho}_{mix} \sum_{i=1} \frac{y_i \gamma_i^{1/4}}{\overline{\rho}_i} \tag{3.2.30}$$

In Equation 3.2.30, y_i is the mole fraction of the i^{th} species and $\overline{\rho}$ is either the molar density of the i^{th} component or the mixture depending on the subscript. Then, given that the surface tension of a supercritical fluid is essentially zero, Equation 3.2.30 becomes:

$$\gamma_{mix} = \left(\frac{\overline{\rho}_{mix}}{\overline{\rho}_{polymer}} \right)^4 y_{polymer}^4 \gamma_{polymer} \tag{3.2.31}$$

This can be further simplified to:

$$\gamma_{mix} = \gamma_{polymer} \left(\frac{\rho_{mix}}{\rho_{polymer}} \right)^4 \left(1 - w_{gas} \right) \tag{3.2.32}$$

where ρ is now the mass density of the mixture or the polymer and w_{gas} is the weight fraction of the absorbed gas.

In their work, Goel and Beckman (1994) attempt to create a homogenous polymer system. To that end, they polymerize neat (no solvents present) PMMA with UV light in the presence of 1000 ppm of azo bis(iso-butyronitrile) or AIBN, a free radical initiator.

This approach minimizes possible contaminants from the initiator and avoids solvents that could act as heterogeneous nucleation sites. Thus, they have a system that is as homogeneous as possible. There are still issues related to unreacted monomer and low molecular weight oligomers but the systems should be made up entirely of repeating PMMA units (with monomer assumed to be nearly equivalent to a repeat unit) and carbon dioxide blowing agent. The AIBN units at the beginning of the chains should be negligible because of their very low concentration. Even with the different approach used to estimate the surface tension, Goel and Beckman still needed to use a fitted parameter as a first approximation for the frequency factor to obtain results that were reasonable when compared to experimental data.

Other approaches to modifying the surface tension was also considered by Lee and Flumerfelt (1996) and Su and Flumerfelt (1996). This approach utilized the Lifshitz theory to modify the contribution of the intermolecular potential fields between the polymer chains that affect the surface tension. Lee and Flumerfelt (1996) and Su and Flumerfelt (1996) both estimate local or microscopic surface tensions that are evaluated through the use of Hamaker constants (see below). Both groups of authors use the same experimental system to study the nucleation phenomena, polyethylene with nitrogen as the blowing agent. The range of saturation pressures examined in the Lee and Flumerfelt work was from about 4 to 15 MPa while that of the Su and Flumerfelt work was done at one pressure, 11 MPa. Both works cover a fairly narrow temperature range, 386-423 K and 408-438 K, respectively.

From Lifshitz theory, the Hamaker constant, A_{iji}, is defined as follows (Ross and Morrison, 1988):

$$A_{iji} = 12\pi z^2 G(z) \tag{3.2.33}$$

where z is the separation distance between molecules and $G(z)$ is the non-retarded Lifshitz-van der Waals free energy.

Lee and Flumerfelt calculate Hamaker constants for the components in their system (polyethylene and nitrogen) using Equation 3.2.33. These Hamaker constants are then used with a surface mass density coefficient, κ, to estimate local or microscopic surface tensions. The surface mass density coefficient, κ, is calculated from the following:

$$\kappa = \frac{\left[-3z_1 z_2\left(\rho_1^* y_1 + \rho_2^* y_2\right)\left(2\pi z_1^2 z_2^2 \gamma - A_{212} z_2^2 y_1^2 - A_{212} z_1^2 y_2^2\right)\right]}{\left[4A_{212} O1\right]} \tag{3.2.34}$$

where O1 is defined as:

$$\begin{aligned} O1 = {} & z_1 z_2^3 \rho_1^* y_1^2 - 2z_1 z_2^3 \rho_1^* y_1^3 + z_1^3 z_2 \rho_1^* y_1 y_2 + z_1 z_2^3 \rho_2^* y_1 y_2 + \\ & z_1^3 z_2 \rho_2^* y_2^2 - 2z_2^4 \rho_2^* y_1^2 y_2 - 2z_1^4 \rho_1^* y_1 y_2^2 - 2z_1^3 z_2 \rho_2^* y_2^3 \end{aligned} \tag{3.2.35}$$

In Equations 3.2.34 and 3.2.35, ρ_i^* is the number density of the i^{th} component, γ is the macroscopic surface tension of the system, A_{212} is the Hamaker constant for component 2 separated by component 1 through an intermolecular separation distance of z_1, and z_2 is defined as the repeat unit interaction distance. It is necessary to define what Lee and Flumerfelt (1996) refer to as the intermolecular separation distance, z_1, and as the repeat interaction distance, z_2, in order to allow the calculation of the local surface tension above. The intermolecular separation distance is:

$$z_1 = 2\left(\frac{3\bar{V}_{liquid}}{4\pi L}\right)^{1/3} \tag{3.2.36}$$

The repeat interaction distance is:

$$z_2 = 2\left(\frac{3\overline{V}_{Polymer}}{4\pi L}\right)^{1/3} \tag{3.2.37}$$

In Equation 3.2.36, $\overline{V}_{liquid}$ is the liquid molar volume of the blowing agent dissolved in the polymer matrix. This quantity is substituted for by the molar volume of the polymer repeat unit, $\overline{V}_{polymer}$, in Equation 3.2.37. The surface tension calculated in Equation 3.2.38 is then used in the Equation 2.2.20 to calculate nucleation rates.

The Hamaker constant and the surface mass density coefficient are then used to calculate the microscopic or local surface tension as follows:

$$\gamma_{local} = \frac{1}{\pi z_1^2 R_1^{*2}} O2 \tag{3.2.38}$$

where

$$R_1^* = \frac{r}{\left(z_1/2\right)} \tag{3.2.39}$$

and

$$\begin{aligned} O2 = {} & \frac{A_{212}\kappa y_1}{3R_1^*} - A_{212}\kappa R_1^* y_1 - \frac{2A_{212}\kappa R_1^* y_1}{3} - \frac{5A_{212}y_1^2}{18} + \frac{A_{212}R_1^{*2}y_1^2}{2} - \\ & \frac{A_{212}z_1\kappa R_1^* y_2}{z_2} - \frac{5A_{212}y_2^2}{18} + \frac{4A_{212}\kappa R_1^*\rho_1^* y_1^3}{3\left(\rho_1^* y_1 + \rho_2^* y_2\right)} + \\ & \frac{4A_{121}z_1^3\kappa R_1^{*2}\rho_1^* y_1 y_2^2}{3z_2^3\left(\rho_1^* y_1 + \rho_2^* y_2\right)} + \frac{A_{212}z_2\kappa y_2\left(\rho_1^* y_1 + 4R_1^{*3}\rho_2^* y_1^2 + \rho_2^* y_2\right)}{3z_1R_1^*\left(\rho_1^* y_1 + \rho_2^* y_2\right)} + \\ & \frac{A_{212}z_1^2R_1^{*2}y_2^2}{2z_2^2} - \frac{2A_{212}z_1^2\kappa R_1^{*2}y_2}{3z_2^2} + \frac{4A_{212}z_1^2\kappa R_1^{*2}y_2^2}{3\left(\rho_1^* y_1 + \rho_2^* y_2\right)z_2^2} + \\ & \frac{A_{212}y_2^2\ln\left(z_2/\left(z_1R_1^*\right)\right)}{3} - \frac{A_{212}y_1^2\ln R_1^*}{3} \end{aligned} \tag{3.2.40}$$

In addition to the detailed focus of expressing the surface tension as a function of a Hamaker constant, and system specific variables such as molecular and / or repeat unit

interaction distances, molar fractions of each component, and cluster radius, Lee and Flumerfelt also re-derive the critical free energy (termed as work in their manuscript) based on an overall integral energy balance and the integral form of the Clausius-Duhem inequality. Ultimately, using this alternative approach to determine the work necessary to form a critical cluster, the authors re-derive the standard free energy of formation of clusters used in CNT. By doing so, they have provided a sound method for estimating surface tensions in a polymer system with a dissolved gas, but they do not significantly alter the CNT Equation (2.2.20).

With regard to estimating the surface tension, Su and Flumerfelt (1996) took a similar but simplified approach to Lee and Flumerfelt (1996). Their focus is on accurately measuring what effect the dissolved gas in the polymer has on the surface tension of the system. The equation they developed for the surface tension is again based on Lifshitz theory:

$$\gamma = \frac{A_{212} y_1^2}{8\pi r^2}\left(-\frac{5}{18}+\frac{2r^2}{z_1^2}-\frac{\ln(2r/z_2)}{3}\right)+\frac{A_{212} y_2^2}{8\pi r^2}\left(-\frac{5}{18}+\frac{2r^2}{z_2^2}-\frac{\ln(2r/z_1)}{3}\right) \quad (3.2.41)$$

They point out that macroscopic surface tensions are measured at the interface between two unbounded phases or in the limit as r $\rightarrow \infty$ thus they were able to reduce Equation 3.2.41 to the following simplified form:

$$\gamma = \frac{A_{212}}{4\pi}\left(\frac{y_1^2}{z_1^2}+\frac{y_2^2}{z_2^2}\right) \quad (3.2.42)$$

The surface tensions calculated in Equation 3.3.42 are then used in Equation 2.2.20 to estimate nucleation rates. The authors are able to show good correlation between predicted and experimental surface tensions but the CNT model still over predicts nucleation rates when compared to experimental data.

Ruengphrathuengsuka (1992) modified the homogeneous CNT by suggesting a slightly different form for the free energy of nucleation based on the system being non-ideal. While this author is not the first to come up with a non-ideal correction (Colton and Suh, 1987; Han and Han, 1990), he did it in a slightly different way. Ruengphrathuengsuka suggested the following form for ΔG:

$$\Delta G = V\Delta P - A\gamma + \frac{\rho^{(G)}\mu_G^{(L)}V_G}{MW} \tag{3.2.43}$$

where $\rho^{(G)}$ the density of the blowing agent in the vapor phase, $\mu_G^{(L)}$ is the chemical potential of the blowing agent in the liquid phase, V_G is the volume of the blowing agent, and MW is the molecular weight of the blowing agent. All other terms are consistent with previous definitions. The author also notes that:

$$\mu_G^{(L)} = kT\ln\left(\varphi_G^{(L)}\right) \tag{3.2.44}$$

In Equation 3.2.44, $\varphi_G^{(L)}$ is the activity coefficient of the blowing agent in the liquid phase. This activity coefficient is estimated using the Flory-Huggins equation. The critical value of ΔG is found in the traditional way. When ΔG is maximized with respect to r, the cluster radius, the following expression for ΔG_m is obtained:

$$\Delta G_m = \frac{16\pi}{3}\frac{\gamma^3}{\left[\Delta P + \frac{\rho^{(G)}\mu_G^{(L)}}{MW}\right]^2} \tag{3.2.45}$$

This free energy term is then used in the exponential term in place of the usual expression for ΔG:

$$\Delta G_m = \frac{16\pi\gamma^3}{3\Delta P^2} \tag{3.2.46}$$

Similar to Attar, Ruengphrathuengsuka also included a correction for thermal and mass transfer limitations. The parameter for thermal limitations is defined as follows:

$$\delta_t = \frac{Rh_v\alpha}{(2\pi mkT)^{1/2}K}\left(\frac{\partial P_v}{\partial T}\right)_{C_B T_B} \tag{3.2.47}$$

The one for mass is:

$$\delta_m = \frac{R_v}{(2\pi mkT)^{1/2}D_{AB}}\left(\frac{\partial P_v}{\partial C}\right)_{C_B T_B} \tag{3.2.48}$$

In these equations, α is the thermal diffusivity of the fluid, which is $K/\rho C_p$, where K is the thermal conductivity of the liquid, ρ is the density, C_p is the heat capacity, D_{AB} is the diffusion coefficient, P_v is the vapor pressure, T_B is the temperature of the bulk liquid at equilibrium, and C_B is the concentration of blowing agent in the bulk liquid. Unfortunately terms R and R_v are undefined in the original work. Based on Ruengphrathuengsuka's development, both of the terms, δ_t and δ_m must be dimensionless. A dimensional analysis of Equations 3.2.47 and 3.2.48 indicates that R has units of g-sec/cm and R_v has units of g-cm. Combining all of this, Ruengphrathuengsuka comes up with the following homogeneous steady state nucleation rate equation:

$$J = \frac{C_0}{1+\delta_t+\delta_m}\left[\frac{2\gamma}{\pi m}\left(1-\frac{\rho^{(G)}\mu_G^{(L)}r_c}{\gamma MW}\right)\right]^{1/2}\exp\frac{-\Delta G_m}{kT} \tag{3.2.49}$$

where ΔG_m is defined in Equation 3.2.45.

Using this equation, the author does a theoretical sensitivity study for low-density polyethylene with N_2 as the blowing agent. The work focused on a combination of

nucleation and bubble growth. Experimental results (determination of final foam density) were correlated to the complete model, but a clear connection to the nucleation rate could not be obtained. In examining the construct of Equation 3.2.49, there are correction factors that should improve the results obtained versus those obtained from CNT, which always over predicts the nucleation rates. The first correction in the denominator of the exponential term ($\rho^{(G)}\mu_G^{(L)}/MW$ from Equation 3.2.45) reduces the value of ΔG_m. The second correction term is in the denominator of pre-exponential term (refer to the $1+\delta_t+\delta_m$ in Equation 3.2.49), and it will also help reduce the predicted result. The theoretical sensitivity studies using the nucleation model did show the typical trends for all the various well-known relationships (i.e. the effect of surface tension on critical bubble size). The results of the model, which in general, relate to foam density (not nucleation rate) are presented as non-dimensionalized ratios relative to a standard set of results. There is one result specific to a nucleation rate which is also reported as a non-dimensional ratio (nucleation rate for a given set of conditions compared to the nucleation rate of the model base case). As will be seen below, Shafi et al. (1996) did some work using this model, but reverted back to a more traditional form in subsequent efforts. Without knowing what R and R_v are, it is difficult to evaluate the true effectiveness of the model.

Shafi and Flumerfelt (1996) have proposed a model combining nucleation and bubble growth. The work simply uses the Laplace-Kelvin Equation (2.2.4) from CNT as the starting point for bubble growth calculations. Additionally, they used the modified CNT equation developed by Ruengphrathuengsuka to determine nucleation rates. While the work includes a nucleation model, the focus of it seems to be clearly on bubble

growth. The results that are obtained are generalized and presented in non-dimensional form since the integral mass and momentum equations are solved in a non-dimensionalized form. The authors use hypothetical parameters from an arbitrary polymeric system in their model.

A second manuscript by Shafi, Lee and Flumerfelt (1996) also combine bubble nucleation and bubble growth in one model. In this case, however, the authors adopt the nucleation model proposed by Lee (1995). Lee attempted to improve the CNT by incorporating rheological effects into the calculation of the Gibbs free energy. In essence, rather than assuming all of the surface energy contributions can be adequately described by an appropriate surface tension, Lee attempted to incorporate the energies required to overcome the viscous and elastic effects. The exponential term in the CNT equation is modified accordingly in an attempt to incorporate these additional forces, however, the classical pre-exponential term is retained:

$$J = N\left(\frac{2\gamma}{\pi m}\right)^{1/2} \exp\left(\frac{-16\pi\gamma^{3}}{3kT\left(\Delta P - I + P_i \ln\frac{\varphi}{Z'}\right)^{2}}\right) \tag{3.2.50}$$

In Equation 3.2.50, Z' is the compressibility of the dissolved gas solute in the molten polymer matrix, φ is the activity coefficient of the dissolved gas solute, and I is the elasticity number for nucleation. It is a function of the rheology of the system and can be calculated from the following:

$$I = \int_0^1 \frac{9}{2\tau} \ln\left(1 + \tau \frac{\left(\left(1-\vartheta^3\right)^{4/3} + 2\left(1-\vartheta^3\right)^{-2/3} - 3\right)}{3}\right) \frac{d\vartheta}{\vartheta^4} \sum_{k=1}^{m} \frac{G_k^*}{4N_{De}} \tag{3.2.51}$$

In Equation 3.2.51, τ is the Larson parameter, ϑ is the ratio of characteristic bubble radius to the actual bubble radius, G_k^* is the modulus of the polymer, and N_{De} is the Deborah number defined as relaxation time, λ_t, divided by the bubble growth time, t_c.

Shafi et al. (1996) creates a dimensionless nucleation equation and couples it to an elaborate bubble growth model. The coupled equations are solved simultaneously using a variety of numerical techniques. Theoretical sensitivity studies are completed using the model, but the results are not correlated to experimental data. The study included the effect of both the Peclet number and the Solubility number on bubble growth dynamics. The Peclet number is defined as the ratio of the surface tension squared to the product of the diffusion coefficient, pressure difference, and viscosity. The Solubility number is the product of the Henry's constant, the universal gas constant, and temperature. The simulation parameters were based on a low-density polyethylene system using nitrogen as the blowing agent.

Two other works, one by Shafi and Flumerfelt and the other by Shafi et al. (both 1997) are also more concerned with a coupled nucleation and bubble growth model. In these works, however, the authors revert to the classical form of the heterogeneous nucleation equation (Equation 2.3.6) with one subtle correction. In their work, they add a correction factor, $\wp$, to the pre-exponential term to account for the surface area of the nucleating agent per unit volume of bulk metastable phase. This simple correction term changes the equation to:

$$J = \wp N_G^{2/3} \frac{1+\cos\theta}{2}\left(\frac{2\gamma}{\pi m F}\right)^{1/2} \exp\frac{-16\pi\gamma^3 F}{3kT\left(P_G - P_B\right)^2} \tag{3.2.52}$$

In both works, however, the emphasis remains on predicting a foam with an existing nucleation model and a bubble growth model. The inclusion of the correction term for the nucleating agent surface area relative to the volume of the metastable phase is not a significant improvement to the theory. Colton and Suh (1987) used a similar approach based on the concentration of the nucleating agent particles to account for the effect from the nucleating agent. Shafi et al. simply scaled this correction factor differently. As in their previous works in 1996, the results are presented in dimensionless terms as this is how the authors have solved the complicated set of coupled equations created by the model. Again, the simulations are based on hypothetical parameters, and not necessarily based on experimental data.

The work of Shafi et al. (1996) was extended by Joshi et al. (1998) who did not further alter the nucleation model. As in the previous works by Shafi et al. cited above, Joshi, et al. also employs a dimensionless nucleation equation and couples it to an elaborate bubble growth model. The coupled equations are also solved simultaneously using a variety of numerical techniques. Joshi's work extends the sensitivity studies initially done by Shafi to include the effects of the Deborah number and a dimensionless quantity representing the ratio of back-pressure in the system vs. the pressure difference across the bubble surface on bubble growth dynamics. Shafi's work had only included the Peclet and Solubility numbers. The simulation parameters were based on a system of low-density polyethylene and nitrogen.

The problem with the methods suggested by Shafi et al. and by Joshi et al. is that they require a sophisticated understanding of the rheology of the system under investigation and many of the required parameters may be unavailable or difficult to

measure and / or estimate. The effects of the blowing agent (concentration or chemical type) on the rheological properties of the system also need to be understood. Finally, it is difficult to evaluate the usefulness of this model because the theoretical results are not compared to experimental results.

3.3 Other Mechanisms

Ramesh, Rasmussen, and Campbell (1993, 1994) have suggested an alternative heterogeneous nucleation model for systems of two polymers. The basic principle behind the theory is that a distribution of microvoids is created when the system is cooled if the two polymers have dissimilar thermal expansion coefficients and T_g's. The microvoids are created when one polymer contracts at a faster rate then the other. These microvoids serve as nucleation sites for the foaming process. This eliminates the need for a new phase to be created as is indicated in the classic theory because the voids act as the new phase.

In their work, the authors use a polystyrene-polybutadiene copolymer (high impact polystyrene or HIPS). Nitrogen is used as the blowing agent and the polystyrene is the continuous phase. The polybutadiene phase is discontinuous and forms discrete particles of varying size. The polybutadiene is grafted to the polystyrene, however, therefore the particles have the ability to transmit tensile forces through both polymers.

Further, in this system the polybutadiene has a higher thermal expansion and lower glass transition temperature (by more than 100K) than the polystyrene so that when the mixture is cooled, the polybutadiene continues to shrink after the polystyrene has frozen. This causes stresses in the polybutadiene. The magnitude of the stresses within

an individual rubber particle can be calculated from elasticity theory. Ramesh, Rasmussen, and Campbell give this triaxial tensile stresses as:

$$\Sigma_{rr} = \Sigma_{\theta\theta} = \Sigma_{\phi\phi} = \frac{4(K_B - K_S)(1-\nu_B)g_B g_S \Delta T}{6(1-2\nu_B)g_S + 3(1+\nu_B)g_S} \tag{3.3.1}$$

where K is the thermal conductivity, ν is Poisson's ratio, ΔT is the temperature change upon cooling, and g is the modulus. The subscripts B and S refer to polybutadiene and polystyrene, respectively. The idea of evaluating the stresses can be extended to the polymer matrix and these stresses can be estimated from the following:

$$\Sigma_{rr} = \left(\frac{r_p}{r}\right)\frac{4(K_B - K_S)(1-\nu_B)g_B g_S \Delta T}{6(1-2\nu_B)g_S + 3(1+\nu_B)g_S} \tag{3.3.2}$$

In Equation 3.3.2, r_p is the radius of the polybutadiene particle and r is the radial distance to the center of an inclusion. An inclusion is stiff occluded polystyrene that is trapped inside the polybutadiene particle. From Equation 3.3.2, the authors point out that the radial stress within the matrix depends strongly on r_p so the microvoid size distribution is assumed to follow the polybutadiene particle size distribution. Additionally, through SEM and TEM (scanning and transmitting electron microscopy, respectively), the authors measure the size distribution of the polybutadiene particles and the foam cells. The particles range in size from about 10 angstroms to 1 micrometer. They note that both the particle and the cell distributions follow a log-normal distribution. The slope of both lines is very similar indicating that the polybutadiene particle size has a significant influence on the foam cell size distribution. Based on this, Ramesh et al. (1993, 1994) choose a log-normal distribution to model the foam cell distribution.

The authors also noted that only the largest voids will survive in the rubber particle, the smaller voids are destroyed by coalescence. Based on this, Ramesh et al.

assumes that each particle will only provide one void for nucleation. The authors make the following other assumptions in their model. They neglect mass transfer and assume that a neo-Hookean model adequately describes the elastic forces that oppose the formation of the microvoid, in other words, the forces trying to collapse the void. They assume spherical symmetry and neglect losses in blowing agent to the surroundings during the process. Finally, the authors assume that the solubility of the nitrogen is the same in both polymers (supported by the fact that the Henry's constant for nitrogen in each polymer differ by less than 10%, 0.045 vs. 0.049 $cm^3(STP)N_2/cm^3atm$ for polystyrene and polybutadiene, respectively).

Ramesh et al. start with a material balance on the saturated gas to obtain an equation for the amount of gas remaining in the polymer:

$$K_{h_1}P = K_{h_0}P_0 - \frac{4\pi T_0}{3V_p P_0}\left(\frac{r^3 P}{T} - \frac{r_0 P^{sat}}{T^{sat}}\right) \tag{3.3.3}$$

In this equation, K_h with subscript 0 or 1 is the appropriate Henry's constant for the system, P is the pressure, P^{sat} is the saturation pressure at temperature T^{sat}, P_0 is a reference pressure, T_0 is a reference temperature, V_p is the volume of polymer surrounding the bubble, r is the radius of the bubble and r_0 is the initial radius of the microvoid. The left hand term in the equation represents the volume of the remaining gas in the polymer, the first term on the right is the initial amount of gas in the polymer, the first term in the parentheses is the gas volume in the nucleated bubble and the last term (still in the parentheses) in the expression is the gas volume of the initial microvoid. From this equation, using appropriate expressions for the Henry's constants, the authors are able to calculate the pressure inside the microvoid.

Ramesh et al. next considers the two resisting forces trying to collapse the microvoid. These forces are the surface tension forces and the elastic forces of the polymer. The authors give the following expression for the equilibrium pressure necessary to maintain mechanical equilibrium of the void:

$$\Delta P = \frac{2\gamma(T)}{R} + 2g_c\left[\frac{1}{4}\left(\frac{y+r^3}{y+r_0^3}\right)^{-4/3} + \left(\frac{y+r^3}{y+r_0^3}\right)^{-1/3} - \frac{1}{4}\left(\frac{r^3}{r_0^3}\right)^{-4/3} - \left(\frac{r^3}{r_0^3}\right)^{-1/3}\right] \tag{3.3.4}$$

where the first term is due to the surface tension effects and the second term is due to the elastic effects. In Equation 3.3.4, γ is the surface tension, g_c is the composite modules, and y is what the authors call a convected coordinate transformation variable that represents the amount of polymer surrounding the microvoid. Large values of y indicate that the microvoid behaves as if it is an infinite pool of liquid and small values indicate that it is in close contact with other voids. The latter is similar to the cell model of Amon and Denson (1984). In their model, the internal pressure of the microvoid needs to be greater than the ΔP indicated in Equation 3.3.4 for the void to nucleate and grow. Voids with pressures lower than ΔP will succumb to the external pressures and collapse.

As stated earlier, the authors assume that the cumulative distribution will follow a log-normal behavior. The distribution is then given as:

$$\mathcal{P}_r = \frac{1}{\sigma\sqrt{2\pi}}\int_{-\infty}^{r}\exp\left[\frac{-\left(\log\frac{r}{\bar{r}}\right)}{2\sigma^2}\right]d\log r \tag{3.3.5}$$

In Equation 3.3.5, $\mathcal{P}_r$ is the probability of a given microvoid of size r, and $\bar{r}$ and σ are the logarithmic average and standard deviations, respectively. Ramesh et al. use a mathematical identity to put the distribution function into a more manageable form:

$$\mathcal{P}_r = \frac{1}{2}\left[2 - erfc\left(\frac{\log\frac{r}{\bar{r}}}{\sigma\sqrt{2}}\right)\right] \tag{3.3.6}$$

In Equation 3.3.6, the complimentary error function is denoted as "erfc". The tail of this distribution curve represents the distribution (or population) of microvoids larger than a given radius. In order to determine what the cumulative distribution of microvoids smaller than that limiting size is, this probability needs to be subtracted from 1 or:

$$f_n = N_0(1-\mathcal{P}_r) = \frac{N_0}{2} erfc\left(\frac{\log\frac{r}{\bar{r}}}{\sigma\sqrt{2}}\right) \tag{3.3.7}$$

where the term f_n is the distribution of microvoids in the system (used here analogously to the f_n for the cluster distribution function in the other chapters). N_0 is estimated from the total number of polybutadiene particles present.

Ramesh et al. noted experimentally that particles smaller than 0.6 microns did not create effective microvoids. To account for this in the model they adjusted the parameter N_0 by determining the number of particles that would be larger than this limiting value. This time they use Equation 3.3.7 again, since the particles follow the log-normal distribution to determine the number of particles larger than a certain value:

$$f_n = \frac{n_p}{2} erfc\left(\frac{\log\frac{r_p}{\bar{r}_p}}{\sigma_p\sqrt{2}}\right) \tag{3.3.8}$$

In the equation, the subscript p designates that the particles are at least of a certain cut off size. The term, N_p is estimated as:

$$N_p = \frac{6\Phi}{\pi d^3} \tag{3.3.9}$$

where Φ is the volume fraction of the polybutadiene particles in the nucleated polystyrene, and d is the average domain size of the particle that can be obtained from the particle size distribution.

Ramesh et al. obtain good correlations between their model predictions and experimental results for such things as the effect of polybutadiene particle size and polybutadiene concentration on cell density. It is important to point out that the model does not extend to homogeneous systems, or even heterogeneous systems with low levels of impurities. In the authors' case, the concentration of polybutadiene particles ranged from about 10^8 to 10^{10} particles per cm^3 of bulk phase. This is an adequate number of particles to create sufficient microvoids to support the nucleation phenomena. Generally, commercial HIPS resins have about 6-10 wt% polybutadiene providing for the potential to have a very large number of nucleation sites. Other types of resins could contain significantly lesser amounts of nucleating agents and these resins may need to rely on the more traditional nucleation phenomena which including the creation of a new phase. The model by Ramesh et al. described here disregards this step. Finally, Ramesh et al. (1993, 1994) did not attempt to include the influence of other heterogeneous materials such as zinc stearate, which are commonly found in HIPS resins. This is understandable because these other impurities are probably present in insignificant concentrations when they are compared to the polybutadiene.

The cavity model is another model used to describe the formation of bubbles in polymeric foams from extrusion processes (Lee, 1991; 1994). This type of model was originally proposed to describe the formation of gas bubbles in blood vessels caused by

drastic pressure changes which can be seen after deep sea diving (Harvey, et al., 1944). Figure 3.1 describes the cavity model. Lee suggests that cavities result when thousands of nucleating agent particles clump together to form a porous surface. The surface of these porous clump cannot be completely wetted by a polymer melt creating the cavities. Blowing agent molecules are better able to diffuse into the porous cavities where they can collect at the base of them (see Figure 3.1(a)). As more blowing agent molecules

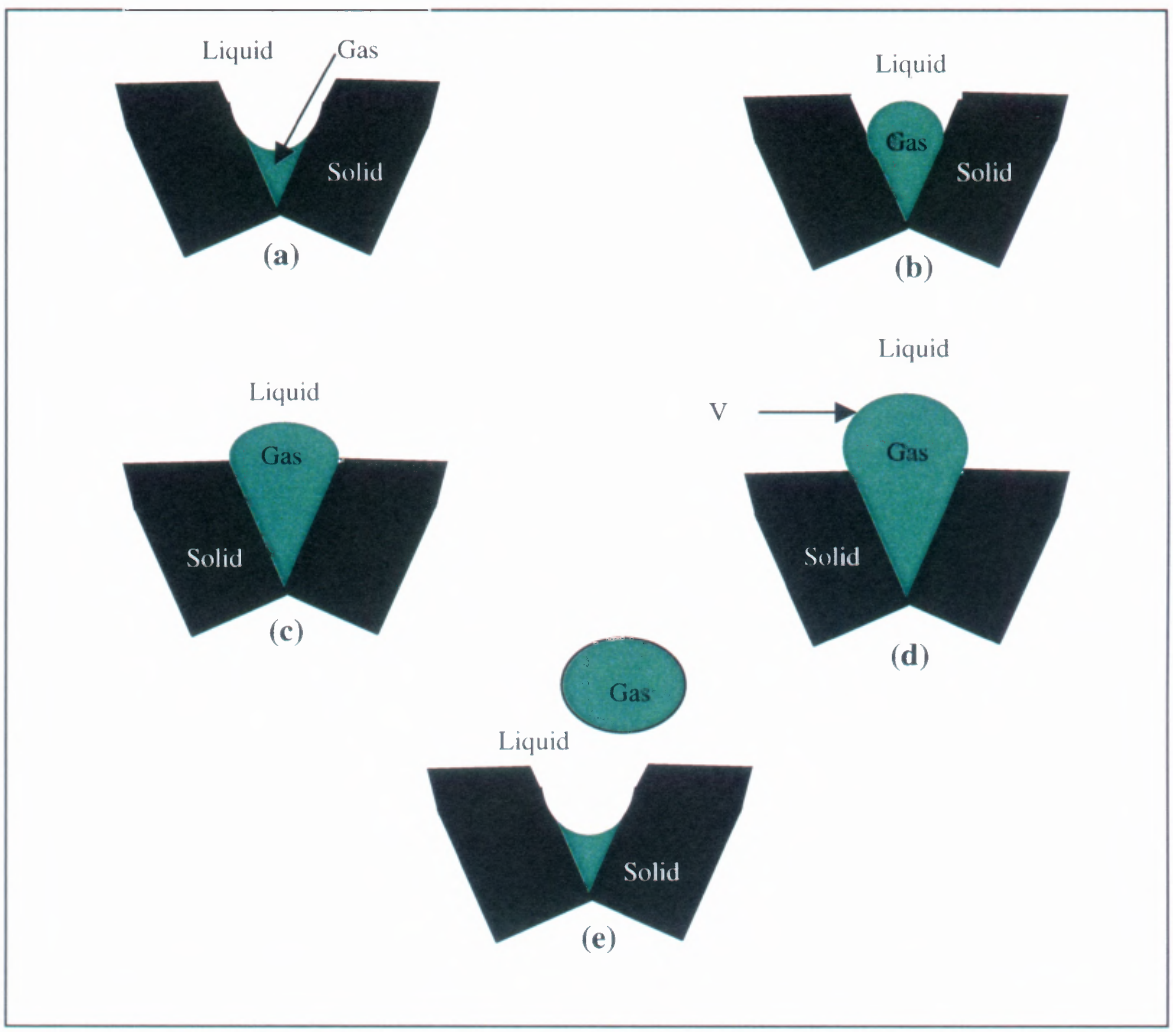

Figure 3.1 Cavity Model Proposed by Lee (1991).

diffuse into the cavities, the bubbles begin to grow filling the voids (Figure 3.1(b)). Lee also indicates that the shape of the bubble meniscus is strongly dependent on the pressure of the system. At a certain point, a bubble will grow large enough to extend beyond the volume of the cavity (Figure 3.1(c)) and it becomes subject to the shear and flow forces in the process (see Figure 3.1(d)). Finally, the bubble continues to grow and detaches from the cavity (Figure 3.1(e)).

The presence of "shear" will help detach the bubble from the cavity in Figure 3.1(d). In order to determine this effect, Lee completes a force balance equating the holding forces and the detaching forces on the bubble. The force balance is summarized below:

Surface Tension = Buoyant + Extensional + Shear (3.3.10)

In mathematical terms, this is:

$$2\pi r\gamma = \frac{4}{3}\pi r^3\left(\rho_l - \rho_g\right) + 3\pi R_p{}^3 \frac{d\bar{v}}{dz} + \frac{\pi}{2}\eta\dot{\gamma}_{avg} \tag{3.3.11}$$

In the above equation, γ is the surface tension, R_p is the radius of the mouth on the porous cavity, and r is the radius of the gas cavity (similar to the cluster radius in previous notations). The terms ρ_l and ρ_g are the densities of the liquid and gas respectively, $\bar{v}$ is the average linear velocity, and $\dot{\gamma}_{avg}$ is the average shear rate in the process.

Lee suggests that the buoyant forces are negligible and the shear forces are more than 2 orders of magnitude larger that the extensional forces, so he defines the Capillary number as:

$$Ca = \frac{R_p\eta\dot{\gamma}_{avg}}{4\gamma} \tag{3.3.12}$$

which is the ratio of shear forces ($R_p \eta \dot{\gamma}_{avg}$) to the surface tension forces (γ). The shear forces are given by the product of the shear rate, $\dot{\gamma}$, and the viscosity, η. Lee indicates that in the limit when R_p is much greater than r, it is not possible for the gas phase to form a large enough angle to slip to the top of the porous cavity and be dislodged. At the other limit, when r is much greater than R_p, the shear rate effects are limited. Based on the inadequacy of these two limits, Lee chooses the situation for R_p = r as a reasonable starting point for the model. He also points out that the shear forces are highly dependent on the degree of superheat in the system. Finally, based on this, Lee suggests that the Capillary number should be used in place of the Gibbs free energy in the exponential term of a typical Arrhenius type nucleation rate equation.

Experimentally, Lee (1991) uses polyethylene with a dichlorodifluoromethane blowing agent as the system and magnesium silicate as a nucleating agent. He blends and gasifies in a twin screw intermeshing counter-rotating extruder. Foams are extruded through a variety of different dies creating different pressure drops. Lee suggests that the key variable is not the nucleation rate, but rather cell density, because the nucleation process is instantaneous as the polymer-gas blend leaves the extruder. The author shows a fairly good correlation between the experimental data and the model, but he does not go into detail about how the pre-exponential constant is determined. He does indicate that this constant is a function of the system. Lee (1994) provides additional experimental evidence in his second work, but again, does not describe how the pre-exponential constant is determined.

For completeness in this chapter, a series of manuscripts focused on experimental methods and / or findings are briefly discussed below. Additionally, a few manuscripts

focusing on polymer devolatilization are mentioned. The manuscripts on experimental techniques generally discuss methods for making polymeric foam, and do not focus on the theoretical treatment of nucleation. The manuscripts on the devolatilization of polymers draw on the natural parallels to the nucleation phenomena since a result of the devolatilization process is the formation of bubbles in the polymer. These bubbles are formed as the volatile component is removed from the polymer matrix.

Ramesh and Malwitz (1995) present a method for extruding water-soluble and biodegradable polyvinyl alcohol with non-CFC blowing agents. The blowing agent used was a methanol-water mixture. A foam growth model coupled with heat transfer effects was used to predict foam densities that were in good agreement with experimental results. The experimental work looked at the effects of two key parameters on foam density, the concentration of cross-linking agent in the polyvinyl alcohol and the concentration of the blowing agent mixture. Foams with densities as low as 35.2 kg/m^3 were obtained.

The design of rapid pressure drop nozzles or rapid decompressive elements necessary to produce microcellular foams is detailed in Park, Baldwin, and Suh (1995). The authors provide an experimental technique to calibrate the nozzles for flow rate and pressure drop and are able to produce a variety of different microcellular polystyrene foams with three differently sized nozzles. The experimental system was high impact polystyrene (HIPS)-carbon dioxide. The choice of HIPS may have been based on the fact that the rubber particles contained in the HIPS copolymer would serve as excellent heterogeneous nucleation sites. The authors refer to the CNT equations as a means to predict the nucleation rate and experimentally determine the effects of different pressure drops on microcellular nucleation. Ultimately, they conclude that the pressure drop rate

plays an important role in determining the cell density, which results from the competing effects of nucleation and bubble growth.

Park and Suh (1996) further detail a continuous extrusion process for manufacturing microcellular HIPS. In addition to looking at how the magnitude of the pressure drop affects cell nucleation as in their first work, the authors also investigate the effect that the concentration of dissolved gas in the polymer has on the nucleation phenomena. The results that are presented indicate that both variables can significantly affect the nucleation process.

In a third manuscript, Park and coworkers further discuss producing microcellular foams from HIPS in a continuous extrusion process (Park, Behravesh, and Venter, 1998). In this work, they improve their earlier results (increased cell density) to some degree by adding a cooling heat exchanger/static mixer to improve the cool down rate for foam. Increasing the cool down rate reduces the amount of bubble collapse and bubble coalescence thereby increasing cell density. The authors report expansion ratio results from 1.5 to 23 and cell densities on the order of 10^{10} cells/cm^3. The authors define the expansion ratio as the total volume of the polymer and gas divided by the polymer volume. As in the previous manuscripts, however, no efforts are made to correlate the experimental results to predictive nucleation rate models.

Baldwin, Park, and Suh (1996) experimentally investigate the formation of polymeric foams from amorphous and semi-crystalline polymers. They use a homopolymer of poly(ethylene terephthalate) (PET) and PET containing a polyolefin nucleating agent (PET-b, where the b designates blend with polyolefin). Carbon dioxide was the blowing agent used for the studies. Their experimental results indicate that the

nucleation mechanism is different between the semi-crystalline and amorphous states. When both polymers were in the semi-crystalline state, they showed similar nucleation mechanisms and a less pronounced cell density dependence on saturation pressure. Additionally, the semi-crystalline polymers had higher (10-1000 times) cell densities when compared to their amorphous counterparts. From the experimental cell density data, the authors concluded that heterogeneous nucleation dominated at low pressure and homogeneous effects were added as pressure was increased. This is based on the fact that there were higher cell densities at higher pressures believed to be the result of higher nucleation rates. The heterogeneous nucleation is based on the PET having sufficient inherent flaws to facilitate the process. In the case of the PET-b, the heterogeneous sites are believed to be the inherent flaws in the PET and the polyolefin nucleating agent that was added. The authors compare their experimental results to CNT and conclude that the CNT was inadequate to describe the phenomena.

As previously mentioned, similarities exist between the formation of polymeric foams and the devolatilization of polymers. Polymers can be devolatilized for a number of reasons. One common reason is to remove unreacted monomers and oligomers from the product after the polymerization reaction. The design and optimization of devolatilization units has been the subject of many investigations and is far beyond the scope of this work. In these investigations, however, experimenters often will indicate the similarities between the formation of volatile vapor bubbles during the devolatilization process and the formation of bubbles from physical blowing agents added to polymers for the purpose of creating foams. Biesenberger and Todd (1983),

Werner (1981), and Biesenberger and Lee (1987) are all references that examine the study of devolatilization and how it can parallel foam nucleation.

3.4 A Need for a New Approach

For a nucleation theory to adequately describe a polymeric system, it needs to correctly represent two phenomena. First, it must accurately identify the Gibbs free energy change associated with the process. This is the exponential term in the classical Arrhenius type nucleation equation. Second, it must accurately determine the rate at which molecules impinge or add to critically-sized clusters. This is the pre-exponential term in the classical Arrhenius type equation that is often used.

As discussed in Sections 3.1-3.3, numerous authors have tried to correct the free energy barrier for polymeric systems. Colton and Suh (1987) appear to have been the first and examined what effect the changes in free volume that occur in a polymeric system would have on ΔG. They found that their modifications, which were based on a Lennard-Jones intermolecular potential force, had only a negligible effect. Colton and Suh ultimately used what appear to be fitted parameters as part of the pre-exponential term to obtain reasonable correlations with experimental results.

Han and Han (1990) also looked to modify the free energy term. Their approach consisted of two corrections, one for the non-ideal polymer system and the other for the non-equilibrium condition that they claimed exists between the bubble pressure and the saturated vapor pressure of the blowing agent at the processing temperatures. Han and Han proposed a non-ideality correction based on Flory-Huggins theory and a non-equilibrium correction based on the degree of supersaturation. They also added

corrections to the pre-exponential term, which included two fitted constants based on the experimental data for the specific system under investigation. The effectiveness of their correction for ΔG is difficult to determine, however, because the changes to the pre-exponential term rely on experimentally fitted parameters. Additionally, they did their work in a concentrated polymer solution instead of a polymer melt.

Lee (1995) looked at incorporating elastic and viscous effects into the free energy term. Their approach requires a very high level of understanding of the complicated rheology of polymer systems. Lee retained the classical pre-exponential term, however.

A number of investigators have looked at improved ways to determine the surface tension, which appears in the free energy term with mixed success. Goel and Beckman (1994) use a correlation proposed by Reid, et al. (1987) and take advantage of the fact that their blowing agent is above the critical point (supercritical) to simplify their estimation of the surface tension. They retain a fitted parameter in the pre-exponential term, however, to obtain a good fit between theoretical prediction and experimental results. Lee and Flumerflet (1996) and Su and Flumerflet (1996) look at estimating microscopic surface tensions, no doubt trying to avoid the constraint of the capillary approximation that is fundamental to CNT. They develop surface tension models based on Lifshitz theory. The authors are able to show good correlation between calculated and experimental surface tensions, however, they do not necessarily make improvements in predicting nucleation rates.

Ruengphrathuengsuka (1992) incorporated three corrections into a nucleation rate equation. The first was a non-ideal term to correct the free energy of nucleation and the second two were both related to transport limitations. One was a thermal limitation and

the other was a mass limitation. Both of these transport correction terms had similar forms as the ones proposed by Attar for coal pyrolysis. Ruengphrathuengsuka's results were presented in a non-dimensional form and compared to a "base case" nucleation rate. The base case nucleation rate needs to be validated experimentally to be accurate. Therefore the model is still relying on experimental data to be effective. Without the experimental validation of the base case, an evaluation of the effectiveness of the model cannot be determined.

Shafi and coworkers (1996, 1996, 1997, 1997) provide a combined nucleation and bubble growth model to predict foam formation in polymeric materials. Initially, they used a nucleation model described by Ruengphrathuengsuka (1992), but then changed to the model described by Lee (1995). The focus of the work appears to be more on the bubble growth equations, however, and not nucleation theory.

Ramesh and co-workers (1993, 1994) developed a completely different nucleation model based on the formation of microvoids. The microvoids are formed when two dissimilar polymers are cooled and one polymer has a significantly different rate of contraction. As the two polymers contract, shear forces are created as one polymer reaches its "freeze" temperature and stops contracting while the other continues to contract. These forces create the microvoids. Ramesh et al. experimentally determined that the voids followed a log-normal distribution and proposed this as the basis for their theory. There are two significant requirements for using this theory. The first is having enough accurate physical property and rheological data on the system (including the effect of the blowing agent on these properties) and the second is having a system with two polymers dissimilar enough to form the microvoids. Additionally, the number of

particles creating the microvoids needs to be estimated for the theory to be useful. Finally, the number of these particles present in the system needs to be sufficient to support the nucleation process.

Lee (1991, 1994) attempts to use a cavity model to include shear effects in the extrusion process into a nucleation model. Lee defines a capillary number, which is the ratio of the shear forces to the surface tension forces and proposes using this in place of the free energy in the exponential term of the nucleation equation. The issue here is that the model does not have applicability in a system undergoing free expansion and can only be applied when a significant shear force is present in the system.

Finally, as has been mentioned before, many of the models discussed above have retained the traditional pre-exponential factor from CNT. This appears to be highly problematic as this term is based on gas molecules traveling through vapor and impinging on the surface of critical clusters (Becker and Döring, 1935; Farkas, 1927; Feder, et al. 1966; Volmer, 1929 and 1939; Zeldovich, 1942). This is a very poor representation of the true physical situation in the polymeric system (and for that matter, in any liquid systems where bubble formation is occurring) and should be addressed.

A new theory could address the motion of the molecules in the polymeric system by incorporating a diffusion-based approach for estimating impingement rates. Further, the new theory will need to recognize the complicating factors that surround a polymeric system and what impact these factors can have on estimating the Gibbs free energy in the exponential term. Examples of these complicating factors are the large discrepancy between the blowing agent molecules and the polymer molecules, the complicated

rheology of these systems, and the difficulties often encountered in trying to obtain experimental data.

Given all of this, it would be a significant improvement to nucleation theory to develop a model that was neither system dependent, nor based on fitted parameters from experimental data. This is the originally stated goal of this investigation. In the subsequent chapters, such a model will be developed and proposed.

CHAPTER 4

A NEW APPROACH FOR ESTIMATING NUCLEATION RATES IN THERMOPLASTIC POLYMERS

The development of any nucleation model must first begin with an accurate physical depiction of the system under investigation. The development of a model for the thermoplastic polymer/blowing agent systems of interest here is no different. The system can be envisioned as a two-component system made up of a thermoplastic polymer that has been impregnated with a blowing agent. . This investigation is limited to homogeneous systems. In such a system, the molecules of the blowing agent are assumed to be completely miscible with the polymer and only a single phase exists. In general, the polymer molecules are expected to be on the order of a few hundred to a thousand times larger than the blowing agent molecules. The type of blowing agent, physical or chemical, is unimportant if all required physical and chemical property data are available for the blowing agent.

In the systems of interest, the gas impregnated polymer is initially below its glass transition temperature, T_g, therefore it is considered a solid. At this time, the blowing agent molecules, which are frozen in place in the free volume between the polymer chains, are unable to move except possibly from very slow solid-state diffusion. This however, should not affect the dynamics of the process. The polymer and blowing agent are then heated to a constant temperature above the T_g of the system and held there until nucleation occurs creating a polymeric foam. The T_g of the polymer becomes an inverse function of the blowing agent concentration. Increasing the blowing agent concentration decreases the T_g and decreasing the blowing agent concentration will increase the T_g. The foaming or nucleation process is assumed to be carried out in a mechanically open

system; therefore the polymer is free to expand in all directions. The system, however, is considered "closed" in the thermodynamic sense, i.e. it can transfer heat but not mass. This constant mass constraint is only expected to hold for the initial phase of heating the polymer. As heat is applied to the system for longer periods of time, some blowing agent will ultimately be lost to the surrounding environment and it becomes unrealistic to expect the constant mass constraint to hold. Most, if not all of the nucleation, however, should have occurred before the system begins to loose mass justifying the constant mass assumption. Perfect heat transfer is assumed ensuring that the entire polymer sample is at a uniform equilibrium temperature above T_g. It is also assumed that this temperature is obtained in a relatively short time frame.

Once above T_g, the polymer melt softens and becomes fluid (albeit, a highly viscous fluid). In this state, the blowing agent molecules are free to move throughout the system. As has been described previously (Lothe and Pound, 1962; Reiss, Katz, and Cohen, 1968; Ellerby and Reiss, 1992), these molecules are expected to partition into naturally occurring groups or clusters of varying size. Since the molecules are in constant motion, the configuration of the molecules is changing continuously. The term configuration is used here to denote the specific arrangement of the molecules in the system, not the different possible conformations that the polymer chains can exist in. The total number of differently sized clusters is assumed to be constant, however, as a steady state in the molecular movement is anticipated. This is because there is no concentration gradient of the blowing agent at the macroscopic level. The nucleation process ultimately occurs as molecules add to clusters of a critical size. In this process, only the movements of single molecules are considered. Consistent with Reiss, Katz, and Cohen (1968) and

Reiss, Tabazadeh, and Talbot (1990), the movement of groups of molecules as single entities is excluded. This is necessitated because the model assumes that the clusters are sufficiently separated in space so that they will not interact with each other. If groups of molecules were treated as single entities, then the groups could interact and this assumption would be violated.

The one significant difference that this model for polymeric systems will offer over the CNT model (Becker and Döring, 1935; Farkas, 1927; Feder, et al. 1966; Volmer, 1929 and 1939; Zeldovich, 1942; Blander and Katz, 1975) is how the motion of the molecules forming the new phase is handled. The use of an impingement rate based of the kinetic theory of gases is ill equipped to handle the complicated motion of the blowing agent molecules in the polymer system. A better approach is one based on diffusion.

4.1 A Diffusion Based Model

A diffusion-based approach was investigated after reviewing work on coagulation of colloidal suspensions (Ross and Morrison, 1988). In Ross and Morrison's work, the stability of colloidal suspensions was examined. In their review, the authors were concerned with estimating the time it would take for individual colloidal particles to agglomerate into larger flocculates. Ross and Morrison modeled the kinetics of these coagulations with a simplified diffusion model utilizing Fick's law and they assumed that the concentration of the colloidal particles followed a Boltzmann distribution. This assumption with regard to the particle distribution is consistent with the assumptions found in CNT for the individual molecules. Their approach led to a model with a binary

diffusion coefficient as the key parameter. A similarity between the colloidal particles agglomerating into the larger flocculates and the blowing agent molecules in the polymeric system coalescing into bubbles can be envisioned. Work by Slezov (1996) using a diffusion model for the low viscosity systems described in Chapter 2 and a second manuscript by Schmelzer and Schmelzer (1999) which is a follow-up to the Slezov work also supported the idea of trying to use a diffusion based model for predicting nucleation rates. This has been extended to polymers in this work.

To extend the diffusion concept to polymers, an approach similar to Slezov et al. (1996) will be followed. One specific issue that needs to be addressed when dealing with a polymeric system is how the molecular size of the components will be determined. This size is important because it impacts the diffusion distance (the distance a molecule needs to travel before it will collide with a cluster) and how the number of molecules in a cluster will be determined. Slezov et al. defined a characteristic molecular length and used it as a radius to calculate volumes based on a spherical geometry. This was not a significant issue in Slezov's case because he was dealing with systems that contained relatively small and similar sized molecules (water and argon for example) as apposed to the large molecules typically found in polymer systems.

Since the difference in molecular size between the blowing agent and the polymer can be very large, it is unreasonable to expect the long polymer chains to occupy a volume based on a simple spherical model similar to Slezov's. This simple model, however, has some appeal because it simplifies the numerical calculations that are involved so efforts will be made to retain it. The characteristic molecular length will be defined as the radius of gyration. Data for this parameter for many common blowing

agents are readily available. A useful measure of the space occupied by a molecule is the van der Waals volume and it will be used for any estimations of molecular volume in the model. In order to account for the volume of the polymer chains in a reasonable way, the van der Waals volume of the polymer repeat unit will be used. The van der Waals volume can be estimated from a group contribution method outlined by van Krevelen (1990). This van der Waals volume can then be multiplied by the number of repeat units in the polymer chain to estimate the actual chain volume. All of the other physical properties used in the model, such as density, are based on the polymer and not the repeat unit or monomer.

4.1.1 Derivation of the Diffusion Based Model

The starting point for the development of this diffusion based nucleation theory is the Fokker-Planck equation (Equation 2.2.8) given in Chapter 2:

$$\frac{\partial f(n,t)}{\partial n} = \frac{\partial}{\partial n}\left\{\mathcal{P}_D\left[\frac{\partial f(n,t)}{\partial n} + \frac{f(n,t)}{kT}\frac{\partial \Delta G(n)}{\partial n}\right]\right\}$$

The diffusion probability, $\mathcal{P}_D$, is defined as:

$$\mathcal{P}_D = \frac{4\pi r_c^2 D_{AB} C_0}{\ell} \tag{4.1.1}$$

where r_c is the critical cluster radius, ℓ is the radius of gyration of the blowing agent, D_{AB} is the binary diffusion coefficient between the polymer and the blowing agent, and C_0 is the initial concentration of the blowing agent.

Following Slezov et al. (1996), changes in the cluster size distribution are related to the flux in the cluster size space, therefore:

$$\frac{\partial f(n,t)}{\partial t} = -\frac{\partial J(n,t)}{\partial n} \tag{4.1.2}$$

where

$$J(n,t) = -\mathcal{P}_D\left[\frac{\partial f(n,t)}{\partial n} + \frac{f(n,t)}{kT}\frac{\partial \Delta G}{\partial n}\right], \qquad n \le g \tag{4.1.3}$$

In Equation 4.1.3, g is an arbitrary size limit to the clusters and it will be defined later. Assuming that the cluster size distribution function f(n) follows a Boltzmann distribution, as is the case traditionally, then:

$$f(n) = \xi \exp\left(-\frac{\Delta G}{kT}\right) \tag{4.1.4}$$

At steady state, the number of different size clusters in the cluster size distribution function does not change with time (sizes of clusters are continuously changing but the net rate of change in the number of each size cluster is zero). In order to determine what this steady state distribution is, Equation 4.1.4 is substituted into Equation 4.1.3. To do this, the cluster size distribution function f(n) (Equation 4.1.4) must be differentiated with respect to n. This gives:

$$\frac{\partial f(n)}{\partial n} = -\frac{\xi}{kT}\exp\frac{-\Delta G}{kT}\left[\frac{\partial(\Delta G)}{\partial n}\right] + \frac{\partial \xi}{\partial n}\exp\frac{-\Delta G}{kT} \tag{4.1.5}$$

The steady state condition is then obtained by substituting this into Equation 4.1.3. Steady state implies that the flux is a constant and J is no longer dependent on n or t. That gives:

$$J = -\mathcal{P}_D\left[\frac{-\xi}{kT}\exp\frac{-\Delta G(n)}{kT}\frac{\partial \Delta G}{\partial n} + \frac{\partial \xi}{\partial n}\exp\frac{-\Delta G(n)}{kT} + \frac{\xi}{kT}\exp\frac{-\Delta G(n)}{kT}\frac{\partial \Delta G}{\partial n}\right] \tag{4.1.6}$$

Equation 4.1.6 is valid in the range of $0 < n < g$ where g must be larger than the critical cluster size, n_c. Simplification leads to the desired steady state result:

$$J = -\mathcal{P}_D\left[\frac{d\xi}{dn}\exp\frac{-\Delta G(n)}{kT}\right] \tag{4.1.7}$$

A limiting case for the cluster distribution is that none of the clusters contain more than one molecule or, in other words, clusters with n ≥ 2 cannot exist in this limit. In this limit, the value of ΔG in Equation 4.1.4 must be zero. Likewise, the value of f(n) is equal to ξ and this must equal C_0. Equation 4.1.4 can be re-written in this limit as:

$$f(n) = \xi\exp\frac{-0}{kT} = C_0 \tag{4.1.8}$$

Equation 4.1.7 can be rewritten as the following by separating variables:

$$\int_0^{\xi} d\xi = \int_0^{n}\frac{J\exp\frac{\Delta G}{kT}}{\mathcal{P}_D}dn \tag{4.1.9}$$

The integration with respect to n from zero to n then results in:

$$\xi = C_0 - J\int_0^{n}\frac{\exp\frac{\Delta G}{kT}}{\mathcal{P}_D}dn \tag{4.1.10}$$

The C_0 in the above equation is the result of evaluating the integral at the lower limit (n = 0) and the second term, which is still written in the form of an integral, results from evaluating the upper term (n = n). The term g can now be defined as the smallest non-zero value of n that makes ξ = 0 as in Slezov's work. This is then substituted in as the upper limit of the integral and ξ is set to zero. This gives:

$$0 = C_0 - J\int_0^{g}\frac{\exp\frac{\Delta G}{kT}}{\mathcal{P}_D}dn \tag{4.1.11}$$

This can then be rearranged to:

$$C_0 = J\int_0^g \frac{\exp\frac{\Delta G}{kT}}{\mathcal{P}_D} dn \tag{4.1.12}$$

and finally solving for J:

$$J = \frac{C\mathcal{P}_D}{\int_0^g \exp\frac{\Delta G}{kT}\, dn.} \tag{4.1.13}$$

As in the classical development, ΔG is expected to be a steep function of n, therefore contributions to the value of ΔG from values of n far removed from n_c, the number of molecules in a critical cluster, will be negligible (Cohen, 1970; Blander and Katz, 1975). This allows ΔG to be expanded in a Taylor series and truncated after the quadratic term as a reasonable approximation for its value. The truncated expansion for ΔG can then be readily integrated.

In order to complete the expansion, a variety of terms and derivatives are required. These include the first and second derivatives of ΔG with respect to n, the value of n_c and the value of ΔG at n_c. The first step will be to take the standard form of ΔG as a function of cluster radius and put it in terms of the number of molecules in a cluster, n_c. The change in free energy can be written as:

$$\Delta G(r) = \frac{4}{3}\pi r^3 \Delta P + 4\pi r^2 \gamma \tag{4.1.14}$$

Here, Δγ, which is the difference in surface tension between the final and initial states has been replaced with γ because the metastable phase is a single phase and its surface tension is zero. Thus, the change in surface tension, Δγ, is the surface tension differences between the two newly formed phases. Using the notion of spherical volumes, the volume of a blowing agent molecule, v_m is given by:

$$v_m = \frac{4}{3}\pi\ell^3 \tag{4.1.15}$$

Likewise the volume of a cluster, v is given by:

$$v = \frac{4}{3}\pi r^3 \tag{4.1.16}$$

The number of molecules in a cluster of radius r, assuming perfect packing with no voids, is then given by:

$$n = \frac{v}{v_m} = \frac{r^3}{\ell^3} \tag{4.1.17}$$

This simplified expression, which is used as a limiting case, eliminates the potential problems and inconsistencies that arise from trying to determine a consistent packing factor for all possible types of systems. This gives an expression for n in terms of r that can be substituted into Equation 4.1.14:

$$\Delta G(n) = \frac{4}{3}\pi n\ell^3\Delta P + 4\pi n^{2/3}\ell^2\gamma \tag{4.1.18}$$

As before, in order to find the value of $n = n_c$, the derivative of $\Delta G(n)$ with respect to n needs to set equal to zero, and then solved. This derivative is:

$$\frac{d[\Delta G(n)]}{dn} = \frac{4}{3}\pi\ell^3\Delta P + \frac{8}{3}\pi\ell^2\gamma n^{-1/3} \tag{4.1.19}$$

Setting this equal to zero and solving gives the maximum value of n or n_c:

$$n_c = \frac{8\gamma^3}{\ell^3\Delta P^3} \tag{4.1.20}$$

The second derivative will also be required. The second derivative of Equation 4.1.19 is:

$$\frac{d^2[\Delta G(n)]}{dn^2} = \frac{-8\pi\gamma\ell^2}{9n^{4/3}} \tag{4.1.21}$$

The next step is to evaluate both of these derivatives and the original function, ΔG, at n_c.

Substituting Equation 4.1.20 into Equations 4.1.18, 4.1.19, and 4.1.21 respectively results in:

$$\Delta G\big|_{n_c} = \frac{16\pi\gamma^3}{3\Delta P^2} \tag{4.1.22}$$

$$\left.\frac{d[\Delta G(n)]}{dn}\right|_{n_c} = 0 \tag{4.1.23}$$

$$\left.\frac{d^2[\Delta G(n)]}{dn^2}\right|_{n_c} = \frac{-\pi\ell^6\Delta P^4}{18\gamma^3} \tag{4.1.24}$$

Note that in Equation 4.1.22, the value of ΔG_m at $n = n_c$ is the same as the value obtained using CNT and as expected, the value of the first derivative is zero.

The formula for a Taylor series expansion is (Thomas and Finney, 1982):

$$\Delta G(n) \approx \Delta G(n_c) + \frac{d\Delta G(n_c)}{dn}(n-n_c) + \frac{1}{2!}\frac{d^2\Delta G(n_c)}{dn^2}(n-n_c)^2 + \cdots + \frac{1}{n!}\frac{d^n\Delta G(n_c)}{dn^n}(n-n_c)^n \tag{4.1.25}$$

Truncating higher order terms above the quadratic leads to:

$$\Delta G(n) \approx \Delta G(n_c) + \frac{d\Delta G(n_c)}{dn}(n-n_c) + \frac{1}{2!}\frac{d^2\Delta G(n_c)}{dn^2}(n-n_c)^2 \tag{4.1.26}$$

Substituting the values from Equations 4.1.22 through 4.1.24 into Equation 4.1.26 leads to the following expression for ΔG:

$$\Delta G(n) \approx \frac{16\pi\gamma^3}{3\Delta P^2} - \frac{\pi\ell^6\Delta P^4}{36\gamma^3}(n-n_c)^2 \tag{4.1.27}$$

This expression can then be substituted into Equation 4.1.13 and the integration can be completed:

$$J = \frac{C\mathcal{P}_D}{\int_0^g \exp\frac{1}{kT}\left[\frac{16\pi\gamma^3}{3\Delta P^2} - \frac{\pi\ell^6\Delta P^4}{36\gamma^3}(n-n_c)\right]dn} \tag{4.1.28}$$

To simplify this integration, let:

$$\chi = \frac{16\pi\gamma^3}{3\Delta P^2} \tag{4.1.29}$$

and

$$w = \frac{\pi\ell^6\Delta P^4}{36\gamma^3} \tag{4.1.30}$$

This leads to:

$$\int_0^g \exp\frac{1}{kT}\left[\chi - w(n-n_c)^2\right]dn \tag{4.1.31}$$

In order to integrate, the following substitution is employed. Let:

$$z = n - n_c \tag{4.1.32}$$

then

$$z^2 = (n-n_c)^2 \tag{4.1.33}$$

and

$$dz = dn \tag{4.1.34}$$

Again making the appropriate substitutions leads to:

$$\int_0^g \exp\frac{1}{kT}\left[\chi - wz^2\right]dz \tag{4.1.35}$$

As χ/kT is a constant relative to n (or z), this expression can be further rearranged giving:

$$\exp\frac{\chi}{kT}\int_0^g \exp\frac{1}{kT}\left[-wz^2\right]dz \tag{4.1.36}$$

Using standard integration tables, the solution to an integral of this form is:

$$\int_0^g \exp\frac{1}{kT}\left[-wz^2\right]dz = \frac{1}{2}\sqrt{\frac{\pi kT}{w}}erf\left(g\sqrt{\frac{kT}{w}}\right) \tag{4.1.37}$$

For most cases, the error function, erf, will be approximately equal to 1, allowing the above to be simplified to:

$$\int_0^g \exp\frac{1}{kT}\left[-wz^2\right]dz = \frac{1}{2}\sqrt{\frac{\pi kT}{w}} \tag{4.1.38}$$

Also of note is the fact that the error function is a steep Gaussian function so that the upper limit of integration can be extended to infinity without introducing any computational error.

The result to this point only accounts for the positive half of the cluster distribution (from 0 to infinity). Since the distribution is Gaussian and symmetrically centered, the contribution from the negative side of the distribution (negative infinity to 0) also needs to be included. If the lower limit of integration is extended to minus infinity, then the result in Equation 4.1.38 is obtained again. When this is added to the results of the first integration from zero to infinity, the overall result doubles and the ½ term in the original result is eliminated.

Multiplying this result by expχ/kT and substituting it back into Equation 4.1.28 with the appropriate expressions for χ and w gives:

$$J = \frac{C\mathcal{P}_D}{\left(\frac{36kT\gamma^3}{\Delta P^4 \ell^6}\right)^{1/2}\exp\frac{16\pi\gamma^3}{3kT\Delta P^2}} \tag{4.1.39}$$

This can be rearranged and put in the following final form:

$$J = \mathcal{P}_D Z C \exp \frac{-\Delta G|_{n_c}}{kT} \tag{4.1.40}$$

where the Z is the Zeldovich factor (see Appendix B) given by:

$$Z = \frac{\ell^3 \Delta P^2}{6(kT)^{1/2} \gamma^{3/2}} \tag{4.1.41}$$

and

$$\Delta G|_{n_c} = \frac{16\pi\gamma^3}{3\Delta P^2} \tag{4.1.42}$$

4.1.2 Results and Discussion of the Diffusion Model

Equation 4.1.40 provides a means to estimate steady state nucleation rates in polymer systems based on diffusion. The results from this model will be compared to the experimental results for a PMMA/CO_2 system used by Goel and Beckman (1994). Table 4.1 summarizes physical property data that were used in the calculation.

Table 4.1 Physical Property Data for PMMA/CO_2 System used to Determine Nucleation Rates

Physical Property	Units	PMMA	CO_2	Mixture[a]
Molecular Weight	g/mole	100[b]	44	-
Mass Density @ 298 K	g/cm^3	1.188	0.800[c]	1.17[d]
Solubility Parameter	(J/cm^3)$^{0.5}$	19.4	12.3	-
van der Waals Volume	cm^3/mole	56.93	19.70	-
Radius of Gyration	cm	-	1.04×10^{-8}	-
Diffusion Coefficient	cm^2/sec	-	-	4.58×10^{-7}
Surface Tension	dyne/cm	42.0	-	5.0[e]

[a] Example is for 37.25 wt% CO_2 @ 27.5 MPa and 313 K
[b] Based on repeat unit, all other data based on polymer.
[c] Based on "liquid molar volume" at 273K, Prausnitz at el., (1986)
[d] Determined at 313 K.
[e] Individual component surface tension not necessary, mixture data given in Goel and Beckman (1994).

The surface tension of the system is highly dependent on the blowing agent concentration, which is shown in Figure 4.1. In this figure, the CO_2 concentration is represented by the saturation pressure. This is the experimental variable Goel and Beckman used to obtain PMMA samples with different CO_2 concentrations. The pressure can be related to the concentration through a variety of different methods or measured experimentally. Goel and Beckman used a mean field lattice gas model to determine the different CO_2 concentrations. Their results for concentration were used in all of the calculations done here with the diffusion-based model.

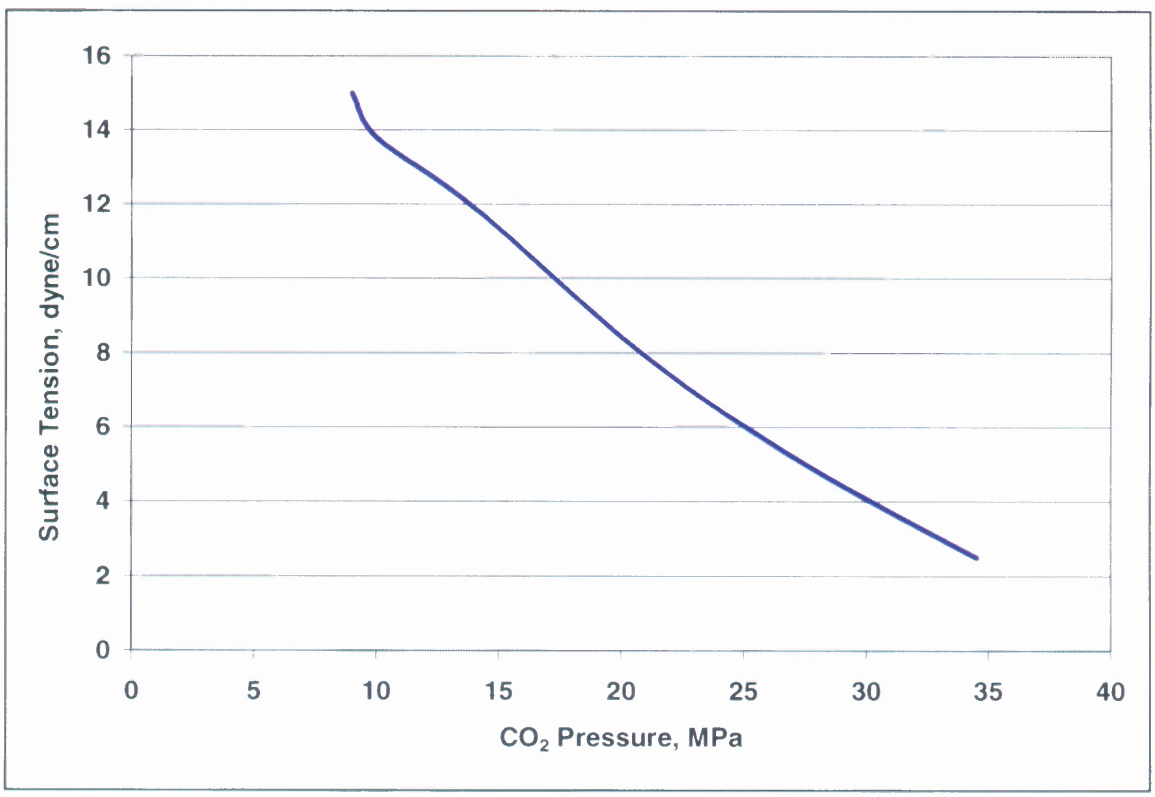

Figure 4.1 Surface Tension vs. Concentration for PMMA/CO_2 @ 313K. Data from Goel and Beckman (1994).

The strong effect of concentration on surface tension helps to explain the behavior of the critical radius size as a function of CO_2 pressure, see Figure 4.2 and Figure 4.3. Figure 4.2 highlights a sharp drop in critical radius size with increasing CO_2 pressure, which parallels the drop in surface tension. This behavior is expected, as the size of the critical radius is directly proportional to the surface tension (see Equation 2.2.4), which decreases as CO_2 pressure increases. The critical radius is also inversely proportional to ΔP, which is increasing.

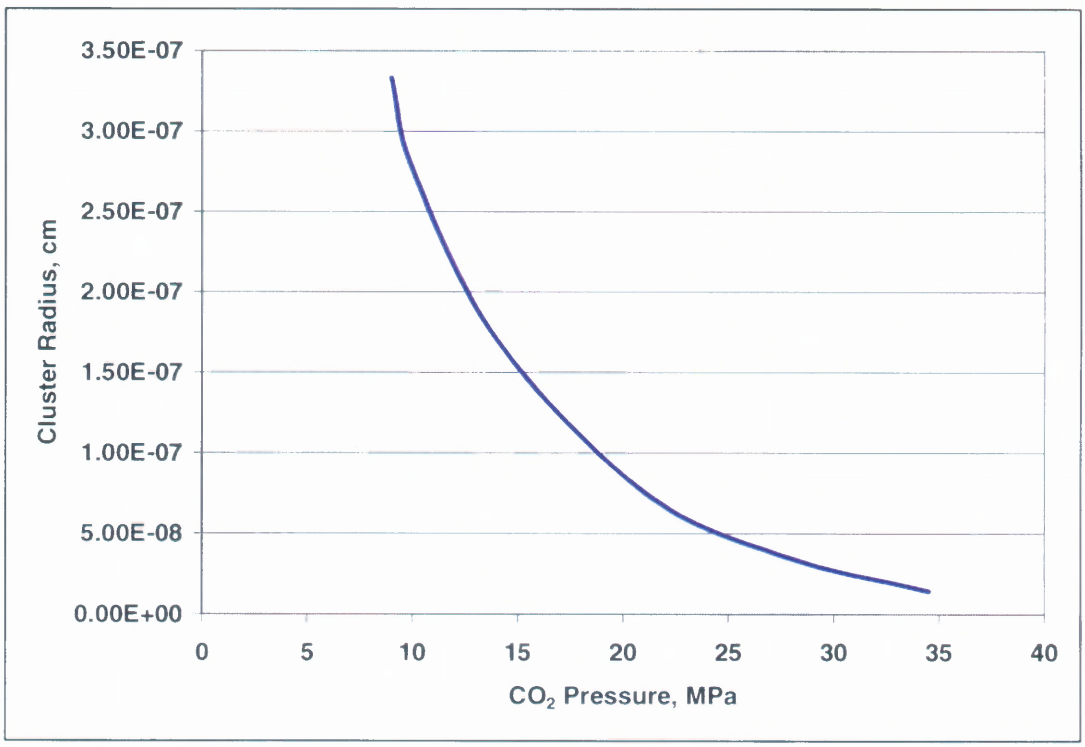

Figure 4.2 Critical Cluster Radius (cm) vs. CO_2 Pressure (MPa) for the PMMA/ CO_2 System @ 313 K. Data from Goel and Beckman (1994).

Figure 4.3 highlights how the number of molecules in a cluster changes with pressure. This is directly related to how the cluster volume changes (as calculated using

the cluster radius) with CO_2 pressure. The actual number of molecules in a cluster ranges over a few orders of magnitudes from ten molecules when the pressure is over 30 MPa to more than 30,000 molecules at pressures below 10 MPa.

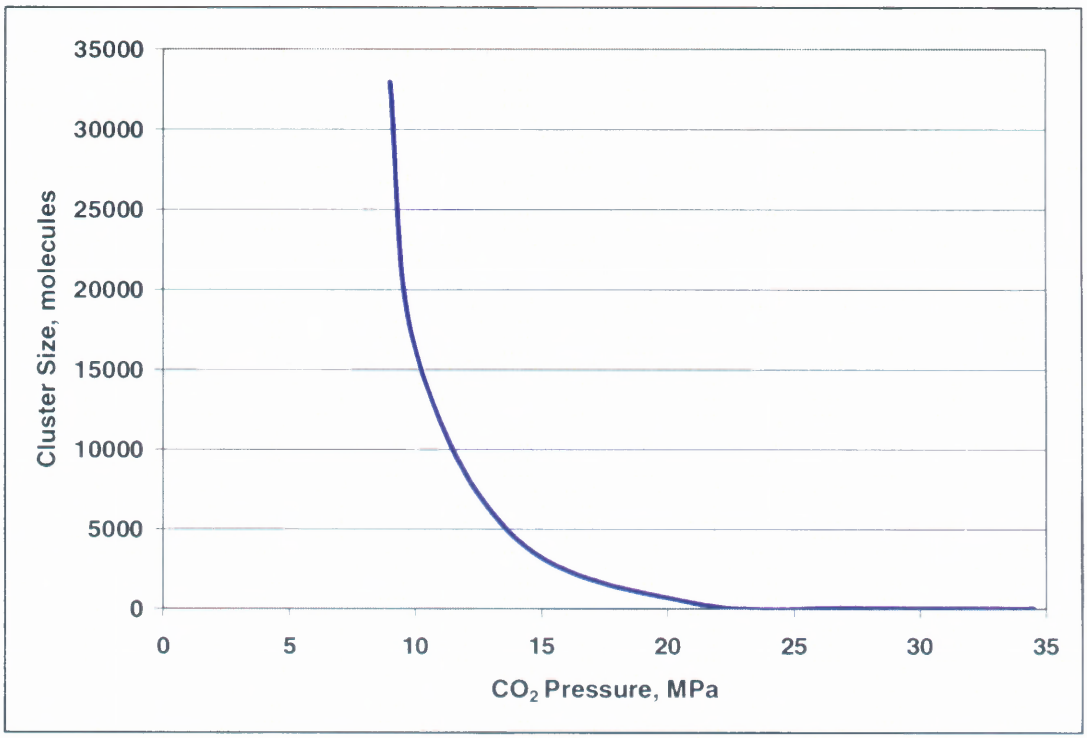

Figure 4.3 Molecules in the Critical Cluster vs. CO_2 Pressure (MPa) for the PMMA/CO_2 System @ 313 K. Data from Goel and Beckman (1994).

Figure 4.4 shows the behavior of $\Delta G/kT$ as a function of CO_2 pressure. Since the exponential term in the original CNT has not been altered, this is the same curve that would have been obtained using the original CNT. The shape of this curve dictates the shape of the nucleation rate curve in the diffusion model (just as it did in the CNT model) because the ΔG term in the exponential part of the equation dominates. A few observations about Figure 4.4 are warranted. First, at high saturation pressure (or CO_2 concentrations), the free energy plateaus at a nominally low level suggesting that the

nucleation process can occur readily. Second, at low pressure, very small changes in pressure will lead to significant changes in the final nucleation rate. Additionally, the figure suggests that the nucleation rate will be significantly lower at low pressure relative to high pressure. This is a reasonable fit with intuition, as higher concentrations of CO_2 are expected to lead to a larger number of clusters. The larger number of clusters coupled with the more molecules being present at the higher concentrations should increase the probability of a molecule impinging on a cluster.

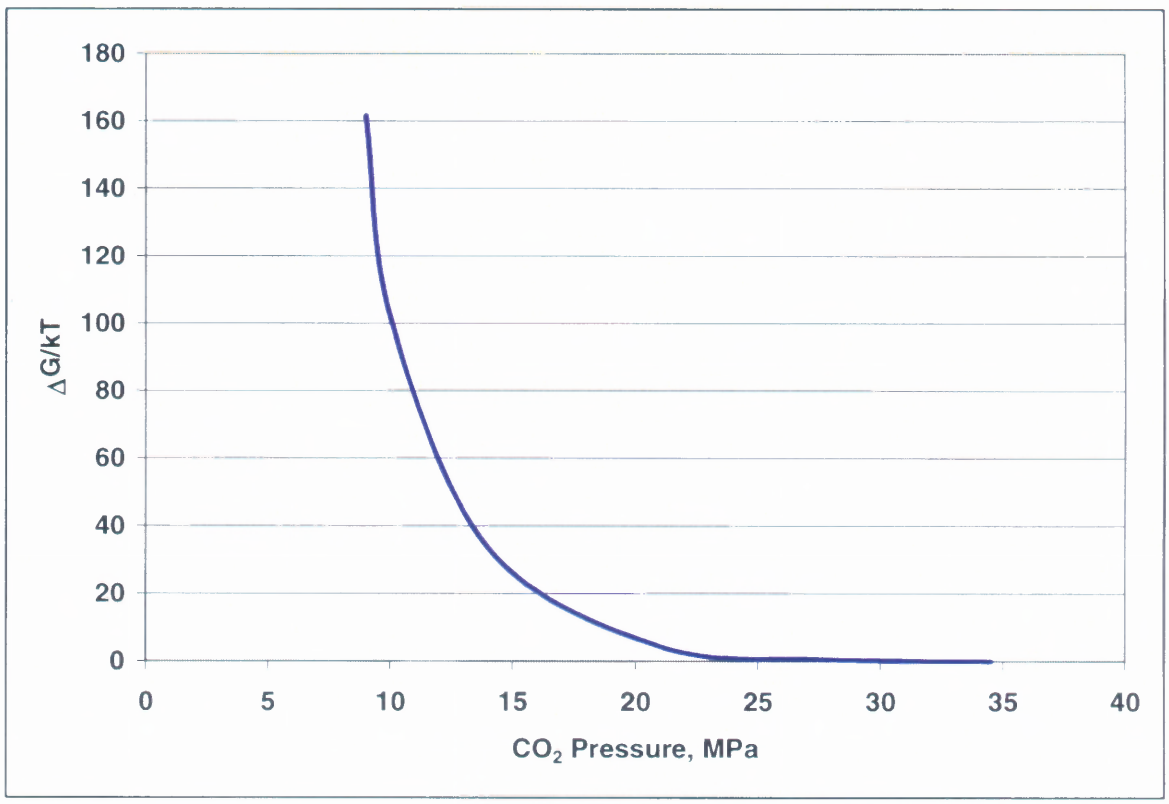

Figure 4.4 $\Delta G/kT$ vs. CO_2 Pressure for the PMMA/CO_2 System @ 313 K. Data from Goel and Beckman (1994).

Figure 4.5 compares the results of the new diffusion based nucleation rate model to the classical (CNT) model and the actual experimental data from Goel and Beckman.

It is immediately apparent that the diffusion model is better than the classical model but still unacceptable. Both models and the experimental data have similar shaped curves indicating that the exponential function originally suggested in the CNT is a reasonable starting point for the theory. Further, both models seem to describe the plateau in the nucleation rate behavior that occurs at high pressure, even though both grossly overpredict the actual experimental results.

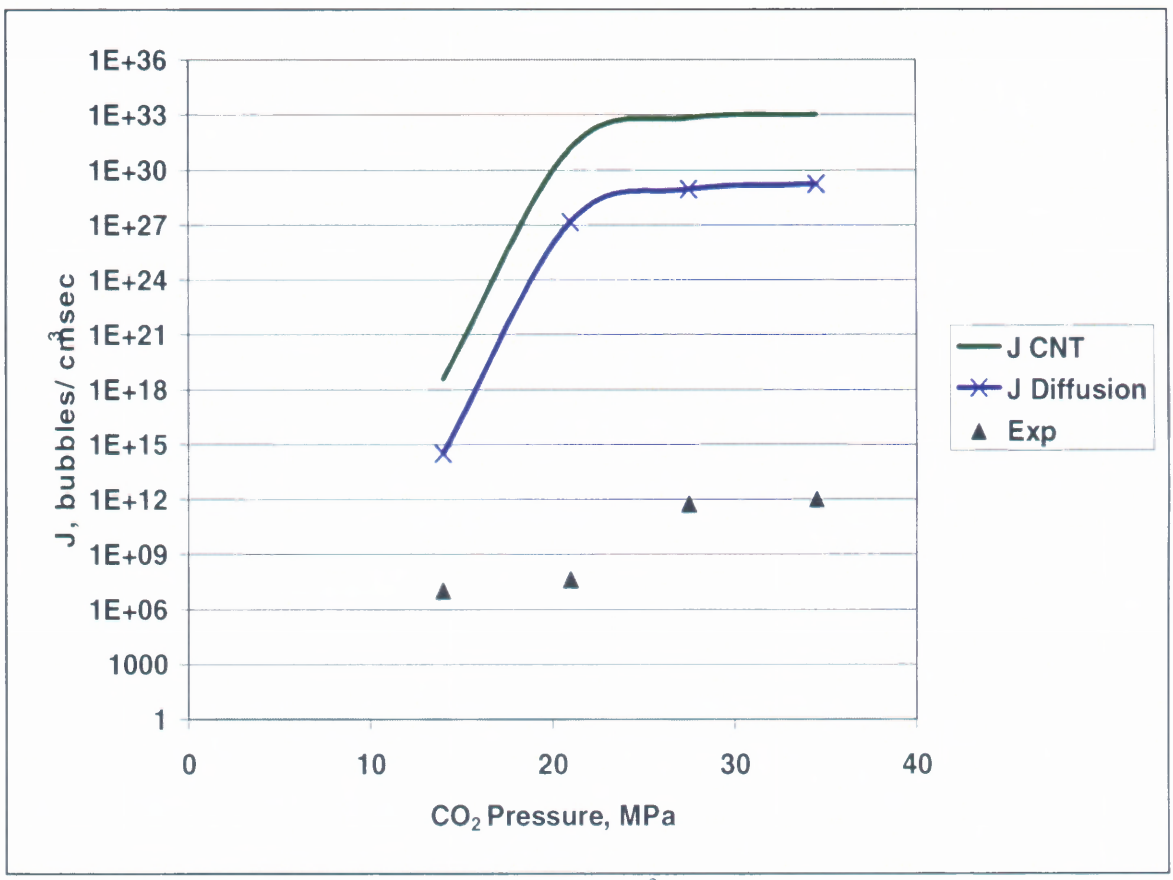

Figure 4.5 Nucleation Rate, J, (bubbles/cm^{3}sec) vs. CO_2 Pressure (MPa) for PMMA/CO_2 system @ 313 K. Data from Goel and Beckman (1994).

In an effort to further examine the diffusion-based theory, experimental results were obtained for a polystyrene (PS)/n-pentane (n-C_5) system and modeled. This system

is known commercially as expandable polystyrene or EPS. It is important to point out that the PS/n-C_5 system used in the experiments (described below) contained impurities and was not a perfectly homogeneous system. As such, some heterogeneous nucleation was expected and a difference in the experimental results and those predicted by the model were anticipated. The impurities are introduced during the manufacturing process and cannot be avoided. EPS is suspension polymerized and the stabilization system used to maintain the suspension provides significant amounts of impurities that are trapped in the final polymer. Depending on the grade of EPS used, additional impurities can be introduced from additives such as flame-retardants that the manufacturer will incorporate to enhance or alter the product performance. In order to minimize the error caused by these impurities, only commercial grades of EPS that did not contain any extra additives were used in the experiments.

Two commercial resins supplied by BASF Corp. were used, Styropor® BRL 315 and Styropor® BR 315 in the experiments. BRL 315 is a PS product that contains 4.0-wt% n-pentane and BR 315 is a product that contains 6.0-wt% n-pentane. Table 4.2 summarizes key physical property data for the PS and the blowing agent. Both products use the same PS and the only difference between the two (BR 315 and BRL 315) is the pentane content as indicated above.

In order to initiate the nucleation process, both resins were expanded in contact with atmospheric steam in a static expansion chamber. Details of the steam chamber design can be found in Appendix C. The EPS was free to expand in all directions in this device. In this steam expansion process, samples of the EPS beads were subjected to different steam times in a batch process. Steam times are the actual times, in seconds,

Table 4.2 Physical Property Data for PS/n-C_5 System Used to Determine Nucleation Rates

Physical Property	Units	Polystyrene	n-Pentane	Mixture[a]
Molecular Weight	G/mole	104[b]	72	-
Mass Density @ 273 K	g/cm^3	1.05	0.63	1.01[c]
Solubility Parameter	$(J/cm^3)^{0.5}$	17.6	14.4	-
van der Waals Volume	$cm^3/mole$	62.83	58.03	-
Radius of Gyration	cm	-	3.34×10^{-8}	-
Diffusion Coefficient	cm^2/sec	-	-	1.00×10^{-7}
Surface Tension	dyne/cm	34	7.6	30.1[c]

[a] Example is for Styropor® BR 315 which contains 6.0-wt% n-pentane.
[b]Based on repeat unit, all other data based on polymer.
[c]Concentration dependent, example for BR 315 (6.0 wt% n-C_5) at 373 K.

that the EPS beads are exposed to atmospheric steam. The resulting foamed beads were analyzed via SEM photography. The images were digitized and computer software was used to estimate the cell density or the number of cells using software that is proprietary to BASF, however; commercial software such as Visilog Image Analysis is available. The expansion behavior of the beads can be seen in Figures 4.6 and 4.7.

Figures 4.6 and 4.7 show that even after steaming times of more than 60 seconds, nucleation has not begun. A low level of nucleation begins to occur somewhere between 75 and 105 seconds. At 120 second, the nucleation process is essentially complete. The effect of bubble growth on foam density can be seen from Figure 4.8. In this figure, the BRL 315 and the BR 315 have been expanded for different steaming times up to 12 minutes. An obvious result is that the resin with the higher pentane content reaches an overall lower minimum density and does so in a slightly faster time. The slight increase in density for the BR 315 at steaming times below 100 seconds can result from either experimental error in the density measurement or a slight increase in the sample weight, which is caused by the EPS absorbing moisture during the steaming process.

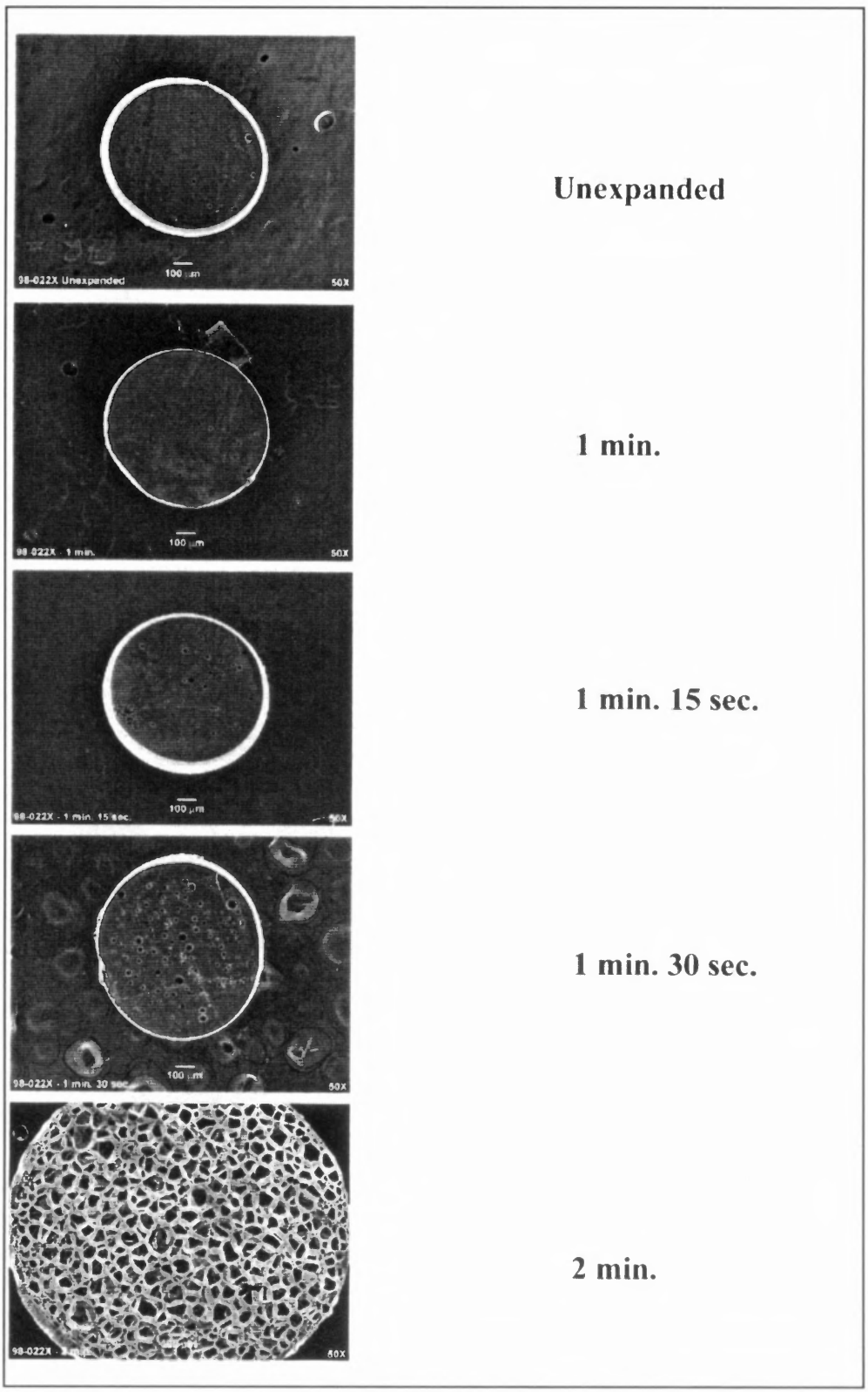

Figure 4.6 Expansion and Nucleation Behavior of BR 315 at 101.3 kPa and 373 K.

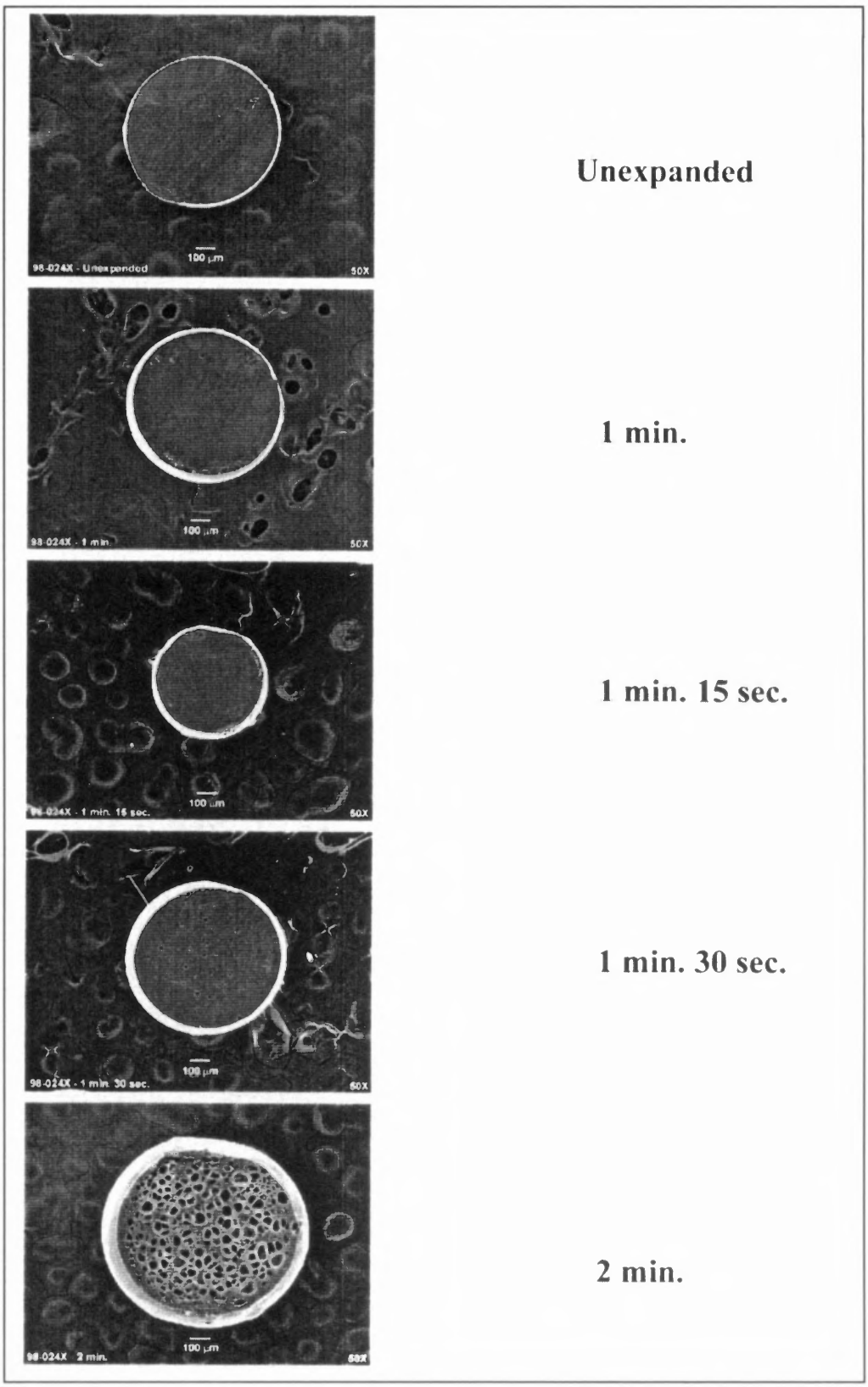

Figure 4.7 Expansion and Nucleation Behavior of BRL 315 at 101.3 kPa and 373 K.

The density increase is not significant, however, and does not interfere with the experimental analysis in either case.

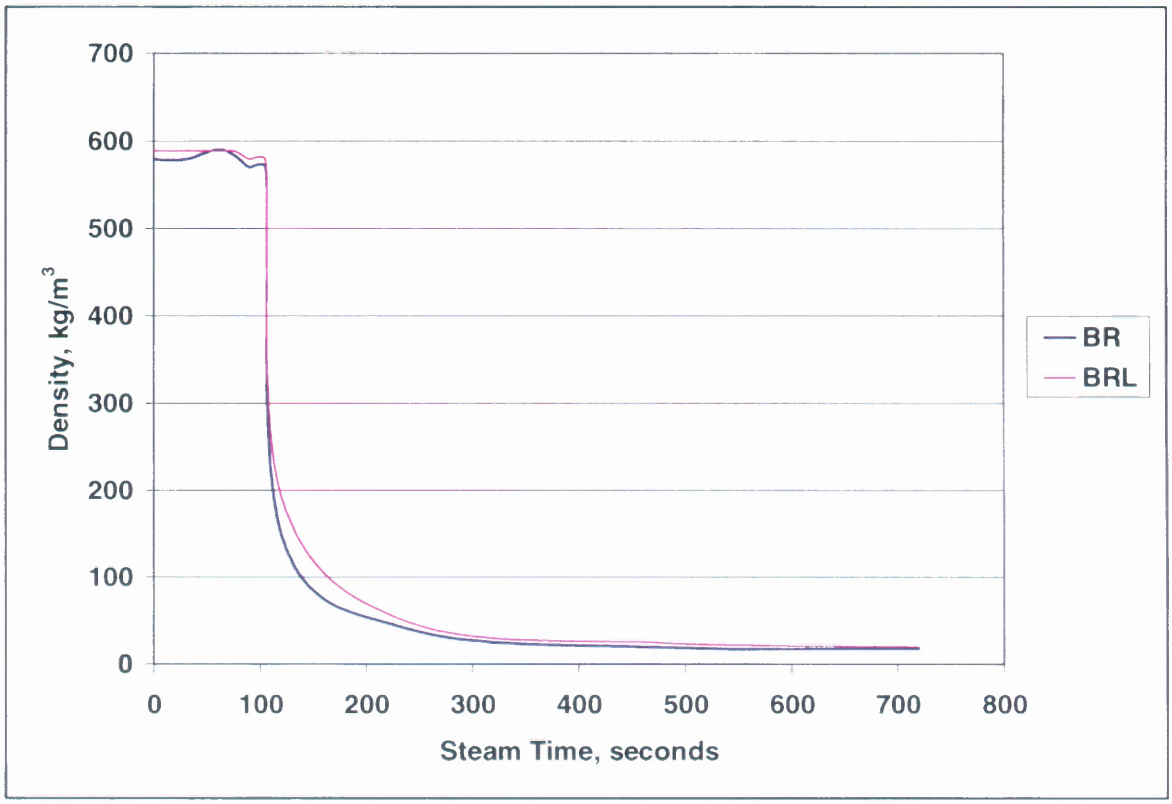

Figure 4.8 Density vs. Steam Time for BR and BRL at 101.3 kPa and 373 K.

Figures 4.6 and 4.7 are useful because the chronology of the nucleation event can be followed. Each individual cross section in these figures is relatively small, however, therefore additional larger cross sectional images of BR 315 are presented in Appendix C, Figures C.3 through C.12. Those images, which were developed from a second experiment, are taken from samples expanded over the same time scale as the samples in the original experiment used to develop the data for Figure 4.8. Further evidence that the majority of the nucleation takes place between steam times of 105 and 120 seconds can

be seen. The figures indicate that bubble growth dominates at steam times longer than 120 seconds.

It is hypothesized that most of the nucleation occurs almost instantly after a certain lag time. Thinking the lag could be the result of poor heat transfer, an unsteady state heat transfer calculation was completed to determine how long it would take the beads to heat up. This calculation, which was based only on convective heat transfer (i.e. no steam permeating the surface of the polymer), indicated that the beads reach their expansion temperature in about 6 seconds; see Appendix E. Based on this result, the lag observed in Figures 4.6 and 4.7 is not likely to be due to any heat transfer effects and there must be an actual time lag in the system. Such time lags have been the focus of other investigations (Feder, et al., 1966; Slezov, et al., 1996; Kanne-Dannetschek and Stauffer, 1981; Olson and Hamill, 1996; Schmelzer and Schmelzer, 1999). The time lag should not affect the steady state nucleation rate and it should only act as a shift in the time scale. Based on this and the fact that the principal concern of this investigation is steady state nucleation, the time lag will not be considered further. Information on the time lag in nucleation can be obtained from the above-cited manuscripts.

The model results for the PS/n-C_5 system are summarized in Figures 4.9-4.12. Figure 4.9 shows the effect of the n-pentane concentration on the surface tension of the system and Figure 4.10 illustrates the effect of pentane content on the critical cluster size. Figure 4.11 is a plot of $\Delta G/kT$ vs. r_c while Figure 4.12 shows the effect of pentane concentration on the free energy of formation for clusters, $\Delta G/kT$. In the model, the surface tension was calculated utilizing a method proposed by Reid, et al. (1987):

$$\gamma_{mix}^{1/4} = \overline{\rho}_{mix} \sum_{i=1} \frac{x_i \gamma_i^{1/4}}{\overline{\rho}_i} \tag{4.1.43}$$

In Equation 4.1.43, $\overline{\rho}_{mix}$ is the molar density of the mixture, $\overline{\rho}_i$ is the pure component molar density, and x_i is the mole fraction. The pressure inside the bubble or cluster is also required for the model. It was estimated using a standard VLE approach for polymers and solvents (Gabbard and Knox, 2000). The details of the method are summarized in Appendix D.

The model results for the EPS system are qualitatively similar to those obtained from the PMMA/CO_2 system, however, they are quantitatively very different. For the EPS system, as expected, the surface tension drops with increasing blowing agent concentration. This can be seen Figure 4.9. The actual drop in surface tension from 34 dyne/cm for pure polystyrene to about 29 dyne/cm at 8-wt% pentane is significantly smaller than the drop in surface tension in the PMMA/CO_2 system. The larger decrease in the surface tension of the PMMA/CO2 system is due to the higher concentrations of CO_2 relative to pentane concentration in the PS/n-C_5 system. The EPS system only dropped about 15% whereas the PMMA/CO_2 system decreased from about 15 dyne/cm to 3 dyne/cm or about 80%. A greater reduction of the surface tension of the EPS system may have been observable at higher pentane concentrations, however, concentrations greater than 8-wt% pentane were not investigated because it has been found that the n-pentane is no longer miscible with the polystyrene above this concentration.

The sharp decrease in the critical cluster radius with increasing blowing agent concentration seen in the PMMA/CO_2 system is also observed in the PS/n-C_5 system (Figure 4.10). The critical cluster size dropped dramatically at pentane concentration in

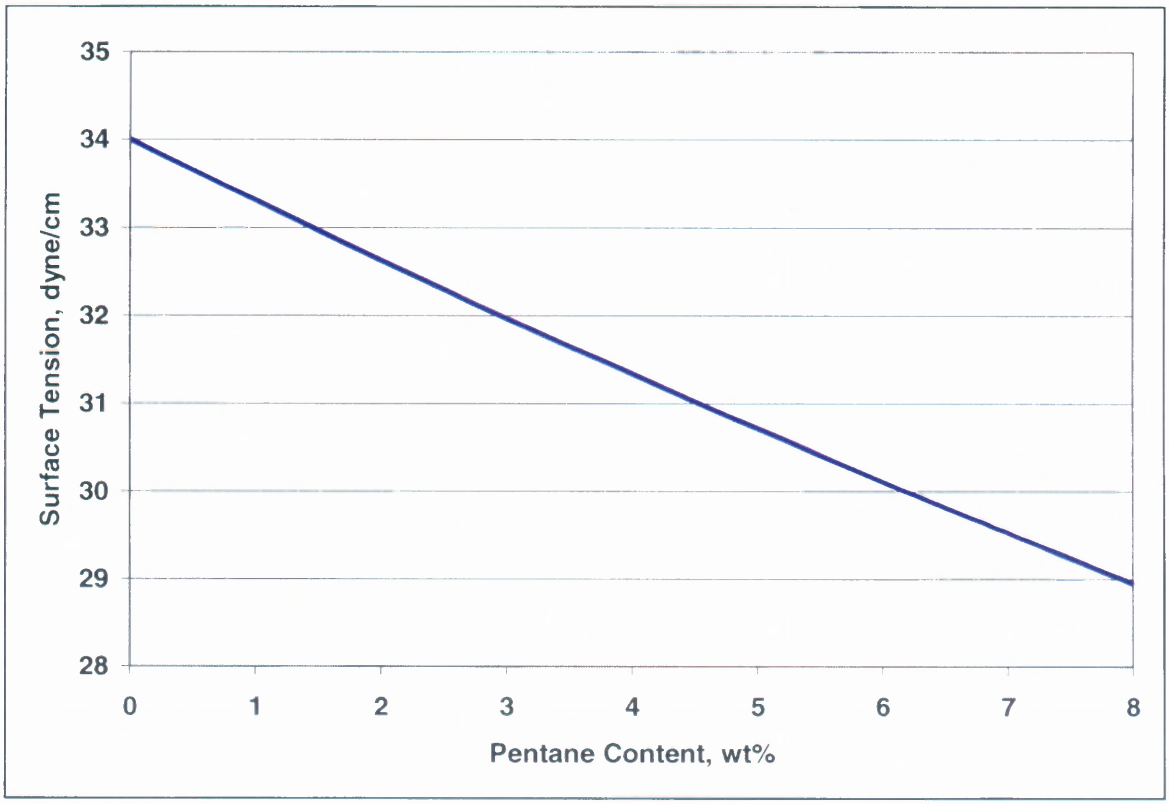

Figure 4.9 Surface Tension (dyne/cm) vs. n-Pentane Concentration (wt%) in EPS @ 373 K .

the region of 2-3.5-wt% but then leveled off at concentrations greater than 6 wt%. The size of the critical cluster is significantly larger in the PS/n-C_5 system (on the order of $1x10^{-4}$cm) vs. the PMMA/CO_2 system ($1x10^{-7}$ to $1x10^{-8}$ cm).

In comparing the micrographs of the EPS developed here with the micrographs in the Goel and Beckman (1994) manuscript, the cell density of the EPS system looks to be lower. This is consistent with the larger cell size found in the EPS samples. In fact, the PMMA foam should be considered micro-cellular as most of the cells are smaller than 10 microns but the EPS sample is simply cellular as most of the cells are larger than 10 microns. The larger cell size in the EPS sample makes sense since EPS system had

critical clusters with significantly larger radii. It should be pointed out, however, that an absolute comparison of the two foam samples is very difficult because they are not necessarily at the same foam density and the cell size and final foam density are strongly related. This is because the cells continue to grow even after the nucleation process has been completed as the final foam density of the sample is achieved.

Figure 4.10 also indicates the effect of the processing temperature and blowing agent concentration on the critical radius. The pentane used in the EPS system acts as a good plasticizer, so the same critical radius size can be achieved at lower temperatures as the pentane content is increased. This can be seen as a critical radius of 0.003 cm can be

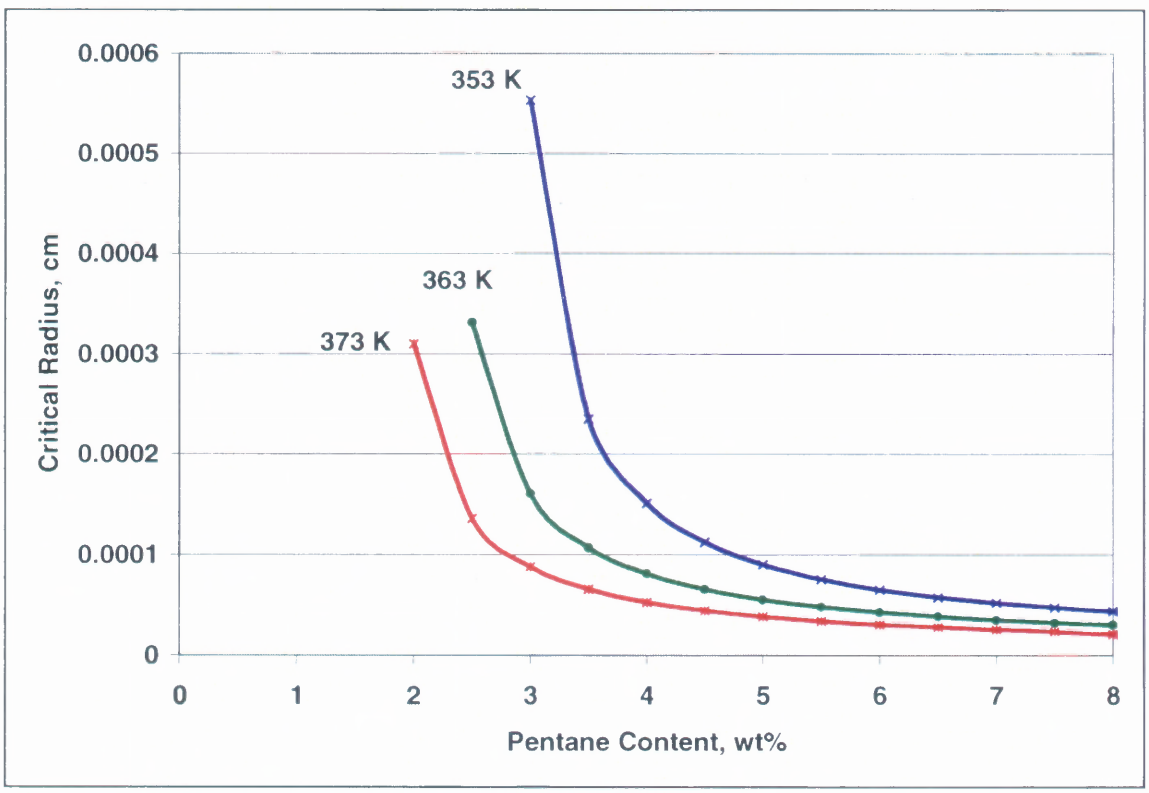

Figure 4.10 Critical Cluster Radius (cm) vs. n-Pentane Concentration (wt%) in EPS @ Various Temperature.

achieved at all three temperatures (353, 363, and 373) and the only difference is the pentane content which is approximately 2.0, 2.8, and 3.5 wt% respectively.

Figure 4.11 illustrates the change in ΔG as the cluster radius is increased. At 373 K and 101.3 kPa, the figure indicates that the radius of the critical cluster is about 3.5 x 10^{-5} cm. The Aγ and VΔP contributions to ΔG are shown separately.

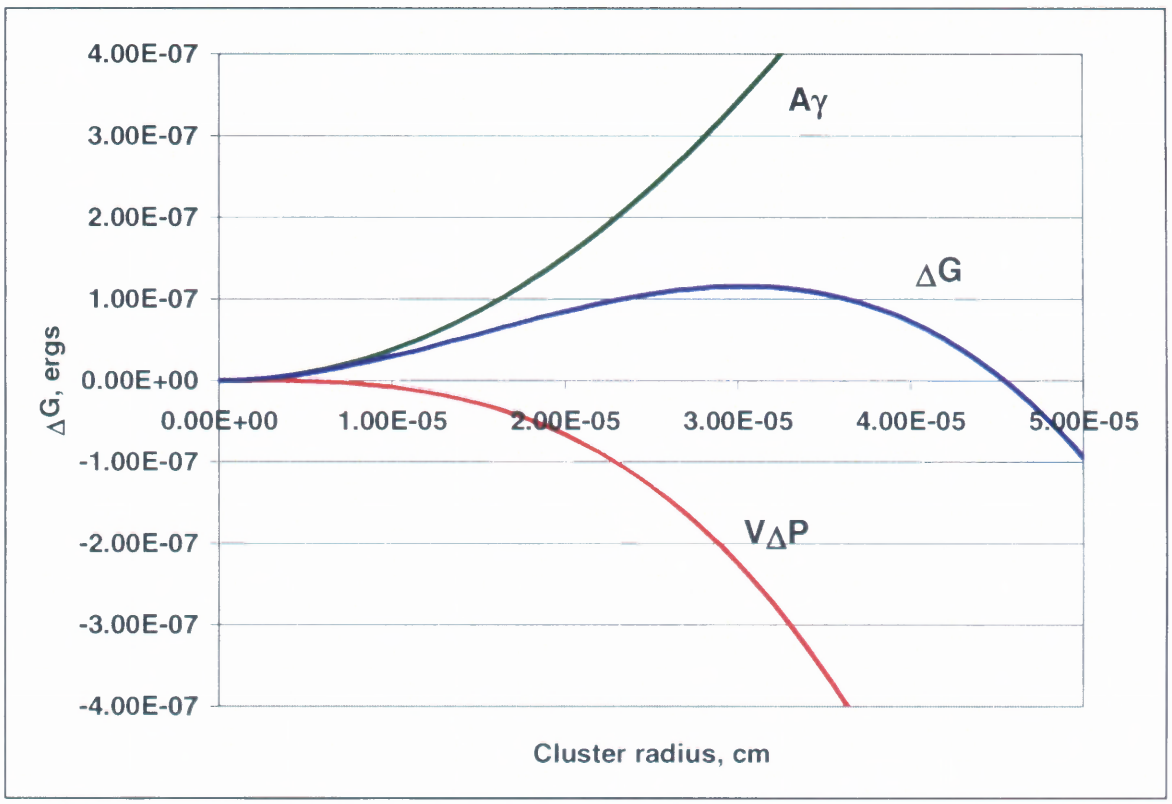

Figure 4.11 ΔG vs. r_c for BR 315 at 101.3 kPa and 373 K.

Finally, Figure 4.12 shows the effect of pentane concentration on ΔG/kT for the PS/n-C_5 system. The values of ΔG/kT are quite large and actually drive the exponential part of the nucleation equation (Equation 4.1.40) to zero. Hence, the new diffusion based theory predicts that no nucleation will take place just as the CNT does. The error is

obviously due to the fact that there is a significant amount of heterogeneous nucleation taking place and the EPS cannot be construed to be a homogeneous system.

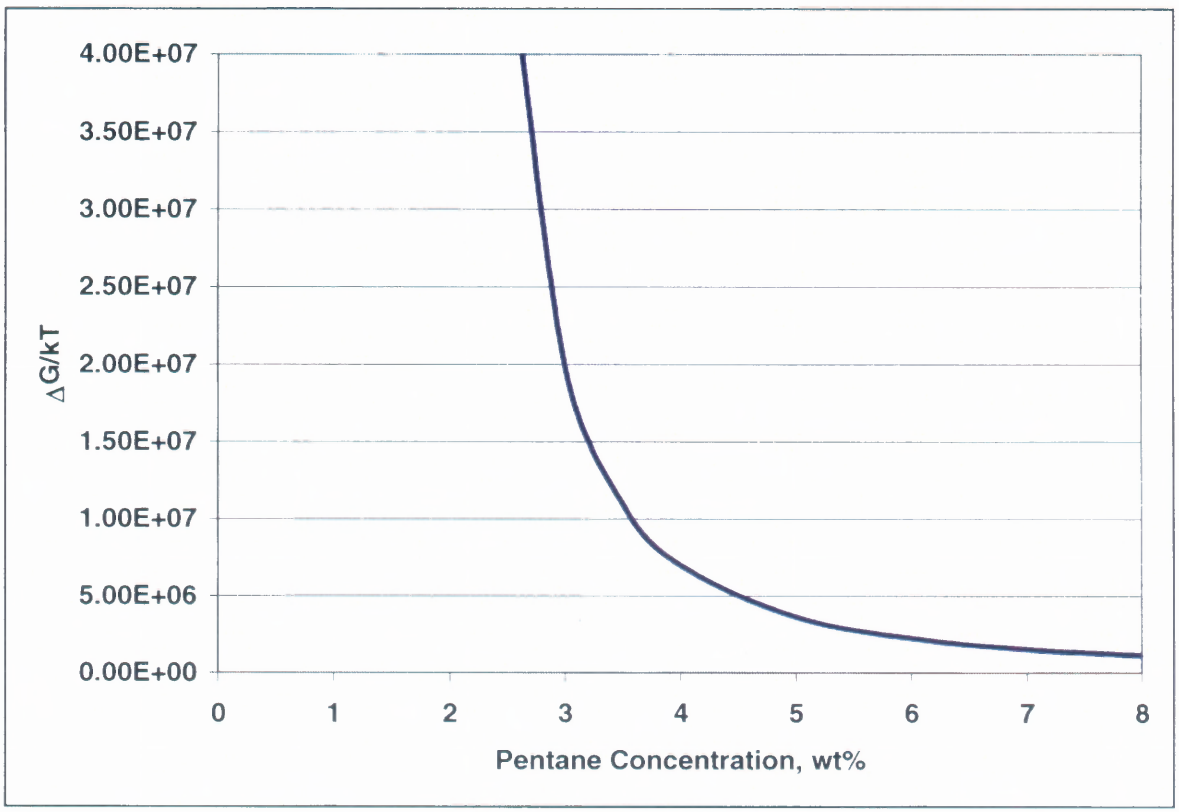

Figure 4.12 ΔG/kT vs. Pentane Concentration for EPS at 101.3 kPa and 373 K.

4.2 Investigations of Alternatives

The alternatives investigated in this Section are those that did not improve the results of the nucleation model. They are discussed here to help avoid wasted efforts by other investigators. Alternatively, they could serve as the beginnings of a successful approach for another investigator who uses the basic idea with yet another slightly different approach.

Since the PS/n-C_5 system appears to be dominated by heterogeneous nucleation, the PMMA/CO_2 system will become the focus. Given the significant overprediction of the diffusion-based model, it appears that still another improvement is needed. To explain the overprediction of the nucleation rates by the diffusion based model, a closer examination of Equation 4.1.40 is in order. Equation 4.1.40 is:

$$J = \mathcal{P}_D Z C_0 \exp \frac{-\Delta G|_{n_c}}{kT}$$

Re-iterating, the first term in the pre-exponential, $\mathcal{P}_D$, is the diffusion probability based on Fick's law. It accounts for the diffusion of CO_2 through the system and thereby determines the net impingement rate of CO_2 molecules on the clusters. The second term, Z, is the Zeldovich correction factor. Finally the last term, C_0, is the concentration of the blowing agent molecules initially present in the system. This can be coupled with the exponential term and thought of as the cluster distribution function.

As the first term (see Equation 4.1.1) is derived from Fick's law, it appears to be a reasonable approach to determining the net rate of movement of the CO_2 molecules. Further, the diffusion coefficient used in the model (4.58×10^{-7} dyne/cm) is of the right order of magnitude when compared to other diffusion coefficients for polymer/blowing agent systems and as a result, the actual numeric value of it will not change the model results significantly.

The Zeldovich factor appears throughout the literature and seems to be reasonable. Additionally, Z only ranges over a few orders of magnitude in the calculations. Based on this, it does not seem like it would be significant.

This diffusion probability term, however, may have one deficiency in predicting the impingement rate of individual molecules on critical clusters. It treats all molecules

exactly the same regardless of what energy they possess. This may be a problem because all of the CO_2 molecules can have different energy levels and not all of them will have sufficient energy to cause nucleation after impinging on a critical cluster. Treating all of the molecules as if they have the same energy may lead to significant overprediction. One possible way to correct this may be with the use of fluctuation theory.

4.2.1 Fluctuation Theory

The result obtained for a "mechanical" property in a statistical thermodynamic system is the average that results when all of the contributions from every molecule in the system are included. Every molecule will make a slightly different contribution to this average, which is often referred to as an ensemble average (see Appendix A). A fluctuation is defined as a deviation from the mean value. Fluctuation theory is the investigation of the probability of the deviations from the average of these "mechanical" properties (McQuarrie, 1976).

Mechanical properties are those properties that can be well defined in a given quantum state. A quantum state is defined by a specific discrete energy level. As previously stated, the polymer systems under investigation can be considered as closed systems with fixed N, V, and T. This assumption seems reasonable during nucleation and up until the point of bubble growth. This type of system is often associated with a specific ensemble, the canonical ensemble (Hill, 1986). For a closed system with fixed N, V, and T, two mechanical variables that can have fluctuations are energy, and pressure. It is the fluctuations in energy that are of interest here. Recalling the nucleation mechanism, a molecule of sufficient energy needs to impinge on a critical cluster before

another molecule leaves the cluster in order for nucleation to occur. If all of the blowing agent molecules have different energy levels, then only collisions of molecules with sufficient energy will result in nucleation. The diffusion-based model proposed in the last section did not attempt to determine which fraction of the molecules actually had sufficient energy. The model assumed that all of the molecules had sufficient energy and were all equally likely to cause nucleation. Since only a very small percentage of the molecules are likely to contain sufficient energy, this assumption could have led to the erroneously high nucleation rates that the model predicted. In order to correct this error the diffusion probability term in Equation 4.1.40 would need to be modified with an additional probability, the probability that the impinging molecule was one with sufficient energy. This probability can be obtained from fluctuation theory.

Looking at fluctuation theory, the basic concept is that every molecule will have a certain discrete energy level or quantum state. Numerous individual molecules can have the same energy level but molecules cannot exist between energy levels (or quantum states). The distribution of the molecules over the various energy levels is anticipated to be Gaussian in nature. Fluctuation theory takes advantage of this Gaussian distribution and the ensemble average is calculated using basic statistical concepts. Fluctuation theory will be used to determine how many of the molecules in the system have sufficient energy to cause nucleation. This fraction will then define the probability that is needed to correct the diffusion probability discussed above. The energy of nucleation will be based on how much energy a cluster needs to overcome the nucleation energy barrier, $\Delta G/kT$.

To estimate the probability, first assume that there is an average energy for the system. This average will be called the background energy. Individual molecules can

have higher or lower energies relative to this average. The energy barrier to nucleation, ΔG/kT, can be looked at as the aggregate energy above this average that a cluster needs to attain in order to nucleate into a bubble. Since the cluster needs a higher energy than the background energy to nucleate, the molecules in the cluster will have, on average, higher energies. The average energy of these individual cluster molecules can be estimated by dividing the free energy of the cluster by the number of molecules in it. This energy can be considered the minimum energy that a molecule needs in order to cause nucleation. Since the distribution of the molecules over the energy levels is Gaussian, it can be represented by (Vining, 1998):

$$f(D)=\frac{1}{\sqrt{2\pi\sigma^2}}\exp\left[-\frac{1}{2}\left(\frac{D-\overline{D}}{\sigma}\right)^2\right] \tag{4.2.1}$$

Above, f(D) is the distribution function for the variable Y, σ is the standard deviation, and $\overline{D}$ is average of D.

Equation 4.2.1 simplifies to:

$$f(D)=\frac{1}{\sqrt{2\pi\sigma^2}}\exp\left[-\frac{1}{2}\left(\frac{D}{\sigma}\right)^2\right] \tag{4.2.2}$$

The standard deviation or variance for a given distribution of molecules in these different energy levels can be estimated from fluctuation theory (McQuarrie, 1976; Hill 1986):

$$\sigma^2=\frac{kT^2C_v}{n} \tag{4.2.3}$$

In Equation 4.2.3, C_v is the constant volume heat capacity of the system, k is Boltzmann's constant, and T is the temperature. (The complete derivation of this

equation is given in Appendix A.) Substituting Equation 4.2.3 into Equation 4.2.2 leads to:

$$f(E)=\frac{1}{\sqrt{2\pi kT^2c_v}}\exp\left[\frac{1}{2}\left(\frac{E^2}{kT^2c_v}\right)\right] \tag{4.2.4}$$

The desired probability is proportional to the number of molecules that will have the necessary energy divided by the total number of molecules. It can be obtained from integrating Equation 4.2.44 from ΔG/kT to infinity or:

$$\mathcal{P}(E)=\int_{\Delta G/kT}^{\infty}\frac{1}{\sqrt{2\pi kT^2c_v}}\exp\left[\frac{1}{2}\left(\frac{E^2}{kT^2c_v}\right)\right]dE \tag{4.2.5}$$

Making use of the fact that the sum of all the probabilities from minus infinity to infinity must equal 1 and that the probability distribution is symmetric this probability can be rewritten as:

$$\mathcal{P}(E)=\frac{1}{2}-\int_{0}^{\Delta G}\frac{1}{\sqrt{2\pi kT^2c_v}}\exp\left[\frac{1}{2}\left(\frac{E^2}{kT^2c_v}\right)\right]dE \tag{4.2.6}$$

This type of integral is commonly encountered in statistics and is usually solved by transforming the integral of interest to a standard normal integral. This is possible because any normal random variable (the distribution of molecules among different energy levels in this case) can be related to the standard normal variable, **Z** through the following simple transformation (Vining, 1998).

$$\mathbf{Z}=\frac{D-\overline{D}}{\sigma} \tag{4.2.7}$$

In Equation 4.2.7, as before, D is any normal random variable, $\overline{D}$ is the average of the normal random variable, and σ is the standard deviation. The standard normal distribution, **Z** is defined as a distribution with a mean centered on zero and a standard

variable equal to one. The correlation between a normal random variable and the standard normal variable can be seen in Figure 4.13. In Equation 4.2.7, the average is subtracted from each random variable to center the actual distribution on zero and then these values are divided by the standard deviation to scale or normalize the variables so the newly transformed distribution has a variance equal to 1 (Vining, 1998). Once the standard normal variable, **Z**, is obtained, it can be related to the probability through standard mathematical tables for the "Cumulative Distribution Function for the Standard Normal Distribution" available in most Probability and Statistics books (i.e. Vining, 1998) and Mathematical handbooks like CRC's Standard Mathematical Tables (1987). In the event that the value of **Z** needed to determine the necessary probability is not available in the tables, then the Equation 4.2.6 can be integrated numerically.

For the specific case here where the background energy has been set equal to zero, Equation 4.2.7 reduces to:

$$\mathbf{Z} = \frac{\Delta G}{kTc_v/n} \tag{4.2.8}$$

when ΔG is substituted for the necessary energy and Equation 4.2.3 is used to substitute for σ. The values of **Z** and the corresponding value of the probability for a molecule to have sufficient energy to cause nucleation are summarized in Table 4.3 for the PMMA/CO_2 system at three different pressures.

Table 4.3 Value of **Z** and the Corresponding Probabilities for the PMMA/CO_2 System @ 313 K for Different Pressures

Pressure, MPa	**Z**	$\mathcal{P}$
21	1.24	0.1038
27.5	0.19	0.4247
34.5	0.02	0.4920

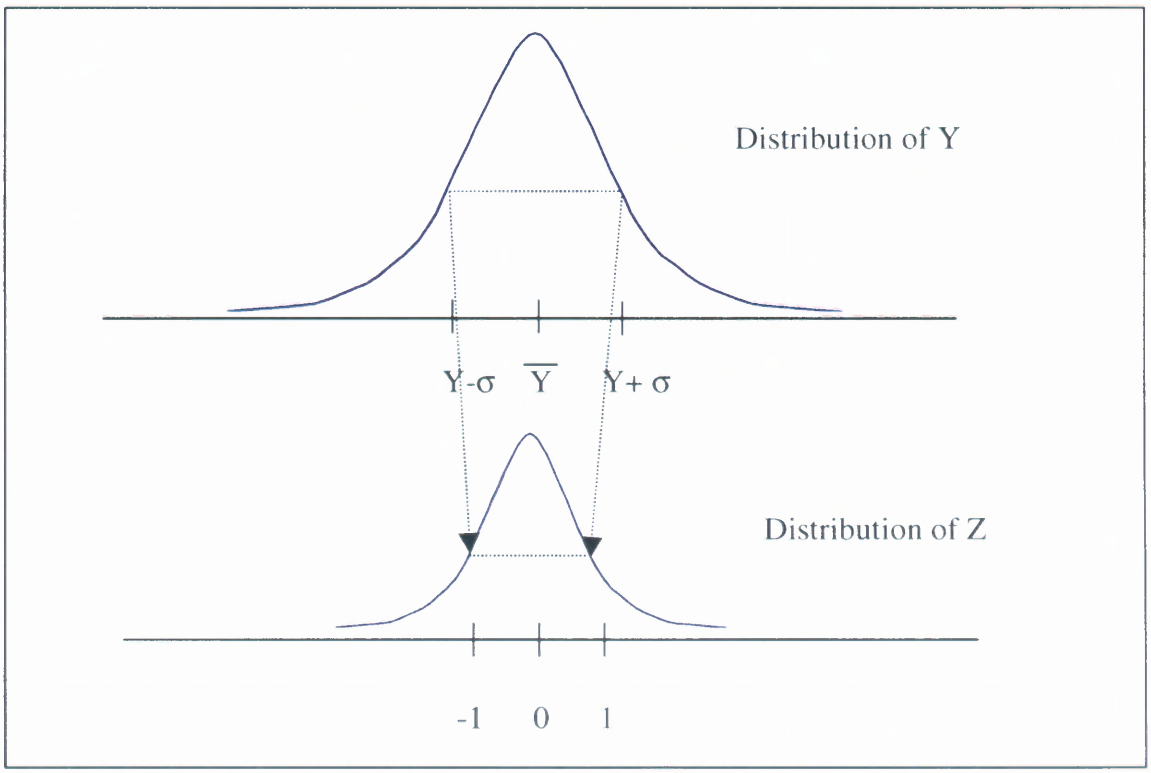

Figure 4.13 The Transformation of a Normal Random Variable Distribution to a Standard Normal Distribution.

These probabilities are compared to values of experimentally determined probabilities in Table 4.4. In Table 4.4, the experimental probability was determined by dividing the predicted nucleation rate by the actual nucleation rate. In reviewing Table 4.4, it is apparent that this approach is not effective.

Table 4.4 Comparison of Experimental and Theoretical Probabilities for the PMMA/CO_2 System at 313 K for Various Pressures[1]

Pressure MPa	Experimental Nucleation Rate Bubbles/cm^3 sec	Model Nucleation Rate Bubbles/cm^3 sec	Experimental Probability Dimensionless	Model Probability Dimensionless
21	4.0×10^{7}	1.4×10^{27}	2.08×10^{-20}	0.1038
27.5	5.0×10^{11}	8.8×10^{28}	5.7×10^{-18}	0.4247
34.5	1.0×10^{12}	1.7×10^{29}	5.9×10^{-18}	0.4920

[1]Experimental Data from Goel and Beckman (1994).

Based on the experimental data, the probability term needs to be many orders of magnitude more than what the fluctuation theory approach is providing. One possible reasons for this is that the use of an average energy for the molecules in the cluster (above the background energy) as determined by the free energy of the cluster is not appropriate.

With regard to this, the cluster requires a certain energy level in order to overcome the nucleation energy barrier. If the molecule adding to the cluster has exactly the same energy as the average energy of the cluster molecules, then by a simple energy balance over all of the molecules, it is easy to see that average energy of the cluster is unchanged. If this is the case, the energy level of the cluster is not sufficient to move the cluster over the nucleation energy barrier. In actuality, the molecule that adds to the cluster to increase it to n + 1 molecules must have an energy greater than the average energy of the cluster in order to move the cluster over the energy barrier. Unfortunately, at this time, there is no apparent method to estimate how much more energy (above the average cluster energy) this molecule needs to have. The calculated probability is still too high because the energy level used in the calculation is not set high enough to exclude a sufficient number of molecules. As an alternate, a completely new method based on a lattice hole theory will be investigated it the next section.

4.2.2 Lattice Hole Theory

This approach is based on the concept of a lattice that has less than 100 percent occupation. Polymer systems have been described by lattice theory for many years (Flory, 1953, Sanchez and Lacombe, 1978). The approach here will be to estimate the

number of vacancies in the lattice for a given system. These vacancies will then be used to estimate the nucleation rate. In this approach, the vacancies act as cavities similar to the cavity model proposed by Lee (1991). The key becomes estimating the number of lattice vacancies and then the number of these vacancies that actually can create bubbles.

The first step is to create a lattice. The lattice will be constructed of a number of cells of fixed volume. The volume of an individual lattice cell will be set equal to the volume of the blowing agent molecule. It can be estimated from:

$$V_l = \frac{4}{3}\pi\ell^3 \tag{4.2.9}$$

In this equation, the lattice volume is denoted by V_l, and ℓ is the radius of gyration of the blowing agent molecule. Note that V_l is equal to v_m. Alternatively, if the van der Waals volume of the blowing agent is known, it can be used directly for V_l.

The next step is to fill the lattice, see Figure 4.14. The lattice will be filled with blowing agent molecules and polymer repeat units. Here, just as in the development of Section 4.1.1, the volume of a polymer repeat unit will be used rather that the volume of the polymer chain. The total polymer volume is again determined by multiplying the repeat unit volume by the number of repeat units. As before, the repeat unit volume will be estimated by the van der Waals volume. In the case of the polymer repeat unit, one repeat unit will occupy multiple lattice cells as given by the following Equation.

$$\mathcal{N} = \frac{V_{vdw}}{V_l} \tag{4.2.10}$$

In Equation 4.2.10, $\mathcal{N}$ is the number of lattice sites occupied by a polymer repeat unit and this is not necessarily a whole number. The term V_{vdw} is the van der Waals volume.

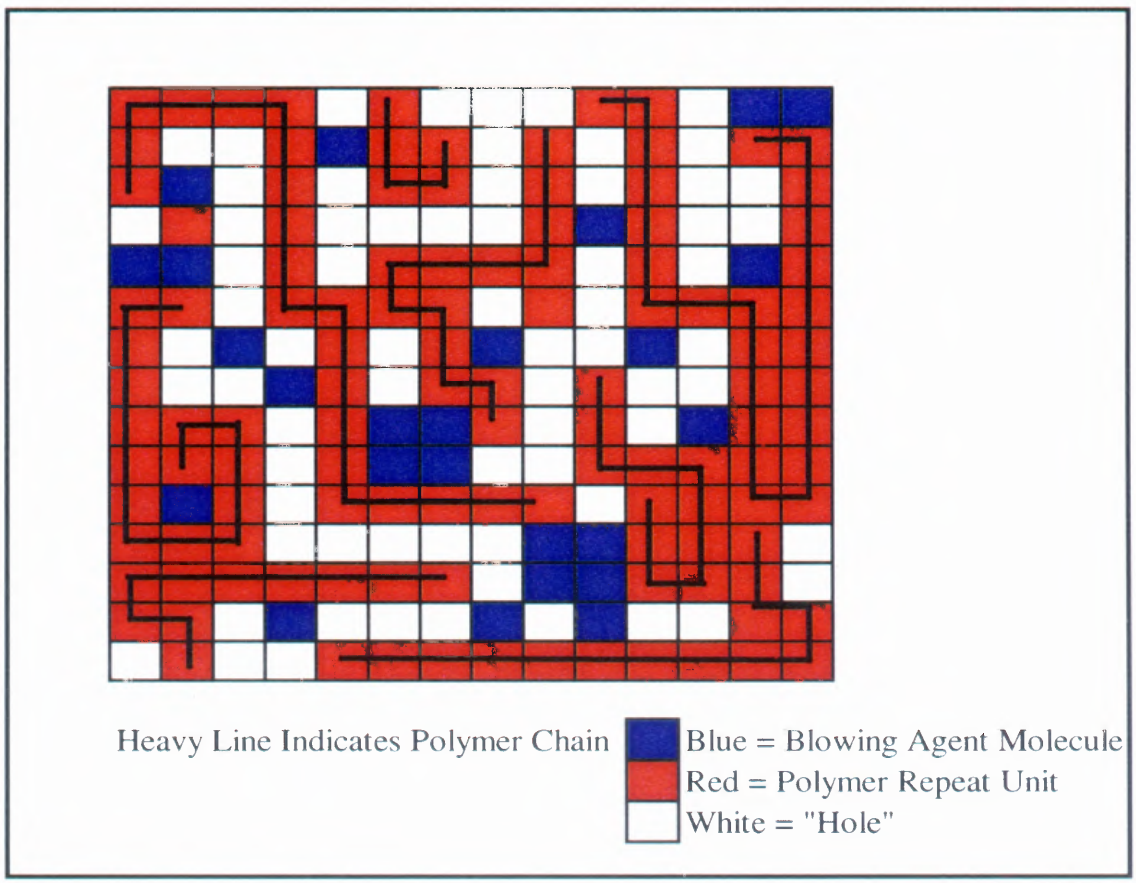

Figure 4.14 Schematic Representation of a Lattice with "Holes".

A blowing agent molecule will occupy one lattice cell. If the total number of repeat units in the system is given by N_R and the total number of blowing agent molecules in the system by N_G, then the total number of occupied lattice sites, $\mathcal{N}_0$ is given by:

$$\mathcal{N}_0 = \mathcal{N} N_R + N_G \tag{4.2.11}$$

The total number of lattice sites for the system is then given by:

$$\mathcal{N}_T = \mathcal{N}_0 + \mathcal{N}_V \tag{4.2.12}$$

where $\mathcal{N}_v$ is the number of vacant lattice sites or "holes" in the system.

If the mass of the repeat unit is given by m_R and the mass of the blowing agent

given by m_G, then the total mass of the system is given by:

$$M = N_R m_R + N_G m_G \tag{4.2.13}$$

The density of the system is given by:

$$\rho = \frac{M}{(n_T)V_l} = \frac{N_R m_R + N_G m_G}{(n_0 + n_V)V_l} \tag{4.2.14}$$

where ρ is the density of the polymer system. If the number of vacant lattice cells is known, then Equation 4.2.14 can be used to estimate the density and this can be compared to experimentally determined densities.

If the number of vacant lattice cells or "holes" is not known, it can be determined by solving Equation 4.2.14 for n_v using the experimentally determined density:

$$n_V = \frac{N_R m_R + N_G m_G}{\rho V_l} - n_0 \tag{4.2.15}$$

Equation 4.2.15 was used to determine the number of holes in the PMMA/CO_2 system and the PS/n-C_5 system. In both cases, the number of holes in the lattice was estimated to be about the same order of magnitude as the original number of blowing agent molecules. The results are summarized in Table 4.5.

With this approach, it was hoped that the number of holes identified in the lattice would be significantly (many orders of magnitude) smaller than the number of blowing agent molecules. These vacancies, acting like cavities, could then become the basis of the nucleation model. Unfortunately, the number of holes estimated in the lattice was of the same order of magnitude as the blowing agent molecules so no real advantage was identified and the need for a different approach remained.

Table 4.5 Results of the Lattice Hole Calculation for the PMMA/CO_2 System and the PS/n-C_5 System

System	PMMA/CO_2[a]	PS/n-C_5[b]
Lattice Cell Volume, cm^3	3.27×10^{-23}	9.64×10^{-23}
Density of System, g/cm^3	1.1725[c]	1.035[d]
Mass of Polymer Repeat Units[e], g	0.851	0.9565
Number of Polymer Repeat Units[f]	5.12×10^{21}	5.58×10^{21}
Volume of Repeat unit, cm^3/molecule	7.85×10^{-23}	1.04×10^{-22}
Number of Lattice Sites Occupied by Polymer	1.58×10^{22}	6.36×10^{21}
Mass of Blowing Agent Molecules[f]	0.322	0.0435
Number of Lattice Sites Occupied by blowing agent	4.4×10^{21}	3.63×10^{20}
Number of Vacant Lattice Sites	1.04×10^{22}	3.29×10^{21}

[a]PMMA sample at 21 MPa.
[b]EPS with 4.35-wt% n-C_5. Typically has 1.0-wt% moisture, actual sample had 0.98-wt% moisture, water content did not have an effect on the number of vacant lattice sites, it was estimated both with and without the moisture with virtually no change in the result.
[c]Density as determined in Goel and Beckman (1994) at 313 K. The authors used a mean field lattice gas model to estimate physical properties such as density.
[d]Density experimentally determined at 298 K.
[e]Mass of repeat units based on 1 cm^3.
[f]Number of repeat units or molecules based on 1 cm^3.

An alternative to looking at either of these methods to correct the nucleation rate model is to look at the distribution of the molecules in the system. From the distribution, it may be possible to develop a molecular partition function that will improve the result. This partition function approach will be developed in the next chapter and coupled with the concept of the diffusion-based model discussed earlier in this chapter, which will be retained since it makes more sense physically.

CHAPTER 5

A STATISTICAL APPROACH

5.1 Developing the Molecular Partition Function

To this point, the efforts to improve the predictive capability of a nucleation rate model without experimentally fitted parameters have not been very successful. In general, most, if not all of the investigations in the literature have ultimately resorted to some sort of experimental parameter. Efforts to correct the nucleation rate in this work as discussed in Chapter 4 have not been very successful either. So far, these efforts have included the use of a diffusion-based model, a diffusion based model modified with fluctuation theory and a lattice hole model that extended to a cavity model. Hence, a more sophisticated approach is necessary. The approach adopted here is the creation of a molecular partition function (MPF).

This concept is not completely new, as the work of Reiss and his co-workers (Chapter 2) used just such an approach for estimating nucleation rates of simple systems like condensing argon gas. This approach, however, has not been used to investigate polymer systems. The task of modeling polymer systems is often more difficult because of the size disparity between the polymer chains and the blowing agent molecules. In order to take a MPF approach, the first step is to define a physically consistent cluster; this will be done in Section 5.1.1. The second step will is to develop the actual cluster distribution function. This is derived in Section 5.1.2. Finally, Section 5.1.3 determines the most probable, or equilibrium distribution.

5.1.1 Defining the Cluster

In any system, the molecules will tend to be distributed into various sized groups or clusters. Before the cluster distribution function or MPF can be developed, a definition of a cluster is required. This definition must possess two key factors. Primarily, it must make sense physically. This suggests that the envisioned physical construct should intuitively match our current understanding of the microscopic situation. As a secondary factor, the model should be mathematically manageable. With the advent of high-powered computers, this factor is becoming less and less important. The cluster model of Ellerby, Weakliem, and Reiss (1991) will be used as the model here. It will be adjusted accordingly to account for the polymer in the system.

The following mathematical terms are defined for the polymer systems under investigation:

- N is the total number of molecular units in the system. A molecular unit is either a blowing agent molecule or a polymer repeat unit. The polymer repeat unit will be used in place of the polymer chain to minimize the size differences of the molecular constituents in the system. The actual polymer chain size can be obtained as before, by multiplying the size of the repeat unit by the number of repeat units. Throughout the derivation, the total sum of the number of blowing agent molecules and the number of repeat units in the bulk phase will be referred to as simply the number of molecules even though the repeat unit is not technically a molecule.
- N_P is the number of the polymer repeat units. This quantity is estimated by dividing the mass of polymer by the molecular weight of the repeat unit.

- N_G is the number of blowing agent molecules in the system.
- n is the number of molecules in a cluster.
- Λ is a the inverse of the thermal de Broglie wavelength cubed:

$$\Lambda = \left(\frac{2\pi mkT}{h^2} \right)^{3/2} \tag{5.1.1}$$

This term is multiplied by the system volume when used for an ideal gas translational contribution to a MPF. In the equation above, all terms are defined in the traditional way; h is Planck's constant, k is Boltzmann's constant, m is the mass of a molecule, and T is the temperature.

The cluster will be defined in the following way:

- A cluster will contain n molecules
- It will occupy a volume v
- The density within the cluster is given by (n+1)/v which can be approximated by n/v
- The cluster is assumed to be spherically symmetric
- One blowing agent molecule from the surrounding bulk mixture can be found inside a differential shell volume defined as dv. This shell volume molecule defines the outer limit of the cluster.
- The center of mass (c.m.) of the cluster is determined only by the n molecules in the cluster and the one molecule in the shell.
- The n molecules inside the cluster can only be blowing agent molecules.
- The n molecules in the cluster are treated as an ideal gas.
- The cluster can be found anywhere in the system volume, V.

- The remaining N-(n+1) molecules must be found outside the cluster volume, v, either in other clusters or in the bulk metastable phase.
- The clusters are sufficiently small and sufficiently separated in space so that they do not interact with each other.
- The clusters do not interact with the surrounding metastable bulk phase.

A schematic representation of a cluster is shown in Figure 5.1. The system description is completed by assuming that the metastable bulk phase is a regular liquid. The term regular liquid implies that the excess volume and entropy are both zero and the excess enthalpy, free energy, and internal energy are all equal.

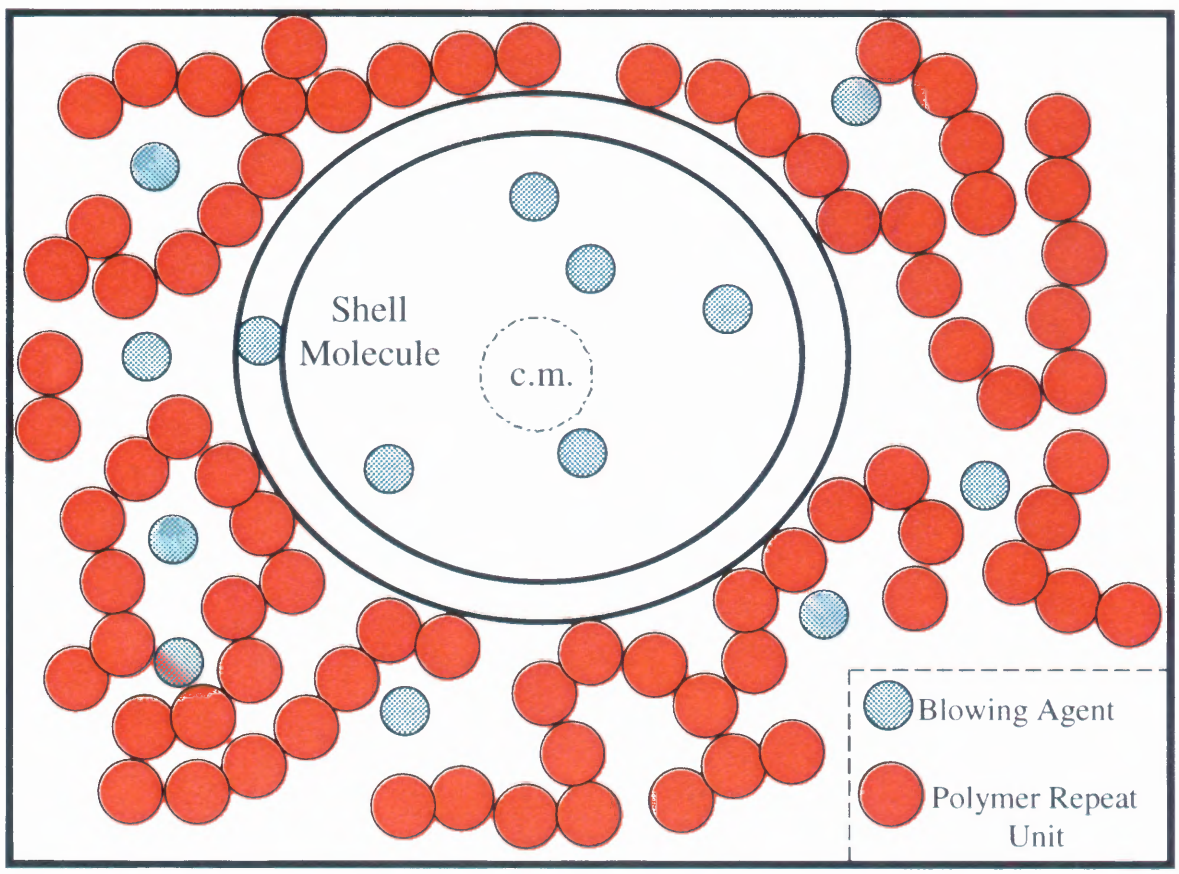

Figure 5.1 Schematic Representation of the Blowing Agent Cluster. The polymer chains are shown as multiple polymer repeat units connected in series.

5.1.2 Determining the Cluster Distribution Function

The development of the MPF is a complicated process. In order to simplify this process, a "road map" of the involved steps may be helpful. In developing the road map, all of the molecules are initially considered distinguishable. One of the last steps in the procedure corrects this.

- Step 1: Determine the contributions of a particular distribution of molecules, otherwise known as a configuration. The configuration will have a certain number of molecules that are polymer (or polymer repeat units) in the bulk phase, blowing agent molecules in the bulk phase, and blowing agent molecules in clusters. The cluster positions in this configuration will be fixed at $\mathbf{R_1}$, $\mathbf{R_2}$, $\mathbf{R_3}$, ... $R_{n_{nv}}$. The $\mathbf{R_i}$'s designate the c.m. of the clusters in cluster space.
- Step 2: Determine the contributions of all of the different configurations that have clusters in the same physical locations in the cluster space, i. e. at $\mathbf{R_1}$, $\mathbf{R_2}$, $\mathbf{R_3}$, ... $R_{n_{nv}}$, but with the molecules in different places. The only restriction is that molecules in a cluster must remain in a cluster. They can move anywhere else in that cluster so long as the end result is that the cluster c.m. is the same. Molecules outside the clusters are free to move anywhere in the bulk phase but can not join a cluster.
- Step 3: Account for double counting. Configurations that have clusters of exactly the same size switch positions should not actually be counted as two different configurations. Therefore an appropriate correction factor will be developed.

- Step 4: Relax the constraint that clusters must have exactly the same c.m. and allow clusters to move throughout the entire system volume.
- Step 5: Correct the result because the process was developed using "distinguishable" molecules. In reality, the molecules are indistinguishable. Sum the results over all possible cluster configurations from Step 4 to finish the task.

Each step will now be described in detail.

In order to determine the MPF for a given system, it is helpful to visualize the distribution of the molecules in space at a given time. This is facilitated by imagining that all of the molecules in the system are frozen in time for an instant. While frozen, a picture of the molecules is taken. This picture represents one of the many possible configurations that the molecules can be in or occupy. In taking this picture, the molecules have been made "distinguishable" because in theory, they can be labeled.

The contributions of all of the molecules in this configuration need to be included in the MPF. This is accomplished by including the contributions from the four different types of molecules in the configuration. The first contribution is for the n molecules that are in each cluster. The second is for the single molecule that is contained in the shell volume, dv, of each cluster. The third contribution is for the blowing agent molecules in the bulk metastable phase (not in a cluster). Finally, the last contribution is for the polymer repeat units that are located in the bulk metastable phase.

Since the blowing agent molecules inside the cluster (including the molecule in the shell) are considered ideal, their contributions are nothing more than the translational

contribution to the partition function; Λ multiplied by the volume (Hill, 1986). For the n molecules inside the cluster, this contribution is given by:

$$(\Lambda d\tau)^n \tag{5.1.2}$$

In this equation, dτ is an arbitrary differential volume. The quantity Λdτ is raised to the n^{th} power because there is a contribution for each of the n molecules in the cluster. The term for the single molecule inside the differential shell volume that physically defines the outer limit of the cluster is similarly:

$$\Lambda d\tau^* \tag{5.1.3}$$

The only difference between this equation and Equation 5.1.2 is that the arbitrary volume is denoted as dτ* and the term is not raised to any power (there is only one shell molecule per cluster). The shell molecule resides in a volume element that is different from the cluster volume (it is actually a small subspace of the total cluster volume) so the * is used to denote that this volume is different from the actual differential cluster volume, dτ. The contributions of the polymer repeat units and the blowing agent molecules in the bulk phase (all of the molecules that are not in clusters) are more complicated because of their non-ideality. The polymer repeat unit contributions can be obtained from (Hill, 1986):

$$\left[\Lambda d\tau_{f_P} \exp\left(\frac{u}{2kT}\right)\right]^{N_P} \tag{5.1.4}$$

In Equation 5.1.4, $d\tau_{f_P}$ is the differential free volume of the polymer and u is the potential energy of interaction between one molecule and all of the others. This term is raised to the N_P power in order to account for the fact that there are N_P polymer repeat units in the system.

A similar expression can be obtained for the blowing agent molecules in the bulk phase, however, this number first needs to be determined. This is done by a simple mass balance on the blowing agent. The number of blowing agent molecules in every cluster is n + 1. This accounts for the n molecules inside the cluster volume plus the shell molecule. This number is then multiplied by the number of clusters, f_{nv}, to be determined later. The result is subtracted from the total number of blowing agent molecules originally present in the system to give the number of blowing agent molecules in the bulk phase, or:

$$N_G - \sum_{nv}(n+1)f_{nv} \tag{5.1.5}$$

This becomes the exponent for the contribution of the blowing agent in the bulk phase to the MPF below:

$$\left[\Lambda d\tau_{f_G} \exp\left(\frac{u}{2kT}\right)\right]^{N_G-\sum_{nv}(n+1)f_{nv}} \tag{5.1.6}$$

In Equation 5.1.6, $d\tau_{f_G}$ is the differential free volume of the blowing agent in the bulk phase. Equations 5.1.2, 5.13, 5.1.4, and 5.1.6 can be combined to provide the contributions to the MPF from this one configuration. The result of this is:

$$\left[\Lambda d\tau_{f_G} \exp\left(\frac{u}{2kT}\right)\right]^{N_G-\sum_{iv}(n+1)f_{nv}} \left[\Lambda d\tau_{f_P} \exp\left(\frac{u}{2kT}\right)\right]^{N_P} \prod_{nv}\left[(\Lambda d\tau)^n \Lambda d\tau^*\right]^{f_{nv}} \tag{5.1.7}$$

The cumulative product for the last two terms in Equation 5.1.7 accounts for the fact that there are nv clusters, each with their shell and n internal molecules that contribute to the MPF. The last two terms are raised to the f_{nv} power to account for each cluster size occurring f_{nv} times. Refer to Figure 5.2

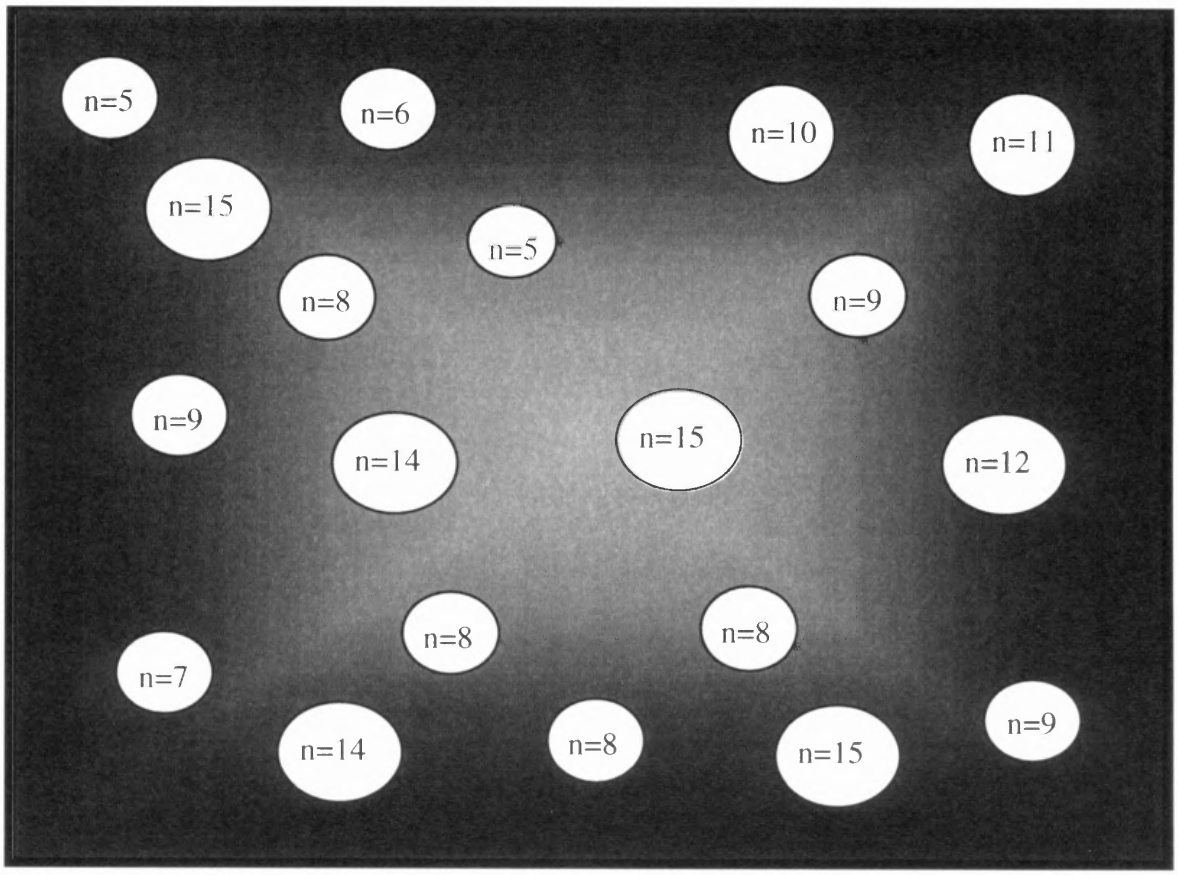

Figure 5.2 Schematic Representation of a Distribution of Various Sized Clusters in the System. The schematic shows clusters of varying size from n = 5 to n = 15, however, all cluster sizes up to n = n_c are possible. Note that some clusters of the same size occur more than once. In actuality, the size range of the clusters and the number of each of the various sized clusters would be a function of the particular system under investigation.

Equation 5.1.7 already differs from the original approach of Ellerby et al. (1991) in that it has been extended to a two-component system. Reiss et al. did not deal with this complexity, as the development of their MPF was for the condensation of a pure ideal vapor. The extension of the MPF theory to a two-component (or multi component) system creates one significant problem. The nucleating clusters will need to occupy a certain volume. In doing this, the clusters exclude volume that is otherwise available in the overall system and the molecules not contained inside the clusters will need to be

re-partitioned in the new smaller system volume. The volume that the clusters need has an effect on the volume for both the blowing agent molecules and the polymer repeat units. It is, however, impossible to determine how each of their respective volumes, $d\tau_{f_G}$ and $d\tau_{f_P}$, will be affected. One solution to this problem is to combine these two terms (Equations 5.1.4 and Equation 5.1.6). In order to do this, the total number of molecules, N_B, (blowing agent molecules and polymer repeat units) in the bulk phase needs to be determined. This number is equal to the total number of polymer repeat units in the system plus the number of blowing agent molecules not in clusters. Using Equation 5.1.5, N_B is given by the following equation:

$$N_B = N_p + \left[N_G - \sum_{nv} (n+1) f_{nv} \right] \tag{5.1.8}$$

The contributions of all of the molecules in the bulk phase can be given by:

$$\left[\Lambda d\tau_f \exp\left(\frac{u}{2kT} \right) \right]^{N_B} \tag{5.1.9}$$

where $d\tau_f$ and u now are properties of the mixture, not the individual components and will need to be described by an adequate mixing rule. The mixing rule will be discussed a little later in this Chapter.

The contributions of all of the molecules from this first configuration (the first picture) can now be combined:

$$\left[\Lambda d\tau_f \exp\left(\frac{u}{2kT} \right) \right]^{N_B} \prod_{nv} \left[(\Lambda d\tau)^n (\Lambda d\tau^*) \right]^{f_{nv}} \tag{5.1.10}$$

This is essentially the result of the first step in the road map outlined at the beginning of this section. The next step (Step 2) is to account for all of the possible

configurations that have the c.m. of the clusters fixed but still have the individual molecules in different positions. Each of these configurations can be envisioned as the result of repeating the process of taking pictures of the system. Many different pictures will result with the molecules of the system in different places but with the c.m. of the clusters in the same place. Eventually, all of the possible locations of the molecules providing the same cluster distribution (i. e. clusters of the same size with c.m. in the same place) will be exhausted and no other contributions to the MPF will be observed. Under this constraint, that is the equivalent to integrating for all possible configurations over the excluded free volume of the system (Ellerby, et al., 1991). In order to facilitate this integration, it is helpful to define the excluded volume for the system. It is the volume not occupied by individual molecules or by clusters. In physical terms, it is essentially the space between the molecules in the bulk phase.

The free volume, V_f, of the bulk phase is given by:

$$V_f = V - N_B b \tag{5.1.11}$$

where V is the system volume if there are no clusters present, N_B is the number of molecules in the bulk or liquid phase given by Equation 5.1.9, and b is the van dar Waals volume. This free volume can be considered the sum of the "holes" in a lattice (relating back to the lattice concept in Chapter 4). This volume needs to be corrected further for the volume of the clusters to represent the actual excluded volume of the bulk phase in the system. This volume is given the symbol $\overline{V}_f$, and is obtained by subtracting the total volume occupied by clusters from V_f or:

$$\overline{V}_f = V - N_B b - \sum_{nv} v f_{nv} \tag{5.1.12}$$

Now that $\overline{V}_f$ has been defined, it is now possible to carry out the desired integration. The result of this integration is that the differential free volume in the first term of Equation 5.1.10 is replaced with the actual free volume, the differential shell volume, $d\tau^*$ is replaced with a differential cluster volume, and for the moment, dv, and the differential cluster volumes, $d\tau$'s is left un-integrated (this is to show that there are multiple integrals, one for every cluster):

$$\left[\Lambda\overline{V_f}\exp\left(\frac{u}{2kT}\right)\right]^{N_B}\prod_{nv}\left[\Lambda^n\int\cdots\int\exp\left(\frac{u_n'}{2kT}\right)d\tau^n(\Lambda dv)\right]^{f_{nv}} \tag{5.1.13}$$

Note in Equation 5.1.13 that there is an integral for every cluster, hence the symbol for multiple integrals. Additionally, in Equation 5.1.13, a potential energy term, $\exp(u_n'/2kT)$, has been added to the cluster molecules for technical completeness. This term could have been included in Equations 5.1.2 and 5.1.3 just as easily. As these molecules are being treated as an ideal gas, u_n' is zero, and this is only a formality. Equation 5.1.13 reduces to:

$$\left[\Lambda\overline{V_f}\exp\left(\frac{u}{2kT}\right)\right]^{N_B}\prod_{nv}\left[\Lambda^n\int\cdots\int d\tau^n(\Lambda dv)\right]^{f_{nv}} \tag{5.1.14}$$

when the substitution $u_n' = 0$ is made. With the potential energy term eliminated from the second factor of Equation 5.1.14, the integration can be completed and the result is:

$$\left[\Lambda\overline{V_f}\exp\left(\frac{u}{2kT}\right)\right]^{N_B}\prod_{nv}\left[\Lambda^n v^n\Lambda dv\right]^{f_{nv}} \tag{5.1.15}$$

At this point, it is important to recognize that since the molecules are being treated as distinguishable, the number of ways that a given configuration can be obtained is equal to

the number of different permutations that can be developed by selecting each molecule in the system, one at a time. The number of these permutations is obtained by selecting:

- the polymer repeat units in the bulk phase one by one,

then by selecting the

- blowing agent molecules in the bulk phase, one by one,

then by selecting the

- blowing agent molecules in the clusters, one by one, for each cluster,

and then finally by selecting the

- shell molecule for each cluster, one by one.

Mathematically, this is equivalent to

$$\frac{N_P!N_G!}{N_P!\left[N_G-\sum(n+1)f_{nv}\right]!(n!\,cluster\,1)^{f_{nv}}(n!\,cluster\,2)^{f_{nv}}\cdots(n!\,cluster\,n_{nv})^{f_{nv}}(1!)^{f_{nv}}} \tag{5.1.16}$$

In Equation 5.1.16, each of the terms $(n!\,cluster\,n_{nv})^{f_{nv}}$ has been shortened so that the equation format is manageable, these terms should actually read $(n!\ for\ cluster\ size\ n_{nv})^{f_{nv}}$.

Equation 5.1.16 can be rewritten:

$$\frac{N_P!N_G!}{N_P!\left[N_G-\sum(n+1)f_{nv}\right]!\prod_{nv}(n!)^{f_{nv}}(1!)^{f_{nv}}} \tag{5.1.17}$$

and simplified slightly:

$$\frac{N_P!N_G!}{N_P!\left[N_G-\sum(n+1)f_{nv}\right]!\prod_{nv}(n!)^{f_{nv}}} \tag{5.1.18}$$

The expression in Equation 5.1.15 must be multiplied by this number of different possible permutations giving:

$$\frac{N_P!N_G!}{N_P!\left[N_G-\sum(n+1)n_{nv}\right]!\prod_{nv}(n!)^{f_{nv}}}\left[\Lambda\overline{V_f}\exp\left(\frac{u}{2kT}\right)\right]^{N_B}\prod_{nv}\left[\Lambda^n v^n \Lambda dv\right]^{f_{nv}} \qquad (5.1.19)$$

Rearranging and collecting terms:

$$\frac{N_P!N_G!\left[\Lambda\overline{V_f}\exp\left(\frac{u}{2kT}\right)\right]^{N_B}}{N_P!\left(N_G-\sum(n+1)f_{nv}\right)!}\prod_{nv}\frac{\left[\Lambda^n v^n \Lambda dv\right]^{f_{nv}}}{(n!)^{f_{nv}}} \qquad (5.1.20)$$

At this point, the contributions of all of the possible configurations with the clusters confined to the same place have been accounted for. The third step in the road map set out at the beginning of this section is to correct for the double counting that goes on when the same configuration is obtained by clusters of exactly the same size simply switching position with one another. When this happens, there is no new contribution to the MPF and the configuration should only be counted once. Equation 5.1.20 can be divided by a factor of $\prod f_{nv}!$ to correct this problem. The result is:

$$\frac{N_P!N_G!\left[\Lambda\overline{V_f}\exp\left(\frac{u}{2kT}\right)\right]^{N_B}}{N_P!\left(N_G-\sum(n+1)f_{nv}\right)!}\prod_{nv}\frac{\left[\Lambda^n v^n \Lambda dv\right]^{f_{nv}}}{(n!)^{f_{nv}}}\frac{1}{f_{nv}!} \qquad (5.1.21)$$

At this point, it is convenient to introduce a cluster partition function, q:

$$q=\frac{(\Lambda v)^n}{n!} \qquad (5.1.22)$$

This individual cluster partition function has the same properties as the individual molecular partition function, q, for an ideal gas because the cluster definition was set up exactly the same as the definition for molecules in an ideal gas. That definition included the clusters being small enough and sufficiently spaced so that they would not interact with each other. This is the same as saying the potential energy of the ideal gas

molecules is zero and there are no interactions between molecules. Just as in an ideal gas where the contributions of the individual molecules can simply be multiplied together to obtain the system partition function, the individual cluster partition functions can be multiplied to give the system MPF. Rearranging Equation 5.1.21 using Equation 5.1.22 leads to:

$$\frac{N_P!N_G!\left[\Lambda\overline{V_f}\exp\left(\frac{u}{2kT}\right)\right]^{N_B}}{N_P!\left(N_G-\sum(n+1)f_{nv}\right)!}\prod_{nv}\frac{[q\Lambda dv]^{f_{nv}}}{f_{nv}!} \tag{5.1.23}$$

The next step in the development of the MPF is to relax the requirement that the c.m. of the clusters must remain fixed and allow the clusters to be found anywhere in the system V. This is accomplished by integrating all of the coordinates of the various c.m.'s over V. This integration produces a factor $\prod V^{f_{nv}}$ (Ellerby et al., 1991) by which Equation 5.1.23 is multiplied:

$$\frac{N_P!N_G!\left[\Lambda\overline{V_f}\exp\left(\frac{u}{2kT}\right)\right]^{N_B}}{N_P!\left(N_G-\sum(n+1)f_{nv}\right)!}\prod_{nv}\frac{[qV\Lambda dv]^{f_{nv}}}{f_{nv}!} \tag{5.1.24}$$

The result is simply the inclusion of a V in the cumulative product above.

One of the last steps that is needed in developing the MPF is to correct for the fact that the molecules are indistinguishable. This is necessary because the entire development up until this point has treated the molecules as distinguishable. This is done by dividing Equation 5.1.24 by $N_P!N_G!$. The result is:

$$\frac{\left[\overline{\Lambda V_f}\exp\left(\frac{u}{2kT}\right)\right]^{N_B}}{N_P!\left(N_G-\sum(n+1)f_{nv}\right)!}\prod_{nv}\frac{[qV\Lambda dv]^{f_{nv}}}{f_{nv}!} \tag{5.1.25}$$

Finally, the last thing that needs to be done in creating the MPF is to sum all of the contributions of all of the cluster configurations that satisfy the following constraining equation:

$$N = N_P + \left\{N_G - \sum (n+1) f_{nv}\right\} + \sum (n+1) f_{nv} \tag{5.1.26}$$

This leads to

$$Q = \sum_{f_{nv}} \frac{\left[\Lambda \overline{V_f} \exp\left(\frac{u}{2kT}\right)\right]^{N_B}}{N_P!\left(N_G - \sum (n+1) f_{nv}\right)!} \prod_{nv} \frac{[qV\Lambda dv]^{f_{nv}}}{f_{nv}!} \tag{5.1.27}$$

In Equation 5.1.27, it is important to remember that the f_{nv} in the sum is over the entire set of possible nv values. Equation 5.1.27 is the MPF for the system.

5.1.3 Determining the Most Probable or Equilibrium Distribution

The next step will be to determine which of the many possible distributions is actually the most probable. This will be done using the method of Lagrange multipliers (Thomas and Finney, 1982). In order to apply the method of Lagrange multipliers to Equation 5.1.27, it is useful to rewrite it in terms of two variables, f_{nv} and N_B. Expressing Q in terms of f_{nv} and N_B results in:

$$Q = \sum_{f_{nv}} \frac{\left[\Lambda \overline{V_f} \exp\left(\frac{u}{2kT}\right)\right]^{N_B}}{N_P!(N_B - N_P)!} \prod_{nv} \frac{[qV\Lambda dv]^{f_{nv}}}{f_{nv}!} \tag{5.1.28}$$

In the equation above, a mass balance on the blowing agent molecules has been used to replace the $\left(N_G - \sum (n+1) f_{nv}\right)!$ term, which is the number of blowing agent molecules in the bulk phase, with $(N_B - N_P)!$. In order to maximize Q, it needs to be put into a more

tractable form. To do this, the sum will be replaced with its maximum term. This is done by writing out one of the terms from the series, however, one comment is necessary before proceeding. Since it becomes awkward to take factorials for large values of N, rather than writing out a term of Q as it is cast in Equation 5.1.28, the natural log of a term in Q will be used. This allows Stirling's approximation to be used for the factorials and makes the problem significantly easier to deal with. The replacement of Q with its maximum term does not lead to any significant error because of the numerically large factorials involved in the calculation (McQuarrie, 1976). This leads to the following equation:

$$\begin{aligned}\ln Q = {} & N_B \ln \Lambda + N_B \ln \overline{V_f} + N_B \ln\left(\exp\frac{u}{2kT}\right) - N_P \ln N_P + N_P - \\ & (N_B - N_P)\ln(N_B - N_P) + (N_B - N_P) + \\ & \sum f_{nv} \ln(qV) + f_{nv} \ln \Lambda dv - f_{nv} \ln f_{nv} + f_{nv}\end{aligned} \tag{5.1.29}$$

Now, just as Q was put in terms of n_{nv} and N_B, the constraining equation (Equation 5.1.26) also needs to be recast in these terms. Designating this constraining equation as $g(f_{nv}, N_B)$ then:

$$g(f_{nv}, N_B) = N_P + [N_B - N_P] + \sum (n+1) f_{nv} - N = 0 \tag{5.1.30}$$

Equation 5.1.30 is set equal to zero to facilitate the maximization process.

Following the method of Lagrange multipliers, the following equation needs to be maximized:

$$d \ln Q(f_{nv}, N_B) - \lambda dg(f_{nv}, N_B) = 0 \tag{5.1.31}$$

Taking the total differential of Equation 5.1.31 leads to:

$$\frac{\partial \ln Q}{\partial f_{nv}} df_{nv} + \frac{\partial \ln Q}{\partial N_B} dN_B - \lambda\left(\frac{\partial g}{\partial f_{nv}} df_{nv} + \frac{\partial g}{\partial N_B} dN_B\right) = 0 \tag{5.1.32}$$

Combining terms of like coefficients:

$$\left(\frac{\partial \ln Q}{\partial n_{nv}} - \lambda \frac{\partial g}{\partial n_{nv}}\right) dn_{nv} + \left(\frac{\partial \ln Q}{\partial N_B} - \lambda \frac{\partial g}{\partial N_B}\right) dN_B = 0 \tag{5.1.33}$$

The four necessary derivatives are:

$$\frac{\partial \ln Q}{\partial f_{nv}} = \frac{-N_B v}{\overline{V_f}} + \ln qV + \ln \Lambda dv - \ln f_{nv} \tag{5.1.34}$$

$$\frac{\partial \ln Q}{\partial N_B} = \ln \Lambda \overline{V_f} - \frac{N_B v}{\overline{V_f}} + \frac{u}{2kT} - \ln(N_B - N_P) \tag{5.1.35}$$

$$\frac{\partial g}{\partial f_{nv}} = -(n+1) \tag{5.1.36}$$

and

$$\frac{\partial g}{\partial N_B} = -1 \tag{5.1.37}$$

For like terms of f_{nv},

$$\frac{\partial \ln Q}{\partial f_{nv}} - \lambda \frac{\partial g}{\partial f_{nv}} = 0 \tag{5.1.38}$$

Substituting in the appropriate derivatives gives:

$$-\frac{N_B v}{\overline{V_f}} + \ln qV + \ln \Lambda dv - \ln f_{nv} + (n+1)\lambda = 0 \tag{5.1.39}$$

Equation 5.1.39 can be solved for $\ln f_{nv}$:

$$\ln f_{nv} = -\frac{N_B v}{\overline{V_f}} + \ln qV + \ln \Lambda dv + (n+1)\lambda \tag{5.1.40}$$

Reiss and Katz (1967) showed that:

$$\lambda = \frac{\mu_1}{kT} \tag{5.1.41}$$

This can be used in Equation 5.1.40 to obtain f_{nv}:

$$f_{nv} = \Lambda dv \exp\left[-\frac{N_B v}{\overline{V}_f} + \ln qV + \frac{(n+1)\mu_1}{kT} \right] \tag{5.1.42}$$

The above equation can be rewritten if the last term on the in the square brackets is split up into two separate exponential terms:

$$f_{nv} = \Lambda dv \exp\left(\frac{\mu_1}{kT}\right) \exp\left[-\frac{N_B v}{\overline{V}_f} + \ln qV + \frac{n\mu_1}{kT} \right] \tag{5.1.43}$$

Hill (1986) shows that the Helmholtz energy can be related to ln q in the following way:

$$A_H = -kT \ln qV \tag{5.1.44}$$

Equation 5.1.43 can be rewritten to take advantage of this fact:

$$f_{nv} = \Lambda dv \exp\left(\frac{\mu_1}{kt}\right) \exp\left[-\frac{1}{kT}\left[\frac{N_B vkT}{\overline{V}_f} - kT \ln qV - n\mu_1 \right] \right] \tag{5.1.45}$$

Using the ideal gas law, it is also easy to note that the term:

$$\frac{N_B vkT}{\overline{V}_f} \tag{5.1.46}$$

is actually a PV term. Also noting from thermodynamics:

$$G = A_H + PV \tag{5.1.47}$$

Using Equation 5.1.47, Equations 5.1.44 and 5.1.46 can be combined to give:

$$G_f = \frac{N_B vkT}{\overline{V}_f} - kT \ln qV \tag{5.1.48}$$

where G_f is the final Gibbs free energy of formation of a cluster. The initial Gibbs free energy, G_i, is given by:

$$G_i = n\mu_1 \tag{5.1.49}$$

The difference between G_f and G_i is obviously ΔG. Equation 5.1.44 can then be rewritten again as:

$$f_{nv} = \Lambda dv \exp\left(\frac{\mu_1}{kT}\right)\exp\left[-\frac{\Delta G}{kT}\right] \tag{5.1.50}$$

This is actually a very convenient form for Equation 5.1.50 because even though it has been developed at the molecular level, macroscopic properties can still be used to evaluate the change in the Gibbs free energy, ΔG. In reviewing Equation 5.1.50, the only undefined term left at this point is μ_1/kT. The definition of this term can be obtained by returning to the method of Lagrange multipliers and looking at the other equation that was used. For like terms of N_B:

$$\frac{\partial \ln Q}{\partial N_B} - \lambda\frac{\partial g}{\partial N_B} = 0 \tag{5.1.51}$$

Again, substituting in the appropriate derivatives gives:

$$\ln \Lambda\overline{V_f} - \frac{N_B b}{\overline{V_f}} + \frac{u}{2kT} - \ln(N_B - N_P) - \lambda = 0 \tag{5.1.52}$$

Also substituting Equation 5.1.41 for λ again gives:

$$\ln \gamma\Lambda\overline{V_f} - \frac{N_B b}{\overline{V_f}} + \frac{u}{2kT} - \ln(N_B - N_P) - \frac{\mu_1}{kT} = 0 \tag{5.1.53}$$

This can be solved for μ_1/kT:

$$\frac{\mu_1}{kT} = \ln \Lambda\overline{V_f} - \frac{N_B b}{\overline{V_f}} + \frac{u}{2kT} - \ln(N_B - N_P) \tag{5.1.54}$$

Substituting Equation 5.1.54 into Equation 5.1.50 leads to the complete cluster distribution function:

$$f_{nv} = \Lambda\left(4\pi r^2 dr\right)\exp\left(\ln\Lambda\overline{\overline{V_f}} - \frac{N_B b}{\overline{\overline{V_f}}} + \frac{u}{2kT} - \ln\left(N_B - N_P\right)\right)\exp\left[-\frac{\Delta G}{kT}\right] \qquad (5.1.55)$$

where $4\pi r^2 dr$ has been substituted for dv. One other simplification can be made with regard to this equation. As it is cast now, a trial and error calculation would be required to obtain the cluster distribution function because the function is dependent on the excluded volume, $\overline{V}_f$. This trial and error calculation can be eliminated by assuming that the excluded volume of the clusters, $\sum_{nv} vf_{nv}$ in Equation 5.1.12 is very small. This is based on the original cluster definition. Neglecting this term in Equation 5.1.12 given earlier:

$$\overline{V}_f = V - N_B b - \sum_{nv} vf_{nv}$$

results in the traditional free volume which was given in Equation 5.1.11:

$$V_f = V - N_B b$$

Making this substitution gives a cluster distribution function of:

$$f_{nv} = \Lambda\left(4\pi r^2 dr\right)\exp\left(\ln\Lambda\overline{V}_f - \frac{N_B b}{\overline{V}_f} + \frac{u}{2kT} - \ln\left(N_B - N_P\right)\right)\exp\left[-\frac{\Delta G}{kT}\right] \qquad (5.1.56)$$

In order to evaluate the terms in the first exponential, the mixing rules discussed earlier in the chapter become necessary. The simplest composition-dependent mixing rule that can be used is one that is also common for many equations of state. It has the following form:

$$\mathcal{B}_M = \sum_i y\mathcal{B}_i \qquad (5.1.57)$$

In Equation 5.1.57, $\mathcal{B}$ is used to designate any property of the mixture, y_i is the mole fraction, and $\mathcal{B}_i$ is the pure component property. The three properties that are required are the free volume, V_f, the excluded volume, $N_B b$, and a mass term, m. Applying Equation 5.1.57 to these three properties gives:

$$V_f = y_1 V_{f_1} + y_2 V_{f_2} \tag{5.1.58}$$

$$N_B b = y_1 N_B b_1 + y_2 N_B b_2 \tag{5.1.59}$$

$$m = y_1 m_1 + y_2 m_2 \tag{5.1.60}$$

Since ΔG can be evaluated from macroscopic properties, as stated earlier, the traditional expression (Equation 5.1.56) from CNT can be retained:

$$\Delta G_m\big|_{r_c} = \frac{16\pi\gamma^3}{3\Delta P^2}$$

At this point, the only issue left is dealing with the potential energy term, u/2kT. One of the originally stated assumptions of the model was that the bulk metastable liquid would be considered a regular liquid. This assumption allows the molecules in the liquid to be treated as if they are all in a uniform potential field (an oversimplified mean field approximation). Regular solution theory will be used to estimate this potential. Additionally, regular solution theory seems to be a reasonable approach in that it is the foundation for the Flory–Huggins theory which dominates in application to polymeric systems (Flory, 1953; Billmeyer, 1984; Walas, 1985; Brandrup and Immergut, 1989).

Regular solution theory, which is also known as the Scatchard-Hildebrand theory, is based on the premise that the potential energy is related to the composition and a cohesive-energy density of a system (Prausnitz, et al., 1986). The cohesive-energy

density, $\Re$, is defined as the ratio of the complete energy of vaporization, ΔE^v, to the liquid molar volume, V_L:

$$\Re \equiv \frac{\Delta E^v}{V_L} \tag{5.1.61}$$

The term ΔE^v is the energy change upon isothermal vaporization of the saturated liquid to the ideal gas state. The solubility parameter, δ, is then defined as:

$$\delta \equiv \Re^{1/2} = \left(\frac{\Delta E^v}{V_L} \right)^{1/2} \tag{5.1.62}$$

The next step is to define the volume fractions that will be used in the calculation. The volume fraction is:

$$\Phi_i = \frac{V_{Li} y_i}{\sum V_{Li} y_i} \tag{5.1.63}$$

where the yi's are the mole fractions of the various components. The potential energy that is needed for Equation 5.1.56 can now be estimated from:

$$-u = \left(y_1 V_{L1} + y_2 V_{L2} \right) \left(\Re_{11} \Phi_1^2 + 2\Re_{12} \Phi_1 \Phi_2 + \Re_{22} \Phi_2^2 \right) \tag{5.1.64}$$

In Equation 5.1.64, $\Re_{11}$ accounts for the interactions between molecules of type 1 with each other, $\Re_{22}$ accounts for the interactions of molecules of type 2 with each other, and $\Re_{12}$ accounts for the interactions between the different molecules. When the forces of attraction are primarily due to dispersion forces, there is a simple relation between the different cohesive-energy densities given by London's formula (Prausnitz, et al., 1986):

$$\Re_{12} = \left(\Re_{11} \Re_{22} \right)^{1/2} \tag{5.1.65}$$

At this point, all of the necessary components to the cluster distribution function have been developed. While the traditional change in Gibbs free energy of formation of

the clusters originally used in CNT was retained, the rest of the equation is very different. Typically, as developed in CNT, the pre-exponential term has just been based on the initial blowing agent concentration. This has been based on the argument of taking the system to the limit of having only clusters of one molecule in size and recognizing that ΔG would need to be zero in this case. The coefficient in front of the ΔG term derived here is very different as can be seen in Equation 5.1.56. It is not just a function of the blowing agent concentration, but also of the polymer repeat unit concentration, the potential energy of the system, and the volumetric properties of the system. The next step will be to combine this new cluster distribution function into a nucleation rate equation.

5.2 A New Nucleation Model

The development of this improved nucleation model will include two concepts previously identified in the literature and in previous sections of this work. The first concept is the incorporation of the Zeldovich correction factor. The Zeldovich factor, as discussed in Chapter 2 (and derived in Appendix B), is a correction factor to account for the fact that the molecular partition function will predict a greater number of clusters in the equilibrium distribution than are actually present during the steady state nucleation process. The second concept is the use of a diffusion-based expression to account for the impingement rate of the blowing agent molecules on the clusters. The diffusion-based expression will be used because it seems to be a much more realistic representation of what physically happens in the process.

5.2.1 Combining the Molecular Partition Function with the Diffusion Model

In its most fundamental definition, nucleation is the formation of a new phase when the molecules of the material forming the new phase collide or impinge on the critically sized clusters of those same molecules. These clusters arise naturally in the system and will have a certain size distribution. Estimating the nucleation rate of the new phase becomes a matter of accurately predicting the cluster distribution function and the net rate of collision or impingement of molecules into clusters of the "right" size. This can be summarized in the following equation:

$$\text{Nucleation Rate} = \left[\begin{array}{c}\text{Rate Molecules Impinge} \\ \text{on the Surface of} \\ \text{Critically Sized Clusters}\end{array}\right] \text{X} \left[\begin{array}{c}\text{Total Surface Area} \\ \text{of the Critically} \\ \text{Sized Clusters}\end{array}\right] \qquad (5.2.1)$$

In developing Equation 5.2.1, the energies of the individual molecules have not been considered. It is implied that as long as a molecule has sufficient energy to have a collision, it will lead to nucleation if the collision was with a critically sized cluster.

Each term in Equation 5.2.1 will now be looked at separately. The first term, which is the collision or impingement rate, will be based on liquid diffusion and Fick's law. From the developments of Chapter 4, the diffusion probability can be defined as:

$$\mathcal{P}_D = \frac{D_{AB} C_0}{\ell} \qquad (5.2.2)$$

The terms in Equation 5.2.2 are defined in the usual way; D_{AB} is the liquid diffusion coefficient for the blowing agent and the polymer, C_0 is the initial blowing agent concentration, and ℓ is the diffusion distance.

The second term in Equation 5.2.1 accounts for the total surface area of critically sized clusters. This is the area available to the impinging molecules and is made up of three different terms. The first is the surface area of a critically sized cluster, the second is the cluster distribution function evaluated specifically for the number of critically sized clusters, and the third is the Zeldovich factor. Combining all three of these terms results in:

$$A_T = Z\left(4\pi r_c^2\right)\Lambda\left(4\pi r_c^2 dr\right)\exp\left[\ln\Lambda\overline{V_f} - \frac{N_B b}{\overline{V_f}} + \frac{u}{2kT} - \ln\left(N_B - N_P\right)\right]\exp\left[-\frac{\Delta G_m}{kT}\right] \tag{5.2.3}$$

Combining Equations 5.2.2.and 5.2.3, one obtains the following nucleation rate equation:

$$J = \mathcal{P}_D A_T \tag{5.2.4}$$

This equation can be put into a more familiar form by re-writing some of the key terms. First, the cluster distribution function, Equation 5.1.56 can be rewritten as:

$$f_{nv} = \mathcal{N}\exp\left[-\frac{\Delta G_m}{kT}\right] \tag{5.2.5}$$

with:

$$\mathcal{N} = \Lambda\left(4\pi r_c^2 dr\right)\exp\left(\ln\Lambda\overline{V_f} - \frac{N_B b}{\overline{V_f}} + \frac{u}{2kT} - \ln\left(N_B - N_P\right)\right) \tag{5.2.6}$$

Equation 5.2.3 can then be rewritten as:

$$A_T = ZA\mathcal{N}\exp\left[-\frac{\Delta G_m}{kT}\right] \tag{5.2.7}$$

Substituting this into Equation 5.2.4 leads to:

$$J = \mathcal{P}_D ZA\mathcal{N}\exp\left(\frac{-\Delta G_m}{kT}\right) \tag{5.2.8}$$

Equation 5.2.8 now has the same common Arrhenius form as most of the equations in the literature.

Finally, before moving on to a discussion of the results in the next section, one last simplifying estimation needs to be discussed. The difference N_B-N_P in Equation 5.2.3 or Equation 5.2.6 can be replaced with N_G with little error. This difference (N_B-N_P) is the number of blowing agent molecules contained only in the bulk phase (not in the clusters) but this number should be reasonably the same as the total number of blowing agent molecules, N_G, because the number of molecules in clusters should be small relative to the entire system. This is a result of the cluster definition employed throughout the development of the MPF. With that, the nucleation model is complete and the results will be discussed next.

5.2.2 Results and Discussion of the New Nucleation Model

An example of a cluster distribution for the PMMA/CO_2 system at 313K and 21 MPa given by Equation 5.1.55 can be seen in Figure 5.3. In Equation 5.1.55, the dv term has been replaced with $4\pi r^2 dr/3$ where the radius of gyration, 1.04 x 10^{-8} cm, for CO_2 has been used for dr. When examining Figure 5.3, it is important to note that the distribution function as shown has been plotted as if r is a continuous variable. In actuality, there are certain limitations on allowable values of r. Values of r smaller than the radius of gyration are not possible because the smallest radius a cluster can have is the radius of one molecule. Values smaller than this would have no physical meaning. The values that r can have also have an upper limit. This upper limit is equivalent to the critical cluster radius.

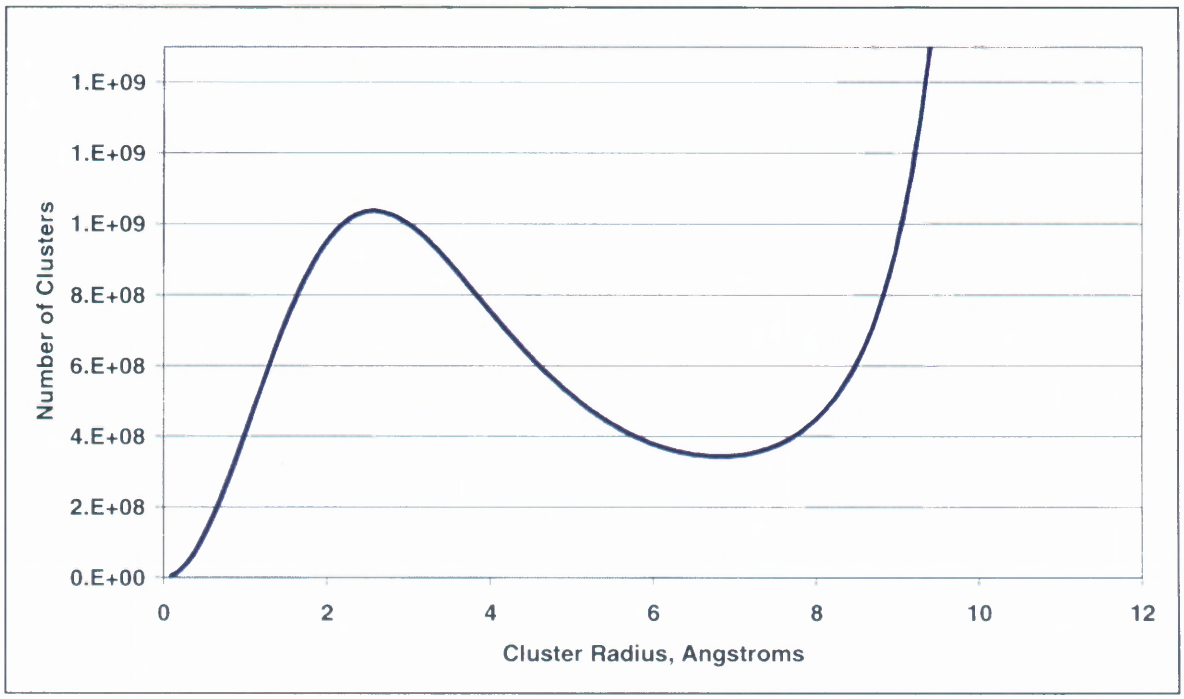

Figure 5.3 The Cluster Distribution Function for PMMA/CO_2 at 313 K and 21 MPa.

As the model has been defined, values greater than r_c would indicate that the cluster had already nucleated into a bubble and is undergoing bubble growth. For Figure 5.3, the minimum value of r would then be 1.04 x 10^{-8} cm and the maximum value would be about 7.5 x 10^{-8} cm.

In this region, the curved has a local maximum around 2.5 x 10^{-8} cm and then, as expected, declines exponentially until the critical cluster is reached. The sharp increase in the distribution function for values of r greater than r_c is caused by the $\Delta G/kT$ term decreasing steadily. As this term continues to decrease, it turns negative providing a very large positive exponential contribution to the function. This causes the function to increase sharply.

The cluster distribution function described above was then coupled with the diffusion probability term to create the improved nucleation model. The natural log of the nucleation rate results (in bubbles per cm^3-sec) are plotted vs. CO_2 saturation pressure (in MPa) in Figure 5.4. In this figure, the improved model is compared to the diffusion model developed in Chapter 4 and to classical nucleation theory. Comparisons to the other nucleation models described in Chapter 3 have not been done because of the lack of detailed experimental and or rheological data that was required. Even though the model results do not match the experimental results for the PMMA/CO_2 system, there is a significant improvement using this new approach. In fact, the approach is up to 12 orders of magnitude better.

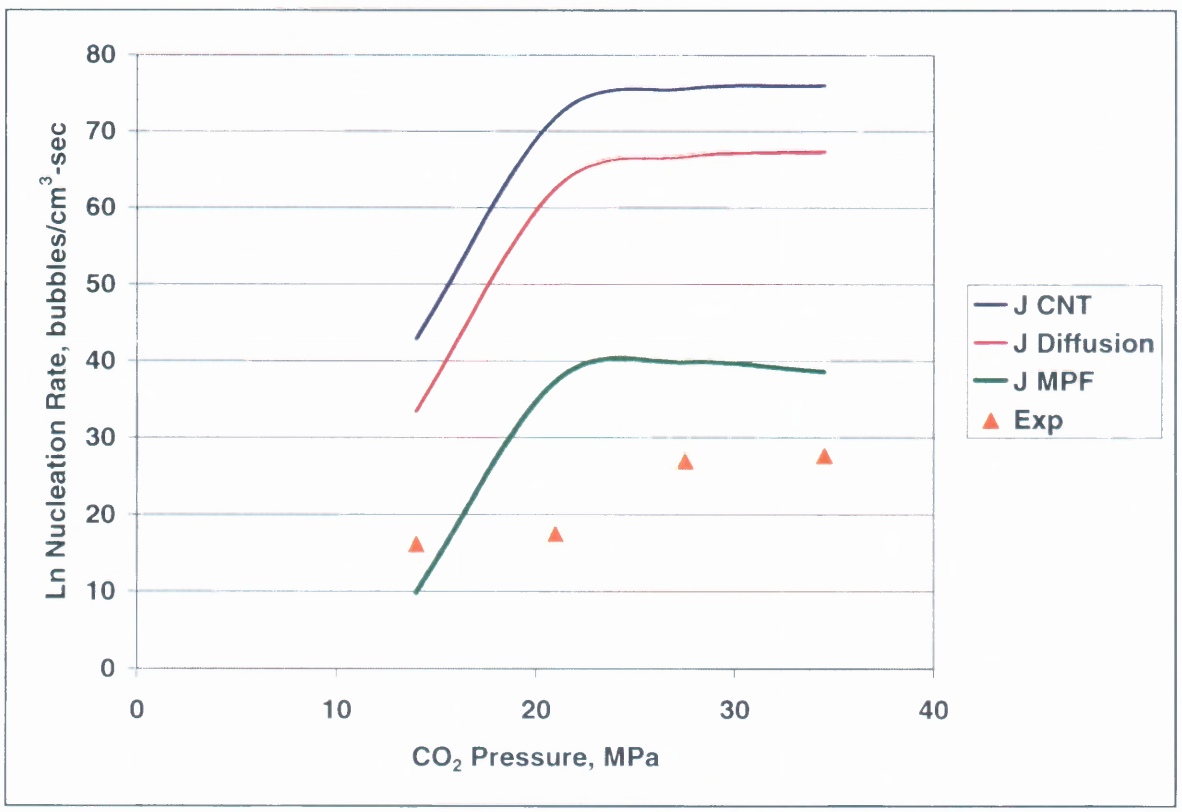

Figure 5.4 Nucleation Rate, J, (bubbles/cm^3sec) vs. CO_2 Pressure (MPa) for PMMA/CO_2 System @ 313 K

The characteristic shape of the curve with the new MPF/diffusion approach is similar to the CNT equation in that there is a region where the curve rises sharply and then plateaus off. In all the cases examined, CNT, the diffusion model proposed in Chapter 4 and the new approach proposed here in Chapter 5, the break point in the curve is at 21 MPa. All of the models predict that the nucleation rate will be very sensitive to changes in pressure below this value and much less sensitive to it above that value.

In order to understand this behavior, Equation 5.2.8:

$$J = \mathcal{P}_D Z A \mathcal{N} \exp\left(\frac{-\Delta G_m}{kT}\right)$$

needs to be examined further. Initially, the behavior of ΔG needs to be examined as a function of pressure. In order to do this, it is helpful to divide the pressure range up into two separate ranges, a low one and a high one with 21 MPa as the dividing point. Then using Figure 5.4, it becomes easy to see that ΔG varies greatly at pressures below 21 MPa and becomes almost completely independent of pressure at pressures greater than 21 MPa.

At pressures greater than 21MPa, ΔG/kT approaches zero so that exp(-ΔG/kT) approaches 1. Hence, at pressures above 21 MPa, the nucleation rate is dominated by the diffusion term and the coefficient of the cluster distribution function, $\mathcal{N}$, given by Equation 5.2.6. As the model results still err on the high side, the value of $\mathcal{N}$ is likely too large. Possible reasons for this include: First, the estimation of the potential energy of the system using regular solution could be low. This estimate was based on an regular liquid assumption and a non-ideal liquid may have a higher potential energy. Since the potential energy term appears as a negative term in the expression for $\mathcal{N}$, a higher

potential energy would ultimately reduce the value of $\mathcal{N}$ and subsequently, the value of the nucleation rate. Second, a similar error caused by the regular solution approximation could be an under prediction of the free volume estimates. The simplified approach of estimating the polymer chain volume by multiplying the number of repeat units by the van der Waals volume of the repeat unit could lead to free volumes that are too small in the presence of intermolecular forces. This is because the polymer chain volume will incorporate a certain amount of free volume based on which conformation the chains are in (tight coil, extended, etc.). Third, another possibility is that the simple mixing rule used to account for the mixture of blowing agent and polymer in the bulk phase was inadequate. A more complicated mixing rule may need to be developed.

For pressures below 21 MPa the nucleation model actually under predicts the nucleation rate for the PMMA/CO_2 system. In this low-pressure region, the model is dominated by the exponential ΔG term, not the pre-exponential constant, N, from the cluster distribution function. That is because the value of ΔG rises very rapidly at lower pressures. Given that ΔG is a function of the pressure and surface tension, it is certainly possible that the surface tension estimate is in error. This is not surprising knowing how dramatically plasticizers can influence other polymer properties like T_g. These effects can be particularly impressive at low concentrations and it is possible that the effects of the plasticizer on the surface tension have been under-estimated.

It is unfortunate that another homogeneous or nearly homogeneous system could not be identified other than the PMMA/CO_2 system used by Goel and Beckman (1994). The improved nucleation model shows significant improvement over the CNT model and over the diffusion-based model proposed earlier in this work, however, it would have

been useful to apply the model to a second system. This shortcoming can be overcome in one of two ways. An investigator can take great pains to develop a different homogeneous system similar to the way Goel and Beckman developed theirs or the model developed here can be extended to include the heterogeneous case. As there are data from numerous heterogeneous systems in the literature, extending this model to include the heterogeneous case seems to be the more pragmatic approach. As such, the steps to do this will be outlined in the final chapter as part of the possibilities for future work.

CHAPTER 6

SUMMARY OF CONTRIBUTIONS

An improved nucleation rate model for predicting bubble formation in thermoplastic polymers has been developed. This fundamental improvement in the model is accomplished without resorting to the use of experimentally determined parameters or fitted data in the nucleation rate equation. The model is instead based on a statistical mechanics approach that required the development of a molecular partition function. This partition function is then combined with a rate component to complete the model. The improvement over the results obtained from the equations based on Classical Nucleation Theory is many orders of magnitude. In creating the molecular partition function, three key aspects of the model had to be developed.

First, a molecular cluster needed to be defined. The physical construct of the cluster definition proposed by Ellerby, Weakliem, and Reiss (1991) for condensing argon was adapted to the more complicated polymer system. The adaptation included moving the shell molecule from the bulk phase to the inner edge of the cluster. By doing this, the shell molecule was treated as an ideal vapor molecule in the same way as the other blowing agent molecules in the cluster.

Second, the molecular partition function needed to be developed. The use of molecular partition functions for nucleation theory can be found in the prior literature (Reiss, Katz, and Cohen, 1967; Reiss, Tabazadeh, Talbot, 1990; and Ellerby, Weakliem, and Reiss, 1991), however, all of these were for single component ideal vapor systems. The work here extends the molecular partition function to a multi-component system and

deals with the complexity of a bulk phase that is not an ideal vapor and is in fact a complex polymer/ blowing agent mixture.

Third, an appropriate mixing rule needed to be selected to further deal with the complications added by the multi-component nature of the system. A traditional equation of state composition-dependent mixing rule was chosen, however, the compositions were based on the number of molecules of each species. Further, to account for the size discrepancy between the blowing agent and the polymer, the number of polymer repeat units in the system was used as the number of molecules for the polymer species rather than the actual number of polymer chains. This is similar to using a Flory-Huggins type volume fraction.

The rate component of the model is based on Fick's law for diffusion. A liquid diffusion coefficient is used to more accurately estimate the rate at which blowing agent molecules can move in the system. This eliminates the need to use the traditional impingement rate term, β, which is based on the kinetic theory of gases. In addition to this improved nucleation rate model, three other less successful approaches were investigated at length. Unfortunately, none of these approaches were very successful but they have been described here to help other investigators avoid erroneous paths and/or serve as inspiration.

The first attempt looked at replacing β in the original CNT with a diffusion-based term. Originally, there were no further modifications. The diffusion-based model offered modest improvements but was still grossly incorrect.

The second approach was to couple the diffusion-based approach with fluctuation theory. This approach recognized that the diffusion-based model assumed that all

molecules had an equally likely chance to cause nucleation regardless of their energy level. This in fact is not true, as not all of the molecules would have enough energy to cause nucleation. Using the total concentration of blowing agent molecules would then overpredict the nucleation rates. Fluctuation theory was unsuccessfully used to determine what fraction of the molecules actually had enough energy to cause nucleation. This approach failed, however, because the actual required energy level could not be properly determined.

The third and final approach was completely different. This approach used the concept of a lattice model. Vacancies in the lattice were identified as possible "holes" which could be future nucleation sites. The idea was an attempt to build on the concepts of Ramish, Rasmussen, and Campbell (1994) who devised a nucleation model based on voids that were created in the heterogeneous systems they were investigating. The difference with this approach is that the voids do not need the existence of a second heterogeneous material in order to be created. The approach failed when the lattice model determined vacancy levels that were on the same order of magnitude as the number of blowing agent molecules in the system.

Finally, the results here are based on a very limited data set as it is very difficult to obtain homogeneous polymeric systems. The one system that was identified as a homogeneous system was the PMMA/CO_2. While there were no other homogeneous systems found, the author feels fortunate to have found the PMMA/CO_2 system.

CHAPTER 7

FUTURE WORK

The development of a multi-component molecular partition function (MPF) that could be included into a nucleation rate equation was a daunting task. To make this task more manageable, some simplifying assumptions were made. Now that the foundation has been developed, improvements in the theory may be obtained with a more rigorous approach to some of the assumptions that were made.

First, the potential energy contribution to the MPF was based on the assumption of a regular liquid. This is similar to the Flory-Huggins approach taken for polymeric systems and allows the potential energy to be estimated with regular solution theory. A more sophisticated approach, possibly one accounting for intermolecular potentials, could be used to estimate the potential energy of the system. A more accurate representation of the potential energy will be beneficial since this term has a significant effect on the results that are obtained (refer to Equation 5.1.56).

Second, the shell molecule was moved into the inside edge of the cluster in the cluster definition so that it could be treated as an ideal vapor along with the rest of the cluster molecules. With an appropriate intermolecular potential, this molecule could be moved back to the outside edge of the cluster (actually be part of the bulk phase), and this would change the MPF slightly. This step is also important as will be discussed below to extend the theory to heterogeneous systems.

Third, more sophisticated mixing rules could be employed or developed. For this initial development of the theory, the simplest composition-dependent rules typically used for equation of state theory were adopted. Some slight adjustment was

made to account for the size discrepancy between the polymer and the blowing agent molecules but more could be done in this area.

The most obvious area where more work can be done is in the development of truly homogeneous experimental data. There was a significant lack of homogeneous data and most systems that were identified as homogeneous were in fact, heterogeneous. There is little practical incentive for the development of such systems, however, because most industrially relevant systems are heterogeneous. The development of these homogeneous systems would only serve as means to further understand the complicated phenomenon of nucleation in polymer systems. Further, this exercise is not trivial as the development of a truly homogeneous polymer system is very difficult and will take a great deal of laboratory expertise. Even the smallest amounts of catalysts, stabilizers, and solvents can jeopardize the homogeneity of the system.

Given the difficulty in conducting experiments on truly homogeneous systems, it may be more desirable to extend the theory to heterogeneous systems. The homogeneous model that was developed here was done so with this in mind. In taking this approach (using heterogeneous systems), there will be a much broader base of experimental systems to evaluate and the true effectiveness of this type of an approach can then be measured. The approach to extend this homogeneous model to a heterogeneous one would be very similar to the one used here and the steps will be briefly outlined below.

The development of the heterogeneous model could begin with the assumption that nucleation occurs at the interface between the two immiscible phases (Blander and Katz, 1975; Colton and Suh, 1987). Working from this hypothesis, the shell molecule in the current homogeneous model becomes critical as it can be used to differentiate the

boundary of the immiscible phases. This can be accomplished by moving the shell molecule back to the outer edge of the cluster and placing it at the edge of the bulk phase. In doing this, the ideal vapor contribution of the shell molecule to the cluster will need to be eliminated and a new contribution to the system will have to be incorporated. This contribution could be another "regular liquid" contribution similar to the bulk phase contributions in the homogeneous model here.

The new molecular partition function could possibly take on the following form if this type of an approach were adopted:

$$Q = \sum_{f_{nv}} \frac{\left[\Lambda \overline{V_f} \exp\left(\frac{u}{2kT}\right)\right]^{N_B}}{N_P!(N_B - N_P)!} \prod_{nv} \frac{\left[qV\Lambda dv \exp\left(\frac{u_{shell}}{2kT}\right)\right]^{f_{nv}}}{f_{nv}!} \tag{7.1.1}$$

At this point, one of the difficulties would be determining a suitable intermolecular potential to estimate the potential energy of the shell molecule if the simplified regular solution approach is ineffective. The rest of the steps would be fairly straightforward.

The molecular partition function would be used to determine the most probable distribution using the Lagrange method of undetermined multipliers. This would then be multiplied by a suitable Zeldovich correction factor to account for the difference between the number of clusters at equilibrium and during the steady state condition. The total surface area of the critical clusters would be determined by multiplying the number of critically sized clusters found from the distribution function by the surface area of a critically sized cluster. This then can be multiplied by a diffusion-based rate expression to create the final nucleation model.

The selection of the appropriate potential energy function for the shell molecule could potentially include a correlation to the wetting angle that is created between the

immiscible phases. This would serve the purpose of tying this potential energy function to something that is experimentally tangible.

Finally, even with all of the heterogeneous systems in the literature, experimentation is needed on developing "pure" heterogeneous systems. Most if not all of the heterogeneous systems in the literature contain multiple impurities and it is very difficult to discern how each different impurity affects the system. Carefully designed experiments could develop systems that contained only one impurity. These experiments could lead to better information on such physical properties as the wetting angle and could help identify the specific effects of the investigated impurity on nucleation and foam morphology.

APPENDIX A

FLUCTUATION THEORY

The following Appendix briefly summarizes the mathematical development behind fluctuation theory. Three texts are referenced for this discussion, Prausnitz et al. (1986), McQuarrie (1976), and Hill (1986). Fluctuation theory looks at estimating deviations from a mean value for certain "mechanical" variables in a statistical thermodynamic system. A mechanical variable is one that has a well-defined value in a given quantum state. For example, if the canonical ensemble (see definition below) is used, then properties with well-defined values in different quantum states are E_i, the energy in the i^{th} quantum state; N, the number of molecules; V, the volume; and P_i which is $-\partial E_i / \partial V$. Examples of variables that are not considered mechanical (because they are not well defined in individual quantum states) are S, the entropy; T, the temperature; and μ, the chemical potential (Hill, 1986). Before a discussion on fluctuation theory can continue, some comments regarding statistical thermodynamics and ensemble averaging are appropriate. In order to define what an ensemble average is, it is first important to understand the difference between thermodynamic and quantum states.

A thermodynamic state is a macroscopic interpretation of a system. For instance, if the system under investigation is a salt solution, then the thermodynamic state of the system can be accurately and completely described using only a few variables. They would be for example, the volume, temperature, total mass of the system, and the mass fractions of the components. These few variables are enough to completely describe the system at the macroscopic level, however, they are by no means enough to describe the state of the system at the microscopic level. In order to do that, one would have to

specify the position and momentum of each of the individual molecules. It is this molecular view that leads to the concept of a quantum state.

A quantum state can be viewed as a discrete microscopic state that is defined by a particular energy level. Each molecule in a given quantum state will have an energy level corresponding to that quantum state. Each thermodynamic state is made up of very many quantum states and a macroscopic property (i.e. energy) of the thermodynamic system is the average of that property taken over all quantum states. This leads to the concept of an ensemble and an ensemble average.

An ensemble is nothing more that a mental collection of a very large number of systems, each an exact replica of the original thermodynamic system. While all of these systems or ensembles are identical from a macroscopic (or thermodynamic) perspective, they are not identical at the molecular level. This is because each system can have many different quantum states. The ensemble average is taken over all of these different quantum states by utilizing probabilities that are associated with each of the different quantum states in the different ensemble systems. The probabilities used in these calculations are based on a fundamental postulate of statistical mechanics that states all quantum states are equally likely or equally probable. This assumption or postulate is often referred to as the property of "equal a priori" probabilities in many statistical mechanics and thermodynamics texts (Prausnitz, et al., 1986; Hill, 1986; McQuarrie, 1976).

In order to calculate an ensemble average, an ensemble must first be created. For a closed system with the number of molecules, temperature, and volume as the independent thermodynamic variables, the ensemble that is created is referred to as the

canonical ensemble. To further explain this, the developments in McQuarrie and Hill will be followed. A large number of systems equal to the original thermodynamic system are constructed. The entire group of systems is placed in an insulated container and brought to some temperature, T. Each system is defined by walls that allow heat conduction thus allowing all of the systems to obtain an equilibrium temperature consistent with the large insulated heat bath. These walls will not conduct mass, however, so the systems can be considered closed. Hence, each system has the same N and V and both are constant. Once at equilibrium, the entire ensemble made up of the many systems, (call the number of systems ω) is now a single system containing ωV volume and ωN molecules. The total energy of the system is denoted as E_t. While each of the ω systems can be in different quantum energy state, they all have the same quantum energy states available. These states are denoted as $E_1, E_2, E_3, \ldots E_j$. Now as discussed in Chapters 2 and 5, a picture of each system is taken so that the energy state of each system in the ensemble can be observed simultaneously and noted. This procedure provides the distribution of the systems in the different energy states. If n_1 is the number of systems found in state E_1, n_2 the number of systems found in state $E_2, \ldots$ to n_j, the number of systems found in state E_j then the numbers $n_1, n_2 \ldots n_j$ are the distribution. Many different distributions can exist but all must satisfy the following constraining relations:

$$\omega = \sum_j n_j \tag{A.1}$$

and

$$E_t = \sum_j n_j E_j \tag{A.2}$$

At this point, the ensemble has been defined and the next step is to calculate the ensemble average. In order to do that, the necessary probability must be determined.

In essence, this probability is the probability of finding a given quantum state in one of the systems of the ensemble. For a given distribution of n_1, n_2 , . . . n_j, the probability is simply n_j/ω. Unfortunately, there are too many possible distributions for a given N, V, E_t, and ω to identify a specific probability (n_j/ω) and what is really required is an overall probability or average of n_j/ω over all the different possible distributions. This average probability is denoted as $\overline{n}_j / \omega$ and is given by:

$$\mathcal{P}_j = \frac{\overline{n}_j}{\omega} = \frac{1}{\omega} \frac{\sum_k \mathcal{C}(n) n_j(n)}{\sum_k \mathcal{C}(n)} \tag{A.3}$$

where:

$$\mathcal{C}(n) = \frac{(n_1 + n_2 + \cdots +)!}{n\,!n_2!\cdots} = \frac{\omega!}{\prod_j n_j!} \tag{A.4}$$

is a well known combinatorial formula (McQuarrie, 1976). As with all probabilities, the sum of all the probabilities must equal 1. The desired ensemble average for the energy is given by:

$$\overline{E} = \sum_j \mathcal{P}_j E_j \tag{A.5}$$

Unfortunately, while the probability given in Equation A.3 is technically correct, it is not in a convenient form to do calculations. In order to deal with this, the concept of the most probable distribution is introduced. There are many different possible distributions of n consistent with the original constraining equations (A.1 and A.2) for a system defined by N, V, T, and ω. For each of these possible distributions, the weight of

their contribution to the overall average is given by $\mathcal{C}(n)$. However, because there are so many systems involved, it has been shown that the determination of the average will be dominated by those distributions that are equal to the most probable distribution or those which only differ from it by a negligible amount (Hill, 1986). Of course, the most probable distribution is the one with the largest value of $\mathcal{C}(n)$ and it is denoted as n*. In essence, this means that as the limit of $\omega \rightarrow \infty$, the contributions to the calculation of the average of the distributions that are not close to the n* can be neglected. Of course, as $\omega \rightarrow \infty$ holding N, V, and T fixed, each n_j must also go to ∞. However, the ensemble average is only dependant on the ratio of n_j to ω and this remains finite. This allows Equation A.3 to become:

$$\mathcal{P}_j = \frac{\bar{n}_j}{\omega} = \frac{1}{\omega}\frac{\sum_k \mathcal{C}(n^*) n_j^*}{\sum_k \mathcal{C}(n^*)} = \frac{n_j^*}{\omega} \tag{A.6}$$

This implies that the computation of $\mathcal{P}_j$ can be based on the most probable distribution instead of the mean value of the distribution. In order to take advantage of this, the most probable distribution needs to be determined. This is done by the method of Lagrange multipliers.

To move forward, we note that the distribution giving the largest value of $\mathcal{C}$ will also give the largest value of $\ln\mathcal{C}$ because $\ln\mathcal{C}$ increases monotonically with $\mathcal{C}$. Since it is easier to work with $\ln\mathcal{C}$, this will be used in place of $\mathcal{C}$. Taking the log of Equation A.4 gives:

$$\ln \mathcal{C} = \ln \omega! - \sum_j \ln n_j! = \ln\left(\sum_j n_j!\right) - \sum_j \ln n_j! \tag{A.7}$$

In order to further simplify Equation A.7, Stirling's approximation is employed. Stirling's approximation states that for large n, the following is a reasonable approximation for ln n!:

$$\ln n! = \sum_{m=1}^{n} \ln m \approx \int_{1}^{n} \ln x dx = n \ln n - n \tag{A.8}$$

Remembering that ω is the sum of n_j and using this approximation, Equation A.7 can be rewritten:

$$\ln \mathcal{C} = \left(\sum_j n_j \right) \ln \left(\sum_j n_j \right) - \sum_j n_j - \sum_j \left[n_j \ln n_j - n_j \right] \tag{A.9}$$

Simplification leads to:

$$\ln \mathcal{C} = \left(\sum_j n_j \right) \ln \left(\sum_j n_j \right) - \sum_j n_j \ln n_j \tag{A.10}$$

According to the Lagrange method of undetermined multipliers, the set of n_j's that lead to the maximum value of ln $\mathcal{C}$ subject to the constraints of Equations A.1 and A.2 is found from:

$$\frac{\partial}{\partial n_j} \left[\ln \mathcal{C} - \mathcal{R} \sum_j n_j - \mathcal{S} \sum_j n_j E_j \right] = 0, \quad j = 1, 2, \cdots \tag{A.11}$$

In Equation A.11, $\mathcal{R}$ and $\mathcal{S}$ are the undetermined multipliers. Differentiating leads to:

$$\ln \left(\sum_j n_j \right) - \ln n_j^* - R - SE_j = 0, \quad j = 1, 2, \cdots \tag{A.12}$$

This can be rearranged and put in terms of n_j*:

$$n_j^* = \omega \exp(-\mathcal{R}) \exp(-\mathcal{S} E_j) \tag{A.13}$$

Equation A.13 is the most probable distribution. The undetermined multipliers $\mathcal{R}$ and $\mathcal{S}$ are found by substituting Equation A.13 back into the original constraining equations, A.1 and A.2. The results are:

$$\exp(\mathcal{R}) = \sum_j \exp(-\mathcal{S}E_j) \tag{A.14}$$

and

$$\overline{E} = \frac{\sum_j E_j \exp(-\mathcal{S}E_j)}{\sum_j \exp(-\mathcal{S}E_j)} \tag{A.15}$$

Upon substituting A.14 into A.13, the probability defined in Equation A.6 is obtained:

$$\mathcal{P}_j = \frac{n_j^*}{\omega} = \frac{\exp(-\mathcal{S}E_j)}{\sum_j \exp(-\mathcal{S}E_j)}, \quad j = 1, 2, \cdots \tag{A.16}$$

Hill (1986) and McQuarrie (1976) have shown that the undetermined multiplier $\mathcal{S}$ is equal to 1/kT. Finally, it is also common to define the canonical partition function as Q:

$$Q = \sum_j \exp\left(-\frac{E_j}{kT}\right) \tag{A.17}$$

The probability can then be put into a final form using $\mathcal{S}$ = 1/kT and Equation A.18:

$$\mathcal{P}_j = \frac{\exp\left(-\frac{E_j}{kT}\right)}{Q}, \quad j = 1, 2, \cdots \tag{A.18}$$

Additionally,

$$\sum_{j=1}^{\infty} P_j = 1 \tag{A.19}$$

From statistics, the dispersion or spread of such a probability distribution is given by the standard deviation, σ:

$$\sigma^2 = \overline{\left(E - \overline{E}\right)^2} = \overline{E^2} - \left(\overline{E}\right)^2 \tag{A.20}$$

where the symbol E has been used since we are interested in the energy. Note that

$$\overline{E^2} = \sum_{j=1}^{\infty} E_j^2 \mathcal{P}_j \tag{A.21}$$

Using Equation A.18, Equation A.21 can be rewritten:

$$\overline{E^2} = \frac{1}{Q} \sum_{j=1}^{\infty} E_j^2 \exp - \frac{E_j}{kT} \tag{A.22}$$

Now note that:

$$-kT^2 \frac{\partial}{\partial T} \sum_{j=1}^{\infty} E_j \exp - \frac{E_j}{kT} = \sum_{j=1}^{\infty} E_j^2 \exp - \frac{E_j}{kT} \tag{A.23}$$

This can be substituted into Equation A.22 to give:

$$\overline{E^2} = -\frac{kT^2}{Q} \frac{\partial}{\partial T} \sum_{j=1}^{\infty} E_j \exp - \frac{E_j}{kT} \tag{A.24}$$

Next, from Equation A.18:

$$\exp - \frac{E_j}{kT} = \mathcal{P}_j Q \tag{A.25}$$

This can be substituted into Equation A.24 giving:

$$\overline{E^2} = \frac{kT^2}{Q} \frac{\partial}{\partial T} \sum_{j=1}^{\infty} E_j \mathcal{P}_j Q \tag{A.26}$$

This can be further simplified to:

$$\overline{E^2} = \frac{kT^2}{Q} \frac{\partial}{\partial T} \overline{E} Q \tag{A.27}$$

Taking the differential with respect to T leads to:

$$\overline{E^2} = \frac{kT^2}{Q} \left[\overline{E} \frac{\partial Q}{\partial T} + Q \frac{\partial \overline{E}}{\partial T} \right] \tag{A.28}$$

This can be rewritten as:

$$\overline{E^2} = \overline{E}\frac{kT^2 \ln Q}{\partial T} + kT^2 \frac{\partial \overline{E}}{\partial T} \tag{A.29}$$

In Equation A.28, $\partial Q / Q \partial T$ has been replaced with $\partial \ln Q / \partial T$. Also note that (McQuarrie 1976):

$$\overline{E} = kT^2 \frac{\partial \ln Q}{\partial T} \tag{A.30}$$

Substituting this result into Equation A.29 results in:

$$\overline{E^2} = \left(\overline{E}^2\right) + kT^2 \frac{\partial \overline{E}}{\partial T} \tag{A.31}$$

Now Equation A.31 can be substituted into Equation A.20 leading to

$$\sigma^2 = kT^2 \frac{\partial \overline{E}}{\partial T} \tag{A.32}$$

Finally, recognizing that:

$$\frac{\partial \overline{E}}{\partial T} = c_v \tag{A.33}$$

leads to the final result:

$$\sigma^2 = kT^2 c_v \tag{A.34}$$

Equation A.34 as derived is for a thermodynamic system, however, Equation A.34 needs to be divided by n for systems that contain independent elements as is the case in this work. Hence, Equation A.34 becomes:

$$\sigma^2 = \frac{kT^2 c_v}{n} \tag{A.35}$$

which is consistent with Equation 4.2.3, which was used in Chapter 4.

APPENDIX B

DERIVATION OF THE ZELDOVICH FACTOR

The Zeldovich factor was developed to account for difference between the number of clusters that exist in the meta-stable phase at equilibrium and in the meta-stable phase during the steady-state nucleation process. It is defined as derivative of the ratio of these two values with respect to n, the number of molecules in the cluster (Shafi and Flumerfelt, 1996):

$$Z = \frac{d\left(f_{n,s}/f_{n,0}\right)}{dn} = \left[-\frac{1}{2\pi kT}\frac{d^2\Delta G}{dn^2}\right]^{1/2}\Bigg|_{n_c} \tag{B.1}$$

where the expression is evaluated at the value of a critically sized cluster, n_c. In Equation B.1, $f_{n,0}$ has been defined as the equilibrium number of clusters of size n in the meta-stable phase (before nucleation begins) and $f_{n,s}$ as the number of clusters of size n formed during the steady state nucleation process. In classical nucleation theory, when dealing with vapor systems, the Zeldovich factor can be taken as (Blander and Katz, 1975):

$$Z = \frac{(\gamma kT)^{1/2}}{P_B A} \tag{B.2}$$

where γ is the surface tension of the system, k is Boltzmann's constant, T is the absolute temperature, P_B is the pressure inside the bubble, and A is the surface area of the bubble.

For a liquid system, the Zeldovich factor needs to be re-derived based on the above definition. This derivation is provided below. First, assume spherical symmetry holds for the blowing agent molecules and the clusters. Then define ℓ as the radius of

gyration of the blowing agent molecule and let the volume occupied by a molecule be defined as:

$$v = \frac{4}{3}\pi\ell^3 \tag{B.3}$$

Similarly, the volume of a cluster can be defined as:

$$V = \frac{4}{3}\pi r^3 \tag{B.4}$$

where r is the size of a cluster of n molecules. Then, the number of molecules in that cluster, n, can be found by:

$$n = \frac{V}{v} = \left(\frac{r}{\ell}\right)^3 \tag{B.5}$$

In Equation B.5, packing of the molecules has been neglected.

Having done this, the next step is to re-write ΔG in terms of n rather than r. The expression for ΔG in terms of r, the cluster radius

$$\Delta G(r) = \frac{4}{3}\pi r^3 \Delta P + 4\pi r^2 \gamma \tag{B.6}$$

can be put in terms of n, the number of molecules in the cluster:

$$\Delta G(n) = \frac{4\pi n \ell^3 \Delta P}{3} + 4\pi n^{2/3} \ell^2 \gamma \tag{B.7}$$

by replacing r with $\ell n^{1/3}$ from Equation B.5. Taking the first and second derivatives of ΔG with respect to n results in (dropping the (n) notation on the ΔG):

$$\frac{d\Delta G}{dn} = \frac{4\pi\ell^3 \Delta P}{3} + \frac{8\pi\ell^2 \gamma n^{-1/3}}{3} \tag{B.8}$$

and

$$\frac{d^2\Delta G}{dn^2} = -\frac{8}{9}\pi\ell^2\gamma n^{-1/3} \tag{B.9}$$

In order to evaluate the second derivative at the critical number of molecules, n_c, as prescribed by the definition, the value of n_c needs to be identified. This is done by maximizing the first derivative, Equation B.8 with respect to n. Setting the first derivative (Equation B.8) equal to zero and solving for n_c results in:

$$n_c = \frac{8\gamma^3}{(\ell\Delta P)^3} \tag{B.10}$$

Substituting Equation B.10 into Equation B.9 leads to an expression for the second derivative of ΔG with respect to n evaluated at the critical cluster size:

$$\left.\frac{d^2\Delta G}{dn^2}\right|_{n_c} = -\frac{\pi\ell^6\Delta P^4}{18\gamma^3} \tag{B.11}$$

This expression can then be used in Equation B.1 to obtain a new expression for the Zeldovich factor. The result is:

$$Z = \frac{\ell^3\Delta P^2}{6(kT)^{1/2}\gamma^{3/2}} \tag{B.12}$$

APPENDIX C

EXPERIMENTAL APPARATUS FOR EPS EXPANSIONS

The following Appendix outlines the design and operation of the atmospheric steam chamber that was used to expand the EPS samples. The steam expansion chamber consists of a well-insulated metal chamber that is vented and a sample pan. Steam is supplied to the chamber from a low-pressure steam header (typically 4-7 bar) and is reduced to 1 bar just before entering the chamber, but upstream of the steam control valve. The actual flow of steam is controlled via a control valve that is tied to the steam timer. Refer to Figure C.1. A steam time, in seconds, is put into the set point of the timer. Once the timer is started, the steam control valve automatically opens. When the preset time is reached, the timer automatically closes the steam valve. The bottom of the chamber is pitched slightly to allow condensate to collect and drain through a low point drain in one corner of the unit.

The actual design of the steam chamber is very simple and it can be readily constructed by most machine shops. The size can be determined based on convenience; the unit used for this work had a working steam volume of about 1-m^3. The sample pan is placed into the chamber manually through a door that is provided in the front of the unit. This pan has sides that are about 10 cm tall and the pan itself has dimensions of about 400 cm by 800 cm. A tight stainless steel mesh is used for the bottom of the pan. The size of the mesh only needs to be small enough to make sure that the beads do not fall through during the steaming process.

The actual EPS bead sample is contained in a metal pan during the steaming process. The mesh allows the steam to surround the beads on all sides. In the expansion process, about 50 grams of EPS is weighed out. The actual weight of the beads is not critical as 50 grams is more than enough for the density measurement that will be taken in a subsequent step. Each sample is steamed for a different period of time. Typical steaming times can be as short as 30 seconds and as long as 12 minutes. Once the beads have been expanded, they are allowed to air-dry overnight and then their density is measured.

The density measurement is done by weighing the beads in a known volume on a Mettler analytical density scale. This scale is programmable and reads out directly in density units (the volume of the sample container is programmed into the scale). The actual mass accuracy of the scale is 0.01 grams. Before experiments are started, the system is pre-heated for 12 to 15 minutes. This is to insure that the temperature will be constant. The samples with the longest steam times are done first. This is because samples with long steam times will be well into the bubble growth region (nucleation should be complete) and the density may have even reached its minimum value. In doing the experiments this way, little error is introduced in the event that the pre-heating step was not sufficient.

As indicated above, after each sample is steamed, it is removed and allowed to dry. This drying process is done to insure that moisture does not affect the densities obtained in the experiment. The last step is to obtain Electron Scanning Microscopy images to evaluate the cell structure. This can be done through standard analytical means available to any laboratory familiar with ESM procedures, all of the images in this work

were prepared internally at BASF Corp. Figures C.3 through C.12 highlight the nucleation and expansion behavior of a PS/n-C_5 product (Styropor® BR 315).

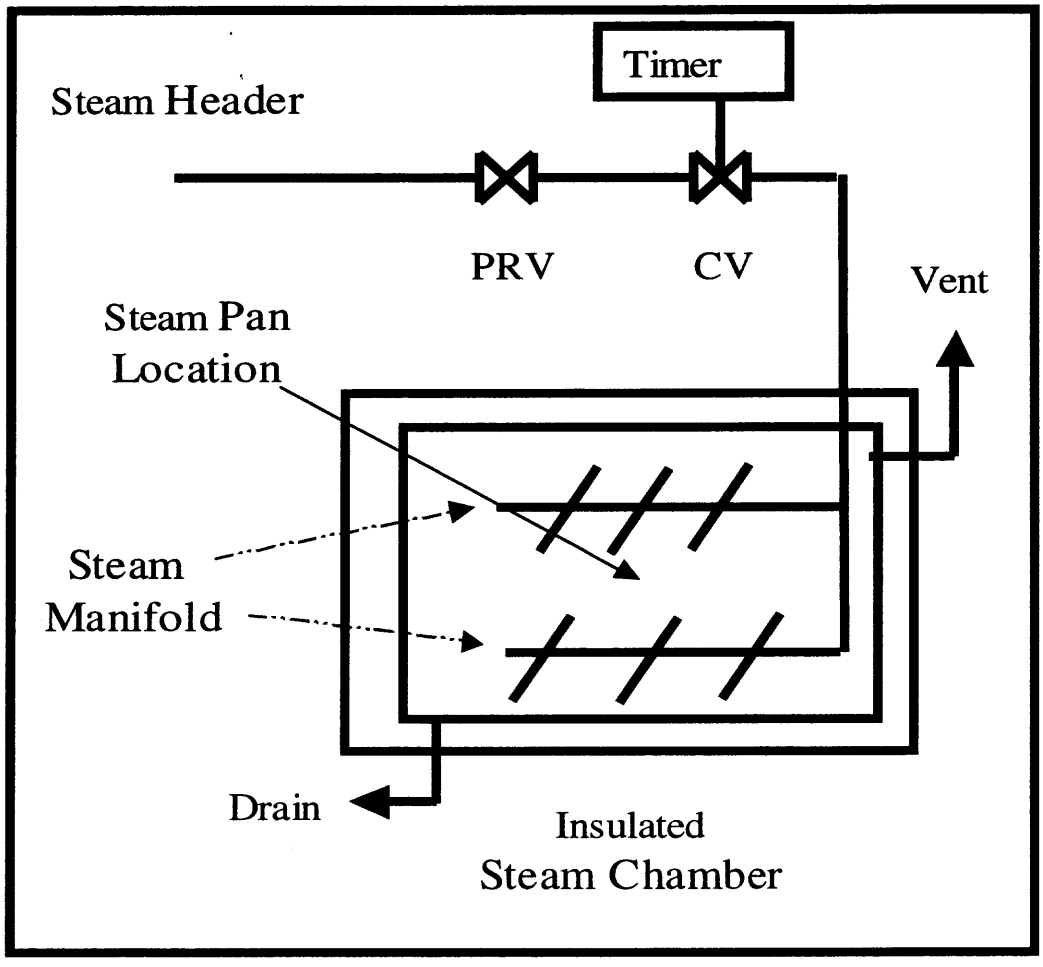

Figure C.1 Insulated Steam Chamber for Expansion of EPS Samples.

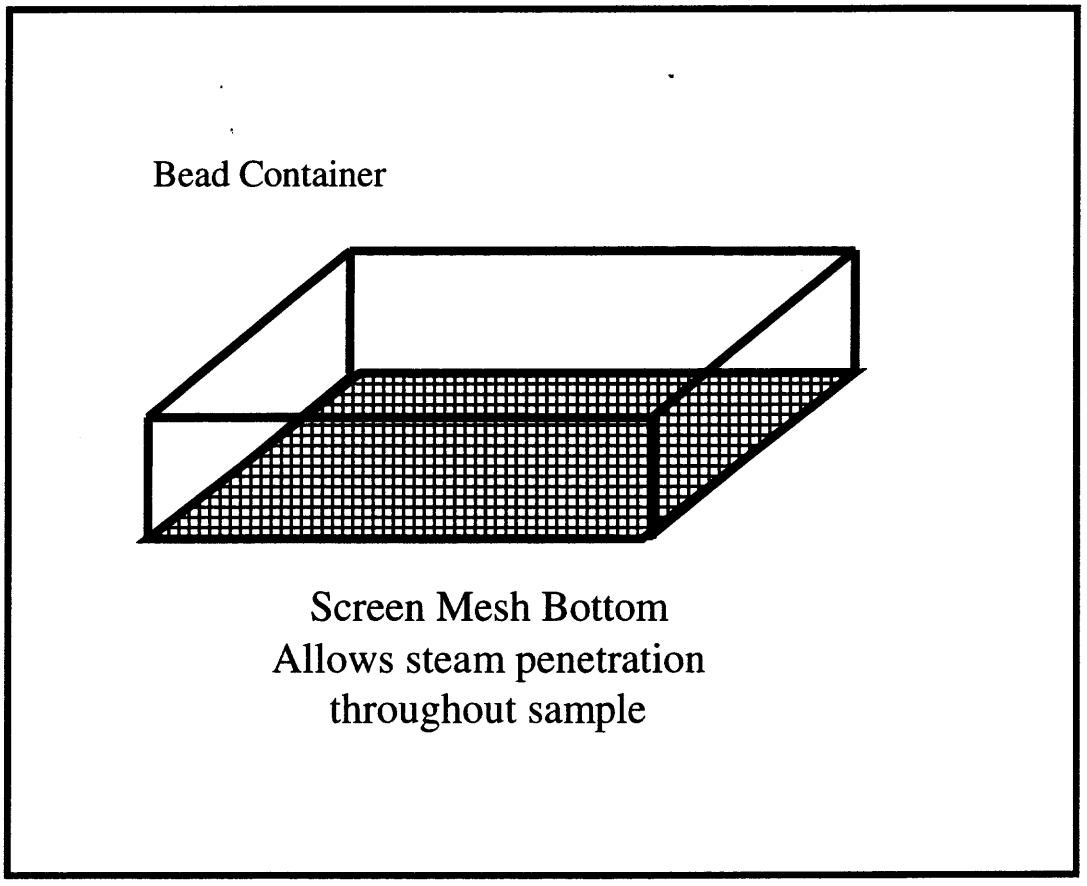

Figure C.2 Sample Container for Steam Expansion Chamber.

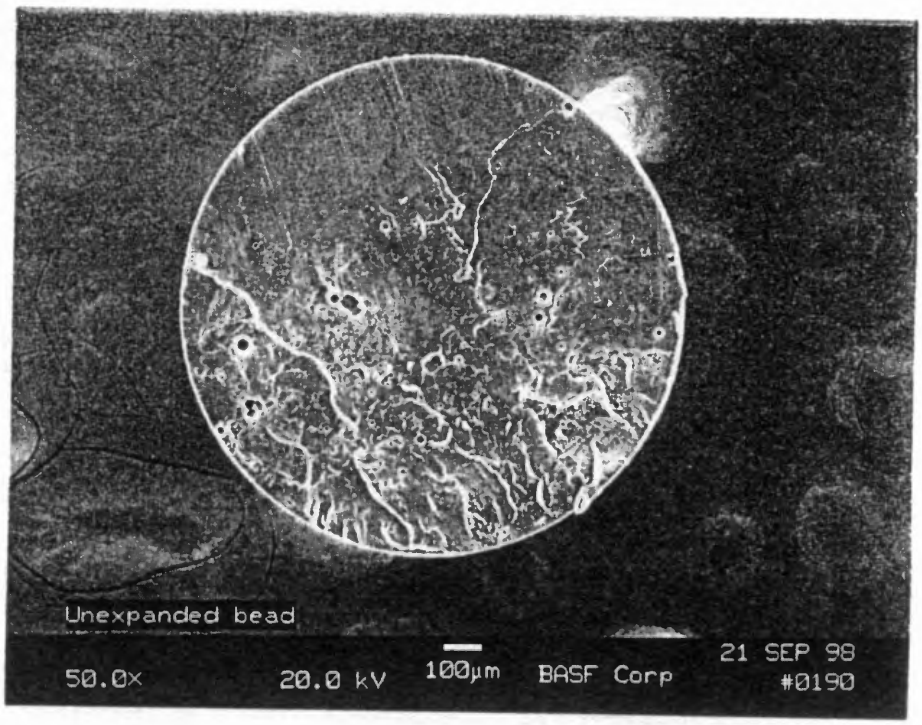

Figure C.3 Cross Sectional View (50X) of EPS Bead Before Steaming.

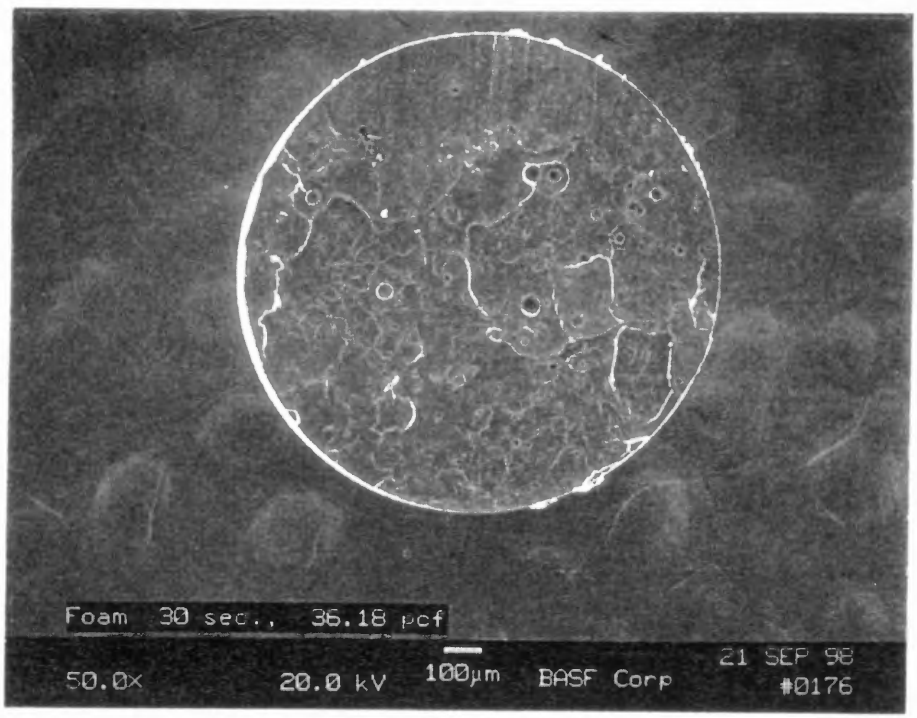

Figure C.4 Cross Sectional View (50X) of EPS Bead After Steaming for 30 Seconds.

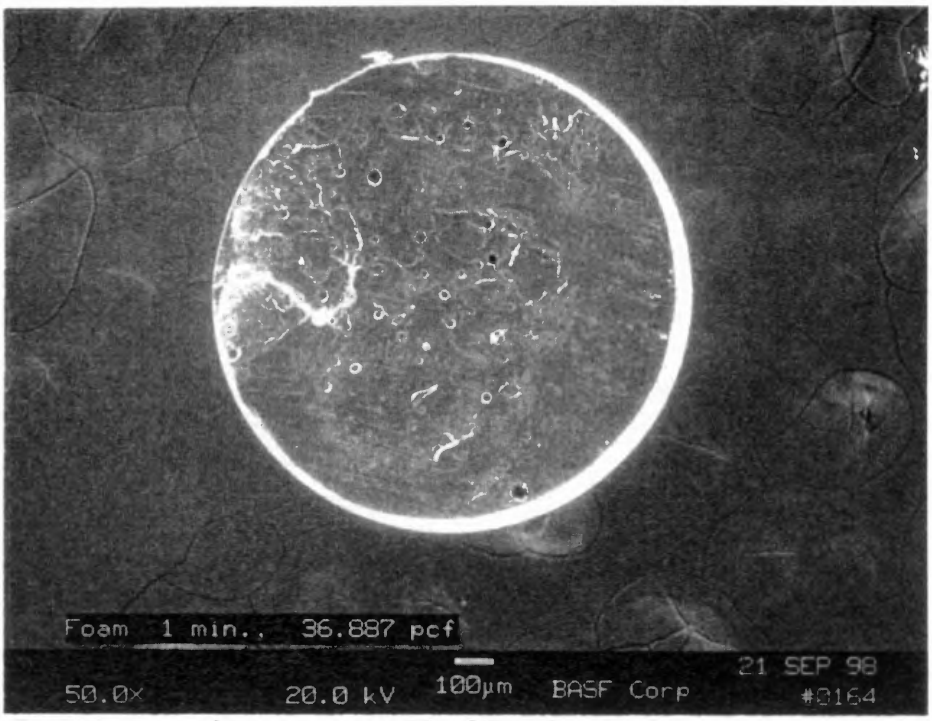

Figure C.5 Cross Sectional View (50X) of EPS Bead After Steaming for 60 Seconds.

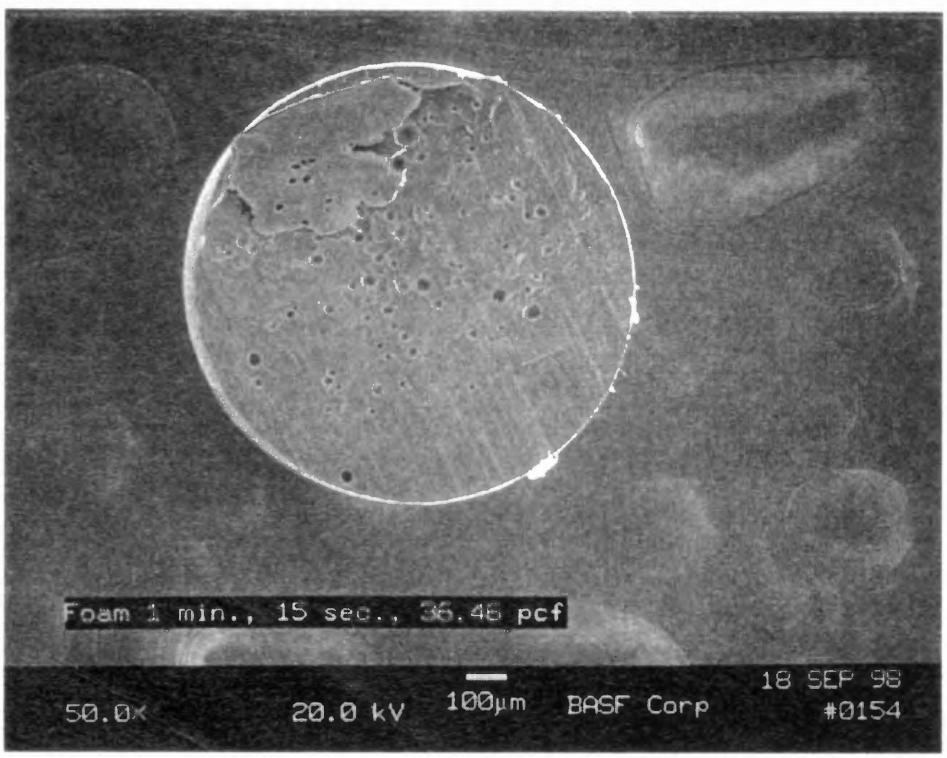

Figure C.6 Cross Sectional View (50X) of EPS Bead After Steaming for 75 Seconds.

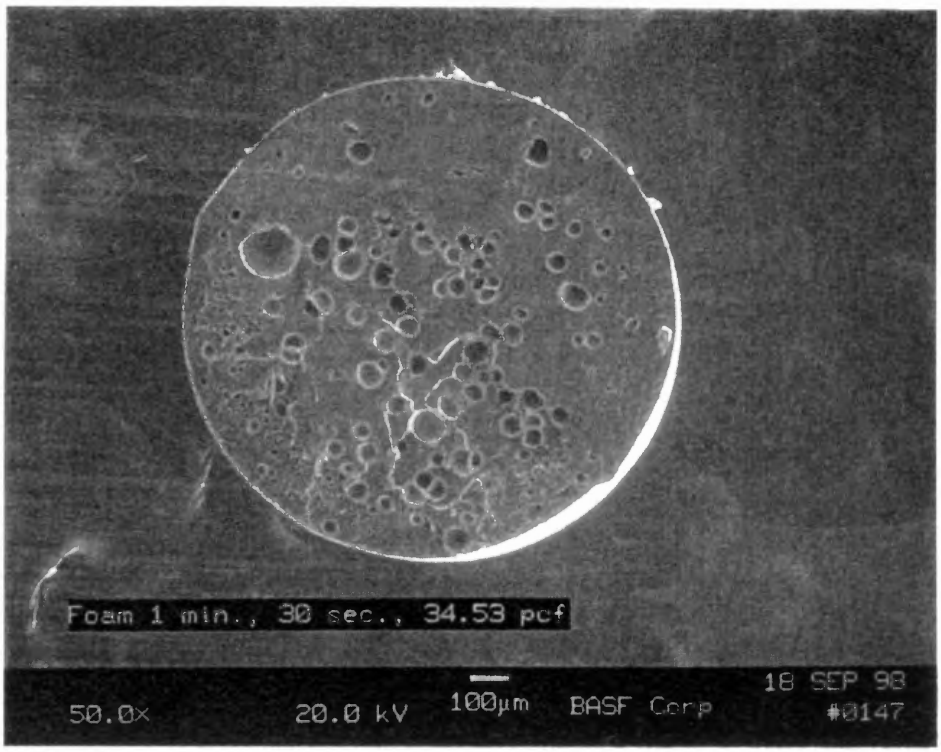

Figure C.7 Cross Sectional View (50X) of EPS Bead After Steaming for 90 Seconds.

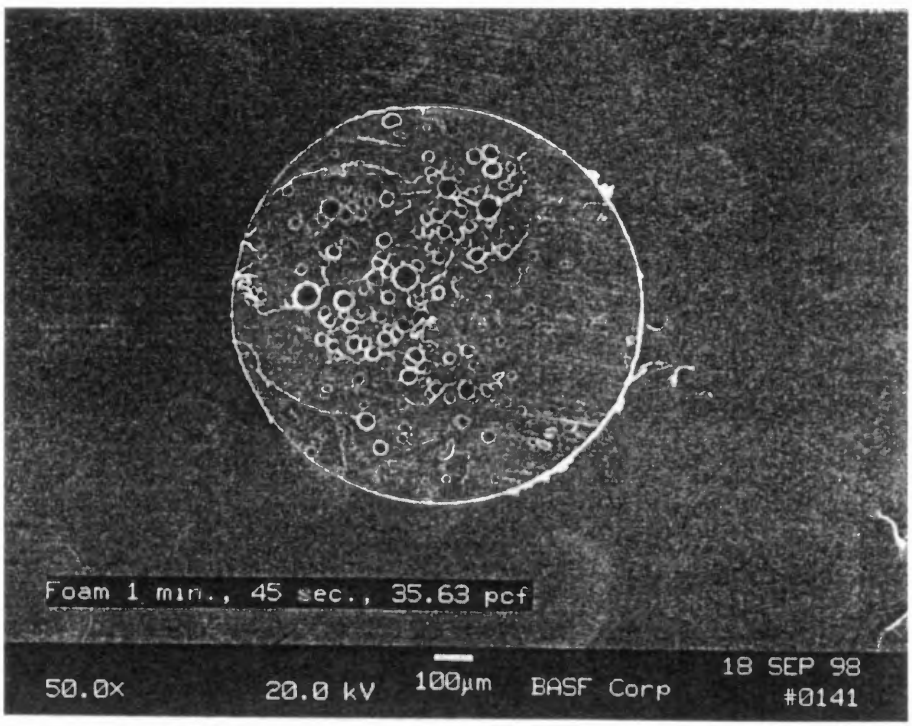

Figure C.8 Cross Sectional View (50X) of EPS Bead After Steaming for 105 Seconds.

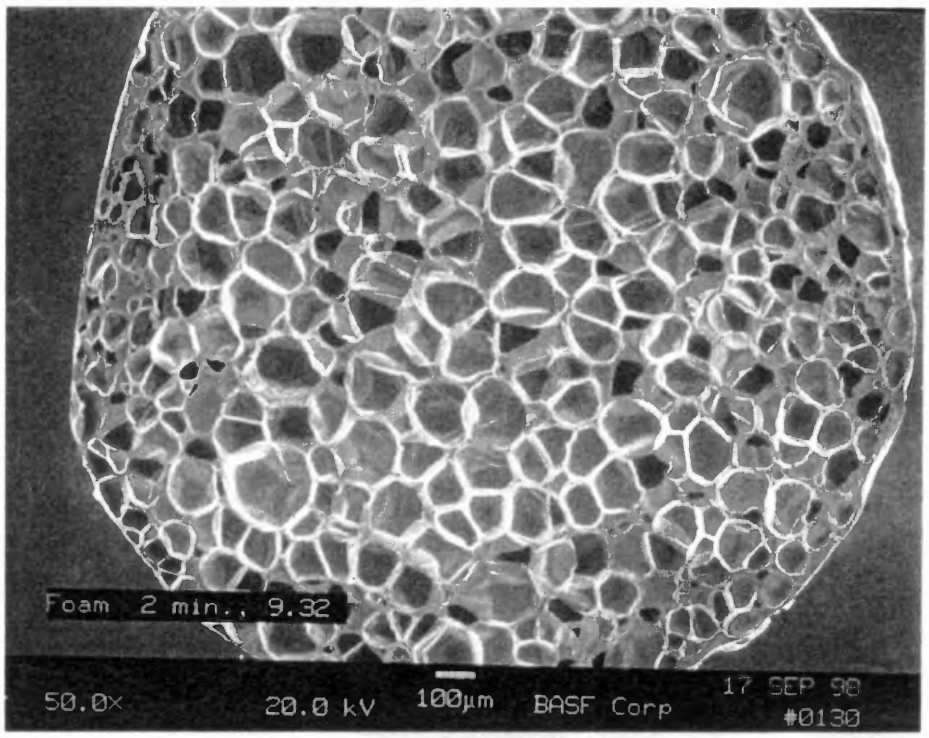

Figure C.9 Cross Sectional View (50X) of EPS Bead After Steaming for 120 Seconds.

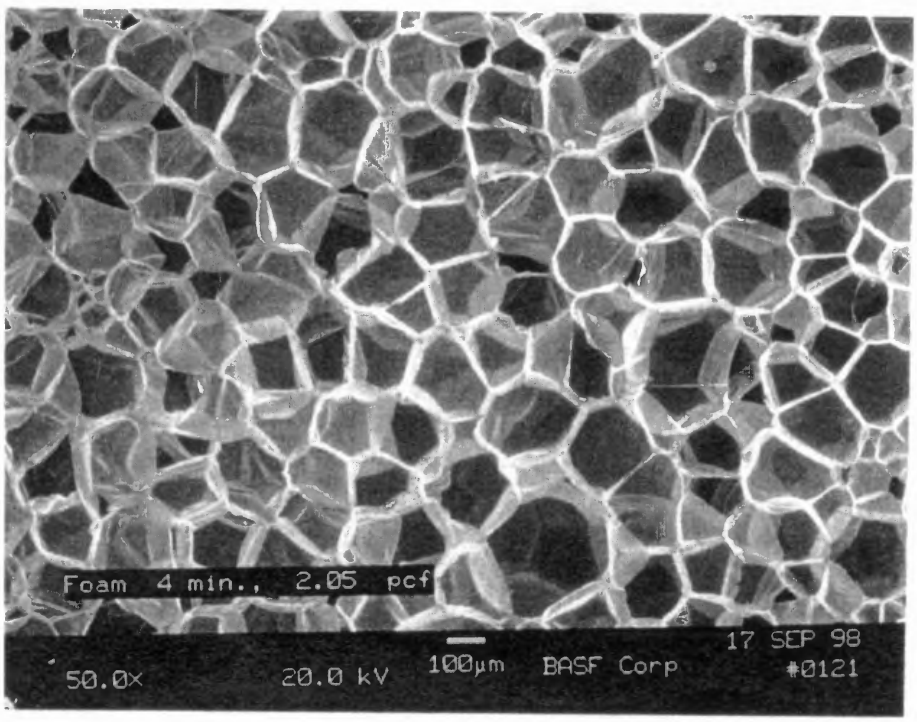

Figure C.10 Cross Sectional View (50X) of EPS Bead After Steaming for 240 Seconds.

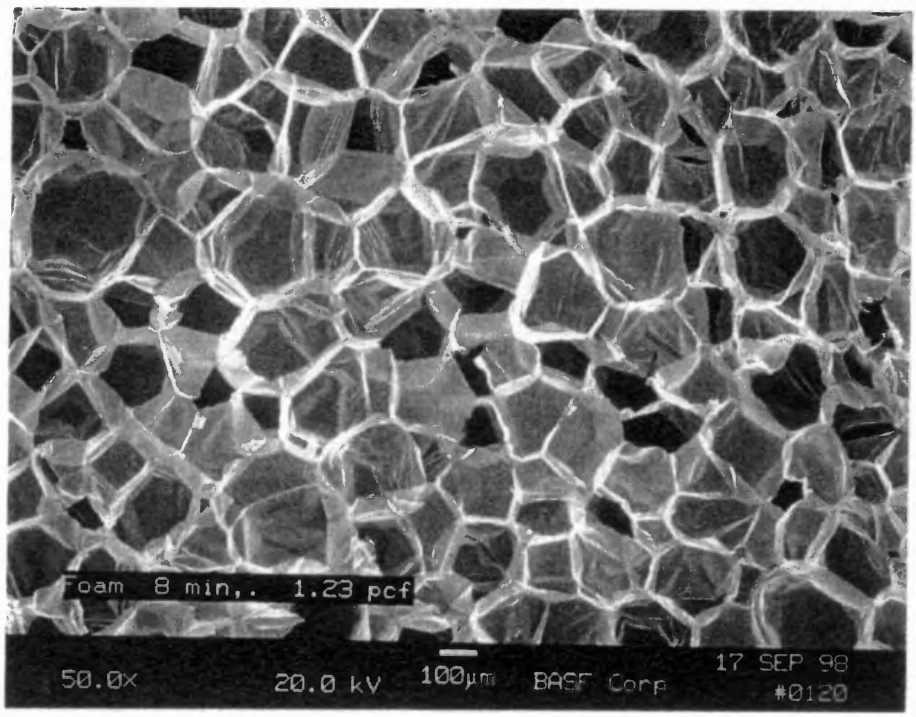

Figure C.11 Cross Sectional View (50X) of EPS Bead After Steaming for 480 Seconds.

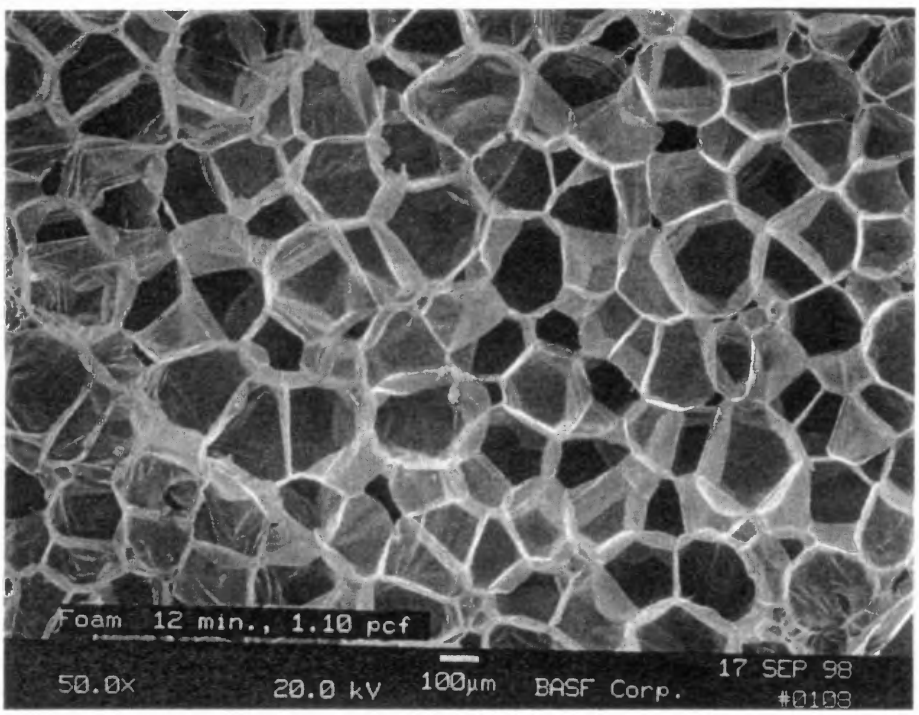

Figure C.12 Cross Sectional View (50X) of EPS Bead After Steaming for 720 Seconds.

APPENDIX D

THERMODYNAMIC CONSIDERATIONS: ESTIMATING INTERNAL PRESSURES OF THE BUBBLES IN POLYMERIC FOAMS

Much, if not most of the literature dealing with nucleation in polymers is based on work using gaseous blowing agents. For these situations, it is perfectly reasonable to describe the pressure inside the gas bubbles of the newly formed second phase with a form of Henry's law (Smith and Van Ness, 1975):

$$P_G = K_h x \tag{D.1}$$

There are instances, however, where Henry's law is not sufficient to accurately describe this equilibrium. In particular, Henry's law falls short when the liquid phase can no longer be treated as ideal. A simple approach to correcting this can be to modify Henry's law with the addition of an appropriate activity coefficient to account for this non-ideality in the liquid phase:

$$P_b = K_h \gamma_a x \tag{D.2}$$

There are still instances where Henry's law will not be sufficient. Such instances can be when the Henry's constant is not available or is unreliable, when the system is at extreme conditions, or when the system components are highly incompatible.

In such instances, a traditional vapor-liquid equilibrium (VLE) approach is required to adequately describe the pressure inside the bubbles of the new second phase (Gabbard and Knox, 2000). In such an approach, the fugacity of the blowing agent in the polymer solution, f^{l}, is defined to be equal to the fugacity of the blowing agent vapor in the bubble, f^{v}:

$$f^{v} = f^{l} \tag{D.3}$$

The fugacities can then be replaced with well-known expressions:

$$f^{v} = y_i \hat{\phi}_i P \tag{D.4}$$

and

$$f^{l} = x_i \gamma_i \phi_i^{sat} P_i^{sat} \frac{f_i}{f_i^{sat}} \tag{D.5}$$

where the last term in Equation (D.5) is the Poynting correction given by:

$$\frac{f_i}{f_i^{sat}} = \exp\left[\frac{v_i\left(P_{liq} - P_i^{sat}\right)}{RT}\right] \tag{D.6}$$

The term v_i is the molar liquid volume of the vapor blowing agent, P_{liq} is the pressure in the polymer solution, and P_i^{sat} is the vapor pressure of the pure vapor blowing agent. Combining these equations leads to the familiar expression for VLE:

$$y_i \hat{\phi}_i P_G = x_i \gamma_{a_i} \phi_i^{sat} P_i^{sat} \exp\left[\frac{v_i\left(P_{liq} - P_i^{sat}\right)}{RT}\right] \tag{D.7}$$

If one assumes that the vapor inside the bubble is pure and ideal, Equation (D.7) can be solved for the pressure inside the bubble:

$$P_G = a_i P_i^{sat} \exp\left[\frac{v_i\left(P_{liq} - P_i^{sat}\right)}{RT}\right] \tag{D.8}$$

The quantity $x_i\gamma_i$ has been replaced with the activity, a_i. The switch from an equation with the activity coefficient, γ_i, to one with the activity is desirable in polymeric systems because most commercial polymers have polydispersed molecular weights making the

determination of a mole fraction, x_i, very difficult. The switch to the activity facilitates the calculation by eliminating the need for this quantity.

The activity can than be estimated through any number of different polymer-solvent models. The choice of model depends on the system under investigation. For a system such as polystyrene containing pentane (pure or a blend of isomers) as the vapor blowing agent, Flory-Huggins theory can be used. The activity is given by (Walas, 1985):

$$\ln a_1 = \ln \Phi_1 + \left[1 - \frac{1}{m_v}\right]\Phi_2 + \chi \Phi_2^2 \tag{D.9}$$

where the subscripts refer to the blowing agent (1) and polymer (2) respectively. The Flory parameter, χ, is given by (Brandrup and Immergut, 1989):

$$\chi = \chi_0 + \frac{v_1}{RT}(\delta_1 - \delta_2)^2 \tag{D.10}$$

where χ_0 is usually a handbook value and δ_i is the solubility parameter for the i^{th} component. The volume fraction, Φ_i is given by:

$$\Phi_i = \frac{\rho_i m_i}{\sum \rho_i m_i} \tag{D.11}$$

This type of approach is reasonably consistent with the regular solution approach taken for estimating the potential energy in the regular liquid in Chapter 5 since Flory-Huggins theory is, in essence, an extension of regular solution theory as can be seen since Equation D.10 is based on solubility parameters.

APPENDIX E

UNSTEADY-STATE HEAT TRANSFER CALCULATION FOR THE EPS BEAD USING THE LUMPED CAPACITANCE METHOD

A common unsteady-state heat transfer problem that often arises is one where a solid at some equilibrium temperature experiences a sudden change in its thermal environment. An example of such a problem would be a hot forged metal at uniform temperature T suddenly being submerged in cold water to quench it. The same type of situation exists for the EPS bead in the expansion chamber. The bead initially at ambient temperature is placed into the steam chamber and then the steam is turned on. The temperature of the environment surrounding the bead rapidly goes from ambient to 373 K. The temperature of the bead will begin to increase until some equilibrium temperature, T_e, is reached. The convective heat transfer of the solid-fluid interface causes the bead temperature to rise. The lumped capacitance method assumes that the temperature of the solid will be spatially uniform at any instant during the transient process and this implies that the temperature gradients in the solid are negligible (Incropera and De Witt, 1990).

The time it takes the center of a sphere to reach the equilibrium temperature is given by:

$$t = \frac{\rho D_p c_p}{6h_c} \ln \frac{T_i - T_e}{T - T_e} \tag{E.1}$$

In Equation E.1, D_p is the diameter of the particle, h_c, is the convective heat transfer coefficient and c_p is the heat capacity. For this method to be applicable, the Biot number, N_{Bi}, must be less than 0.1. The Biot number is given by:

$$N_{Bi} = \frac{h_c\left(\frac{r_p}{3}\right)}{K} \tag{E.2}$$

The physical properties of polystyrene used in the calculation are summarized in Table E.1. The pentane content was neglected in this calculation and all of the properties are based on pure polystyrene.

Table E.1 Physical Properties of Polystyrene Used in the Unsteady-state Heat Transfer Calculation

Property	Units	Value
Bead Diameter, D_p	cm	0.1
Thermal Conductivity, K	W/mK	0.128
Heat Capacity, C_p	KJ/kgK	1.838

Additionally, typical values of h_c for forced convection with steam can range anywhere from 25-250 W/m^2K. A value of 25 W/m^2K was chosen for the calculation since the longest possible time to reach T_e would be the worst-case situation with respect to the nucleation time lags discussed in Chapter 4. Using these values, the value of the N_{Bi} was 0.0325, which is well below the 0.1 maximum value indicating that the lumped capacitance method is appropriate.

For the actual experimental situation described in Chapter 4, the critical time would be the time it takes for the center of the bead to reach the glass transition temperature, T_g. Once this happens, the polymer begins to become a melt and the trapped gas molecules become free to move around starting the nucleation process. For the two resins discussed in Chapter 4, BR 315 and BRL 315, the T_g is between 333-353 K. To determine the longest possible lag times, an internal temperature of 353 K was used in the calculation. Figure E.1 summarizes the results of the calculation and one can see that the 353 K temperature is reached in only about six seconds. Further, it takes less than ten seconds for the temperature to exceed 363 K, which is well above the T_g for either of the

products used in the experiments. Since the nucleation process did not start until well after 45 seconds (refer to results in Chapter 4; specifically Figures 4.6 and 4.7), the nucleation time lag is not likely the result of heat transfer limitations.

Finally, as expected, the calculation was repeated with higher values of h_c, but the times needed to reach the 353 K temperature were only reduced. This calculation did not account for heat transfer from steam permeation into the bead. This would only further reduce the time required to achieve the desired temperature.

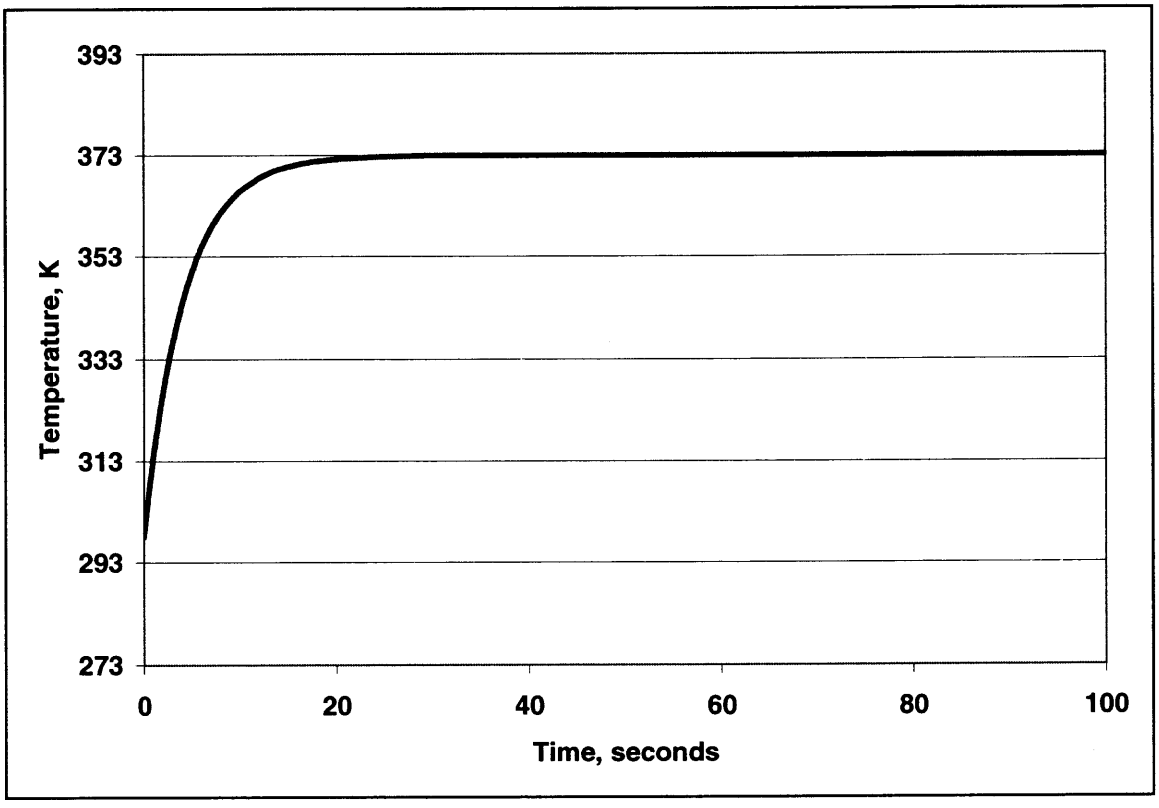

Figure E.1 Theoretical Temperature Profile of the EPS in the Steam Expansion Chamber.

REFERENCES

Alsoy, S. (1999). Modeling of Diffusion in Closed Cell Polymeric Foams. *Journal of Cellular Plastics, 35,* 247-271.

Amon, M., & Denson, C. D. (1984). A study of the Dynamics of Foam Growth: Analysis of the Growth of Closely Spaced Spherical Bubbles. *Polymer Eng. Sci., 24,* 1026-1034.

Arefmanesh, A. (1991). *Numerical and Experimental Study of Bubble Growth in highly Viscous Fluids, Ph.D. Thesis.* Mechanical Engineering Department, University of Delaware.

Attar, A. (1978). Bubble Nucleation in Viscous Material Due to gas Formation by a Chemical Reaction: Application to coal Pyrolysis. *AIChE J., 24* 106-115.

Baldwin, D. F., Park, C. B., & Suh, N. P. (1996). A Microcellular Processing Study of Poly(ethylene Terephthalate) in the Amorphous and Semi-crystalline States, Part I: Microcell Nucleation. *Poly. Eng. Sci., 36,* 1437-1445.

Barlow, E. J. & Langlois, W. E. (1962). Diffusion of Gas from a Liquid into an Expanding Bubble. *IBM J. Res. Dev., 6,* 329-337.

Becker, R & Döring, W. (1935). The Kinetic Treatment of Nuclear Formation in Supersaturated Vapors. *Ann. Physik, 24,* 719-752.

Benning, C. J. (1969). *Plastic Foams: the Physics and Chemistry of Product Performance and Process Technology, Volumes 1 and 2.* New York, NY: John Wiley and Sons.

Best, J. R., (2001, December 19th). *Plastics Focus.* Toledo, OH: Market Search, Inc.

Beyer, W. H., (1987). *CRC Standard Mathematical Tables* (28th ed.). Boca Raton FL: CRC Press.

Biesenberger, J. A. & Todd, D., (1983). *Section I: Fundamentals in Devolatilization of Polymers.* New York, NY.

Biesenberger, J.A. & Lee, S. T., (1987). Fundamental Study of Polymer Melt Devolatilization. III: More Experiments on Foam Enhanced DV. *Poly. Eng. Sci., 27,* 510-517.

Billmeyer, F. W., (1984). *Textbook of Polymer Science* (3rd ed.). New York, NY: John Wiley and Sons, Inc.

Bird, R. B., Stewart, W. E., & Lightfoot, E. N., (1960). *Transport Phenomena.* New York, NY: John Wiley and Sons, Inc.

Blander, M. & Katz, J. L., (1975). Bubble Nucleation in Liquids. *AIChE J., 21,* 833-848.

Brandrup, J., & Immergut, E. H., (1989). *Polymer Handbook* (3rd ed.). New York, NY: John Wiley and Sons.

Bromberg, J. P., (1980). P*hysical Chemistry.* Boston, MA: Allyn and Bacon, Inc.

Cahn, J.W. & Hilliard, J. E., (1958). Free Energy of a Nonuniform System. I. Interfacial Free Energy. *J. Chem. Phys., 28,* 258-267.

Cahn, J.W. & Hilliard, J. E., (1959). Free energy of a Nonuniform System. III Nucleation in a Two-component Incompressible Fluid. *J. Chem. Phys., 31,* 688-699.

Cohen, E. R., (1970). The Accuracy of the Approximations in Classical Nucleation Theory. *J. Stat. Phys., 2,* 147.

Colton, J. S. & Suh, N. P., (1987). The Nucleation of Microcellular Thermoplastic Foam with Additives, Part I.: Theoretical Consideration. *Poly. Eng. Sci., 27,* 485-492.

Colton, J. S. & Suh, N. P., (1987). The Nucleation of Microcellular Thermoplastic Foam with Additives, Part II: Experimental Results and Discussion. *Poly. Eng. Sci., 27,* 493-499.

Colton, J. S. & Suh, N. P., (1987). Nucleation of Microcellular Foam: Theory and Practice. *Poly Eng. Sci., 27,* 500-503.

Delale, C.F., & Meier, GEA, (1993). A Semiphenomenological Droplet Model of Homogeneous Nucleation form the Vapor Phase. *J. Chem. Phys., 98,* 9850-9858.

Dillmann, A., & Meier, GEA, (1991). A Refined Droplet Approach to the Problem of Homogeneous Nucleation from the Vapor Phase. *J. Chem. Phys., 94,* 3872-3884.

Durill, P. L., & Griskey, R. G., (1966). Diffusion and Solubility of Gases in Thermally Softened or Molten Polymers: Part I. Development of Technique and Determination of Data. *AIChE J., 12,* 1147-1151.

Ellerby, H. M., Weakliem, C. L., & Reiss, H., (1991). Toward a Molecular Theory of Vapor-Phase Nucleation. I. Identification of the Average Embryo. *J. Chem. Phys., 95,* 9209-9218.

Ellerby, H. M., & Reiss, H., (1992). Toward a Molecular Theory of Vapor-Phase Nucleation. II. Fundamental Treatment of the Cluster Distribution. *J. Chem. Phys., 97*, 5766-5772.

Farkas, L., (1927). The Velocity of Nucleus Formation in Supersaturated Vapors. *Z. Phys. Chem., 125*, 236-242.

Feder, J., Russel, K. C., Lothe, J., & Pound, G. M., (1966). Homogeneous Nucleation and Growth of Droplets in Vapours. *Adv. Phys., 15*, 111-178.

Fehn, G. M., (1967). Extrusion Behavior of Cellular High-Density Polyethylene. *J. Cell. Plast., 3*, 456-462.

Fen-Chow, T., Herve, E., DuBault, A., & Halary, J. L., (1999). Viscoelastic Characteristics of Pentane-Swollen Polystyrene Beads. *J. Applied Polym. Sci., 73*, 2463-2472.

Fossey, D. J., & Smith, C. H., (1973). Determination of the Diffusivity of n-Pentane in Polystyrene Bead Foam. *J. Applied Polym. Sci., 17*, 1749-1770.

Flory, P. J., (1953). *Principles of Polymer Chemistry*. Ithaca, NY: Cornell University Press.

Ford, I. J., Laaksonen, A., & Kulmala, M., (1993). Modification of the Dillmann-Meier Theory of Homogeneous Nucleation. *J. Chem. Phys., 99*, 764-765.

Frenkel, J., (1955). *Kinetic Theory of Liquids*. New York: Dover Publications.

Gabbard, R. G. & Knox, D. E., (2000). The Solubility of Blowing Agents in Polymers and Its Impact on Nucleation Rate and Cell Number in Foamed Polymers. 9th Int. Symp. *On Solubility Phenomena (IUPAC)*, Hammamet, Tunisia.

Gabbard, R. G. & Knox, D. E., (2000). Nucleation of Thermoplastic Foams. *AIChE National Meeting*, Los Angeles, CA.

Garcia Garcia, N. & Soler Toroja, J. M., (1981). Monte Carlo Calculation of Argon Clusters in Homogeneous Nucleation. *J. Chem. Phys., 47*, 186-190.

Geankoplis, C. J., (1983). *Transport Processes and Unit Operations* (2nd ed.). Boston, MA: Allyn and Bacon Inc.

Goel, S. K. & Beckman, E. J., (1994) Generation of Microcellular Polymeric Foams Using Supercritical Carbon Dioxide. I: Effect of Pressure and Temperature on Nucleation, *Polym. Eng. Sci., 34*, 1137-1147.

Hagadone Hospitality (2001). The Cour d' Alene A Resort on The Lake Home Page: Golf, Photo Gallery, 2001. Retrieved January 10, 2002 from http://www.cdaresort.com/gallery_golf.asp.

Han, J. H. & Han, C. D., (1990). Bubble Nucleation Polymeric Liquids. II. Theoretical Considerations. *J. Poly. Sci., Part B, 28*, 743-761.

Han, J. H. & Han, C. D., (1990). Bubble Nucleation Polymeric Liquids. I. Bubble Nucleation in Concentrated Polymer Solutions. *J. Poly. Sci., Part B, 28*, 711-741.

Han, C. D., & Yoo, H. J., (1981). Studies on Structural Foam Processing. IV. Bubble Growth During Mold Filling. *Polm. Engg. Sci., 21*, 518-533.

Harvey, E. N., Barnes, D. K., McElroy, W. D., Whiteley, A. H., Pease, D. C., & Kooper, K. W., (1944). Bubble Formation in Animals: I. Physical Factors. *J. Cell and Compar. Physiology, 24*, 1-22.

Hill, T. L., (1956). *Statistical Mechanics, Principles and Selected Applications*. New York: Dover Publishing, Inc.

Hill, T. L., (1986). *An Introduction to Statistical Thermodynamics*. New York: Dover Publishing, Inc.

Helfand, E., (1975). Theory of Inhomogeneous Polymers: Fundamentals of the Gaussian Random-walk Model. *J. Chem. Phys., 62*, 999-1005.

Incropera, F. P., & Witt, D. P., (1990). *Introduction to Heat Transfer* (2nd ed.), New York, NY: John Wiley and Sons.

Joshi, K., Lee, J. G., Shafi, M. A., & Flumerfelt, R. W., (1998). Prediction of Cellular Structure in Free Expansion of Viscoelastic Media. *J. Appl. Polym. Sci., 67*, 1353-1368.

Kanne-Dannetschek, I., & Stauffer, D., (1981). Quantitative Theory for Time Lag in Nucleation. *J. Aerosol Sci., 12*, 105-108.

Kumar, V. & Weller, J. E., (1992). Bubble Nucleation in Microcellular Plolycarbonate Foams. *Polym. Mater. Sci. Eng., 67*, 501-502.

Laaksonen, A., Ford, I. L., & Kulmala, M., (1994). Revised Parameterization of the Dillmann-Meier Theory of homogeneous Nucleation. *Phys. Rev. E49*, 5517-5524.

Laaksonen, A., Talanquer, V., & Oxtoby, D. W., (1995). Nucleation: Measurement, Theory, and Atmospheric Applications. *Annu. Rev. Phys. Chem., 46*, 489-524.

La Mer, V. K., (1952). Nucleation in Phase Transition. *Ind. and Eng. Chem., 44*, 1270-1277.

Lee, J. G., (1995). *Thesis, Controlled Structure Processing of Cellular Materials (Polymer, Bubbles, Foams). Ph.D. Thesis.* Chemical Engineering Department, Texas A&M University, College Station, TX.

Lee, J. G. & Flumerfelt, R. W., (1996). A Refined Approach to Bubble nucleation and Polymer Foaming Process: Dissolved Gas and Cluster Size Effects. *J. Colloid Interface Sci., 31*, 335-348.

Lee, J. K., Barker, J.A., & Abraham, F. F., (1973). Theory and Monte Carlo Simulation of Physical Clusters in the Imperfect Vapor. *J. Chem. Phys., 58*, 3166-3180.

Lee, L. L., (1988). *Molecular Thermodynamics of Nonideal Fluids.* Boston, MA: Butterwoths.

Lee, S. T, (1991). *Shear Effects on Thermoplastic Foam Nucleation.* SPE ANTEC, Conference Proceedings.

Lee, S. T., (1994). *More Experiments on Thermoplastic Foam Nucleation.* SPE ANTEC, Conference Proceedings.

Lothe, J. & Pound, G. M., (1962). Reconsideration of Nucleation Theory. *J. Chem. Phys., 36*, 2080-2085.

Lydersen, A. L., (1983). *Mass Transfer in Engineering Practice.* New York, NY: John Wiley and Sons, Inc.

McDonald, J. E., (1962). Homogeneous Nucleation of Vapor Condensation. I. Thermodynamic Aspects. *Am. J. Phy., 30*, 870-877.

McDonald, J. E., (1963). Homogeneous Nucleation of Vapor Condensation. II. Kinetic Aspects. *Am. J. Phy., 30*, 30-41.

McQuarrie, D. A., (1976). *Statistical Mechanics.* New York, NY: Harper Row.

Meineche, E. A., & Clark, R. C., (1973). *Mechanical Properties of Polymeric Foams.* Westport, CT: Technomic.

Monette, L., (1994). Spinodal Nucleation. *Int. J. Mod. Phys. B, 8*, 1417-1527.

Ohzono, M., Iwai, Y., & Arai, Y., (1984). Correlation of Solubilities of Hydrocarbon Gases and Vapors in Molten Polymers Using Perturbed-Hard-Chain Theory. *J. Chem. Eng. of Japan, 17*, 550-553.

Olson, T., & Hamill, P., (1996). A Time-dependent Approach to the Kinetics of Homogeneous Nucleation. *J. Chem. Phys., 104*, 210-224.

Oxtoby, D. W., & Evans, R., (1988). Nonclassical Nucleation Theory for the Gas-Liquid Transition. *J. Chem. Phys., 89*, 7521-7530.

Park, C. B., Baldwin, D. F., & Suh, N. P., (1995). Effect of the Pressure Drop on the Cell Nucleation in continuous Processing of Microcellular Polymers. *Poly. Eng. Sci., 35*, 432-440.

Park, C. B., Behravesh, A. H., & Venter, R. D., (1998). Extrusion of Low Density Microcellular HIPS Foams Using CO_2. *Poly. Eng. Sci., 38*, 1812-1823.

Park, C. B. & Suh, N. P., (1996). Filametary Extrusion of Microcellular Polymers using a Rapid Decompressive Element. *Poly. Eng. Sci., 36*, 34-48.

Patel, R. D., (1980). Bubble Growth in a Viscous Newtonian Liquid. *Chem. Eng. Sci., 35*, 2352-2356.

Prausnitz, J. M., Lichtenthaler, R. N., & de Azevedo, E. G., (1986). *Molecular Thermodynamics of Fluid-Phase Equilibria* (2^{nd} ed.). Englewood Cliffs, NJ: Prentice-Hall

Prud'homme, R. K., Gregory, W. J., 7 Andres, R. P., (1985). Homogeneous Nucleation Temperatures for Concentrated Polystyrene/benzene Solutions. *J. Polym. Sci. Polym. Symp., 72*, 263-275.

Ramesh, N. S. & Malwitz, (1995). *Extrusion of Novel Water Soluble Biodegradable Foams*. ANTEC '95 Vol. II, Conference Proceedings, 2171-2177.

Ramesh, N. S., Rasmussen, D. H., & Campbell, G. A., (1991). Numerical and Experimental Studies of Bubble Growth During the Microcellular Foaming Process. *Poly. Engg. And Sci., 31*, 1657-1664.

Ramesh, N. S., Rasmussen, D. H., & Campbell, G. A., (1993). The Nucleation of Microcellular Foams in Polystyrene Containing Low Glass Transition Particles. *SPE ANTEC Conference Proceedings, Vol II,* 1828-1831.

Ramesh, N. S., Rasmussen, D. H., & Campbell, G. A., (1994). The Heterogeneous Nucleation of Microcellular Foams Assisted by the Survival of Microvoids in Polymers Containing Low Glass Transition Particles. Part I. Mathematical Modeling and Numerical Simulation. *Poly. Eng. Sci., 34*, 1685-1697.

Ramesh, N. S., Rasmussen, D. H., & Campbell, G. A., (1994). The Heterogeneous Nucleation of Microcellular Foams Assisted by the Survival of Microvoids in Polymers Containing Low Glass Transition Particles. Part II. Experimental Results and Discussion. *Poly. Eng. Sci., 34*, 1698-1706.

Reid, R. C., Prausnitz, J. M., & Poling, B. E., (1987). *The Properties of Gases and Liquids* (4^{th} ed.). New York, NY: McGraw-Hill Book Co.

Reiss, H., & Katz, J. L., (1967). Resolution of the Translation-Rotation Paradox in the Theory of Irreversible Condensation. *J. Chem. Phys., 40*, 2496-2499.

Reiss, H., Katz, J.L., & Cohen, (1968). E. R., Translation-Rotation Paradox in the Theory of Nucleation. *J. Chem. Phys., 48*, 5553-5560.

Reiss, H., Tabazadeh, A., & Talbot, J., (1990). Molecular Theory of Vapor Phase Nucleation: The Physically Consistent Cluster. *J Chem. Phys., 92*, 1266-1274.

Rosen, S. L., (1993). *Fundamental Principles of Polymeric Materials* (2^{nd} ed.). New York, NY: John Wiley and Sons, Inc.

Rosner, D. E., & Epstein, M., (1972). Effects of Interface Kinetics, Capillarity, and Solute Diffusion on Bubble Growth Rates in Highly Supersaturated Liquids. *Chemical Engineering Science, 27*, 69-88.

Ross, S., & Morrison, I. D., (1988). *Colloidal Systems and Interfaces, Chapter IIID*, New York, NY: John Wiley and Sons, Inc.

Ruengphrathuengsuka, W., (1992). *Bubble Nucleation and Growth Dynamics in Polymer Melts, Ph.D. Thesis.* Chemical Engineering Department, Texas A&M University.

Russel, K. C., (1980). Nucleation in Solids: The Induction After Steady State Effects. *Adv. Colloid Interf. Sci., 13*, 205-318.

Sanchez, I. C., & Lacombe, R. H., (1978). Statistical Thermodynamics of Polymer Solutions. *Macromolecules, 11*, 1145-1156.

Schmelzer, J. W. P., & Schmelzer, J., Jr., (1999). Kinetics of Nucleation at Increasing Supersaturation. *J. Colloid Interf. Sci., 215*, 345-355.

Scriven, L. E., (1959). On the Dynamics of Phase Growth. *Chemical Engineering Science, 10*, 1-13.

Shafi, M. A. & Flumerfelt, R. W., (1996). *Prediction of Cellular Structures in Polymer Foaming Process.* Cellular Polymer conference Proceedings, Paper #20, London.

Shafi, M. A. & Flumerfelt, R. W., (1997). Initial Bubble Growth in Polymer Foam Processes. *Chem. Eng. Sci., 52,* 627-633.

Shafi, M. A., Lee, J. G., & Flumerfelt, R. W., (1996). Prediction of Cellular Structure in Free Expansion Polymer Foam Processing. *Poly. Eng. Sci., 36,* 1950-195.

Shafi, M. A., Joshi, K., & Flumerfelt, R. W., (1997). Bubble Size Distributions in Freely Expanding Polymer Foams. *Chem. Eng. Sci., 52,* 635-644.

Shen, V. K., & Debenedetti, P. G., (2001). Density-Functional Study of Homogeneous Bubble Nucleation in the Stretched Lennard-Jones Fluids. *J. Chem. Phys., 114,* 4149-4159.

Slezov, V. V., Schmelzer, J., & Tkatch, Ya. Y., (1996). Number of Clusters Formed in Nucelation-Growth Processes. *J. Chem. Phys., 105,* 8340-8351.

Smith, J. M. & Van Ness, H. C., (1975). *Introduction to Chemical Engineering Thermodynamics* (3rd ed.). New York, NY: McGraw-Hill Book Co.

Stiel, L. I., & Harnish, D. F., (1976). Solubility of Gases and Liquids in Molten Polystyrene. *AIChE J., 22,* 117-122.

Street, J. R., Fricke, A. L., & Reiss, L. P., (1971). Dynamics of Phase Growth in Viscous, Non-Newtonian Liquids. *Ind. Engg. Chem. Fundls., 10,* 54-64.

Su, Y. Z. & Flumerfelt, R. W., (1996). The Effects of Dissolved Gas on Foam Formation Rate in Polymer Melts. *ANTEC '96,* 1937-1940.

Talanquer, V. & Oxtoby, D. W., (1993). Nucleation in Dipolar Fluids: Stockmayer Fluids. *J Chem. Phys., 94,* 4670-4679.

Talanquer, V. & Oxtoby, D. W., (1994). Dynamic Density Functional Theory of Gas-Liquid Nucleation. *J Chem. Phys.,100,* 5190-5200.

Talanquer, V. & Oxtoby, D. W., (1995). Nucleation in Binary Fluids. *J Chem. Phys.,102,* 2156-2164.

Tester, J. W. & Modell, M., (1996). *Thermodynamics and Its Applications* (3rd ed.). Upper Saddle River, NJ: Prentice Hall.

Thomas, G. B., & Finney, R. L., (1982). *Calculus and Analytical Geometry* (5th ed.). Reading, MA: Addison –Wesley Publishing Co.

Van Krevelen, D. W., (1990). *Properties of Polymers Their Correlation with Chemical Structure; Their Numerical Estimation and Prediction From Additive Group Contributions* (3rd ed.). New York, NY: Elsevier.

Vining, G. G., (1998). *Statistical Methods for Engineers.* New York, NY: Cole Publishing.

Volmer, M., (1939). *Kinetik der Phasenbildung.* Dresden: Steinkopff.

Volmer, M., (1029). *Z. Phys. Chem., 25,* 555.

Vrentas, J. S., Duda, J. L., & Hsieh, S. T., (1983). Thermodynamic Properties of Some Amorphous Polymer-Solvent Systems. *Ind. Eng. Chem. Prod. Res. Dev., 22,* 326-330.

Walas, S. M., (1985). *Phase Equililbria in Chemical Engineering,* , Stoneham, MA: Butterworth.

Weakliem, C. L., & Reiss, H., (1993). Towards a Molecular Theory of Vapor-Phase Nucleation. III. Thermodynamic Properties of Argon Clusters from Monte Carlo Simulation and a Modified Liquid Drop Theory. *J. Chem. Phys., 99,* 5374-5383.

Wegener, P. P., (1987). Nucleation of Nitrogen: Experiment and Theory. *J. Phys. Chem., 91,* 2479-2481.

Werner, H. W., (1981). Devolatilization of Polymers in Multi-Screw Devolatilizers. *Kunstoffe, 71,* 18-26.

White, G. M., (1969). Steady-State Random Walks with Applications to Homogeneous Nucleation. *J. Chem. Phys., 50,* 4672-4678.

Wilt, P. M., (1986). Nucleation Rates and Bubble Stability in Water-Carbon Dioxide Solutions. *J. Colloid and Interface Sci., 112,* 530-538.

Wu, S., (1970). Surface and Interfaciual Tension of Polymer Melts. II. Poly(methyl methacrylate), Poly (n-butyl methacrylate), and Polystyrene. *J. Phys. Chem., 74,* 632-638.

Yannas, I. V. & Luise, R. R., (1983). in A. E. Zacharides and R. S. Porters, (Eds.). *The Strength and Stiffness of Polymers.* New York, NY: Marcel Dekker, Inc.

Zhang, Q., Xanthos, M., & Dey, S. K., (2001). Effects of Process Conditions on the Dissolution of Carbon Dioxide in PS in Foaming Extruders. *Intern. Polymer Processing XVI, 3,* 223-228.

Zeldovich, J. B., (1942). *J. Exp. Theor. Phys., 12,* 525.

Zeng, X. C. & Oxtoby, D. W.,(1991). Gas-Liquid Nucleation in Lennard-Jones Fluids. *J. Chem. Phys., 94,* 4472-78.